

Role of Dopamine Tone in Brain Stimulation Reward

Giovanni Hernandez

A Thesis
In the Department
of
Psychology

Presented in Partial Fulfillment of the Requirements

For the Degree of Doctor of Philosophy at

Concordia University

Montreal, Quebec, Canada

October, 2009

© Giovanni Hernandez, 2009



Library and Archives
Canada

Published Heritage
Branch

395 Wellington Street
Ottawa ON K1A 0N4
Canada

Bibliothèque et
Archives Canada

Direction du
Patrimoine de l'édition

395, rue Wellington
Ottawa ON K1A 0N4
Canada

Your file *Votre référence*
ISBN: 978-0-494-67333-1
Our file *Notre référence*
ISBN: 978-0-494-67333-1

NOTICE:

The author has granted a non-exclusive license allowing Library and Archives Canada to reproduce, publish, archive, preserve, conserve, communicate to the public by telecommunication or on the Internet, loan, distribute and sell theses worldwide, for commercial or non-commercial purposes, in microform, paper, electronic and/or any other formats.

The author retains copyright ownership and moral rights in this thesis. Neither the thesis nor substantial extracts from it may be printed or otherwise reproduced without the author's permission.

AVIS:

L'auteur a accordé une licence non exclusive permettant à la Bibliothèque et Archives Canada de reproduire, publier, archiver, sauvegarder, conserver, transmettre au public par télécommunication ou par l'Internet, prêter, distribuer et vendre des thèses partout dans le monde, à des fins commerciales ou autres, sur support microforme, papier, électronique et/ou autres formats.

L'auteur conserve la propriété du droit d'auteur et des droits moraux qui protègent cette thèse. Ni la thèse ni des extraits substantiels de celle-ci ne doivent être imprimés ou autrement reproduits sans son autorisation.

In compliance with the Canadian Privacy Act some supporting forms may have been removed from this thesis.

While these forms may be included in the document page count, their removal does not represent any loss of content from the thesis.

Conformément à la loi canadienne sur la protection de la vie privée, quelques formulaires secondaires ont été enlevés de cette thèse.

Bien que ces formulaires aient inclus dans la pagination, il n'y aura aucun contenu manquant.


Canada

ABSTRACT

Role of Dopamine Tone in Brain Stimulation Reward

Giovanni Hernandez

Concordia University, 2009

The experiments described in the present thesis address the specific role of dopamine (DA) tone in brain stimulation reward (BSR). The level of extracellular dopamine in the rat nucleus accumbens was measured by means of in-vivo microdialysis in rats receiving electrical stimulation of the medial forebrain bundle. The first experiments characterize changes in DA tone as a function of reward predictability and duty cycle under circumstances in which phasic release of DA, as measured by fast-scan cyclic voltammetry, has been reported to be absent (Garris et al., 1999).

The results obtained using several different reinforcement schedules suggest that DA tone reflects the duty cycle of the stimulation rather than the predictability of the reward. In contrast to the transient elevation observed when stimulation is delivered at short (1.5 s) inter-train intervals, stimulation trains separated by long (12 s) inter-train intervals can sustain a stable level of DA tone for up to two hours. This difference in the stability of DA tone has repercussions for the behaviour sustained by BSR, as measured by means of the curve-shift paradigm. When DA tone was measured under similar circumstances to those in the Garris et al. (1999) study, a robust increase in tonic DA release was observed, on each schedule tested, in sharp contrast to the transient changes in phasic DA

release described by Garris et al. (1999). These results suggest that phasic and tonic DA release are under differential control. In an additional experiment, the reinforcement-mountain model and testing paradigm were used to determine the stage(s) of processing at which DA tone influences the pursuit of BSR. The mountain model relates pursuit of BSR to the cost and strength of the electrical stimulation. DA reuptake was blocked by continuous subcutaneous infusion of cocaine in a novel manner that avoids tissue damage. The 3D structure defined by time-allocation, reward cost and reward strength, always shifted rightward along the cost axis but rarely along the strength axis. This result implies that the leftward shifts seen in “rate-frequency” studies of the effect of cocaine on intracranial self-stimulation (ICSS) are misleading: these effects are due to displacement of the diagonally oriented face of the 3D structure along the cost axis. The results demonstrate that DA tone exerts its influence at a later processing stage than originally proposed and long believed.

ACKNOWLEDGMENTS

First and foremost I will like to thank Dr. Peter Shizgal for his support, patience and insight, whose intelligence and understanding I deeply admire. I am grateful to Dr. Kent Conover; his statistical wizardry has greatly improved our life in the Shizgal lab. I am also indebted to Dr. Andreas Arvanitogiannis, Dr. Jane Stewart and Dr. Wayne Brake for their helpful guidance and advice.

Thanks to Dr. Richard Courtemanche, Dr. Wayne Brake and Dr. Andreas Arvanitogiannis for their helpful comments on a previous draft of this thesis.

I would also like to thank all the wonderful people working in the CSBN that help us achieve our academic and research goals, especially Dave Munroe and Steve Cabilio, who keep our entire computers and lab equipment running, Elizabeth Chau and Phyllis Webster who helped me navigate through Concordia's bureaucracy, Aileen Murray who keeps our animal colony in enviable conditions, and Heshmat Rajabi -*the HPLC master*- who taught me a few tricks and whose friendship I deeply cherish.

Heartfelt thanks to my lab mates Rebecca Solomon whose dedication and patience I envy; Marie -Pierre Cossette whose enthusiasm for research and perseverance has no limits; Yannick Breton who has helped many in the lab, including myself with his programming skills; Ivan Trujillo and Brian Dunn who have become good and genuine friends. I am also grateful to those past lab members that helped me in the data collection and encouraged me along the way: Eric Haines and Selma Hamdani.

Thanks to my family who cheers for me from a distance and finally to my wife Marianne Da Costa to who has supported me unfailingly, given me so much and asked nothing in return. I can live a day without science but not a day without you.

TABLE OF CONTENTS

	<i>Page</i>
CONTRIBUTION OF AUTHORS.....	xi
LIST OF FIGURES	xv
LIST OF TABLES.....	xviii
GENERAL INTRODUCTION.....	1
Brain stimulation reward.....	1
The catecholamine system and brain stimulation reward.....	5
BSR and DA release: Phasic vs. tonic	13
The Reinforcement-Mountain.....	18
CHAPTER 1	30
Prolonged Rewarding Stimulation of the Rat Medial Forebrain Bundle:	
Neurochemical and Behavioral Consequences.....	30
Introduction.....	31
Experiment 1	35
Methods.....	35
Subjects.....	35
Surgery.....	36
Self-stimulation training.....	36
In vivo microdialysis.....	37
Analytical chemistry.....	39
Stimulation protocol.....	40
Histology.....	40
Statistics.....	41
Results.....	41
Location of electrode tips and microdialysis probes.....	41
Basal DA levels.....	42
Effect of LH stimulation under an FT12 schedule on locomotion and DA concentration.....	42

Effect of LH stimulation under a VT12 schedule on locomotion and DA concentration	44
Effects of LH stimulation under a VT1.5 schedule on locomotion and DA concentration	47
Statistical comparison of locomotion and DA levels across schedules	47
Discussion Experiment 1	49
Experiment 2	55
Methods	56
Subjects	56
Surgery	56
Self-stimulation training	56
BSR modulation experiment	56
Curve fitting and statistics	57
Results	62
Location of electrode tips	62
Effect of the stimulation schedule on the M50 values	63
General Discussion	68
The role of DA neurons in BSR	69
CHAPTER 2	83
Predictable and unpredictable rewards produce similar changes in dopamine tone	83
Introduction	84
Method	87
Subjects	87
Surgery	88
Self-Stimulation Training	88
In vivo microdialysis	89
Analytic Chemistry	90
Histology	91
Statistics	92
Results	92

Location of Electrode Tips and Microdialysis Probes.....	92
Basal Extracellular Levels of Dopamine, DOPAC and HVA	94
Basal Extracellular Levels of Dopamine, DOPAC and HVA	95
Time courses of Responding Under the FI and VI Schedules	95
Changes in the Concentrations of DA, DOPAC, and HVA during LH Self- Stimulation on an FI-12 Schedule	96
Effect of LH Stimulation under a VI-12 Schedule on Concentrations of DA, DOPAC, and HVA	98
Statistical comparison of DA levels across schedules	102
Discussion.....	104
CHAPTER 3	110
Dopamine tone increases similarly during predictable and unpredictable administration of rewarding brain stimulation at short inter-train intervals	110
Introduction.....	111
Materials and Methods.....	113
Subjects	113
Surgery.....	113
Self-stimulation training and stimulation protocol.....	114
In vivo microdialysis	115
Analytic chemistry	116
Histology	117
Statistics	117
Results.....	118
Location of electrode tips and microdialysis probes.....	118
Basal extracellular levels of dopamine.....	118
Effect of LH stimulation on concentrations of DA	118
Discussion	122
CHAPTER 4	126
Dynamic changes in dopamine tone during self-stimulation of the ventral tegmental area in rats	126
Introduction.....	127

Materials and Methods.....	130
Subjects	130
Surgery	131
Self-Stimulation Training	132
In vivo microdialysis	132
Analytical chemistry	134
Histology	134
Statistics	134
Results.....	135
Location of electrode tips and microdialysis probes	135
Behaviour	135
Basal levels	135
Effects of electrical stimulation on the concentration of dopamine in the intermittent-access condition	138
Effects of electrical stimulation on the concentration of dopamine in the continuous-access condition	138
Discussion.....	142
CHAPTER 5	147
Potential of intracranial self-stimulation during prolonged subcutaneous infusion of cocaine	147
Introduction.....	148
Materials and Methods.....	151
Subjects	151
Surgery	151
Subcutaneous infusions	155
Analytical chemistry	155
Histology	156
Statistics	156
Results.....	157
Time course of DA concentration across conditions	157
Absence of necrosis	158

Discussion Experiment 1	162
Experiment 2.....	163
Material and methods.....	163
Subjects	163
Surgery	163
Self-Stimulation Training	163
Procedure	164
Statistical Analysis	165
Results.....	165
Cocaine-induced curve shifts	167
General Discussion	174
CHAPTER 6	176
<i>At what stage of processing does cocaine influence performance for brain stimulation reward?</i>	176
Introduction.....	177
Subjects	185
Surgery	185
Self-stimulation training	186
Procedure	188
Data analysis	190
Histology	194
Results.....	195
Electrode tip location	195
Fit of the model to the data and cocaine- induced shifts	195
Discussion	213
GENERAL DISCUSSION	218
REFERENCES	228
APPENDICES	261

CONTRIBUTION OF AUTHORS

This is a manuscript-based thesis. Below is a description of the contribution of the authors to each manuscript.

Chapter 1:

- I carried out the research, contributed to the design of the experiment performed the principal analysis of the data, wrote the first draft of the manuscript and contributed to subsequent revisions.
- Selma Hamdani contributed to the data collection.
- Heshmat Rajabi was responsible for the maintenance of the HPLC system, provided advice about the analytic chemistry methods and taught me how to construct the microdialysis probes.
- Kent Conover contributed to the development of the fitting procedure.
- Jane Stewart provided access to the HPLC system, contributed in the interpretation of the results, and provided helpful comments about the manuscript.
- Andreas Arvanitogiannis was involved in designing the experiment and provided helpful feedback on the manuscript drafts.
- Peter Shizgal was involved in designing the experiments, data analysis and the interpretation of the results. He worked on all versions of the manuscript.

Chapter 2:

- I carried out the research, contributed to the design of the experiment performed the principal analysis of the data, made the microdialysis probes, wrote the first draft of the manuscript and contributed to subsequent revisions.

- Eric Haines contributed to the data collection.
- Heshmat Rajabi was responsible for the maintenance of the HPLC system and provided advice about the analytic chemistry methods.
- Jane Stewart provided access to the HPLC system, contributed to the interpretation of the results, and provided helpful comments about the manuscript.
- Andreas Arvanitogiannis was involved in designing the experiment and provided helpful feedback on the manuscript drafts.
- Peter Shizgal was involved in designing the experiments, data analysis and the interpretation of the results. He worked on all versions of the manuscript.

Chapter 3:

- I carried out the research, contributed to the design of the experiment performed the principal analysis of the data, made the microdialysis probes, wrote the first draft of the manuscript and contributed to subsequent revisions.
- Heshmat Rajabi was responsible for the maintenance of the HPLC system and provided advice about the analytic chemistry methods.
- Jane Stewart provided access to the HPLC system, contributed to the interpretation of the results, and provided helpful comments about the manuscript.
- Andreas Arvanitogiannis was involved in designing the experiment and provided helpful feedback on the manuscript drafts.
- Peter Shizgal was involved in designing the experiments, data analysis and the interpretation of the results. He worked on all versions of the manuscript.

Chapter 4:

- I carried out the research, contributed to the design of the experiment performed the principal analysis of the data, made the microdialysis probes, wrote the first draft of the manuscript and contributed to subsequent revisions.
- Peter Shizgal was involved in designing the experiments data analysis and the interpretation of the results. He worked on all versions of the manuscript.

Chapter 5:

- I carried out the research, contributed to the design of the experiment performed the principal analysis of the data, made the microdialysis probes, designed the subcutaneous tubing, wrote the first draft of the manuscript and contributed to subsequent revisions.
- Eric Haines contributed to the data collection.
- Peter Shizgal was involved in designing the experiments and the subcutaneous tubing, in data analysis and in the interpretation of the results. He worked on all versions of the manuscript.

Chapter 6 (*unpublished manuscript*):

- I carried out the research, contributed to the design of the experiment performed the first fit of the data, designed the subcutaneous tubing, wrote the first draft of the manuscript and contributed to subsequent revisions.
- Yannick Breton contributed to the programming of the MATLAB routines
- Kent Conover developed the model-fitting procedures and program.

- Peter Shizgal conceived of and developed the mountain model, as well as the 7-parameter variant. He was involved in designing the experiments, data analysis and fitting procedure, and in the interpretation of the results. He worked on all versions of the manuscript.

LIST OF FIGURES

	<i>Page</i>
Figure 1. Effect of manipulating reward intensity or effort cost on simulated 2D psychometric curves	20
Figure 2. Translation of the stimulation-induced impulse flow into behavior	26
Figure 3. Three dimensional structure describing the dependence of time allocation on pulse frequency and price	27
Figure 4. Location of electrode tips and microdialysis probes	43
Figure 5. Effect of LH stimulation following an FT12 schedule on locomotion and DA concentration.....	45
Figure 6. Time allocation by frequency curves after 2.5 hour of LH stimulation following a VT1.5, VT12 or no stimulation schedule.....	58
Figure 7. Location of electrode tips	65
Figure 8. The feedforward schema	79
Figure 9. Location of microdialysis probes (a) and electrode tips (b) for the FI and VI groups.....	93
Figure 10. Mean normalized response rate (responses/s) for each group as a function of time since last reward.....	97
Figure 11. Effects of electrical stimulation under a FI-12 schedule on the Concentrations of DA, DOPAC, and HVA.	99
Figure 12. Effects of electrical stimulation under a VI-12 schedule on the Concentrations of DA, DOPAC, and HVA	101
Figure 13. DA concentration in Dialysate obtained from NAc under the two reinforcement schedules (VI-12 and FI-12).....	103
Figure 14. Location of microdialysis probes and electrode tips for the FT and VT groups	119
Figure 15. Effect of LH stimulation under a FT-VT1.5 reinforcement schedules on the concentrations of DA.	121
Figure 16. Location microdialysis probes.....	136
Figure 17. Location of electrodes tips.....	137

Figure 18. Effects of electrical stimulation of the VTA throughout 10-minute (intermittent-access) stimulation periods on DA concentration.	139
Figure 19. Effects of electrical stimulation of the VTA under a continuous reinforcement schedule on the concentration of DA.	141
Figure 20. Picture of perforate tubing for prolonged subcutaneous infusion of cocaine	153
Figure 21. Location of microdialysis probes	159
Figure 22. Time course of the changes in DA concentration during subcutaneous infusion of saline or cocaine.	160
Figure 23. Photograph of the dorsal surface of the seven rats in which the subcutaneous tubing remained patent.	161
Figure 24. Location of electrode tips.	166
Figure 25. Cocaine induced curve shifts	168
Figure 26. Across-subject and across-session average of the curve shift observed in each determination	169
Figure 27. Across-subject and across-determination average of the cocaine induced curve shifts for each test session.	171
Figure 28. Translation of the stimulation-induced impulse flow into behavior	184
Figure 29. Simulated time allocation-frequency curves and their average	193
Figure 30. Location of electrode tips	196
Figure 31. Time allocation data from rat MCOC8	197
Figure 32. Contour graphs and bar graph showing the displacement of the mountain along the price axis in the case of rat MCOC8	201
Figure 33. Fit of the time allocation-frequency curves for rat MCOC3 using the 6- parameter and 7-parameter model	204
Figure 34. Time allocation data and projections of the fitted surfaces obtained by allowing the location parameters to vary across sessions.	205
Figure 35. Time allocation data from rat MCOC3, fitted surfaces and their two dimensional projections.	208
Figure 36. Contour graph showing the displacement of the mountain along the price axis in the case of rat MCOC3	210

Figure 37. Time allocation vs. frequency curves obtained at a low price and at a high price under the influence of cocaine 211

Figure 38. Bar graphs showing the displacement of the mountain for all subjects tested. 212

LIST OF TABLES

	<i>Page</i>
Table 1. Summary of the location parameter difference P_e for all subjects.....	206
Table 2. Summary of the location parameter difference F_{hm} for all subjects.....	207

GENERAL INTRODUCTION

Brain stimulation reward

Rats and several species, including humans, will deliver electrical pulse trains to different brain loci through the tip of insulated metallic electrodes (Olds, 1962; Olds & Milner, 1954; Shizgal & Murray, 1989). In humans the activation of certain brain areas by the electrical pulses are accompanied with subjective feelings of pleasure (Delgado, 1975; Heath, 1964). The effect of the electrical stimulation that leads organisms to seek and reinitiate the stimulation is called brain stimulation reward (BSR).

According to Olds (1966), the discovery and study of BSR would have not been possible if two advances had not been made. The first of these advances was the introduction of metallic insulated electrodes to electrically stimulate and electrolytically lesion discrete brain foci in behaving cats. The use of these techniques, by the Swiss physiologist, Hess, allowed him to study brain areas related to autonomic and motor responses and to map the anatomic substrate of complex autonomic functions. Hess, won the Nobel Prize in medicine and physiology in 1949 for his groundbreaking research. The second advance was the design and development of the operant box by B.F. Skinner (1938). The operant box, a ubiquitous apparatus in experimental psychology, allows the experimenter to manipulate external variables and observe how these changes affect a simple repetitive response like pressing a lever. The reinforcing stimulus is one class of such external variables of which response rate is a function. If one modifies the properties of the reinforcing stimulus, a change in the response rate will occur. This simple manipulation opened the door to the quantitative study of rewarding brain stimulation.

The discovery in 1953 that stimulating certain brain areas was rewarding was serendipitous. It occurred when Olds and Milner were looking for aversive responses to stimulation similar to those already reported by Delgado, Roberts and Miller (1954), who showed that the aversive effects of brain stimulation could be used as negative reinforcement. Delgado and colleagues trained their cats to turn wheels in order to avoid the delivery of aversive stimulation to the lateral nuclear mass of the thalamus. As well, the stimulation of this area produced conditioned avoidance of the place where the stimulation was given and it also served as punishment, eliminating feeding behaviour in hungry cats when the stimulation was paired with the onset of feeding. However, what Olds and Milner observed after stimulating the septal area of rats was quite the opposite. They started their rudimentary observations (Olds, 1966) by putting the rats on a table and delivering stimulation every time they approached an arbitrarily chosen corner. Instead of avoiding that particular corner, as would be the case if the stimulation were aversive, the rats returned to the place where the stimulation had been delivered, thus showing signs of place preference. In order to give this observation a quantitative basis, Olds used the operant paradigm and trained the rats to lever press for the electrical stimulation. By using this paradigm, he obtained a measure of the reinforcing properties of the electrical stimulus employed and could compare different brain areas in terms of their potential to sustain intracranial self-stimulation behaviour.

Since its discovery, brain stimulation reward has become the paradigm of choice for studying the neural reward circuitry and goal directed responses. Some of the reasons for this are that the electrical stimulation can be precisely manipulated and that its parameters have neurophysiological meaning. The cathodal current passed through the

electrode depolarizes nearby neurons thereby triggering action potentials. If the train and pulse duration are held constant, the number of action potentials elicited in the neurons close to the electrode tip is determined by the pulse frequency, whereas the stimulation current or pulse amplitude determines the radius of effective stimulation, and thus the number of cells excited by the electrode (Gallistel, Shizgal, & Yeomans, 1981).

The behaviour elicited and controlled by the electrical stimulation, unlike the behaviour controlled by natural rewards (McSweeney & Roll, 1993), is stable both between and within sessions. The electrical signal is injected directly into the brain, bypassing sensory inputs and physiological feedback mechanisms that discount natural rewards over the length of the experimental session. Moreover, it is delivered with a minimal delay after the behaviour that procures the reward has occurred; therefore response-reinforcement delays that degrade natural rewards are avoided.

The rewarding signal that arises as a result of the delivery of electrical pulses is produced at known central nervous system (CNS) sites and it shares properties with natural rewards. Conover and Shizgal (1994), in a series of clever experiments, demonstrated that natural rewards and the rewarding effects of electrical stimulation can compete and can be combined with one another. Their experimental subjects were tested in a forced-choice preference paradigm where they had to select between two manipulanda: one that delivered a train of electrical pulses that varied from trial to trial and the other that delivered a constant concentration of sucrose or a constant concentration of sucrose plus a fixed train of electrical pulses. In order to control for immediacy and for the satiation effects of the natural reward, the sucrose was

administered by means of an oral cannula and removed by means of a gastric cannula. By controlling these two factors, Conover and Shizgal made the two rewards comparable.

In the choice situation in which the experimental subject had to select between the option of variable electrical stimulation pulses or the sucrose alone, the experimental subject would choose the alternative associated with a higher relative reward magnitude. If the rewarding stimulation was strong enough, they would forgo the sucrose reward, but if the rewarding stimulation was weak enough, then they would choose the natural reward. Therefore electrical rewarding stimulation and natural rewards compete with one another.

When the choice was between the variable electrical stimulation pulses or the compound of constant sucrose concentration and a fixed train of electrical pulses, the psychometric function obtained in the previous experiment was right shifted, meaning that the number of pulses required to produce a bias towards the electrical reward had to be increased. The rightward shift observed in the psychometric function suggests that the rewarding effects of electrical stimulation and of a palatable tastant summate. These results suggest that natural rewards and brain stimulation rewards are evaluated using a common scale.

The question of which directly activated neurons are responsible for the rewarding effect of the electrical stimulation has not yet been answered. Part of the difficulty lies in the fact that the sites where the electrode produces rewarding effects are anatomically complex, as the sites contain different subpopulations of fibres with a vast array of physiological characteristics as well as differing anatomical origins and projection fields (Shizgal, 1989). Nevertheless, several attempts have been made to deal

with this question. One of the most influential ideas emphasizes the role of catecholaminergic neurons as the origin of the rewarding signal as well as the neurons that were the most likely candidates to be directly activated by the electrode.

The catecholamine system and brain stimulation reward

Early on in the research on intracranial self-stimulation, it was hypothesized that self-stimulation arises from the activation of catecholamine releasing axons (Stein, 1961). Given the correlation between electrode placement and location of catecholamine projection areas, it was proposed that self-stimulation is due to direct activation of norepinephrine (Crow, Spear, & Arbuthnott, 1972; Poschel & Ninteman, 1963; Stein, 1964) and/or dopamine neurons (Crow, 1969; Crow, 1972; Crow, 1972; Liebman & Butcher, 1974; Lippa, Antelman, Fisher, & Canfield, 1973; Wauquier & Niemegeers, 1972) and that these neurotransmitters were responsible for the transmission of the reward signal (Wise, 1978).

The norepinephrine activation hypothesis received early support by pharmacological and lesion experiments that targeted the norepinephrine (NE) system. The inhibition of the enzyme involved in the final step of the biosynthesis of norepinephrine from dopamine, dopamine- β -hydroxylase, by systematic intraperitoneal administration of disulfiram or intraventricular administration of diethyldithiocarbamate, abolished intracranial self-stimulation. Moreover, intraventricular administration of l-norepinephrine reversed the effects of the NE biosynthesis inhibition (Wise & Stein, 1969). Self-stimulation of the substantia nigra was disrupted by ipsilateral transection of the dorsal and ventral NE bundles by means of knife cuts or by neurotoxic lesions of the NE bundles (Belluzzi, Ritter, Wise, & Stein, 1975).

Although the NE activation hypothesis was supported by this and other positive evidence, it was also challenged on several fronts. Most of the criticism came from discrepant findings and failure to replicate key results. A rigorous examination of the location of electrodes aimed at the locus coeruleus, the principal site for synthesis of norepinephrine in the brain, failed to support the hypothesis that this structure supports self-stimulation (Amaral & Routtenberg, 1975; Simon, Le Moal, & Cardo, 1975). Similarly, several groups reported persistence of self-stimulation following lesions of the ascending NE pathway (Clavier, Fibiger, & Phillips, 1976; Clavier & Routtenberg, 1976; Corbett, Skelton, & Wise, 1977).

From an inferential point of view the assertion that the reduction in self-stimulation behaviour was the exclusive product of the ablation of NE neurons was unwarranted, as suggested by the early studies that supported the NE activation hypothesis. The lesioning techniques used lack specificity (Fibiger, 1978) and the reduction in the self-stimulation behaviour could have been the product of the destruction of other neurons or structures.

Not only were the placement and lesion data challenged, but doubts were also raised about the pharmacological evidence. It was shown that administration of disulfiram disrupted self-stimulation because it induced lethargy; under the influence of the drug, the rats fell asleep, but if the experimenter placed them upon the lever, the rats would resume normal responding (Roll, 1970). Moreover, administration of drugs, such as FLA-63 and U-47, that inhibit dopamine- β -hydroxylase without producing sedation did not disrupt intracranial self-stimulation (Cooper, Cott, & Breese, 1974; Lippa et al., 1973).

As the NE hypothesis lost support, a competing hypothesis positing dopamine (DA) neurons as the neural basis of BSR gained ground. Like the NE hypothesis, the DA hypothesis also leaned heavily on a purported correlation between the location of self-stimulation sites and the anatomical distribution of catecholaminergic projections. It was asserted that intracranial self-stimulation behaviour can be reliably obtained when the electrode is located in known dopaminergic nuclei (Crow, 1972; Crow, 1972). At ventral tegmental sites, current thresholds for BSR and maximal response rates are correlated with the density of DA neurons near the electrode tip (Corbett & Wise, 1980). At more rostral self-stimulation sites, current thresholds were negatively correlated with the amount of DA released by the stimulation in the ventral striatum (Yavich & Tanila, 2007), a finding consistent with the notion that lower thresholds indicate higher densities of reward-related fibers.

Pharmacological studies give further support to the DA hypothesis. In order to avoid confounds in the interpretation of the data, it was necessary to develop testing paradigms that can distinguish effects of drugs on performance capacity from effects on reward strength. Using an ingenious approach to the traditional response rate measurements, Fouriez and Wise (1976) tested whether, independent of performance deficits, the rewarding value of the electrical stimulation was impacted by pimozide, a selective DA receptor blocker. They argued that if this drug produced a change in the rewarding value of the stimulation, the animals should perform as if the lever-press behaviour was being extinguished right after the drug was given. That is, the rats would start with a high response rate similar to previous sessions and then show a steady and steep decline across the session. If the drug produced an effect because of a motor deficit,

then the rats should perform in a stable manner across the session but with a reduced response rate. The behaviour of the rats reliably showed the extinction pattern, in this way lessening the performance deficit interpretation of the effect of pimozide and giving support to the importance of DA neurotransmission on the behaviour sustained by electrical stimulation.

Although in principle, this new addition to the response rate paradigm produced dissociation between reward strength and performance capacity, it came under fire because for some drugs tested it was not clear if the response rate reduction was product of factors other than changes in reward strength. When two different operant responses, lever press and nose poke, are tested with DA receptor blockers, like α -flupenthixol, the decrease in response rate seems to correspond to how much exertion is associated with each operant response and not with a decrease in reward strength (Ettenberg, Koob, & Bloom, 1981). When the DA antagonists fluspirilene and haloperidol were tested and the extinction response pattern was dissociated according to three factors: response initiation, duration of self-stimulation burst and response rate within each burst. The observed behavioural patterns suggest that these drugs have a major impact on response initiation, which some authors have associated with incentive and not reward (Katz, 1981; Katz, 1982).

The criticisms of the extinction method brought to light how difficult is to – dissociate variables that affect reward strength from other variables, including performance capacity when testing paradigms based on response rate measurements are used. This problem is especially acute when measuring the effects of drugs that affect DA

neurotransmission, since DA is implicated both in motor and reward processes (Hamilton, Stellar, & Hart, 1985).

Several testing paradigms have been implemented to minimize the effect of performance variables. These paradigms are known as “rate-free” methods and include titration (Stein & Ray, 1960), the response strength method (Hamilton et al., 1985) and the curve shift-paradigm (Edmonds & Gallistel, 1974) among others; of these the one that has been used most extensively is the curve shift-paradigm.

The curve shift paradigm entails the measurement of the psychometric function relating the vigour of operant performance, such as the rate of lever pressing or time allocation, to the strength of the rewarding stimulation (e.g., the pulse frequency or current). This measurement paradigm was introduced by Edmonds and Gallistel (1974) in a series of experiments in which they changed the number of pulses per train from trial to trial and measured the speed with which rats traversed a straight alley and pressed a lever in the goal box. Since its introduction, this paradigm has been modified by substituting different stimulation parameters or different response measurements (Frank, Markou, & Wiggins, 1987; Stellar, Waraczynski, & Wong, 1988). In this paradigm, lateral curve shifts are interpreted to reflect changes in the potency of the reward, whereas vertical shifts, when using response measurements other than time allocation, are interpreted to reflect changes in performance capacity. (Miliaressis, Rompre, Laviolette, Philippe, & Coulombe, 1986)

When this method has been employed, the dopaminergic hypothesis has stood up to empirical scrutiny. Pimozide, the specific DA receptor antagonist drug, shifts the psychometric function to the right (Franklin, 1978; Gallistel, Boytim, Gomita, &

Klebanoff, 1982; Gallistel & Freyd, 1987; Gallistel & Karras, 1984; Miliareisis, Rompre et al., 1986; Stellar, Kelley, & Corbett, 1983). Similar results have been obtained with haloperidol (Nakajima & Patterson, 1997; Schaefer & Michael, 1980), and raclopride (Nakajima & Patterson, 1997). Thus, the rewarding impact of the stimulation is said to be decreased, because under the influence of DA antagonists, stronger stimulation is required to produce a given level of performance.

The effects of enhancing DA neurotransmission complement those produced by decreasing DA neurotransmission. The specific blockade of the DA transporter by GBR12909, which increases the extracellular concentration of the neurotransmitter, shifts the psychometric function to the left. (Maldonado-Irizarry, Stellar, & Kelley, 1994; Rompré & Bauco, 1990). Apomorphine, another specific DA agonist, has been shown to have mixed effects. In a comprehensive study, Fouriez and Francis (1992) showed that at low dosages, apomorphine reduced the impact of the rewarding effect, whereas at high dosages, the impact of the rewarding effect was enhanced. The perplexing result was explained by the differential affinity of DA receptor subtypes for apomorphine. Apomorphine has higher affinity for presynaptic than for postsynaptic receptors. Therefore at low dosages (0.01 mg/kg-0.10 mg/kg), apomorphine should primarily activate DA presynaptic receptors which would reduce DA release. At higher dosages (0.30mg/kg-1 mg/kg) the presynaptic inhibition should persist but could be overridden by direct activation of postsynaptic receptors. Other non specific agents that boost DA neurotransmission, like cocaine (Baucu & Wise, 1997a; Maldonado-Irizarry et al., 1994) and amphetamine (Colle & Wise, 1988; Roy A. Wise & Munn, 1993), have reliably

produced the leftward displacement of the psychometric function that relates operant performance and stimulation strength.

Neurochemical studies provide further evidence of the involvement of DA in brain stimulation reward. Dopamine release is observed when different areas that support self-stimulation are electrically stimulated. Long-lasting increases of DA concentration, as measured by means of in-vivo microdialysis, have been seen in the nucleus accumbens (Nac) (Nakahara, Ozaki, Miura, Miura, & Nagatsu, 1989; Phillips et al., 1992; Taber & Fibiger, 1995; You, Tzschentke, Brodin, & Wise, 1998; You, Chen, & Wise, 2001) and medial prefrontal cortex (Bean & Roth, 1991; Nakahara, Fuchikami, Ozaki, Iwasaki, & Nagatsu, 1992). Increase in DA overflow after electrical stimulation in the Nac in anesthetized (Blaha & Phillips, 1990) as well as in freely moving subjects (Yavich & Tiihonen, 2000) have been reported using chronoamperometry, an electrochemical technique that measures DA oxidation. With another electrochemical technique, fast-scan cyclic voltammetry (FSCV), DA overflow in the Nac has been observed after each stimulation train if there is a ten-second timeout between stimulations (Cheer, Heien, Garris, Carelli, & Wightman, 2005).

Given the positive evidence offered by mapping, pharmacological and neurochemical studies about the role of DA in intracranial self-stimulation behaviour, it seems plausible to infer, as was done initially, that the rewarding effect of electrical brain stimulation arises from the direct activation of DA cell bodies or fibers by the electrode. However this inference can be rejected almost immediately on anatomical grounds, since self-stimulation can be obtained by electrodes located in the cerebellum (Corbett, Fox, & Milner, 1982) where DA neurons are sparse or absent.

Moreover, psychophysical and electrophysiological studies have shown that dopamine neurons are unlikely to constitute a major component of the neural population stimulated directly by the electrode. The axonal refractory periods of the directly stimulation fibers range between 0.4 to 1.5 ms (Bielajew, Lapointe, Kiss, & Shizgal, 1982; Murray & Shizgal, 1996; Rompré & Miliaressis, 1987; Rompré & Shizgal, 1986; Shizgal, Bielajew, & Rompré, 1988; Yeomans, 1979; Yeomans & Davis, 1975; Yeomans, Matthews, Hawkins, Bellman, & Doppelt, 1979), whereas the refractory periods of DA axons range from 1.2 to 2.5 ms (Anderson, Fatigati, & Rompre, 1996; Yeomans, Maidment, & Bunney, 1988). In addition, DA neurons, unlike the neurons at the tip of the stimulating electrode, have high thresholds for activation by extracellular stimulation via macroelectrodes (Wang, 1981; Yeomans et al., 1988), due to the fact that their axons are unmyelinated and of very fine caliber (Gerfen, Herkenham, & Thibault, 1987). Recently, blocking receptors for excitatory neurotransmitters into the VTA with (\pm)2-amino,5-phosphopentanoic acid (AP-5), an NMDA receptor antagonist while stimulating this area produced a reduction of DA transients observed in the Nac shell as measured by FSCV (Sombers, Beyene, Carelli, & Wightman, 2009). The reduction in DA transients after inactivation of the VTA gives support to the idea that DA neurons are not directly activated by the electrode, but are trans-synaptically activated. If DA neurons were directly activated by the stimulating electrode, inactivation of the cell bodies would have little if any effect on the DA transients. However, if DA neurons were trans-synaptically activated, as the empirical evidence suggests, then inactivation of the VTA would have a direct impact on the release of DA in terminal fields impact on the release of DA in terminal fields.

In summary, DA neurotransmission is important for BSR, and DA neurons are mostly activated trans-synaptically (particularly when short pulse durations and large electrodes are used)(Yeomans et al., 1988). Given these facts, what role do these neurons play in the maintenance of self-stimulation, and where in the reward circuit do they exert their influence?

BSR and DA release: Phasic vs. tonic

Midbrain dopaminergic cells are relatively few in number, between 30.000 - 40.000 in the rat brain, but they project to widely distributed brain areas, in both cortical and subcortical brain structures (Swanson, 1982). DA neurons exert their influence in different neural networks as a function not only of their spatial distribution but also of their activity states. DA neurons have three activity states: an inactive resting state, and an active state that bifurcates into tonic and phasic components (Floresco, West, Ash, Moore, & Grace, 2003).

In a rodent unengaged in active behaviour, about 50% of the DA neuron population is inactive. The inactivation of DA neurons is due to a strong inhibitory drive from GABAergic afferents. Reducing this inhibitory input promotes a transition from the inactive to the active state. Once in the active state, DA neurons fire in a slow and sustained (“tonic”) pattern. The change from tonic to “phasic” bursting firing is produced by activating glutamatergic and cholinergic afferents that innervate DA neurons (Floresco et al., 2003; Smith & Grace, 1992).

These different activity states of DA neurons are translated into different release patterns at the terminal fields. Manipulation of the afferent systems to the VTA, one of

the major mesencephalic DA cell body clusters, produces changes in DA activity states (Floresco et al., 2003). Specifically, manipulations of GABAergic transmission from the ventral pallidum (VP) and manipulations of glutamatergic and cholinergic transmission from the pedunculopontine tegmental nucleus (PPTg) differentially affect tonic and phasic release of DA. Inactivation of the tonically active inhibitory GABAergic input to the VTA by co-infusions of GABA_A (muscimol) and GABA_B (baclofen) agonist into the VP, increases DA neuron population activity without altering phasic burst activity. On the other hand, activation of excitatory glutamatergic and cholinergic afferents to the VTA by infusion of bicuculline into the PPTg increases burst firing in DA neurons without affecting the number of neurons in the active state. Moreover, these changes in tonic and phasic firing have a differential effect on DA efflux registered by means of microdialysis. Inactivation of the VP, which produces an increase in the number of neurons in the active state, also produces a reliable increase in tonic DA efflux in the Nac, whereas activation of the PPTg does not produce any appreciable increase in tonic DA efflux (unless DA reuptake is blocked). The increase in phasic burst activity is believed to be the origin of the transient, local release measured by means of FSCV (Wightman & Robinson, 2002).

Phasic and tonic signaling have direct implications for learning theories and for accounts of intracranial self-stimulation. In reward-mediated learning, it has been shown that phasic dopamine firing in DA neurons located in the VTA and substantia nigra plays an important role in classical conditioning. DA neuron activity seems to fit with temporal difference models of learning in which DA phasic firing works as a teaching signal in the brain (Montague, Dayan, & Sejnowski, 1996; Schultz, Dayan, & Montague, 1997). When

a reward is unpredictable, DA neurons fire in response to the presentation of the reward, but when the reward is paired with a cue, DA phasic firing shift towards the cue (Ljungberg, Apicella, and Schultz, 1992; Mirenowicz, and Schultz, 1994; Schultz, 1998; Schultz et al., 1997). This temporal change in the phasic firing suggests that DA neurons are coding a temporal difference error (Sutton & Barto, 1998).

The temporal difference error represents a disparity between the reward predicted by a given set of stimulus conditions at a particular point in time and the reward received at the next point in time. Before reaching asymptotic learning, each encounter with the reward and the cues associated with it produces a prediction error, which, in turn, changes weights in the neural networks underlying both reward prediction and reward pursuit. The predictions of future rewards are refined so that the organism can improve its predictions of the timing and strength of future rewards, while adjusting action patterns to maximize the reward rate (Dayan & Balleine, 2002; Houck, Adams, & Barto, 1995). Thus, temporal-difference errors are large when unpredicted rewards are received and shrink progressively as the prediction of reward onset is learned.

This property of phasic DA signaling has implications for BSR; Garris et al.(1999) and Kilpatrick et al (2000) showed that in order for rats to learn to self stimulate, the electrical stimulation must produce phasic release of DA. However, DA phasic release under a continuous reinforcement schedule was reported to be short lived in those experiments. During the first few minutes of self-stimulation training, phasic release of DA was detected, but then the phasic signal fell below the detection threshold even though rats continued to self-stimulate vigorously. This observation about the phasic component of DA firing supports the idea that it carries information about the temporal

difference error. During the very first trials, the organisms have no associations between pressing the lever and getting a reward, so in the very first trials the reward is unpredictable. According to the temporal difference error model, this first encounter should produce DA phasic firing. As the training continues and the organism learns the contingency between the lever and the reward, the reward ceases to be unpredictable and therefore DA phasic firing should transfer to the first reward predictor.

The results reported by Garris et al. and Kilpatrick et al. is at odds with ample evidence showing that pharmacological manipulations of the dopaminergic system produce substantial changes in self-stimulation threshold and with microdialysis data demonstrating that DA is present during intracranial self-stimulation. The discrepancy can be resolved by assuming different roles for phasic and tonic DA release. Whereas phasic release may be necessary for the acquisition of self-stimulation, tonic DA signaling may be important for the maintenance and stability of the behaviour.

The difference between the detection of DA release in self-stimulating rats by means of FSCV and microdialysis may reflect the differential sensitivity of these methods to the tonic and phasic components of DA signaling. FSCV is a technique well-suited to register rapid local changes in DA concentration, but due to the digital subtraction of the background signal, DA tone is removed and what is registered is the DA release peak. On the other hand, microdialysis is a technique that is mostly sensitive to the intermediate and/or tonic components of the DA signal. The low sampling rates and the size of the probes used make this technique insensitive towards transients and local concentration changes of DA but bias the technique towards the more spatially and temporally uniform tonic component (Wightman & Robinson. 2002).

Some have argued (Donita, Elaina, Scott, Rueben, & Wightman, 2009) that the signal measured by means of in-vivo microdialysis represents nothing more than a lagged spatiotemporal integral of the local transients recorded by means of FSCV. However, that account ignores the processes that produce the transition from the inactive to the tonic activity state of DA or that tonic and phasic release seem to play different functional roles.

Schultz (1998; 2002), as well as Niv and co-workers (2006) have argued that phasic and tonic DA signaling play different functional roles. The experiments presented in chapters 1, 2, 3, and 4, which describe the changes in tonic DA release that accompany administration of rewarding electrical brain stimulation, are germane to such proposals and to the idea that DA tone is responsible for the maintenance of intracranial self-stimulation (ICSS). Chapters 1, 2 and 3 investigate the role of predictability on DA tone using various schedules of reinforcement that differ not only in the temporal parameters of the stimulation but also in whether or not operant behaviour is required to obtain the rewarding stimulation. Chapter 4 reports the results of a direct test of whether elevated DA tone is present when the phasic signal reported in the initial FSCV studies has faded away.

The role of reward predictability had been investigated almost exclusively in Pavlovian conditioning experiments, and by measuring phasic activation. These studies show that unpredicted rewards produce phasic activation of DA neurons, whereas predicted ones did not (Schultz, 1998; Schultz et al., 1997). Therefore, the experiments presented in these chapters fill a void in our knowledge.

The Reinforcement-Mountain

As the previous sections have shown, ICSS has played a central role in linking dopaminergic neurons to reward. The results of pharmacological challenges (Bauco & Wise, 1997; Fouriezos & Francis, 1992; Maldonado-Irizarry et al., 1994) suggest that DA is important for the maintenance of ICSS.

The question of which functions are modulated by DA is matter of lively controversy. In different accounts DA determines the intensity of rewarding effect (Wise & Rompre, 1989), anticipation of reward (Blackburn, Pfaus, & Phillips, 1992), incentive salience (Berridge, 2007), attention and motor switching (Redgrave, Prescott, & Gurney, 1999a, 1999b), the proclivity of the subject to invest effort in operant performance (Salamone, Correa, Mingote, & Weber, 2005) or the vigor of responding (Niv et al., 2006). The controversy stems partly from the failure to formulate hypotheses in a formal manner and from the exclusive use of a two dimensional plane to relate the observed behaviour to the independent variable(s). Of particular interest for the present thesis are the hypotheses that assign the role of DA tone either to the modulation of reward intensity or the modulation of subjective reward costs. In principle, such a dichotomy is false; not only does performance reflect how good the reward is, but it also reflects the perceived effort required to obtain the reward.

In order to test these hypotheses a new experimental paradigm has to be used because results obtained in the now-standard curve-shift paradigm are ambiguous. Specifically, lateral shifts that have been traditionally attributed to changes in reward potency can be obtained by changes in response effort (Fouriezos, Bielajew, & Pagotto, 1990; Frank & Williams. 1985). More generally, when the curve- shift paradigm is used

indistinguishable changes in a two dimensional plane may ensue from changing either the intensity or the cost of reward, two variables that are at different neural processing stages (Arvanitogiannis & Shizgal, 2008). The inherent ambiguity of the curve shift paradigm is exemplified in the following figures.

When a rat is working in an operant box its behaviour is divided between working in the experimental task, that is holding down the lever or doing other activities that are not under the direct control of the experimenter like, grooming, resting or exploring the environment. When the rat holds down the lever, it can not engage in alternative behaviours; it forgoes the value that would have been obtained from the alternative activities, thus the time the rat has to hold down the lever in order to earn a reward is analogous to an opportunity cost, which will be called the “price” of the reward in this document. Figure 1a shows in blue the psychometric function that theoretically would be obtained after sampling different frequencies and measuring a behavioural output, such as time allocation. Shown in red is the displaced curve produced by manipulating variables that degrade the reward intensity, such as injecting a DA receptor blocker. The superimposed black dotted line is a function that could be obtained by increasing the cost of the reward. Figure 1b shows in blue the theoretical psychometric function obtained when the reward intensity is kept constant and what is modified from trial to trial is the reward cost, the price the rat has to pay in order to obtain a reward. Shown in red is the new function that would be obtained after modifying variables that affect effort cost, such as increasing the force required to depress the lever. The superimposed black dotted line on top is a function that could be obtained after decreasing the reward intensity.

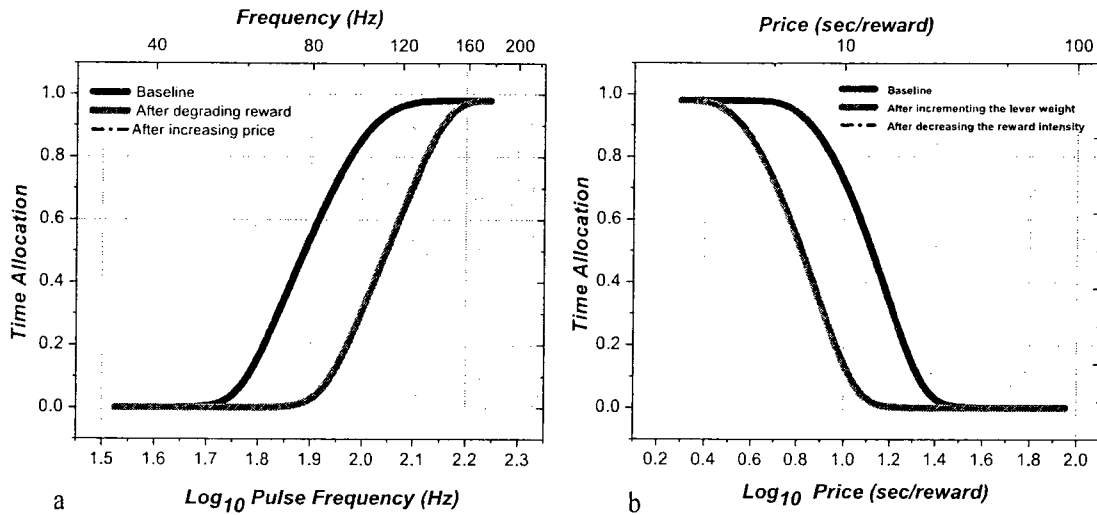


Figure 1. 2D psychometric function measuring time allocation vs. pulse frequency (a) or price (b) theoretically obtained when manipulating reward intensity or reward cost. Panel a shows in blue the time allocation-frequency curve under baseline condition and in red the obtained curve after manipulating variables that degrade the reward intensity. The black dotted line on top is the function that is obtained by increasing the cost of the reward. Panel b shows in blue the theoretical psychometric function when the reward intensity is kept across trials and the reward cost is modified. Shown in red is a the time allocation-price curve obtained after modifying variables that would directly affect reward cost. The black dotted line on top is the time allocation-price curve obtained after modifying the reward intensity. The black dotted line in both panels shows how it is possible to obtain the same psychometric function by manipulating variables that are orthogonal to those of the main independent variable. Changes in the frequency axis can be obtained by changes in cost axis and conversely changes in the cost axis can be obtained by changes in the reward intensity axis.

The black dotted line in both graphical representations shows how it is possible to obtain the same psychometric function by manipulating variables that are orthogonal to those of the main independent variable. Shifts along the frequency axis can be obtained by manipulating costs and conversely changes along the cost axis can be obtained by changing reward intensity. The inability to determine, from two-dimensional data, whether curve shifts are due to changes in the intensity or cost of the reward creates a further ambiguity about the stage of neural processing at which curve-shifting manipulation exerted its influence: variables that alter reward intensity can act at a different stage than variables that affect reward cost, but the two can produce indistinguishable effects in two-dimensional depictions (Arvanitogiannis & Shizgal, 2008; Shizgal, 2004).

When a two-dimensional perspective is adopted, changes along a third dimension that contributes to the behaviour are hidden. Adopting such a perspective can lead to erroneous ascriptions of effects to the independent variable that has been manipulated and depicted rather than to the hidden variable. Thus, the effects of a manipulation on subjective effort costs can be misconstrued as effects on subjective reward intensity and vice versa.

The reinforcement-mountain model and testing paradigm (Arvanitogiannis & Shizgal, 2008) were proposed as means to reduce the inherent ambiguity that is embedded in the traditional two dimensional perspective. When using the reinforcement-mountain testing paradigm researchers measure performance as a product of both the intensity and cost of the rewarding stimulation, two variables that are assumed to make independent contributions to performance; this produces a three dimensional structure

that clearly dissociates changes in the subjective intensity and cost of reward. The reinforcement-mountain is based on the idea that the rewarding stimulation injected by the electrode is processed in a multistage circuit (Gallistel et al., 1981) that translates the induced neural firing into behaviour (Figure 2). Each stimulation pulse triggers a volley of action potentials in the neurons close to the electrode tip. The post-synaptic effects of these firings are integrated over time and space in a manner approximating simple summation of the number of action potentials arriving at the terminals of the directly stimulated neurons within a given “time window.” If the train duration is held constant, a train of high frequency low current pulses produce the same rewarding effects as a train of low frequency delivery at a high current (Gallistel, 1978; Gallistel et al., 1981; Simmons & Gallistel, 1994). Changes in current produce changes in the effective radius of neural activation. Increasing the current will recruit more neurons, and this increase in the number of activated neurons will compensate for a reduction in the stimulation frequency.

The output of the integrator is shaped by a logistic *reward-growth* function into a signal that represents the subjective intensity of the reward (I), according to the following formula:

$$I = I_{\max} \times \frac{f^g}{f^g + f_{hm}^g} \quad (1)$$

where I_{\max} is the maximum reward intensity achievable, f represents the pulse frequency, g is the steepness at which the intensity grows as the frequency increases and f_{hm} is the frequency that produces half-maximal reward intensity (Sonnenschein,

Conover, & Shizgal, 2003). Thus, this function has parameters governing its scale (I_{\max}), slope (g), and location (f_{hm}). The reward-intensity signal rises steeply as the stimulation frequency is increased but then levels-off as the frequency continues to grow (Conover & Shizgal, 2005; Leon & Gallistel, 1992; J.M. Simmons & C.R. Gallistel, 1994; Simmons & Gallistel, 1994; Sonnenschein et al., 2003). Note that absolute reward intensity changes (the reward intensity corresponding to each frequency increases or decreases by the same proportion) will be produced by changes in the reward intensity scale parameter (I_{\max}), whereas relative reward intensity changes (the change in reward intensity is frequency dependent) will be produced by changes in the location parameter (f_{hm}).

At a latter stage, the reward intensity signal is discounted by two costs: price (P) and the perceived exertion ($1+\xi$) required to perform the lever-pressing task to yield the payoff from the stimulation (U_B). In this context P is the time the rat has to hold down the lever in order to earn a reward; as mentioned above, it is analogous to an opportunity cost. While the rat holds down the lever, it forgoes engagement in alternative behaviours, like grooming exploring or resting. Thus, when the rat holds down the lever, it forgoes the value that would have been obtained from the alternative activities. U_B is obtained by the following ratio:

$$U_B = \frac{I}{(1 + \xi) \times P} \quad (2)$$

The constant, 1, has been added to ξ in the term representing the rate of perceived exertion to avoid unrealistic scenarios that arise when small quantities are used as divisors. Note that two of the arguments of U_B , I and ξ , are subjective variables whereas

the third, P , is objective. However, Solomon et al., have shown that when price exceeds 3-4 seconds, subjective price increases at the same rate as objective price (Solomon, Conover, & Shizgal, 2007). Thus, the objective price can be used as a proxy for the subjective price when its value exceeds 3-4 seconds.

The next equation of the model is an extension of Herrnstein's single operant matching law (Herrnstein, 1970, 1974) proposed by McDowell (2005), which is used to convert the suitable transform of U_B into time allocation (TA). In this equation the TA of the organism to BSR is obtained by the ratio between the suitably transformed payoff from the stimulation (U_B) to the sum of the suitably transformed payoffs obtained from all the competing behaviours (U_E). The transformation entails raising each of the payoffs to a power representing price sensitivity (a).

$$TA = \frac{U_B^a}{U_B^a + U_E^a} \quad (3)$$

According to this equation, TA will be 0.5 when U_B and U_E are equal. Therefore, U_E can be expressed in the same terms as U_B , i.e., by dividing I_{max} by the product of the perceived exertion ($1+\xi$) and the price (P_E) at which the rat spends half of his time working for the maximal stimulation intensity.

$$U_E = \frac{I_{max}}{(1 + \xi) \times P_E} \quad (4)$$

By combining equations 1 through 4 and rearranging the terms the following equation is obtained:

$$TA = \frac{\left(\frac{f^g}{f^g + f_{hm}^g} \right)^a}{\left(\frac{f^g}{f^g + f_{hm}^g} \right)^a + \left(\frac{P}{P_E} \right)^a} \quad (5)$$

The surface produced by equation 5 is shown in Figure 3a as a mesh; this surface gives the time allocations for all the possible combinations of prices and frequencies. The different time allocation can be colour-coded, the colour-mapped surface sectioned horizontally at regular intervals, and the resulting profiles projected onto a plane to obtain a contour graph (Figure 3b). In figure 3c, the location of the reinforcement-mountain along the frequency and price axes is specified by lines superimposed on the contour graph, that represent the f_{hm} and P_E parameters.

The values of f_{hm} and P_E reflect different stages of the model. The components prior to the output of the integrator determine f_{hm} and components subsequent to the output of the integrator determine P_E . Thus, the reinforcement-mountain makes it possible to differentiate between variables that determine the pulse frequency required to drive reward intensity to a given proportion of its maximum value and variables such as subjective effort costs, the absolute reward intensity and the value of uncontrolled sources of reward. More importantly, the effect of these two classes of variables can be isolated of the basis of the stage of the ICSS-related circuitry at which they act. Variables acting at stages prior to the output of the integrator will shift the reinforcement-mountain

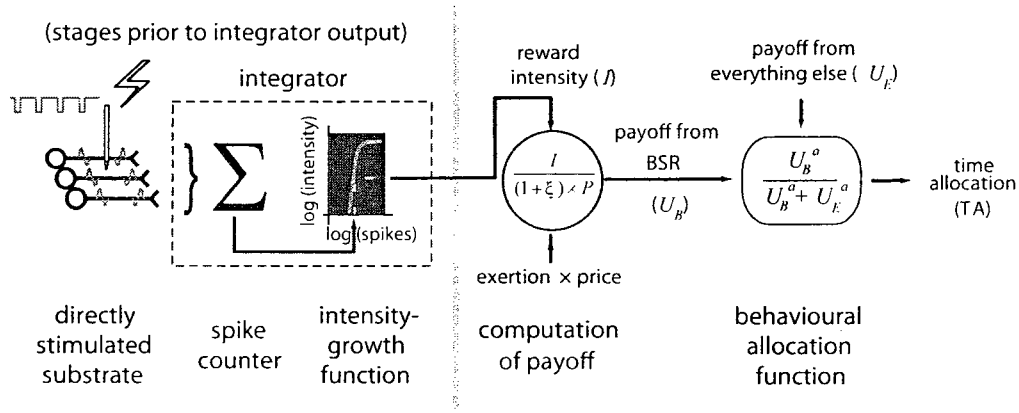


Figure 2. Translation of the stimulation-induced impulse flow into behavior. The stimulation pulses trigger a volley of action potentials in reward-related axons coursing near the tip of the electrode. The output of the directly stimulated stage is integrated, over time and space, by a later stage that functions as if to count spikes within a time window defined by the train duration. The output of the integrator is shaped by a logistic reward-growth function into a signal that represents reward intensity (I), the subjective strength of the reward. Then I gets discounted by two costs: “price” (P), which refers to the opportunity cost of the reward (the total time the rat has to hold down the lever in order to earn a reward) and “effort cost,” the perceived rate of exertion ($1+\xi$) required to perform the lever-pressing task. The comparison between the payoff from the stimulation (U_B) and the payoff from other competitive activities (U_E), like exploring, grooming and resting is described by McDowell’s (2005) extension of Herrnstein’s single operant matching law (Herrnstein, 1970, 1974) which converts the ratio between U_B and U_E into time allocation (TA) to the pursuit of BSR.

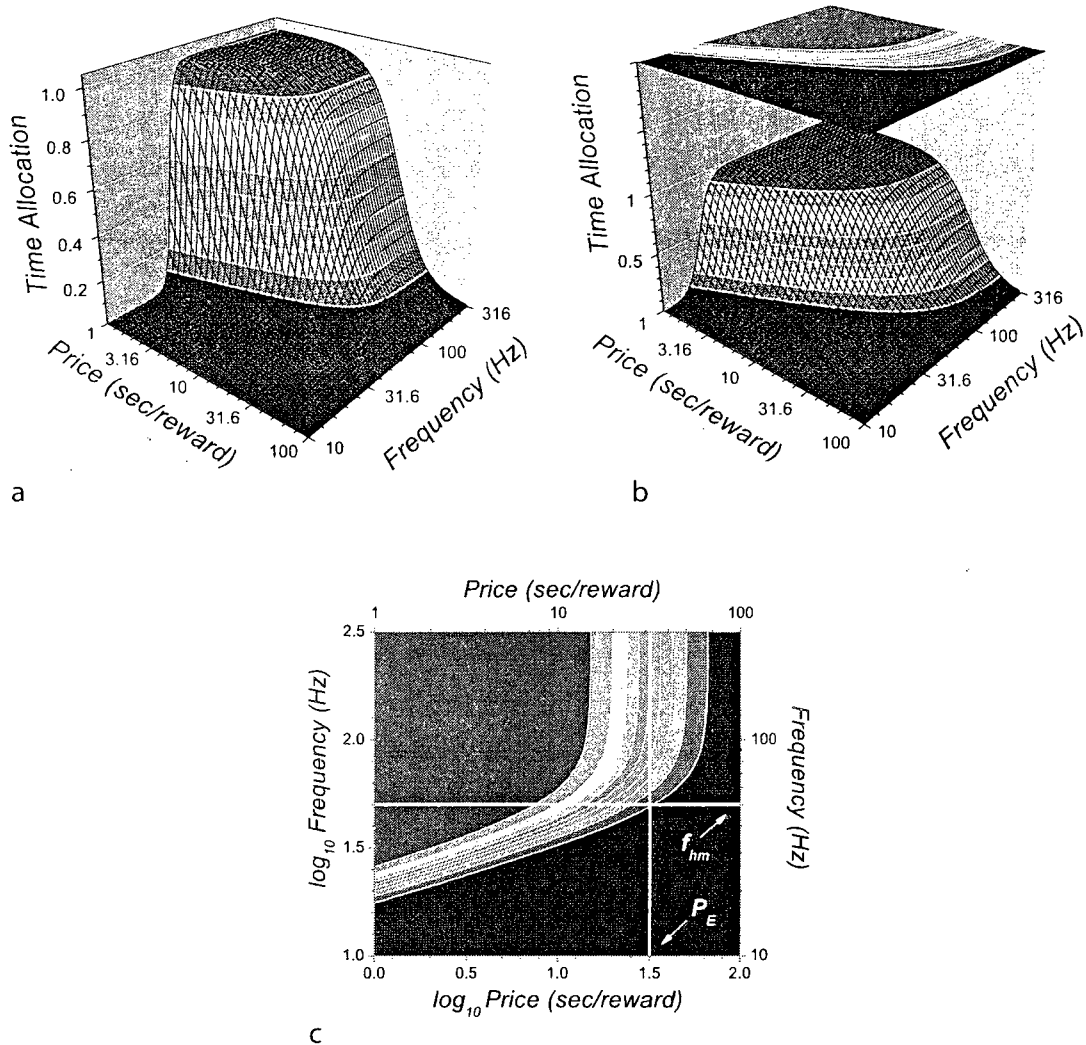


Figure 3. Reinforcement mesh obtained when discrete values of frequency and price axes are combined with the time allocation function. The mesh is the graphical representation of the reinforcement-mountain and gives the time allocations for all the possible combinations of prices and frequencies. The different time allocation can be colour-coded, the colour-mapped surface sectioned horizontally, and the resulting profiles projected onto a plane to obtain the contour graphs (panel b), the location of the reinforcement-mountain can be obtained by plotting the f_{hm} and P_E parameters onto contour graphs (panel c). (Taken from Shizgal, 2004)

along the stimulation-strength (pulse frequency) axis, whereas variables that act at stages beyond the integrator output will shift the mountain along the opportunity-cost (price) axis.

The reinforcement-mountain model and the associated 3D testing paradigm offer a unique opportunity to link DA tone to a particular stage (or stages) of neural processing. One of the most influential and longstanding hypotheses attributes the role of DA tone to the modulation of reward intensity (Wise, 1980); thus this view predicts that DA tone should shift the mountain along the frequency axis. An alternative hypothesis can be interpreted to attribute the role of DA tone to the modulation of the perceived exertion required to perform instrumental responses (Salamone, 2002; Salamone, Correa, Mingote, & Weber, 2003b; Salamone et al., 2005; Salamone, Wisniecki, Carlson, & Correa, 2001); therefore this view predicts that DA tone will produce changes along the opportunity cost axis.

In order to test the role of DA tone in brain stimulation reward, DA tone will be upregulated by blocking the DA transporter with cocaine (Roberts, 1991), Cocaine was used to relate the results obtained with our testing paradigm to the large literature the effects of this drug on ICSS. Another reason for the choice of cocaine to block the DA transporter is the absence of sensitization and tolerance in its influence on BSR (Bauco, Wang, & Wise, 1993); this makes it possible to carry out repeated tests under stable conditions. However, the relatively short half-life of cocaine, between 24 and 28 min (Carmona et al., 2005) when injected intraperitoneally (the most common route of administration in ICSS studies), poses a problem for the 3D measurement method, which requires behavioural and neurochemical stability over several hours. In order to achieve

behavioural and neurochemical stability, we developed a continuous subcutaneous administration method for cocaine that does not produce necrosis, a common problem of using this administration route for delivering cocaine. This method is described in chapter 5. Chapter 6 is devoted to the empirical test of the role of DA in brain stimulation reward.

CHAPTER 1

Prolonged Rewarding Stimulation of the Rat Medial Forebrain Bundle: Neurochemical and Behavioral Consequences

Giovanni Hernandez, Selma Hamdani, Heshmat Rajabi, Kent Conover, Jane
Stewart, Andreas Arvanitogiannis, & Peter Shizgal

Hernandez, G., Hamdani, S., Rajabi, H., Conover, K., Stewart, J.,
Arvanitogiannis, A., Shizgal, P. (2006). Prolonged rewarding stimulation of the rat
medial forebrain bundle: neurochemical and behavioral consequences. *Behavioral
Neuroscience*, 120(4), 888 - 904. Reproduced with permission

Introduction

Midbrain dopamine (DA) neurons are few in number, but via their highly divergent projections to both cortical and sub-cortical forebrain structures, they exert a profound influence on reward, attention, decision making, mood, and motor performance. The nature of the dopaminergic contribution in these domains is the subject of lively controversy. In this article, we re-evaluate the contribution of DA neurons to the powerfully rewarding effect produced by electrical stimulation of the medial forebrain bundle (MFB).

Rats and other vertebrates will work vigorously to trigger the delivery of pulse trains via depth electrodes located in many different brain sites (Olds & Milner, 1954; Olds & Olds, 1962; Shizgal & Murray, 1989; Yeomans, 1988). The effect of the induced neural activity that leads the rat to seek out and re-initiate the stimulation is called “brain stimulation reward” (BSR). This effect is particularly robust in the case of stimulation sites arrayed along the MFB. Dopaminergic neurotransmission plays an important role in the rewarding effect of MFB stimulation, as has been demonstrated by many studies that entail measurement of the psychometric function relating the vigor of operant performance, such as the rate of lever pressing, to the strength of the rewarding stimulation (e.g., the pulse frequency or current). DA receptor antagonists shift this function to the right (Franklin, 1978; Gallistel et al., 1982; Wise & Rompre, 1989). Thus, the rewarding impact of the stimulation is said to be decreased because under the influence of the antagonists, stronger stimulation is required to produce a given level of performance (Edmonds & Gallistel, 1977; Miliareisis, Malette, & Coulombe, 1986).

Blockade of the DA transporter, which increases the extracellular concentration of the neurotransmitter, acts in complementary fashion to the receptor antagonists, shifting the psychometric function to the left (Bauco & Wise, 1997). One way to explain this dependence of BSR on DA neurotransmission is to propose that the stimulation-induced neural signal that maintains lever pressing is encoded in the phasic activation of DA neurons.

The results of an experiment by Garris et al. (1999) fail to support such an explanation. Garris et al. used fast-scan cyclic voltammetry to measure phasic dopamine release in the nucleus accumbens (NAc) of rats working for rewarding MFB stimulation (Garris et al., 1999). Stimulation administered by the experimenters initially triggered phasic changes in DA concentration in all rats that subsequently learned to self-stimulate; four rats in which phasic changes in DA concentration were not observed did not show the usual stimulation-induced exploratory behavior and failed to acquire the lever-pressing task. Following acquisition of self-stimulation by the remaining subjects, DA concentrations were monitored during self-stimulation. It is surprising that phasic increases in DA concentrations were rarely observed. When present, they were short-lived and decreased rapidly as the rats continued to self-stimulate. By 30 min after the start of the self-stimulation session, the few phasic increases in DA concentration that had been noted initially were no longer detectable, but the rats continued to respond vigorously for the stimulation nonetheless. Similar results were obtained with voltammetry probes in the dorsal striatum (Kilpatrick et al., 2000). These findings are not easy to reconcile with the notion that phasic DA activity is the signal responsible for the maintenance of performance for the rewarding stimulation. They also raise a new

conundrum: If DA neurotransmission were important only in learning to self-stimulate and in initiating performance, why does the administration of a DA receptor blocker to rats that have been self-stimulating for many hours (Atalay & Wise, 1983) weaken the rewarding impact of the stimulation and undermine subsequent performance for it?

The view that signaling by DA neurons operates over multiple time scales (Schultz, 2002) offers a means of resolving the paradoxes raised by the fast-scan cyclic voltammetry data (Garris et al., 1999; Kilpatrick et al., 2000). Tonic DA release over a continuous or near-continuous (i.e., over hours) time scale plays a key enabling function in many domains, including the initiation and control of movement, cognition, motivation, and mood. In contrast, brief phasic bursts of firing over a time scale of hundreds of milliseconds have been linked to reward-prediction errors and implicated in learning (Montague et al., 2004; Schultz, Dayan, & Montague, 1997). Schultz points out that the dichotomy between tonic and phasic release is too simplistic; an intermediate time scale of minutes must be considered as well in order to capture DA dynamics associated with reproductive behavior, the procurement and consumption of food, and responses to acute stress (Schultz, 2002). Unless indicated otherwise, we lump the intermediate and continuous time scales together in the remainder of this paper under the rubric “DA tone.”

Phasic DA signaling may well play a crucial role in the acquisition of responding for BSR, as suggested by the observation that rats do not readily learn to lever press for stimulation delivered with electrodes that fail to trigger phasic DA release (Garris et al., 1999; Wightman & Robinson, 2002). However, the effectiveness of DA receptor blockers at reducing BSR long after phasic DA release has declined below the detection threshold

(Atalay & Wise, 1983) suggests that it is the tonic and/or intermediate components of signaling that are crucial to the maintenance of BSR.

The DA signal registered by means of fast-scan cyclic voltammetry is a differential one: the baseline immediately prior to the event of interest (e.g., delivery of a stimulation train) is subtracted from the signals registered during and immediately following that event (Garris et al., 1999; Kilpatrick, Rooney, Michael, & Wightman, 2000; Wightman & Robinson, 2002). Thus, changes in DA tone are removed, and only the phasic component of DA signaling is recorded. If it is the intermediate and/or tonic component of DA signaling that is responsible for the contribution of DA neurons to the maintenance of BSR, then the persistence of self-stimulation following the decay of the phasic DA signal below the detection limit is not necessarily paradoxical. Indeed, measurements of extracellular DA concentration obtained via in-vivo microdialysis, which are sensitive primarily to the intermediate and/or tonic components of the DA signal (Wightman & Robinson, 2002), show that MFB stimulation produces long-lasting increases in DA concentrations in the NAc (Fiorino, Coury, Fibiger, & Phillips, 1993; Hernandez & Hoebel, 1988; Miliareisis, Edmond, & Merali, 1991; Nakahara et al., 1989; Rada, Mark, & Hoebel, 1998; Z.-B. You, Chen, & Wise, 2001). The first experiment reported here extends such measurements of DA tone during prolonged delivery of rewarding MFB stimulation and demonstrates that the magnitude and time course of stimulation-induced changes in DA concentration depend on the temporal density of the stimulation. In a complementary behavioural experiment, we assessed the effect on BSR of prolonged rewarding stimulation of the MFB at two temporal densities that were shown to differentially alter DA tone in the microdialysis experiment.

In Pavlovian conditioning experiments carried out by Schultz's group, unpredicted rewards produced phasic activation of DA neurons whereas predicted rewards did not (Schultz, 1998; Schultz, Dayan, & Montague, 1997). The role of predictability in the control of DA tone has not been established. Thus, another purpose of this study was to compare the effects of predictable and unpredictable delivery of BSR on DA tone in the NAc.

Experiment 1

In-vivo microdialysis was employed to measure extracellular DA concentrations in the NAc during prolonged delivery of rewarding MFB stimulation. To reduce between-subject variability in reward strength, the stimulation frequency was adjusted to yield comparable self-stimulation performance across subjects in behavioral tests carried out prior to the microdialysis measurements. During microdialysis sessions, stimulation trains were delivered at two different rates in order to find out whether the temporal density of the stimulation affects the ability of the DA neurons to maintain elevated extracellular concentrations of DA. The effects of stimulation schedules in which stimulation onset was predictable or unpredictable were compared. In order to ensure precise control of the temporal distribution of the stimulation trains, preprogrammed sequences of experimenter-administered stimulation were employed.

Methods

Subjects

Twelve 300-350g male Long-Evans rats (Charles-River, St. Constant, QC, Canada) served as subjects. The animals were individually housed in hanging cages on a

12 hours light/dark reverse cycle (lights off from 08.00 to 20.00 h), with ad libitum access to water and food (Purina Rat Chow). The experimental procedures were performed in accordance with the principles outlined by the Canadian Council on Animal Care.

Surgery

Atropine sulfate (0.5 mg/kg, sc) was administered to reduce bronchial secretions prior to induction of anesthesia with sodium pentobarbital (65 mg/kg ip). Prior to mounting the rat in the stereotaxic apparatus, the topical anesthetic, xylocaine, was applied to the external auditory meatus to reduce discomfort from the ear bars. A stimulating electrode and a 20 gauge guide cannula (Plastics One, Roanoke, VA) for microdialysis were stereotaxically aimed at the left LH (-2.8 AP, 1.7 ML, and -8.8 DV from skull) and the NAS (1.5 AP, 2.8 ML, and -5.4 DV from skull at a 10 degree angle) respectively. The monopolar stainless steel electrode (0.25 mm diameter) was insulated with Formvar except for the region extending 0.5 mm from the tip. The anode consisted of two stainless steel screws fixed in the skull, around which the return wire was wrapped. The electrode and the cannula were secured with dental acrylic and skull-screw anchors. The rats were allowed to recuperate for 5 to 7 days post-surgery before the self-stimulation training began.

Self-stimulation training

Each rat was shaped to lever press for a 0.5 s train of cathodal, rectangular, constant-current pulses, 0.1 ms in duration. Shaping took place in a Plexiglas Skinner

Box (30 cm L x 21 cm W x 51 cm H) equipped with one retractable lever located on the right wall of the box, and a cue light positioned 1.5 cm above the lever. A continuous reinforcement schedule was in force. The temporal characteristics of the stimulation were set by digital pulse generators, and the amplitude was regulated by constant-current amplifiers. The stimulation currents were monitored with an oscilloscope, by reading the voltage drop across a 1-k Ω resistor (1% precision) in series with the electrode. Initially, low currents (~200 μ A) and low frequencies (~25 Hz) were employed. If sniffing and approach were observed, the rat was trained to press the lever. Otherwise, the stimulation frequency and/or current was increased gradually until either signs of interest or aversion were seen. If the rat displayed signs of aversion, training was discontinued. Once the rat pressed the lever consistently for currents between 250 – 350 μ A, a rate-frequency curve was obtained by varying the stimulation frequency across trials over a range that drove the number of rewards earned from maximal to minimal levels; the stimulation frequency was decreased from trial to trial by 0.08 log₁₀ units. The frequency used during the in-vivo microdialysis session was one log₁₀ unit greater than the lowest frequency that supported a maximal response rate, as determined from the rate-frequency curve.

In vivo microdialysis

Testing was conducted in hexagonal testing chambers (42 x 39 x 33.5 cm), with Plexiglas walls, wooden ceilings, and stainless-steel rod floors; infrared photocells and emitters were mounted in opposed walls of each box. Each testing chamber was housed in a dark wooden enclosure with a small opening at the front. All testing took place during the dark phase of the animals' circadian schedule.

The tip of the microdialysis probe consisted of a 2.5 mm length of semi-permeable dialysis membrane (Spectra/Por; 240 μm o.d., 13000 M.W. cutoff; Spectrum Laboratories, Rancho Dominguez, CA). One end of the membrane was sealed with epoxy, and the other open end was attached to a 20 mm length of 26 gauge, stainless-steel tubing. The stainless-steel tubing was connected to a 50 cm length of polyethylene (PE-20) tubing (HRS Scientific, Montreal, QC). The PE tubing was attached to the stainless steel shaft of an infusion swivel stationed above the testing chamber, which was, in turn, connected by PE tubing to a Harvard infusion pump (Harvard instruments, Holliston, MA). A small diameter fused-silica tube (Polymicro technologies, Phoenix, AZ) extended internally through the probe, and terminated 0.5 mm from the tip. The silica tubing exited the PE tubing, approximately 5 cm from the tip of the probe, and extended along the exterior of the PE tubing. The open end of the silica tubing was positioned within a removable 0.4 ml microcentrifuge tube (Fisher Scientific Canada, Ottawa, ON). All microdialysis probes were designed so that the semi-permeable membrane extended below the tip of the guide cannula when fastened in place.

Sixteen hours before the beginning of each microdialysis experiment, the rats were transported to the testing room and anesthetized lightly with isoflurane. The cannula obturators were removed and then the microdialysis probes were fixed in position and connected to the microdialysis pump. To prevent occlusion, the probes were perfused with artificial cerebrospinal fluid (ACSF; 145 mM Na^+ , 2.7 mM K^+ , 1.22 mM Ca^{2+} , 1.0 mM Mg^{2+} , 150mM Cl^- , 0.2 mM ascorbate, 2 mM Na_2HPO_4 , pH = 7.4 \pm .1) at a rate of 0.07 μl /min. The rats remained in the testing chambers overnight and were provided with ad libitum food and water. Before starting the microdialysis experiment, the food pellets

were removed from the testing cages, but the water drinking tubes were left in place. The flow rate was increased to 0.14 $\mu\text{l}/\text{min}$, and dialysate samples were collected every 20 minutes while motor activity was monitored by a computer system. Baseline sampling continued until three consecutive microdialysis samples showed $\leq 5\%$ fluctuation in DA content before beginning the electrical stimulation.

Analytical chemistry

DA was separated from other chemical species present in dialysate samples by high performance liquid chromatography (HPLC) and quantified by electrochemical detection (ED). The samples were loaded into a reverse-phase column (15 x .46 cm Spherisorb-ODS2, 5 μm ; Higgins analytical) through manual injection ports (Reodyn 7125; 20 μl loop). The separated material passed through Dual-channel ESA coulometric detectors (Coulochem 5100, with a model 5011 analytical cell), which were connected to a computer. The detectors were set to provide the reduction and oxidation currents for DA and its metabolites, 3,4-dihydroxyphenylacetic acid (DOPAC) and homovanillic acid (HVA); one channel reduced DA whereas the other channel oxidized the metabolites. The equipment was calibrated with standard samples of solutions containing known concentrations of DA and metabolites. The mobile phase (20% acetonitrile 40 mg, 0.076 M SDS, 0.1 M EDTA, 0.058 M NaPO_4 , 0.27 M citric acid, pH = 3.35) was circulated at a flow rate of 1.0 ml/min by Waters 515 HPLC pumps. An EZChrom Chromatography Data System (Scientific products & equipment) was used to analyze and integrate the data obtained for DA, DOPAC, and HVA. Two HPLC-ED systems were used in parallel, and the dialysate samples from each rat were always analyzed using the same system.

Stimulation protocol

Following the collection of baseline samples, the rewarding stimulation trains were delivered according to a 12-s variable-time schedule (VT12), a 12-s fixed-time schedule (FT12), or a 1.5-s variable-time schedule (VT1.5). In order to prevent the stimulation trains from overlapping in time or occurring at very short temporal offsets, the intervals composing the variable-time schedules were drawn from lagged exponential distributions. For the VT12 condition, a fixed lag of 1 s was added to each interval drawn from an exponential distribution with a mean of 11 s; in the case of the VT1.5 schedule, both the fixed lag and the mean of the exponential distribution were 0.75 s. The order of the schedules was randomly assigned and counterbalanced. The duration of the stimulation was 120 minutes. The rewarding brain stimulation was delivered by a Master-8 pulse generator (A.M.P.I., Jerusalem, Israel), and a constant-current amplifier (Mundl, 1980). The pulse generator was controlled by LabVIEW software (National Instruments, Austin, TX) installed on an IBM laptop computer. Microdialysis sampling continued for at least two hours following the termination of the electrical stimulation.

Histology

After the completion of the microdialysis experiment, a lethal dose of sodium pentobarbital was administered. With the stimulating electrode serving as the anode, a direct current of 1mA was delivered for 15 sec to deposit iron particles at the site of the electrode tip. The animals were then perfused intracardially with 0.9% sodium chloride, followed by a formalin-Prussian Blue solution (10% formalin, 3% potassium ferricyanide, 3% potassium ferrocyanide, and 0.5% trichloroacetic acid) that forms a blue reaction product with the iron particles. The animals were then decapitated and the brains

fixed with 10 % formalin solution for at least 7 days. Coronal sections of 30 μm thickness were cut with a cryostat. The probe and electrode locations were examined microscopically at low magnification. The locations of the electrode tip and the cannula were determined with reference to the stereotaxic atlas of Paxinos and Watson (1998).

Statistics

The levels of the assayed substances were converted to concentrations ($\text{pg}/\mu\text{l}$). Basal values refer to those obtained before the start of the stimulation; the mean of the three samples preceding the stimulation was defined as the baseline value.

The effect of the electrical stimulation on locomotion, DA and its metabolites were analyzed using Statistica (Statsoft, Inc. Tulsa, OK) to carry out two-way analyses of variance with repeated measures over time. Comparison between the baseline levels, stimulation levels, and post-stimulation levels were carried out using Tukey's DHS for unequal sample sizes. A level of $p < 0.01$ for a two-tailed test was the criterion for statistical significance.

Results

Location of electrode tips and microdialysis probes

Figure 4 shows the location of the electrodes tips (upper panel) and microdialysis probes (lower panel); the placements for one subject are not available due to histological error. All stimulation sites lay within the lateral hypothalamus, at coronal planes corresponding to plates 24 and 25 of the Paxinos and Watson atlas (1998). The tips of all

the microdialysis probes penetrated the shell of the nucleus accumbens, at coronal planes corresponding to plates 13 and 14.

Basal DA levels

The basal amounts of DA collected per 10 μ l of dialysate were 3.4 ± 0.09 pg during delivery of stimulation under the FT12 schedule, 3.47 ± 0.06 pg under the VT12 schedule, and 3.10 ± 0.10 pg under the VT1.5 schedule. Basal levels did not vary significantly across conditions ($F_{(8,42)} = 0.065$, $p = 0.997$).

Results pertaining to the extracellular concentrations of DOPAC and HVA before and after the delivery of LH stimulation were as expected and can be found in the supplementary information available on the journal's web site.

Effect of LH stimulation under an FT12 schedule on locomotion and DA concentration

Delivery of LH stimulation on the FT12 schedule produced increases in locomotor activity and in extracellular DA levels (Figure 5a). Locomotor activity was defined as the consecutive interruption of the two photocell beams. In other words, if a given beam was interrupted two or more times consecutively, this was not counted as locomotion, but if interruption of a given beam followed interruption of the second beam, then the locomotor count was incremented. During baseline sampling, locomotor counts ranged from 1 to 22 across subjects (mean = 3). During the first 20 min of stimulation, the average locomotor count increased to 134, climbed gradually to a peak of 152, 80 min

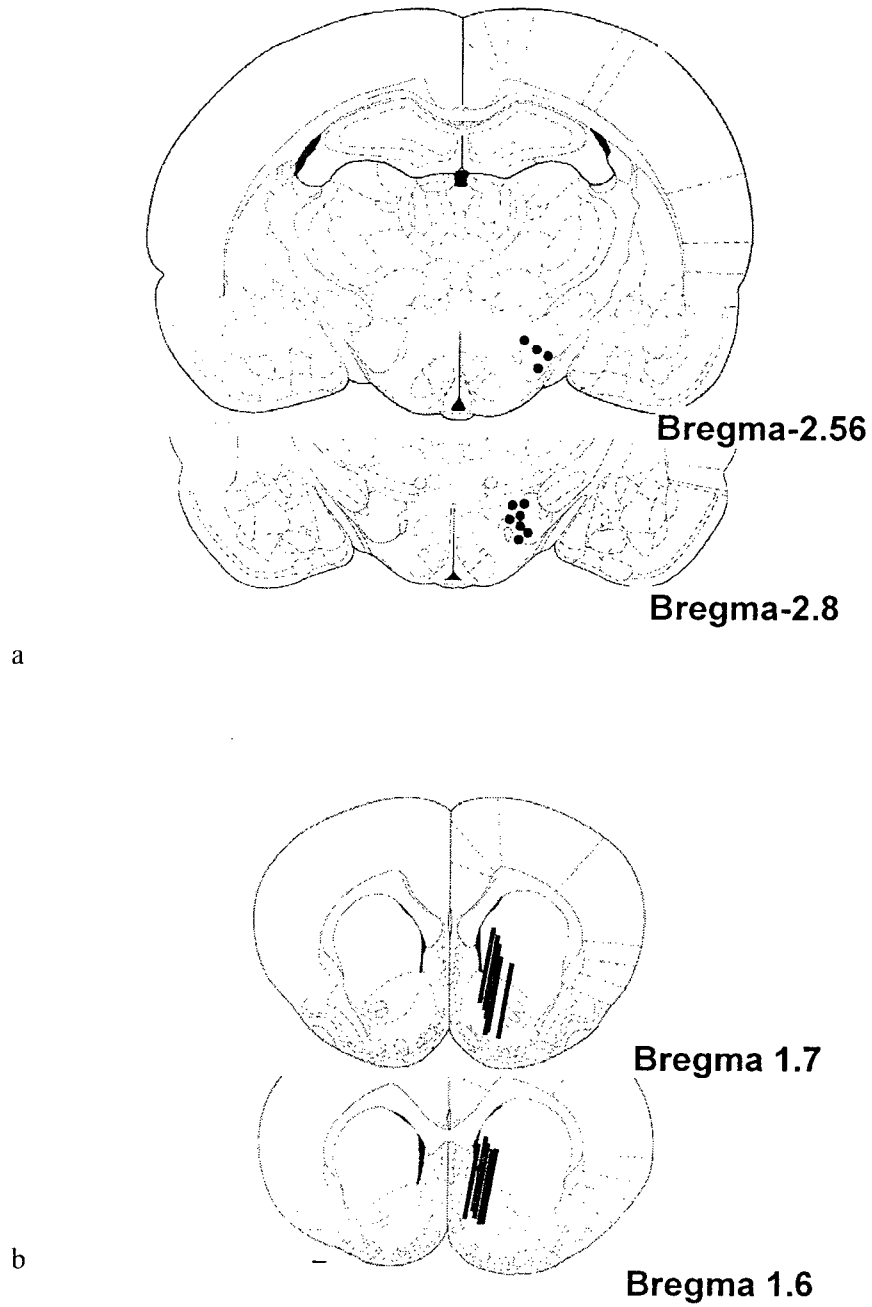


Figure 4. Location of electrode tips (a) and microdialysis probes (b). The coronal drawings are from the Paxinos and Watson atlas (1998). Results from one subject are not available due to histological error.

after stimulation onset, and then declined to 97 at the offset of the stimulation, returning rapidly to the baseline range during the post-stimulation period.

During the first 20 min of stimulation, the DA concentration in the dialysate increased to 172% of the baseline level; it remained near or above this plateau level for 80 min (peak value: 184% at 60 min) before dropping to 160% at the end of the stimulation period. The average DA concentration during the rewarding stimulation was 172% of the baseline value. During the post-stimulation period, DA concentration declined toward the baseline range.

Effect of LH stimulation under a VT12 schedule on locomotion and DA concentration

Similar effects to those observed under the FT12 schedule were found during delivery of LH stimulation under a VT12 schedule. The rewarding stimulation delivered on this schedule produced increases in locomotor activity and extracellular DA levels (Figure 5b).

Following stimulation onset, locomotor activity increased rapidly from a baseline value of 14, reaching a peak of 154 counts, 60 min after stimulation onset, and then declining to 97, at the offset of the stimulation. The average locomotor activity during the stimulation period was 126. During the post stimulation period the locomotor activity returned rapidly to the baseline range.

During the first 20 min of stimulation the DA concentration in the dialysate increased to 148% of the baseline level, peaking at 168% of baseline 60 min after the start of the stimulation. Subsequent to this peak, DA concentration decreased to 155% and remained near or above this plateau for the remaining 40 min of stimulation. The

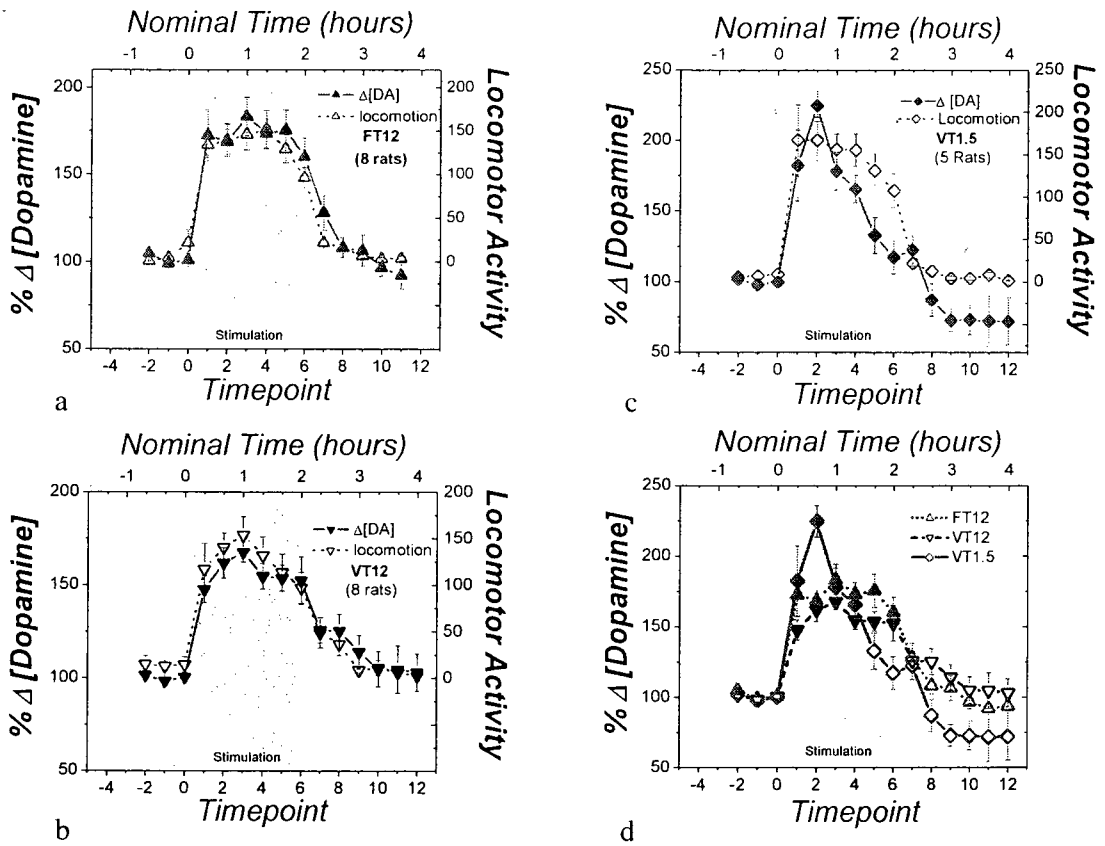


Figure 5.

Figure 5. (a) Effect of electrical stimulation of the MFB under a 12-s fixed-time (FT12) schedule on extracellular dopamine (DA) and locomotion. The onset of stimulation trains was predictable under this schedule. A sustained increase in DA concentration is seen during the 2-hour period of stimulation. Locomotor activity closely mirrors the changes in DA concentration. The “nominal time” represented on the upper abscissa was computed by multiplying the timepoint number by 20 min, the intended sampling interval. The actual sampling intervals averaged 21-22 minutes. (b) Effect of electrical stimulation of the MFB following under an VT12 schedule on extracellular DA and locomotion. The onset of stimulation trains is unpredictable under this schedule. A sustained increase in DA concentration is seen during the 2 hour period of stimulation. Locomotor activity closely mirrors the changes in DA concentration. (c) Effect of electrical stimulation of the MFB following under a VT1.5 schedule on extracellular DA and locomotion. The onset of stimulation trains is unpredictable under this schedule. A large increase in DA concentration is seen during the first 40 min but is not sustained; the DA measurements return to the baseline range before the end of the 2 hour period of stimulation and trend lower after stimulation offset. Locomotor activity lags behind the changes in DA concentration. (d). DA concentrations in dialysate obtained from the NAcc under the three stimulation schedules. Filled symbols represent significant differences from baseline, as revealed by post-hoc tests.

average increase of DA during the rewarding stimulation was 156% of baseline. During the post-stimulation period DA concentration declined toward the baseline range.

Effects of LH stimulation under a VT1.5 schedule on locomotion and DA concentration

As was case under the FT12 and VT12 schedules, the rewarding stimulation delivered during the VT1.5 schedule produced increases in locomotor activity and extracellular DA levels (Figure 5c). However, these increases tended to be larger, to peak earlier, and to be less sustained than those observed under the FT12 and VT12 schedules.

During the first 20 min of stimulation, the average locomotor counts increased quickly from the baseline average of 7, approached the peak value of 167 at 20 min after stimulation onset, and declined to 108 at the offset of the stimulation. The average locomotor count during the stimulation period was 147. During the post-stimulation period the locomotor activity rapidly returned to the baseline range.

During the first 20 min of stimulation the DA concentration in the dialysate increased to 182% of the baseline value, peaking at 225% after 40 min of stimulation onset. Subsequent to this peak, the DA concentration decreased sharply, reaching 117% of the baseline value at the offset of the stimulation. The average increase in DA during the rewarding stimulation was 167% of the baseline value. During the post-stimulation, period DA concentration dropped below the baseline, leveling off around 72%.

Statistical comparison of locomotion and DA levels across schedules

Stimulation of the LH produced a significant increase in locomotor activity under all three schedules studied. Analysis of variance showed a significant main effect for time

of the sample, $F_{(14,252)} = 78.26, p < 0.01$; but not for the schedule under which the stimulation was delivered, $F_{(2,18)} = 0.13, p = 0.87$ nor for the interaction between schedule and time of the sample, $F_{(28,252)} = 0.70, p = 0.86$. The peak increase under the VT1.5 schedule was slightly greater than those observed under the other two schedules, but this difference did not meet the criterion for statistical reliability in a Tukey HSD post-hoc comparison.

The DA concentration in the dialysate increased, under all three schedules studied, during the delivery of stimulation into the LH (Figure 5d). However, the time course of the stimulation-induced changes under the VT1.5 schedule differed from those observed under the two other schedules. Analysis of variance showed a significant main effect for time of the sample, $F_{(14,252)} = 71.59, p < 0.01$; but not for the schedule under which the stimulation was delivered, $F_{(2,18)} = 0.865, p = 0.4$. However, there was a significant interaction between schedule and time of the sample, $F_{(28,252)} = 4.221, p < 0.01$. The rewarding stimulation delivered under the FT12 and VT12 schedules produced significant increases in DA concentration, which remained stable during the two hours of stimulation. The increase during the FT12 was slightly greater than during the VT12 condition, but this difference was not significant. Thus, the VT1.5 schedule was the principal source of the significant interaction. At 40 min following stimulation onset, the DA concentration registered in the VT1.5 condition was significantly higher than the concentrations registered in the FT12 and VT12 conditions. Whereas the DA concentration differed from baseline throughout the stimulation period under the FT12 and VT12 schedules, it was no longer distinguishable from baseline condition during the final 40 minutes of stimulation in the VT1.5 condition. After the stimulation ceased, the

DA concentration stabilized below baseline levels in the VT1.5 condition, but this difference was not statistically significant.

Discussion Experiment 1

When phasic DA release was monitored in self-stimulating rats by means of fast-scan cyclic voltammetry, stimulation-induced increases were rarely noted and were short-lived when observed (Garris et al., 1999; Kilpatrick, Rooney, Michael, & Wightman, 2000). In contrast, the microdialysis measurements obtained in the FT12 and VT12 conditions of the present experiment reveal substantial elevations in DA tone during the entire 2-hour period of stimulation; no systematic differences were observed between the effects of the predictable (FT12) and unpredictable (VT12) stimulation trains. Increasing the temporal density of the stimulation drove DA levels to a higher peak, but this increase was not sustained. These measurements confirm and extend the findings of prior studies in which in vivo microdialysis was used to monitor DA concentrations in the NAc during MFB stimulation (Fiorino, Coury, Fibiger, & Phillips, 1993; Hernandez & Hoebel, 1988; E. Miliaressis, Emond, & Merali, 1991; Nakahara, Ozaki, Miura, Miura, & Nagatsu, 1989; Rada, Mark, & Hoebel, 1998; You, Chen, & Wise, 2001).

Locomotor activity. In the FT12 and VT12 conditions, the time courses of the locomotor scores and DA measurements were strikingly similar (Figures 5a,b). This relationship is not surprising given prior evidence tying exploratory locomotor activity to DA tone in the NAc (Hooks, Colvin, Juncos, & Justice, 1992; Hooks, Jones, Smith, Neill, & Justice, 1991; Kalivas & Stewart, 1991; Kuczenski & Segal, 1989; Sharp, Zetterstrom, Ljungberg, & Ungerstedt, 1987). The very close correspondence between the locomotor and DA measurements implies that any delay between behaviorally meaningful changes

in DA tone in the NAc terminal field and the concentration of DA in the dialysate due to the sheath of damaged tissue around the microdialysis probe (Bungay, Newton-Vinson, Isele, Garris, & Justice, 2003) was insignificant at the available temporal resolution. In the VT1.5 condition (Figure 5c), elevated locomotor activity persisted after the concentration of the DA in the dialysate began to fall, a result opposite to what would be expected if there were a delay between behaviorally meaningful changes in DA concentration in the NAc terminal field and in the dialysate. The observed offset between the DA measurements and the locomotor scores may reflect “superstitious” behavior (Skinner, 1948) due to the frequent coincidence of locomotion and delivery of rewarding stimulation trains. Consistent with this view is the rapid return of the locomotor scores to the baseline range upon cessation of the stimulation, a phenomenon reminiscent of the very rapid extinction of operant responding for BSR under a continuous reinforcement schedule.

Predictability. In the case of the FT12 schedule, train onset was predictable because each train was separated from its predecessor by a fixed interval. In contrast, the inter-train intervals in the VT12 condition were exponentially distributed and hence, train onset was unpredictable. Despite this difference in predictability, the variations in DA levels over time in the FT12 and VT12 conditions are strikingly similar (Figure 5d).

One way to account for the similarity in the time courses observed in the FT12 and VT12 conditions is to propose that reward predictability on a fine temporal scale is not important in the control of tonic DA levels (but see (Zald et al., 2004)). On this view, phasic firing and tonic release have different functions. Phasic firing may play a role in learning the operant task and the timing and intensity of the reward (Garris et al., 1999;

Kilpatrick, Rooney, Michael, & Wightman, 2000; Montague, Dayan, & Sejnowski, 1996; Schultz, Dayan, & Montague, 1997; Wightman & Robinson, 2002) whereas longer-lasting changes in DA tone may play an enabling role (Schultz, 1998, 2002) in processes such as the allocation of effort to task performance (Niv et al., 2006; Salamone, 2002; Salamone, Correa, Mingote, & Weber, 2003a; Salamone, Cousins, & Snyder, 1997); motivation (Blaha & Phillips, 1996), and modulation of the circuitry that computes the intensity of incentive stimuli (Blackburn, Pfaus, & Phillips, 1992) and rewards (Conover & Shizgal, 2005). The latter processes may reflect slowly evolving internal variables, such as homeostatic imbalances, and relatively stable features of the environment rather than predictions of reward timing with sub-second precision.

Alternatively, changes in the timing of DA release might have occurred in the FT condition but over a time scale well beyond the temporal resolution of the microdialysis sampling. Could DA release have come to anticipate train onset in the FT12 condition as the rats learned the inter-train interval? If so, DA release would have followed a scalloped pattern similar to that described by response rates of subjects working on fixed-interval schedules of reinforcement. If some of the DA released prior to each train escaped reuptake, diffused away from the synaptic space, and penetrated the sheath of damaged tissue surrounding the microdialysis probe (Bungay, Newton-Vinson, Isele, Garris, & Justice, 2003), then the concentration of DA in the dialysate would have risen. Due to the 20-min sampling time and the large size of the probe, the microdialysis measurements lack the temporal and spatial resolution to register the local scalloped pattern of DA release in the synaptic space and would reflect instead a broad moving average of the mean concentration of DA across the terminal field during the sample

period. This broad average may well be similar to that observed in response to the unpredictable trains even if the time course over a time scale of seconds is not.

The use of in-vivo voltammetry probes and rapid sampling in future experiments could reveal whether anticipatory release of DA prior to reward delivery (Blackburn et al., 1992; Richardson & Gratton, 1996) indeed emerges during learning of the inter-train interval. Such measurements would help determine whether there are fluctuations in DA levels in the NAc terminal field on a time scale of seconds that could contribute to the changes registered by the microdialysis probes. By coupling voltammetry and microdialysis measurements, it could also be determined whether such fluctuations are superimposed on much slower, plateau-like changes, such as the prolonged increase in the DA-like signal (≥ 1 hour) registered by means of chronoamperometry following stimulation of cholinergic brainstem afferents to the VTA (Forster & Blaha, 2000).

The stimulation delivered during the FT12 condition consisted of 601 trains, providing ample opportunity for learning the inter-train interval. In future experiments, substituting a fixed-interval (FI) schedule for the FT schedule used here and determining whether a scalloped pattern of responding emerges would reveal whether such learning indeed took place.

It is questionable whether any phasic DA release that did occur under the conditions of the present experiment made a major contribution to the DA measurements. The microdialysis method is preferentially sensitive to events on the intermediate and continuous time scales (Wightman & Robinson, 2002). One would expect this bias to be particularly strong at the relatively low rates of reward delivery in the FT12 and VT12 conditions of the present study. Prior work shows that robust changes in DA levels can be

observed by means of microdialysis (Fiorino, Coury, Fibiger, & Phillips, 1993; E. Miliaressis, Emond, & Merali, 1991; You, Chen, & Wise, 2001) under conditions in which phasic DA release is rare and short-lived (Garris et al., 1999; Kilpatrick, Rooney, Michael, & Wightman, 2000).

Effect of increasing temporal density. Raising the rate at which stimulation trains were delivered from 5 / min (FT12 and VT12 conditions) to 40 / min (VT1.5 condition) produced a dramatic change in the time course of DA accumulation in the dialysate: a peak was observed at the 40-min point, well above the levels achieved in the FT12 and VT12 conditions; the DA concentration fell sharply from that point onwards as the stimulation was continued, in contrast to the maintenance of elevated DA levels seen in the FT12 and VT12 conditions. The fall in DA levels during the later portion of the stimulation period may reflect progressive depression of DA release under the relentless afferent drive produced by the MFB stimulation.

Comparison with measurements obtained via fast-scan cyclic voltammetry. To compare stimulation conditions across studies, it is helpful to calculate the average temporal density (duty cycle) of the stimulation, the percentage of the fixed (FT) or average (VT) inter-train interval represented by the train duration. In the FT12 and VT12 conditions, the temporal density was 4% (0.5 sec / 12 sec). Increasing the temporal density to 33% in the VT1.5 condition (0.5 sec / 1.5 sec) yielded a more transient time course of DA release. In the fast-scan cyclic voltammetry experiment of Garris et al. (1999), temporal density was ~60% (a 0.4 sec train divided by an inter-train interval of ~0.67 sec). Had we increased the temporal density of stimulation to that level, would the two sets of results have become congruent?

In the Garris and Wightman study (1999), unpredicted stimulation trains administered by the experimenters triggered phasic DA release in all subjects that learned to self-stimulate. Nonetheless, during repeated delivery of unpredicted trains to untrained rats (playback of the sequence generated by a self-stimulating rat), the magnitude of the DA transients triggered by the stimulation decreased dramatically during the first minute; upon repetition of the playback trial 30 min later, the DA transients were greatly attenuated. In contrast, the DA concentration in the dialysate obtained in the present study climbed steeply from baseline during the first 20 min of stimulation on a VT1.5 schedule and rose further during the next 20 min (Figure 5c). A decrease in DA levels is apparent in the first microdialysis sample obtained following cessation of the stimulation in the FT12 and VT12 conditions, suggesting that any delay due to tissue damage was small in comparison to the sampling period. The discrepancy between the time courses observed by means of microdialysis and voltammetry seems very large in comparison to the difference in temporal density and likely reflects differential control of phasic and tonic DA release. A definitive answer to this question awaits future work combining modeling (Bungay, Newton-Vinson, Isele, Garris, & Justice, 2003; Peters & Michael, 1998) with simultaneous or parallel microdialysis and voltammetry measurements.

Are the observed changes in DA levels behaviorally meaningful? In the VT1.5 condition, the DA concentrations peaked at 40 min and then decayed toward baseline levels while the stimulation continued. Moreover, the DA concentration dropped below the baseline level from the second post-stimulation time-point onwards. Variability was high during this latter period, each mean is based on only 4-5 observations, and the large number of samples obtained (14) necessitated a stringent correction for multiple

comparisons. These factors may have contributed to the failure of the post-stimulation decrease in DA concentration to meet the statistical criterion in the post-hoc tests. In any case, the finding of greatest significance to the behavior of self-stimulating rats is likely the dramatic decrease in the DA concentration during the latter part of the stimulation period. If DA tone modulates the strength of the rewarding effect, then changes in self-stimulation performance should accompany the fall in DA concentration. Experiment 2 addresses the hypothesis that the inability of the stimulated circuitry to sustain elevated DA levels when driven at high temporal densities reflects a behaviorally significant change.

Experiment 2

Administration of drugs that enhance or attenuate DA neurotransmission produces concomitant changes in BSR (Wise & Rompré, 1989). The results from the VT1.5 condition of Experiment 1 show that during prolonged administration of rewarding MFB stimulation at high temporal densities, elevated DA tone is not sustained. The purpose of Experiment 2 was to determine whether the aftereffects of the prolonged stimulation alter the reward effectiveness of subsequently delivered stimulation trains. In an attempt to strengthen the degree to which the prolonged stimulation reduces DA tone, the duration of the experimenter-administered stimulation was lengthened from the 120 minutes used in Experiment 1 to 150 minutes. Performance for rewarding MFB stimulation was assessed following prolonged sessions of experimenter-administered stimulation similar to those in the FT12, VT12, and VT1.5 conditions.

Methods

Subjects

Eight 300-350g experimentally naïve male Long-Evans rats (Charles-River, St. Constant, QC, Canada) were used. The rats were housed and the experimental procedures were performed as in Experiment 1.

Surgery

The surgery procedures were the same as those in Experiment 1, except that stimulation electrodes were aimed bilaterally at the LH level of the MFB.

Self-stimulation training

The self-stimulation training was done as in Experiment 1, but self-stimulation of both sites was assessed, and the electrode that supported the most vigorous lever-pressing in the absence of motoric side-effects was chosen for further testing.

BSR modulation experiment

During each session, two curves were obtained relating the stimulation frequency to the time spent by the rat holding down the lever. The data composing each curve were collected by varying (“sweeping”) the stimulation frequency across a set of 10 trials over a range that drove the number of rewards earned from maximal to minimal levels. The frequency used on the first and second trials of each sweep was the same; the first trial was defined as a warm-up trial, and the data were not included in the analyses. The duration of each trial was set to 25 sec and the inter-trial interval to 10 sec. After each trial, the stimulation frequency was decreased by 0.08 \log_{10} units. The rewarding

stimulation was delivered according to a 1 sec, free-running (zero-hold), variable-interval schedule (FV11). In order to earn a reward under this schedule the rat has to be holding down the lever at the time when the programmed inter-reward interval times out (Conover & Shizgal, 2005).

After the first frequency sweep, the lever retracted, and either the highest frequency tested during the frequency sweep was delivered for 150 minutes according to a VT12 or VT1.5 schedule, or no stimulation was given. At the end of this period another frequency sweep was carried out. This procedure was executed six times, on separate days, during the dark phase of the light/dark cycle.

Histology

The histological procedures were the same as those in Experiment 1.

Curve fitting and statistics

Curve-fitting and normalization procedures were employed to quantify the position of the time allocation versus frequency curves along the frequency axis, to average these curves in a meaningful manner, and to plot them in standardized spaces (Figure 6). Changes in a parameter representing the position of the curves along the frequency axis were tested statistically to determine whether the experimenter-administered stimulation produced reliable displacement of the curves.

The analysis proceeded along two branches. The first was aimed at estimation of a position parameter and at statistical assessment of stimulation-induced changes in this measure. This branch of the analysis yielded a quantitative description of the data from each frequency sweep obtained from every subject and condition. The second branch

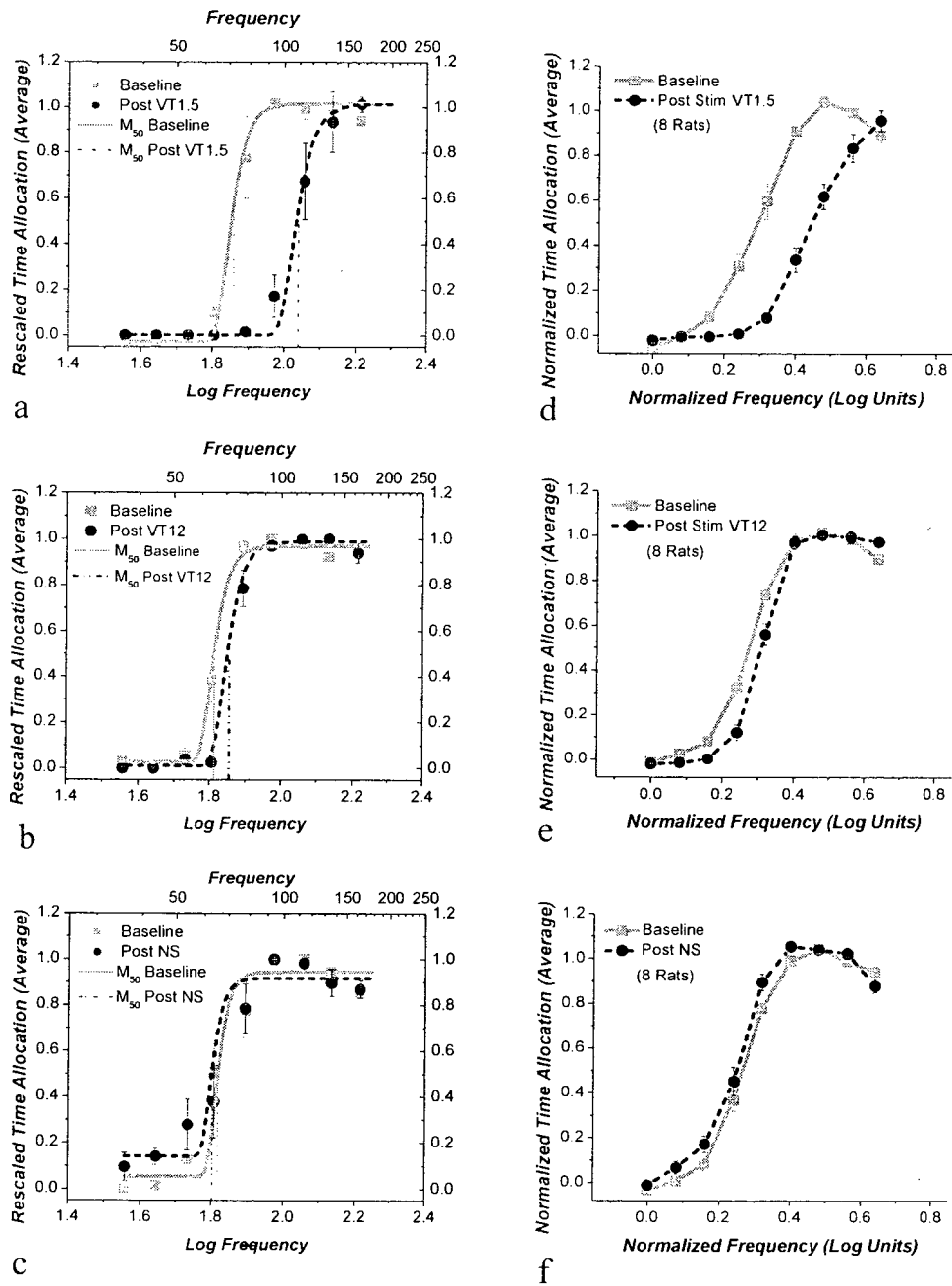


Figure 6.

Figure 6. The left column shows time-allocation data obtained in a single, randomly selected subject (rat SL5). The data shown in black were obtained following 2.5 hr of stimulation under the VT1.5 schedule (a), 2.5 hr of stimulation under the VT12 schedule (b), and 2.5 hr of rest (c). The solid gray and dashed black lines represent the logistic functions fitted to the baseline and poststimulation data, respectively. The positions of the fine vertical lines along the abscissa denote the M50 values for each curve, whereas the intersections of these lines with the fitted functions denote the midpoints between the fitted parameters representing maximal (T_{Amax}) and minimal (T_{Amin}) time allocation. The right column shows average time allocation as a function of stimulation frequency for the entire group of 8 rats. The common logarithm of the lowest frequency tested in the baseline sweep was defined as 0 for the abscissa, and all other frequencies were expressed as displacements from this value along the logarithmic scale. The data denoted by the black symbols and dashed lines were obtained following 2.5 hr of stimulation under the VT1.5 schedule (d), 2.5 hr of stimulation under the VT12 schedule (e), and 2.5 hr of rest (f). Gray symbols and solid lines represent the baseline values.

entailed normalization of the time allocation versus frequency curves along both axes and averaging of the normalized curves. The purpose of this branch was to provide a graphical representation of the effects of the different stimulation schedules.

The following logistic equation was fit to the data from each frequency sweep for each subject:

$$TA = TA_{\min} + \frac{TA_{\max} - TA_{\min}}{(1 + S \times \exp\{-G \times [\log(F) - P]\})^s} \quad (6)$$

where F is the stimulation frequency, G is the growth parameter determining the steepness of the logistic, P is the position parameter denoting the common logarithm of the frequency at which the slope of the curve is maximal. S is the shape parameter determining the asymmetry of the curve, TA is the time allocation, TAm_{ax} is the upper asymptote of the curve, and TAm_{in} is the lower asymptote of the curve. The curve fitting was performed by a non-linear least-squares routine from the MATLAB (The Mathworks, Natick, MA) optimization toolbox. For each set of six curves for a given rat, schedule, and sweep, single best-fitting values of the G, S, TAm_{ax} and TAm_{in} parameters were obtained, whereas best-fitting values of the P (position) parameter were obtained for each individual time allocation versus frequency curve. In this way, any horizontal drift or jitter in the position of the curves along the frequency axis was prevented from artifactually reducing the slope estimate, and the variance of the P parameter could be estimated. Finally, the P parameter was transformed into an M50 value: the common logarithm of the stimulation frequency corresponding to a predicted

time allocation mid-way between T_{Amax} and T_{Amin}. (When S = 1, the curves are symmetrical around P, and P = M50).

Before the M50 values were analyzed statistically, they underwent two transformations. First, the baseline M50 values were normalized across subjects. A vector, $m(R,S,C)$, of M50 estimates for each test session was obtained for each level of subject (R), schedule (S; VT1.5, VT12 or no stimulation) and curve (C; first or second frequency sweep). A global baseline mean for each subject, $m(R,S,1)$, was obtained by pooling the M50 estimates for the first curve (C = 1) across schedules and sessions (1 to 6). This global baseline mean was subtracted from the M50 values for each subject, condition and sweep, $m(R,S,C)$, to produce vectors of normalized data, $m'(R,S,C)$.

$$m'(R,S,C) = m(R,S,C) - m(R,S,1) \quad (7)$$

As a result of the normalization, the average of the baseline M50 values for all subjects was set to zero; the variances and condition effects were not altered by the normalization.

A two-way analysis of variance (schedule by curve) was performed on these transformed M50 values to assess the effect of the stimulation under the VT12 schedule, the stimulation under the VT1.5 schedule, or the period of no stimulation. Comparisons between M50 values were carried out using Tukey's honestly significant difference (HSD) test, with $p < 0.01$ for a two-tailed test chosen as the criterion for statistical significance.

The second branch of the analysis entailed normalization of the data to remove individual differences in maximal and minimal time allocation (the T_{Amin} and T_{Amax} values of the fitted logistics illustrated in Figures 6a-c) and in the position of the baseline curves. Thus, the time-allocation versus frequency curves were rescaled so that T_{Amin} was set equal to zero and T_{Amax} to one. This transformation is described by Equation 8. A vector of rescaled time allocation values, $d(R,S,C)$, for each level of subject (R), schedule (S) and curve (C), was obtained by subtracting the value of the lower asymptote (T_{Amin}) for each vector, $L(R,S,C)$, and dividing the result by the difference between the higher and lower asymptotes, $(H(R,S,C) - L(R,S,C))$.

$$d'(R,S,C) = (d(R,S,C) - L(R,S,C)) / (H(R,S,C) - L(R,S,C)) \quad (8)$$

Finally, the common logarithm of the minimum frequency value tested in each sweep was subtracted from the common logarithms of all the tested frequencies. Thus, the normalized minimum frequency for all subjects was set to zero, and all other frequencies were expressed as deviations from this value. Given that logarithmic steps separating the tested frequencies were the same size for each rat, this normalization aligns the data points along the transformed abscissa.

Results

Location of electrode tips

The histological reconstruction of electrode-tip and microdialysis-probe locations is shown in Figure 7. All of the electrode tips were located within the lateral

hypothalamus, in the coronal planes corresponding to plates 24 and 25 of the Paxinos and Watson atlas (1988).

Effect of the stimulation schedule on the M50 values

For illustrative purposes, Figures 6a-c show time allocation versus frequency curves for a randomly selected individual subject (SL5). The mean time allocations for each frequency are shown along with the corresponding standard errors and the best-fitting logistic functions (Equation 6). The positions of the fine vertical lines along the abscissa denote the M50 values for each curve whereas the intersection of these lines with the fitted functions denote the mid-points between T_{Am} and T_{Amin}. Figures 4d-f show the corresponding group data. The symbols depict average rescaled time allocations for all 8 rats and corresponding standard errors.

Figures 6a and 6d show that 150 min of stimulation under a VT1.5 schedule produces a substantial rightward displacement of the time allocation versus frequency curves. Only a small rightward displacement is seen following 150 min of stimulation under the VT12 schedule and the curve obtained following 150 min after the no stimulation period is very close to the baseline curve.

The analysis of variance carried on the M50 values yielded significant main effects of schedule, $F_{(2,270)} = 103.55, p < 0.01$ and curve $F_{(1,270)} = 68.69, p < 0.01$, as well as a significant interaction, $F_{(2,270)} = 64.54, p < 0.01$. The source of the interaction is evident from inspection of Figure 4 and was confirmed by the post-hoc comparisons: the position of the post-stimulation curve depended on whether it was preceded by stimulation on a VT1.5 schedule, stimulation on a VT12 schedule, or no stimulation. The

post-stimulation curve was displaced from its corresponding baseline curve by $0.18 \log_{10}$ units in the VT1.5 condition, $0.04 \log_{10}$ units in the VT12 condition, and $-0.03 \log_{10}$ units in the no-stimulation condition. Post-hoc comparisons (Tukey's HSD) show that the displacement is statistically reliable only in the case of the VT1.5 condition and that the post-stimulation M50 value for that condition differs from all the others.

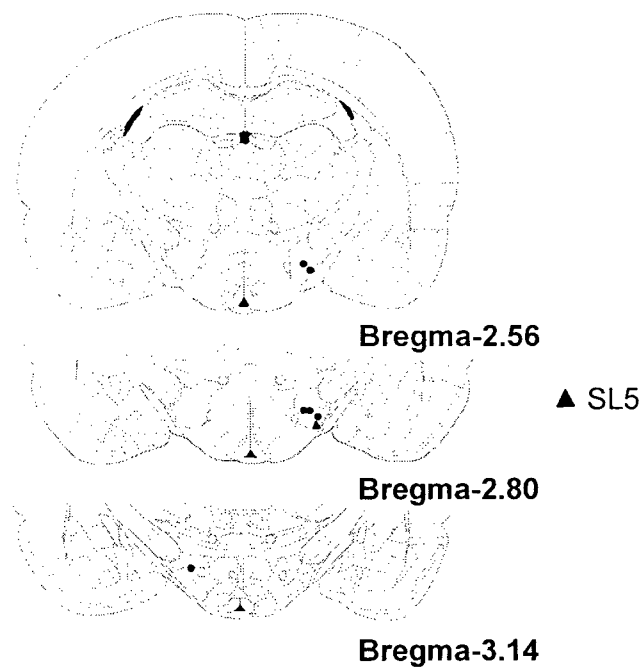


Figure 7. Location of electrode tips in subject from Experiment 2 .Images are from the *The Rat Brain in Stereotaxic Coordinates* (4th ed.), by G. Paxinos and C. Watson, Plates 24–25 (1998).

Discussion Experiment 2

The high reliability of the M-50 estimates is illustrated by the similarity of the results obtained in the baseline and test phases of the “no-stimulation” condition. The curves obtained after a 2.5-hour rest period (dashed black curves in Figures 6c and 6f) are virtually superimposable on those obtained during the baseline sweep (solid grey curves). In sharp contrast, filling the 2.5-hour period separating the two frequency sweeps with delivery of MFB stimulation on a VT1.5-sec schedule shifts the psychometric function (dashed black curve) to the right by $0.18 \log_{10}$ units in the case of the group data in Figure 6d. This shift indicates that a higher stimulation frequency was required in order to obtain a given level of performance and thus, the reward effectiveness of the stimulation was decreased. Reducing the temporal density of the stimulation by substituting a VT12 schedule for the VT1.5 schedule dramatically reduced the curve shift; the dashed black curve in Figure 6b is pulled back toward the solid grey baseline curve, and the residual curve shift falls below the statistical threshold.

In Experiment 1, the DA concentration in the dialysate peaked after 40 min of stimulation on the VT1.5 schedule and then declined during the remaining 80 min of stimulation; following stimulation offset, the DA concentration fell to less than 80% of the baseline level. The VT1.5 schedule was in force for 30 minutes longer in Experiment 2 than in Experiment 1, and the impact on the responsiveness of the DA neurons was likely even larger. It is well established that decreases in DA neurotransmission produce rightward shifts in psychometric functions linking performance for BSR to the stimulation frequency (Franklin, 1978; Gallistel, Boytim, Gomita, & Klebanoff, 1982; Wise & Rompré, 1989). Thus, the rightward curves shifts observed following delivery of

stimulation on the VT1.5 schedule could well be due to the inability of the DA neurons to maintain elevated DA tone in the NAc terminal field following such heavy, prolonged demands. In contrast, elevated DA tone was sustained in the VT12 condition throughout the two-hour stimulation period in Experiment 1. Thus, it is not surprising delivery of stimulation on this schedule failed to produce a significant curve shift in the present experiment.

The results of Experiment 2 have implications for the design of BSR experiments and the interpretation of their results. Rats will lever press steadily for 24 hours or longer when given uninterrupted access to strongly rewarding MFB stimulation (Olds, 1958). The results reported here suggest that such observations of uninterrupted performance for constant-strength stimulation trains may well have hidden significant dynamics in the neural systems underlying the rewarding effect. Note that at the highest frequency tested, time allocation following 150 min of VT1.5 stimulation was as high as during the baseline sweep (Figures 7a & 7d). Had we tested only this frequency, no effect of schedule would have been observed. However, by obtaining psychometric functions over a full range of performance, the impact of the stimulation schedule became evident.

Inherent in the curve-shift method (Edmonds & Gallistel, 1977; Miliareisis, Malette, & Coulombe, 1986) for assessing reward effectiveness is the delivery of stimulation at varying strengths and temporal densities. Due to positive feedback between reductions in stimulation strength and decreases in response rates, the rats take breaks during frequency sweeps when little or no stimulation is delivered and any trains that are received are relatively weak. Such breaks may well forestall both the apparent depression of DA release that was observed in Experiment 1 during the relentless delivery of

stimulation trains on the VT1.5 schedule and the decrease in reward effectiveness observed in the corresponding condition of the present experiment. Moreover, some investigators limit the maximum temporal density of rewarding stimulation by interposing brief blackout periods after reward delivery (Conover & Shizgal, 1994; Sonnenschein, Conover, & Shizgal, 2003) and through the use of non-continuous schedules of reinforcement (Fulton, Woodside, & Shizgal, 2000; Stellar, Hall, & Waraczynski, 1991; Waraczynski & Perkins, 1998). In the quest to obtain stable M-50 values in baseline testing, experimenters have likely found conditions that stabilize the ability of the DA neurons to sustain elevated tone during the periods when the strongest trains are delivered at high temporal density.

General Discussion

Experiment 1 demonstrates that substantial elevations in extracellular DA concentrations in the NAc terminal field can be sustained for as long as 2 hours during delivery of rewarding MFB stimulation. However, when the stimulation is delivered at very high temporal density, DA levels peaked after 40 min and fell back into the baseline range before the end of the two-hour stimulation session. Experiment 2 suggests that due to the failure of the stimulated circuitry to sustain the initially elevated DA levels, the rewarding impact of the stimulation was reduced following prolonged stimulation at high temporal density. To incorporate these new findings as well as results of prior work, we will propose a new schema for the role of DA in BSR. First, we review earlier models.

The role of DA neurons in BSR

The transducer model. Early reviews and studies addressing the role of DA neurons in BSR (Corbett & Wise, 1980; German & Bowden, 1974; Prado-Alcala, Streather, & Wise, 1984; Prado-Alcala & Wise, 1984) emphasized the apparent correspondence between the location of BSR sites and the trajectories of DA neurons. Such correspondence would be expected if the rewarding effect arose from the direct activation of DA neurons by the electrode. On this view, the DA neurons act as transducers, transforming the electrical current pulses into phasic bursts of action potentials that constitute the initial neural encoding of the reward signal. Due to their fine caliber and lack of myelination, dopaminergic fibers are poorly suited for such a role (Gallistel et al., 1981; Shizgal, Bielajew, Corbett, Skelton, & Yeomans, 1980; Shizgal & Murray, 1989). These fibers have high thresholds for activation by extracellular stimulation; their recovery from refractoriness is too slow and their conduction velocity too low to account for much of the behaviorally derived data describing the excitability properties of the directly activated neurons responsible for self-stimulation of the MFB (Anderson, Fatigati, & Rompre, 1996; Yeomans, Maidment, & Bunney, 1988). Whereas dopaminergic MFB fibers project in the caudo-rostral direction, the results of a study employing anodal hyperpolarization to block conduction in MFB reward fibers suggest that the orthodromic direction of conduction is rostro-caudal in at least some of the directly activated neurons responsible for the rewarding effect (Bielajew & Shizgal, 1986). Finally, robust BSR can be elicited along a continuous band of sites near the midline of the pontine and mesencephalic levels of the brainstem (Rompré & Miliareisis,

1985), where DA innervation is sparse or absent. Thus, there are multiple findings inconsistent with the transducer model.

The series model. The abovementioned objections to the transducer model can be circumvented by interposing a synapse between the electrode and the DA neurons, placing these cells in series with the neurons directly activated by the stimulation (Shizgal, Bielajew, Corbett, Skelton, & Yeomans, 1980; Wise, 1980). However, additional data pose problems for the series model. Miliaressis and co-workers (Miliaressis, Emond, & Merali, 1991) determined the current required to support a criterion level of performance for MFB stimulation at each of a series of pulse durations. They then used in-vivo microdialysis to measure extracellular DA concentrations in rats working for behaviorally equivalent pairs of currents and pulse durations. Systematic variations were observed in the DA concentrations measured followed stimulation with these behaviorally equivalent stimulation trains, implying that the reward signal could not have been encoded exclusively by the aspect of DA release measured in their experiment (the tonic component). The studies employing fast-scan cyclic voltammetry (Garris et al., 1999; Kilpatrick, Rooney, Michael, & Wightman, 2000) raise a complementary problem for the series model: phasic DA release was rarely observed in self-stimulating rats and when seen, the signal disappeared rapidly as the rats continued to work vigorously for the stimulation.

The temporal-difference model. Inherent in both the transducer and series models is the notion that the signal representing the reward value of the stimulation is encoded in the phasic activation of DA neurons. At first glance, this notion seems plausible given the well-established dependence of BSR on the state of DA neurotransmission(Adell &

Artigas, 2004; Franklin, 1978; Gallistel, M. Boytim, Y. Gomita, & Klebanoff, 1982; Wise & Rompre, 1989) and the ample evidence that the stimulation-induced neural signal responsible for the rewarding effect builds up and decays rapidly (Fouriez, 1995; Gallistel, 1978; Shizgal & Mathews, 1977; Sonnenschein et al., 2003). However, it is difficult indeed to see how the encoding of the rewarding effect in phasic DA activity can be reconciled with the results obtained by means of fast-scan cyclic voltammetry (Garris et al., 1999; Kilpatrick, Rooney, Michael, & Wightman, 2000). Turning off the stimulation current leads to a very rapid cessation of lever pressing in rats working for BSR on a continuous schedule of reinforcement (Gibson, 1965; Howarth & Deutsch, 1962), indicating that a stimulation-induced neural signal is essential for maintaining performance. The voltammetric results imply that this signal does not arise from the phasic activation of DA neurons.

An alternative approach casts the phasic DA activity as a learning signal rather than as a reward signal (Montague, Dayan, & Sejnowski, 1996). Although it can be recast to avoid the problems of the transducer and series models, this approach also runs into difficulties.

Montague et al. proposed that phasic DA responses act like temporal-difference errors in reinforcement-learning models (Sutton, 1988; Sutton & Barto, 1998) and that BSR is due to the simulation of such errors due to phasic DA activity driven by the electrode. The temporal-difference error represents a discrepancy between the reward predicted by a given set of stimulus conditions at a particular point in time and the reward received during the next instant. By altering the weights in neural networks, these errors serve to improve predictions of the timing and strength of future rewards while adjusting

action patterns so as to maximize the reward rate (Dayan & Balleine, 2002; Houck et al., 1995). Thus, temporal-difference errors are large when unpredicted rewards are received and shrink progressively as the prediction of reward onset is learned.

Among the attractive features of the temporal-difference error hypothesis is that it predicts the disappearance of phasic DA responses as rats learn the contingency between their lever-pressing responses and the delivery of fixed stimulation trains. Thus, this hypothesis predicts important features of the results obtained by means of fast-scan cyclic voltammetry (Garris et al., 1999; Kilpatrick, Rooney, Michael, & Wightman, 2000). However, this proposal faces at least two problems, only one of which is easily surmounted. First, the temporal-difference error signal was attributed by Montague et al. (1996) to the direct activation of DA fibers by the electrode, a proposition that is not supported by psychophysical and electrophysiological evidence (Anderson et al., 1996; Bielajew & Shizgal, 1982, 1986; Shizgal, Bielajew, Corbett, Skelton, & Yeomans, 1980; Yeomans, Maidment, & Bunney, 1986). Such direct activation also generates an unrealistic prediction: If DA fibers were directly activated and the consequent phasic release of DA signaled a temporal-difference error, then the weights in the prediction and action networks would be incremented after each and every train. Depending on the nature of the weight-changing function, the weights would thus either climb towards infinity or saturate. Such outcomes are inconsistent with voluminous data showing that graded adjustment of the strength of MFB stimulation over a substantial range produces correspondingly graded changes in reward strength (Gallistel & Leon, 1991; Miliareisis & Malette, 1987; Simmons & Gallistel, 1994). The model can be rescued from this unrealistic prediction by assuming that the electrode activates the DA neurons trans-

synaptically (as in the “series model”), a proposition that is on firmer empirical ground. If so, the temporal-difference errors could shrink systematically as the reward prediction was learned and relayed to the DA neurons in the form of precisely timed inhibitory input (Brown, Bullock, & Grossberg, 1999); reward strength would stabilize when the inhibitory input representing the prediction matched the excitatory input from the directly stimulated, non-DA fibers.

Although a modified version of the model that incorporates trans-synaptic activation of the DA neurons fits some aspects of the results from the fast-scan cyclic voltammetry studies (Garris et al., 1999; Kilpatrick, Rooney, Michael, & Wightman, 2000), it doesn't readily account for the rapid decline in the phasic DA signal observed in the rats receiving unpredictable stimulation (playback of the pattern of stimulation generated by the lever-pressing of other rats) (Daw & Touretzky, 2002). Moreover, it is not clear in such a model why administration of a DA receptor blocker should weaken BSR in a well-trained subject responding for BSR on a reinforcement schedule that delivers rewards in a predictable fashion (Atalay & Wise, 1983; Franklin, 1978; Gallistel, Boytim, Gomita, & Klebanoff, 1982; Wise & Rompré, 1989). After the weights in the prediction and action networks have stabilized, no systematic temporal-difference error should occur upon reward delivery because the input from the directly-stimulated non-DA neurons would be nulled by the input from the prediction network. Hence, there should be no phasic DA response once the contingency between the operant response and the BSR has been fully learned. If so, why would blocking the output of the DA neurons alter BSR in well-trained subjects?

Daw and Touretzky (2002) have proposed a modified temporal-difference error model that incorporates the tonic as well as the phasic activity of DA neurons. In their model, tonic DA activity falls as the predicted long-term average reward rate grows. This key feature of their model seems discrepant with the continued rise in the DA concentration during the first 40 min of stimulation in the VT1.5 condition and with the achievement of a higher DA peak in the VT1.5 condition than in the VT12 condition (but see (Niv, Daw, & Dayan, 2006)).

The convergence model. The transducer, series, and temporal-difference model all tie BSR to phasic DA signaling. An alternative approach treats the contribution of DA neurons to BSR in a manner analogous to the enabling role played by continuous DA signaling in motor function and other domains (Schultz, 1998, 2000). On this view, the reward signal responsible for the maintenance of self-stimulation performance does not pass through a DA stage. Instead, tonic input from DA neurons modulates transmission at some stage of the circuit that generates the rewarding effect. This model can accommodate the pharmacological data showing that changes in DA neurotransmission alter the strength of BSR. However, it does not account for the activation of the DA neurons by the rewarding stimulation, which is illustrated by the microdialysis data reported here and elsewhere (Fiorino, Coury, Fibiger, & Phillips, 1993; Hernandez & Hoebel, 1988; Miliaressis, Emond, & Merali, 1991; Nakahara, Ozaki, Miura, Miura, & Nagatsu, 1989; Rada, Mark, & Hoebel, 1998; You, Chen, & Wise, 2001), voltammetric measurements (Blaha & Phillips, 1990; Garris et al., 1999; Gratton, Hoffer, & Gerhardt, 1988), and electrophysiological recordings (Anderson, Fatigati, & Rompre, 1996; J.S. Yeomans, Maidment, & Bunney, 1986). (The neurochemical specificity of the

electrochemical measurements is discussed in depth by Blaha and Phillips (1996) and by Wightman and Robinson (2002).

Features of the series, temporal-difference, and convergence models capture aspects of what is known about the contribution of DA neurons to BSR and their responses to rewarding stimulation of the MFB. To circumvent the problems encountered by these models while retaining their successful features, we propose a new “feedforward” schema, which provides a useful framework for explaining the results reported here as well as those of prior experiments.

The feedforward schema. In the feedforward schema (Figure 8), the directly activated neurons are non-dopaminergic, thus accommodating the data that falsify the transducer model. The directly activated neurons project, directly or indirectly (hence the dashed line) to other non-dopaminergic neurons that perform spatio-temporal integration of the reward signal and relay it to later stages of the circuitry. At some stage in the pathway efferent to the directly activated neurons, transmission is modulated by tonic and/or intermediate-timescale changes in DA levels, either by the direct action of this neurotransmitter or via neurons (not shown in Figure 8) that relay the tonic DA input. As in the convergence model, this modulatory input is permissive: Suppression blockade, or removal of this input attenuates or shuts down transmission between the directly activated neurons and the efferent stages of the pathway whereas boosting this input increases the rewarding impact of the stimulation.

The above formulation is purposefully vague about the function of the “efferent stages of the pathway.” In most accounts of the role of DA in BSR, altering transmission in these stages changes the magnitude of BSR. Alternatively, or in addition, changes in

DA tone may alter the proclivity of the subject to invest effort in working for BSR (Niv, Daw, & Dayan, 2006; Salamone, 2002; Salamone, Correa, Mingote, & Weber, 2003; Salamone, Cousins, & Snyder, 1997), thus altering the strength of the stimulation required to support performance. Preliminary data (Conover & Shizgal, 2005) provide support for the former view, but additional work is required to resolve this issue.

A key feature of the feedforward schema the link between DA tone and activation of the directly stimulated, non-DA neurons. As in the series model, DA release is increased by MFB stimulation, but in the feedforward schema, it is the effect on the tonic component of DA signaling that is paramount in the maintenance of self-stimulation performance. Several potentially complementary mechanisms could account for the stimulation-induced increases in DA tone observed in the present study and its predecessors (Fiorino, Cury, Fibiger, & Phillips, 1993; Hernandez & Hoebel, 1988; Miliareisis, Emond, & Merali, 1991; Nakahara, Ozaki, Miura, Miura, & Nagatsu, 1989; Rada, Mark, & Hoebel, 1998; You, Chen, & Wise, 2001). Midbrain dopaminergic neurons receive both monosynaptic (Anderson, Fatigati, & Rompre, 1996; Maeda & Mogenson, 1981) and disynaptic (Yeomans, Mathur, & Tampakeras, 1993) inputs from neurons directly activated by MFB stimulation. By increasing the proportion of DA neurons in the active state and/or increasing the rate of baseline firing in the active neurons, such inputs might increase the tonic and/or intermediate-timescale release of DA in the NAc terminal field. Alternatively or in addition, inputs to DA terminals, such as glutamatergic projections from the cortex, could increase DA levels, even in the absence of a population-wide increase in impulse flow. Thus, multiple mechanisms could explain

the sustained increases in DA levels observed during MFB stimulation. Determining which ones are responsible is an important objective for future work.

Cholinergic afferents to the VTA from the laterodorsal tegmental (LDT) and/or the pedunculo-pontine (PPT) nuclei constitute particularly interesting candidates for coupling MFB stimulation to long-lasting increases in DA tone. These neurons receive descending inputs from the MFB (Yeomans, Mathur, & Tampakeras, 1993). During self-stimulation or experimenter-administered stimulation of the MFB, the concentration of acetylcholine in the VTA increases in a sustained manner (Rada, Mark, Yeomans, & Hoebel, 2000). Blockade of muscarinic receptors in the VTA abolishes or attenuates both MFB self-stimulation (Yeomans & Baptista, 1997) and the long-lasting component of the increase in DA tone following LDT stimulation (Forster & Blaha, 2000). According to the schema in Figure 9, rewarding MFB stimulation increases DA levels, in a manner reminiscent of the effects of exposure to appetizing foods or attractive sexual partners (Blackburn et al., 1992; Di Chiara et al., 2004); in turn, the increased DA tone boosts the rewarding effect. The results of Experiments 1 and 2 suggest that pushing the system too hard results in a state of “overdrive” in which the DA neurons cannot sustain the highly elevated tone produced by very frequent stimulation with intense trains; however, when the stimulation is delivered at lower temporal density, the more modest increase in DA tone that results can be sustained for hours. Such dynamics in the control of DA tone may well have implications for understanding behavioral dynamics in animals seeking and procuring natural rewards (Vorel, Campos, & Gardner, 2002). For example, the positive feedforward influence at the core of the schema in Figure 8 could serve to “lock in” commitment to a particular objective, thus increasing the likelihood that a complex

behavioral sequence is executed to completion and preventing the animal from incurring excessive travel costs between competing sites where rewards are available. An eventual decline in DA levels following achievement of very high peaks could help break the positive feedback between a powerful incentive stimulus and behavior, thus helping prevent a prepotent objective from maintaining exclusive control of behavioral output for excessive periods of time.

To flesh out the schema in Figure 8 into a fully-fledged model, quantitative dynamics will have to be specified and explored by means of simulations and the collection of additional data. Such a model must explain how the positive feedforward relationship between DA tone and BSR is ultimately offset so that both come to stabilize over time. Descending GABAergic projections onto DA somata from striatal terminal fields (Heimer, Zahm, Churchill, Kalivas, & Wohltmann, 1991) and the effect of dendritically released DA onto local autoreceptors (Adell & Artigas, 2004) are examples of long-loop and short-loop negative feedback that could participate in such stabilization. The manner in which the strength, duration and temporal density of stimulation combine to produce DA “overdrive” must be more fully described and then modeled quantitatively.

Feedforward schema

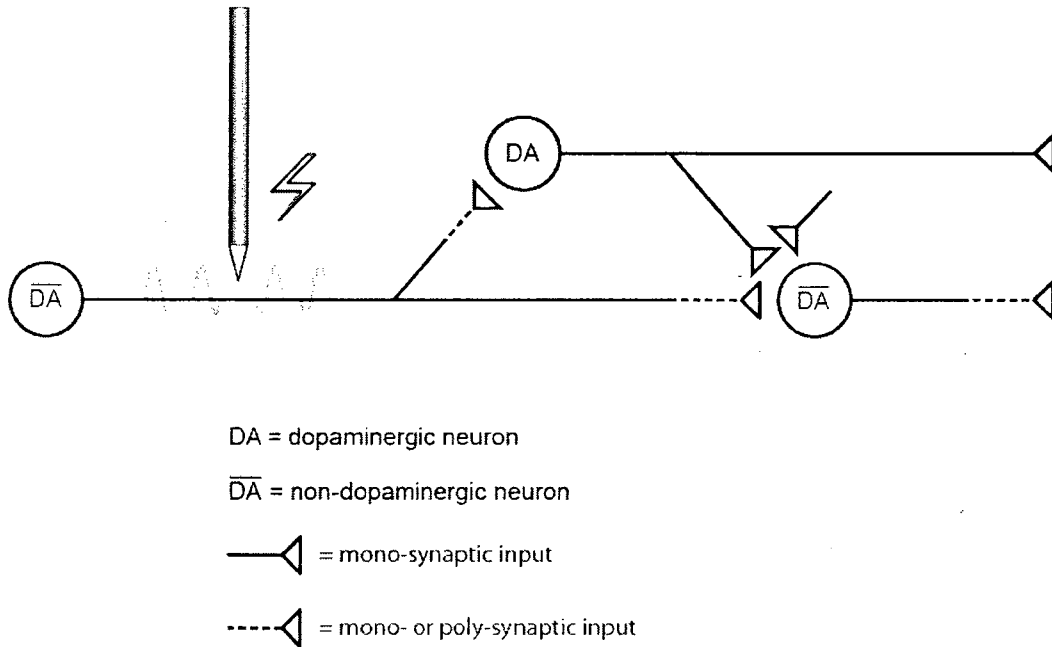


Figure 8. The feedforward schema. DA neurons are trans-synaptically activated by rewarding MFB stimulation. The directly activated neurons are non-dopaminergic. They project, directly or indirectly (hence the dashed line) to other non-dopaminergic neurons that perform spatio-temporal integration of the reward signal and relay it to later stages of the circuitry responsible for self-stimulation performance. Transmission between the directly activated neurons and their non-dopaminergic targets is modulated by DA tone. Suppression blockade, or removal of the DA input attenuates or shuts down transmission between the directly activated neurons and efferent stages of the circuitry that processes the reward signal whereas boosting DA tone enhanced transmission.

Role of phasic DA. The feedforward schema leaves the role of phasic DA activity undefined. Perhaps this aspect of DA signaling conforms to the predictions of the temporal-difference error hypothesis. If so, then phasic DA activity could be involved in learning to predict the timing and strength of BSR as well as the actions required to obtain the stimulation. On this view, phasic DA signaling would decline as learning progressed, and the tonic DA signaling embedded in the feedforward schema would be involved in the maintenance of self-stimulation performance. If so, it is the latter mechanism that would be responsible for the modulation of self-stimulation performance that has been observed in the many studies that have manipulated DA neurotransmission in well trained subjects (Wise & Rompré, 1989).

Limitations and future directions. No single method has yet been shown to provide unambiguous, simultaneous measurement of both phasic and tonic components of temporal profile of extracellular DA concentration at both the local and regional spatial scale. Due to the small size of the probes and high sampling rates employed, fast-scan cyclic voltammetry is well suited to measure local transients in DA concentration. However, due to uncontrolled drift in the state of the electrode-brain interface, a “pre-event” baseline must be subtracted from the signals of interest. Thus, the tonic component of the temporal profile is filtered out. In contrast, the large probe size and low sampling rates used in microdialysis measurements render that method relatively insensitive to transient, local changes in DA concentration, but highly sensitive to the more spatially and temporally uniform tonic component (Wightman & Robinson, 2002). In future work, it would highly informative to combine voltammetry with microdialysis

so as to provide information about DA levels on multiple temporal and spatial scales during delivery of rewarding MFB stimulation.

Pre-programmed patterns of MFB stimulation were employed in Experiment 1 in order to achieve precise control over the temporal distribution of the trains. In future work, it will be important to determine whether similar temporal profiles of DA release are observed in rats working for BSR on fixed- and variable interval schedules. Performance on the fixed-interval schedules would reveal whether the rats had indeed learned to predict the timing of reward availability.

The curve-shift method (Edmonds & Gallistel, 1977; Miliareisis, Rompre, Laviolette, Philippe, & Coulombe, 1986) for estimating changes in the reward effectiveness of electrical brain stimulation can yield strikingly stable results over time, and the remarkable persistence of self-stimulation performance (Olds, 1958) has long been emphasized in accounts of the BSR phenomenon. However, the results of Experiment 2 suggest that self-stimulation performance and DA tone interact to modulate reward strength and/or the “effort price” (Conover & Shizgal, 2005; Salamone, 2002) of the stimulation. It may be that experimenters have tuned their behavioral paradigms in such a way as to stabilize DA tone or have used measures, such as the rate of responding to strong trains, that are relatively insensitive to moderate fluctuations in the state of DA neurotransmission. The results of Experiment 2 argue that it is worth taking a new look at the waxing and waning of BSR over time and the degree to which such fluctuations are tied to tonic DA signaling. Additional positive results would merit extension of this work to prolonged performance for powerful natural rewards.

Early theories of the behavioral role of DA tended to emphasize a single function. In contemporary research, the notion that this neurotransmitter plays multiple roles in different terminal fields and on different time scales has been gaining support (Schultz, 2002). The richness of this view poses a challenge for research on BSR, demanding more nuanced models of how DA alters the rewarding effect of the stimulation and contributes to seeking out additional stimulation. Neurochemical observations obtained by means of multiple methods, coupled to behavioral measurement methods that can distinguish multiple determinants of reward value (Conover & Shizgal, 2005), will be required to meet this challenge. Given the evidence linking BSR to the evaluation and selection of natural goal objects (Conover & Shizgal, 1994; Green & Rachlin, 1991; Hoebel, 1974), such work could have broad implications for our understanding of the neural basis of goal-directed behaviour.

CHAPTER 2

Predictable and unpredictable rewards produce similar changes in dopamine tone

Giovanni Hernandez, Eric Haines, Heshmat Rajabi, Jane Stewart, Andreas
Arvanitogiannis, Peter Shizgal

Hernandez, G., Haines, E., Rajabi, H., Stewart, J., Arvanitogiannis, A., & Shizgal, P. (2007). Predictable and unpredictable rewards produce similar changes in dopamine tone. *Behavioral Neuroscience*, 121(5), 887-895. Reproduced with permission.

Introduction

Intensive study of midbrain dopamine neurons has implicated these cells in numerous psychological processes including incentive motivation, investment of effort in the pursuit of appetitive goals, attention, mood, motor performance, decision making, learning, and reward. Lively debate continues about many of these attributions. The present paper addresses a particularly influential hypothesis about dopaminergic function, the notion that reward predictability is a key determinant of dopamine release. Although there is abundant evidence that reward predictability determines the phasic responses of dopaminergic neurons to rewarding stimuli (Schultz, 1998, 2002), the results of the experiment described here support the proposal that dopamine release in the nucleus accumbens over longer time scales does not depend on the predictability of rewards. We show that similar long-lasting increases in nucleus accumbens dopamine levels are produced by self-stimulation of the medial forebrain bundle (MFB) when reward delivery is either predictable or unpredictable.

Rats and other vertebrates will work vigorously to trigger electrical stimulation of many different brain areas. The effect of the stimulation that the subject seeks is called “brain stimulation reward” (BSR). It is well established that DA neurotransmission plays a crucial role in BSR (Wise & Rompre, 1989). However, the exact nature of this role has not yet been determined. It has been argued (Schultz, 1998, 2002) that dopaminergic neurons carry multiplexed signals encoded in firing patterns that extend over different time scales. One mode of firing consists of brief “phasic” bursts lasting a few tenths of a second. These bursts are superimposed on a steady background of low-frequency “tonic” activity. Changes in activity lasting seconds to minutes (intermediate time scale) are

linked to motivationally salient events and bridge the phasic and tonic time scales. In this paper, we lump together the intermediate and tonic timescales and refer to DA signaling on these timescales as “DA tone.” In the case of BSR and other appetitive behaviors as well, phasic DA release and DA tone appear to play distinguishable roles.

Phasic bursts of firing have been linked to reward-prediction errors and implicated in learning (Montague, Dayan, & Sejnowski, 1996; Schultz, Dayan, & Montague, 1997). In contrast, it has been proposed that DA tone plays an enabling role in the initiation and control of movement (Carlsson, 2003; Hornykiewicz, 2002; Sourkes, 2000), the allocation of effort to task performance (Niv, Daw, & Dayan, 2006; Salamone, 2002; Salamone, Correa, Mingote, & Weber, 2003; Salamone, Cousins, & Snyder, 1997), motivation (Blaha & Phillips, 1996), and modulation of the circuitry that computes the intensity of incentive stimuli (Blackburn, Pfau, & Phillips, 1992) and rewards (Conover & Shizgal, 2005).

Rats do not readily learn to lever press for stimulation delivered via ventral tegmental area (VTA) electrodes that fail to trigger phasic DA release (Garris et al., 1999; Wightman & Robinson, 2002). This suggests that phasic DA signaling may play a crucial role in task acquisition (but see Robinson, Sandstrom, Denenberg, & Palmiter (2005)). Nonetheless, phasic DA release is rarely seen after rats have been trained to lever press for BSR under a continuous reinforcement schedule; when observed, phasic DA release disappears rapidly despite the fact that vigorous performance for the rewarding stimulation persists (Garris et al., 1999; Kilpatrick, Rooney, Michael, & Wightman, 2000). Thus, phasic DA release does not appear to be necessary for the maintenance of self-stimulation performance.

Recent results suggest that reward predictability may play a very different role in the control of DA tone than in the control of phasic bursting (Hernandez et al., 2006; Stefani & Moghaddam, 2006). Hernandez et al. (2006) showed that DA levels are elevated throughout prolonged periods of rewarding MFB stimulation, regardless of whether or not train onset was predictable. The rats received a two-hour, pre-programmed sequence of rewarding stimulation trains delivered at inter-train intervals that were either fixed or variable. The concentration of DA in dialysate obtained from nucleus accumbens (NAc) probes was similar during 2 h of stimulation regardless of whether train onset was predictable.

Although the rats in the study of Hernandez et al. received hundreds of stimulation trains and thus had ample opportunity to learn their temporal distribution, no behavioral measures were obtained to confirm that the rats actually did so. In the present study, fixed-interval (FI) and variable-interval (VI) schedules were substituted for the fixed-time (FT) and variable-time (VT) schedules used in the previous study of Hernandez et al. Instead of being passive recipients of the stimulation trains, the rats had to work for them. The different patterns of responding typically seen under FI and VI schedules allowed us to infer whether the rats had actually learned the different contingencies.

Under an FI schedule, the subject is rewarded for the first response emitted once an unsignalled fixed interval has elapsed. This schedule produces a characteristic scalloped response pattern. Following receipt of a reward, there is a pause in responding. After responding commences, its average rate accelerates continuously until the fixed interval elapses. The presence of this scalloped pattern indicates that the animal has

learned the timing and the predictability of reward availability. Under a VI schedule, the subject is also rewarded for the first response emitted once an unsignalled time interval has elapsed, but unlike the FI schedule, the duration of these intervals varies randomly. Thus, the animal cannot predict when the reward will next be available. Performance under this schedule is characterized primarily by stable responding, which may be interrupted by a brief post-reinforcement pause.

We wished to determine whether the profiles of dopamine release observed under the FI and VI schedules would resemble each other and those observed in the study employing FT and VT schedules (Hernandez et al., 2006). If different results were obtained using FI and VI schedules in lieu of FT and VT schedules, this would suggest that the subjects in the previous experiment failed to learn the timing of the stimulation trains. In contrast, if similar results were obtained, this would bolster the case for a differential role of reward predictability in the control of phasic and tonic dopamine signaling.

Method

Subjects

Sixteen 300-350g male Long-Evans rats (Charles-River, St. Constant, QC, Canada) served as subjects. The animals were individually housed in hanging cages on a 12 hour light/dark reverse cycle (lights off from 08.00 to 20.00 h), with ad libitum access to water and food (Purina Rat Chow). Data from eleven of the subject were retained for analysis. The reduction in the sample size was due to lack of stable baselines for the measurement of dopamine levels or histological error. The experimental procedures were

performed in accordance with the principles outlined by the Canadian Council on Animal Care.

Surgery

Atropine sulfate (0.5 mg/kg, sc) was administered to reduce bronchial secretions prior to induction of anesthesia with Ketamine -Xylazine (100 mg/kg ip). Prior to mounting the rat in the stereotaxic apparatus, the topical anesthetic, xylocaine, was applied to the external auditory meatus to reduce discomfort from the ear bars. Isoflurane was used to maintain anesthesia. A stimulating electrode and a 20 gauge guide cannula (Plastics One, Roanoke, VA) for microdialysis were stereotaxically aimed at the left LH (-2.8 AP, 1.7 ML, and -8.8 DV from skull) and the NAS (1.5 AP, 2.8 ML, and -5.4 DV from skull at a 10 degree angle) respectively. The monopolar stainless steel electrode (0.25 mm diameter) was insulated with Formvar except for the region extending 0.5 mm from the tip. The anode consisted of two stainless steel screws fixed in the skull, around which the return wire was wrapped. The electrode and the cannula were secured with dental acrylic and skull-screw anchors. At the end of the surgery the rats were injected with buprenorphine (0.05 mg/kg, sc) to reduce the pain and with sterile saline solution (1 ml/kg, sc) as post-surgery fluid therapy. The rats were allowed to recuperate for 5 to 7 days post-surgery before the self-stimulation training began.

Self-Stimulation Training

The self-stimulation training was carried out as described previously (Hernandez et al., 2006). Stimulation consisted of 0.5 s trains of cathodal, constant-current pulses, 0.1 ms in duration. Once the rat pressed the lever consistently for currents between 250 – 400

μA , a rate-frequency curve was obtained by varying the stimulation frequency across trials over a range that drove the number of rewards earned from maximal to minimal levels; the stimulation frequency was decreased from trial to trial by $0.08 \log_{10}$ units. The frequency used during the rest of the experiment was one \log_{10} unit greater than the lowest frequency that supported a maximal response rate, as determined from the rate-frequency curve. Following measurement of the rate-frequency curve, the rats were separated randomly into two groups. For one of the groups, the stimulation was delivered according to an FI schedule and for the other, according to a VI schedule. The schedules were programmed using LabVIEW software (National Instruments, Austin, TX) installed on an IBM laptop. The intervals of the VI schedule were drawn from lagged exponential distributions with a mean of 11 seconds and a fixed lag of 1 second; the lag was added to each interval in order to prevent the stimulation trains from overlapping in time or occurring at very short temporal offsets. The stimulation was delivered by a Master 8 pulse generator (A.M.P.I., Jerusalem, Israel), and a constant-current amplifier (Mundl, 1980).

The rats were trained under these two schedules until they achieved stable performance. The stability criterion was the C statistic for simplified time-series analysis (Tryon, 1982), which measures systematic deviations in the data points over time. Stability, defined as the absence of any trend in the data, usually was obtained after 15 sessions. Once the behavior was stable, the microdialysis experiment started.

In vivo microdialysis

Testing was conducted in the same boxes in which the rats were trained. All testing took place during the dark phase of the circadian cycle.

The microdialysis probes were designed so that the semi-permeable membrane extended below the tip of the guide cannula when fastened in place. A detailed description of the microdialysis probe can be found in Hernandez et al. (2006).

Sixteen hours before the beginning of each microdialysis experiment, the rats were transported to the testing room and anesthetized lightly with isoflurane. The cannula obturators were removed and then the microdialysis probes were fixed in position and connected to the microdialysis pump. To prevent occlusion, the probes were perfused with artificial cerebrospinal fluid (ACSF; 145 mM Na⁺, 2.7 mM K⁺, 1.22 mM Ca²⁺, 1.0 mM Mg²⁺, 150mM Cl⁻, 0.2 mM ascorbate, 2 mM Na₂HPO₄, pH = 7.4 ± .1) at a rate of 0.7 µl /min. The rats remained in the testing chambers overnight and were provided with food and water ad libitum. Before starting the microdialysis experiment, the food pellets were removed from the testing cages, but the water drinking tubes were left in place. The flow rate was increased to 1.2 µl/min; dialysate samples were collected every 20 minutes and immediately frozen in dry ice. The samples were stored at -80°C until the analytical chemistry was carried out.

Analytic Chemistry

DA was separated from other chemical species present in dialysate samples by high performance liquid chromatography (HPLC) and quantified by electrochemical detection (ED). The samples were loaded into a reverse-phase column (15 x .46 cm Spherisorb-ODS2, 5 µm; Higgins analytical, Mountain View, CA) through manual injection ports (Rheodyn 7125; Rheodyne LLC, Rhonert Park, CA; 20 µl loop). The separated material passed through Dual-channel ESA (Chelmsford, MA) coulometric detectors (Coulochem 5100, with a model 5011 analytical cell), which were connected to

a computer. The detectors were set to provide the reduction and oxidation currents for DA and its metabolites, 3,4-dihydroxyphenylacetic acid (DOPAC) and homovanillic acid (HVA); one channel reduced DA whereas the other channel oxidized the metabolites. The equipment was calibrated with standard samples of solutions containing known concentrations of DA and metabolites. The mobile phase (20% acetonitrile 40 mg, 0.076 M SDS, 0.1 M EDTA, 0.058 M NaPO₄, 0.27 M citric acid, pH = 3.35) was circulated at a flow rate of 1.0 ml/min by Waters 515 HPLC pumps (Lachine, Quebec, Canada). An EZChrom Chromatography Data System (Scientific Software, Inc., San Ramon, CA) was used to analyze and integrate the data obtained for DA, DOPAC, and HVA. Two HPLC-ED systems were used in parallel, and the dialysate samples from each rat were always analyzed using the same system.

Histology

After the completion of the microdialysis experiment, a lethal dose of sodium pentobarbital was administered. A 1 mA current was passed for 15 s, with the stimulating electrode serving as the anode, to deposit iron particles at the site of the electrode tip. The animals were then perfused intracardially with 0.9% sodium chloride, followed by a formalin-Prussian Blue solution (10% formalin, 3% potassium ferricyanide, 3% potassium ferrocyanide, and 0.5% trichloroacetic acid) that forms a blue reaction product with the iron particles. The animals were then decapitated and the brains fixed with 10% formalin solution for at least 7 days. Coronal sections of 30 μ m thickness were cut with a cryostat. The probe and electrode locations were examined microscopically at low magnification. The locations of the electrode tip and the cannula were determined with reference to the stereotaxic atlas of Paxinos and Watson (1998).

Statistics

The levels of the assayed substances were expressed as concentrations. Basal values were estimated as the mean of the three samples preceding the stimulation. The baseline was considered stable if the difference between the 3 samples was inferior to 10%.

The effects of the electrical stimulation on DA and its metabolites were analyzed using a two-way analysis of variance with repeated measures over time. Comparison between the baseline levels, stimulation levels, and post-stimulation levels were carried out using Tukey's DHS for unequal sample sizes. A level of $p < 0.05$ for a two-tailed test was the criterion for statistical significance. The analysis was carried out using Statistica (Statsoft, Inc., Tulsa, OK).

Results

Location of Electrode Tips and Microdialysis Probes

The location of the electrodes tips and microdialysis probes are shown in Figures 9a and 9b. All stimulation sites lay within the lateral hypothalamus, at coronal planes corresponding to plates 24 and 25 of the Paxinos and Watson atlas (1998). The tips of all the microdialysis probes penetrated the shell of the nucleus accumbens, at coronal planes corresponding to plates 13 and 14.

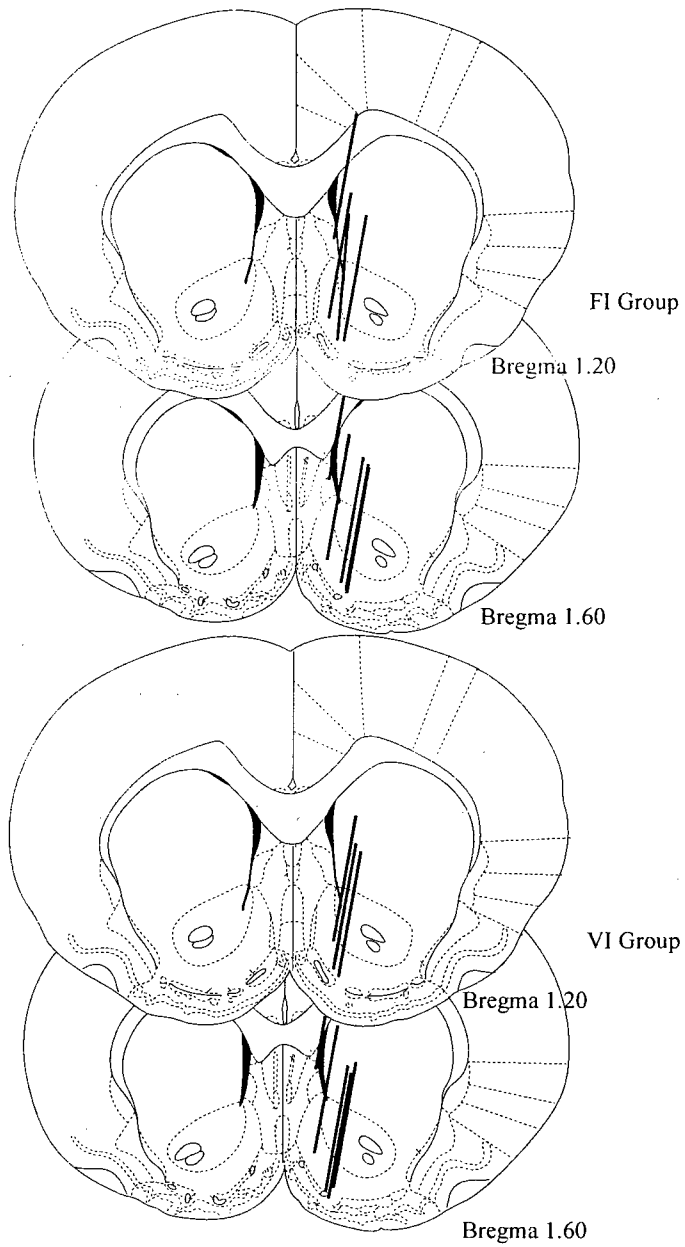


Figure 9a: Location of microdialysis probes for the FI and VI groups. The coronal drawings are from the Paxinos and Watson (1998) atlas, plates 13-14.

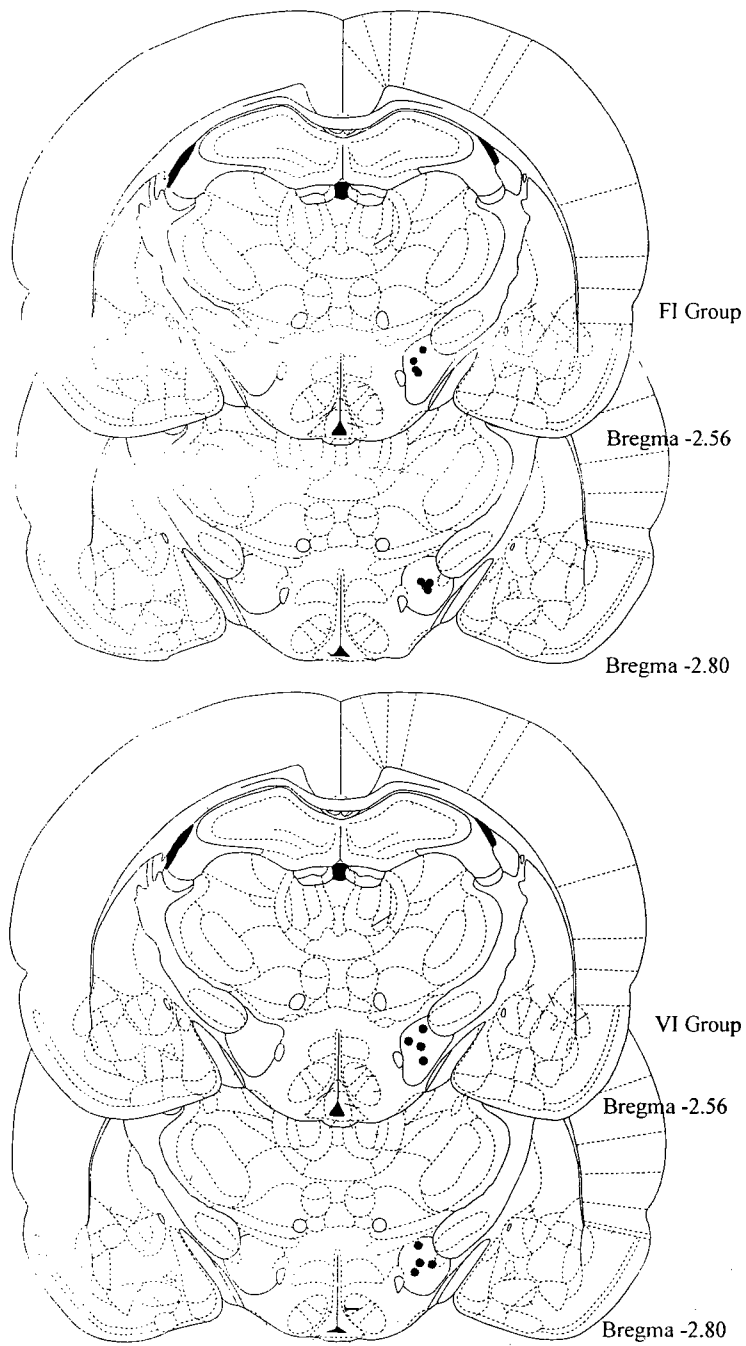


Figure 9b. Location of electrodes tips for the FI and VI groups. The coronal drawings are from the Paxinos and Watson (1998) atlas, plates 24-25.

Basal Extracellular Levels of Dopamine, DOPAC and HVA

Basal amounts of DA, DOPAC and HVA per 10 μ l of dialysate were 1 ± 0.02 pg, 1114 ± 87 pg, and 516 ± 39 pg for the FI-12 schedule, and 1.4 ± 0.16 pg, 1292 ± 47 pg, and 495 ± 43 pg, for the VI-12 schedule. Basal levels did not vary significantly across conditions. (DA $F_{(1,9)} = 2.19$, $p = 0.17$; DOPAC $F_{(1,9)} = 1.07$ $p = 0.32$; HVA $F_{(1,9)} = 0.51$, $p = 0.49$)

Time courses of Responding Under the FI and VI Schedules

The average response rates for the FI and VI group during the microdialysis session were 0.40 ± 0.15 and 0.46 ± 0.09 responses per second, respectively; this difference was not statistically significant ($t_{(9)} = 0.37$, $p = 0.71$). However, the time courses of responding by the two groups were clearly dissimilar, as predicted by prior work (Figure 10).

The FI group showed the classic scalloped pattern of responding (squares), showing that they had learned to predict the time of the reward availability. Little responding was observed during the first 3 seconds of each trial; after that point, the response rate accelerated until the end of the interval. In contrast, there was a two-second pause in responding by the VI group at the beginning of the trial, this pause can be explained by the conjoint effects of the post-reinforcement pause and the fixed lag of 1 second introduced in the time intervals. After the pause, a rapid acceleration of responding occurred during the third second and then a fairly steady response rate for the remainder of the interval. The time of reward availability is unpredictable under a VI schedule, a fact that is reflected in the absence of a well-defined peak in the average response rate of the VI group.

Changes in the Concentrations of DA, DOPAC, and HVA during LH Self-Stimulation on an FI-12 Schedule

The first three samples from one subject in the FI condition greatly exceeded the values from the other subjects, biasing the estimates of the means and standard errors. To control the influence of these outliers, they were replaced by the sum of the mean and two standard deviations (Field, 2005).

Self-stimulation of the LH under a FI-12 schedule was accompanied by an increase in the concentrations of DA, DOPAC and HVA (Figure 11). After 20 min of self-stimulation the average DA concentration in the dialysate increased to 144% of the baseline level and slowly increased across the 120 min of the stimulation period, peaking at the end of this period to 160% of the baseline level. The average DA concentration during the rewarding stimulation was $152\% \pm 2.2$ of the baseline value. During the post-stimulation period, DA concentration declined toward the baseline range.

As shown in the upper panel of Figure 11, the increase in the dialysate concentration of DOPAC during the stimulation period lagged behind the increase in the concentration of DA and rose more gradually to reach a maximum value of 169% of the baseline 80 min after the stimulation onset. The level of DOPAC started declining toward the baseline level 40 min after the stimulation offset. The average concentration of DOPAC during the rewarding stimulation was $148\% \pm 8.2$ of the baseline value.

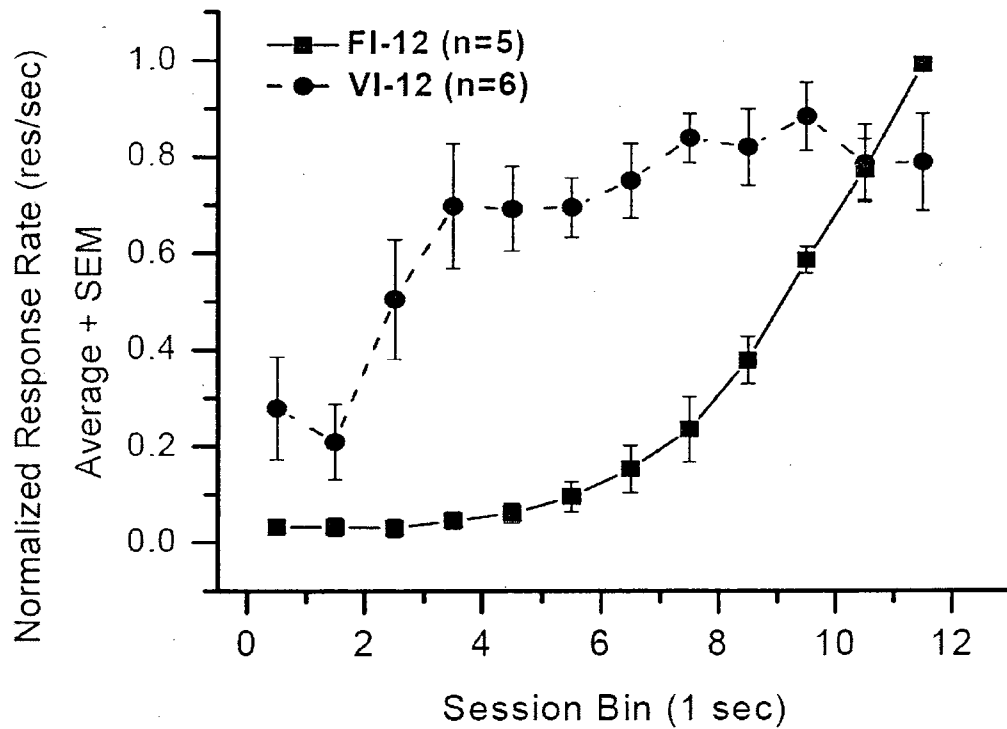


Figure 10: Mean normalized response rate (responses/s) for each group as a function of time since the last reward. These data were collected during the microdialysis session. The error bars denote ± 1 standard error of the mean.

As in the case of DOPAC, the increase in the HVA concentration during the stimulation period was delayed with respect to the rise in DA concentration and was more gradual (lower panel of Figure 11). The maximum level achieved was 158 % of the baseline value, at the end of the stimulation period. The average HVA concentration during the stimulation period was $132\% \pm 9.5$ of the baseline value. The decline in HVA concentration during the post-stimulation period was delayed with respect to the decline in DA and DOPAC concentrations.

Effect of LH Stimulation under a VI-12 Schedule on Concentrations of DA, DOPAC, and HVA

Similar effects to those observed under the FI-12 schedule were found during delivery of LH stimulation under a VI-12 schedule. The electrical stimulation delivered under this schedule produced an increase in DA, DOPAC, and HVA levels (Figure 12). Following stimulation onset, DA concentration in the dialysate increased to 137% of baseline, peaking at 160% of baseline 80 min after the onset of the stimulation. Subsequent to this peak, DA concentration decreased to 151% of the baseline value and remained near this plateau for the remaining dialysate samples. The average increase of DA during the rewarding stimulation was $151\% \pm 3.3$ of the baseline value. During the post-stimulation period, DA concentration declined steadily toward the baseline range.

As shown in the upper panel of Figure 12 the increase in the dialysate concentration of DOPAC during the stimulation period lagged behind the increase in the concentration of DA and rose more gradually, approaching a plateau 80 min after the stimulation onset. The concentration of DOPAC achieved its maximum level, 160% of the baseline value, at the end of the stimulation period and then declined toward baseline

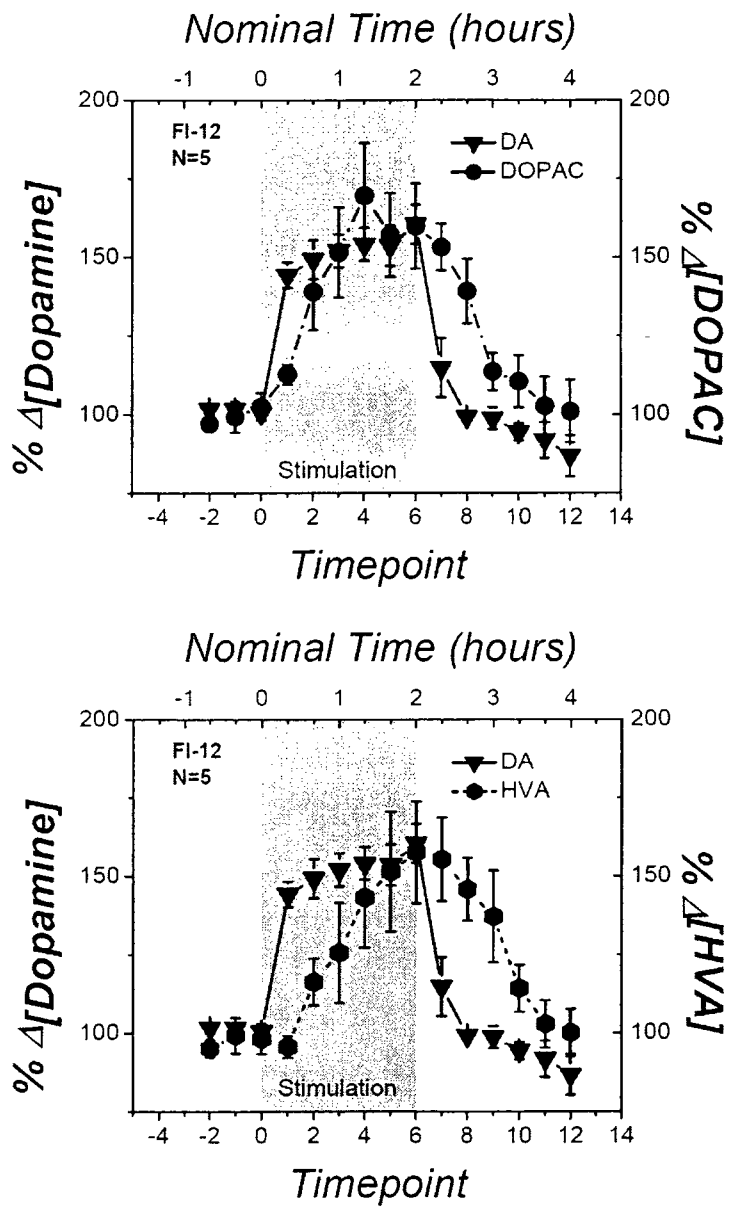


Figure 11.

Figure 11. Effect of electrical stimulation of the medial forebrain bundle (MFB) under a fixed-interval 12-s (FI-12) schedule on the concentrations of dopamine (DA) and its metabolites, dihydroxyphenylacetic acid (DOPAC) (upper panel) and homovanillic acid (HVA) (lower panel), in dialysate obtained from nucleus accumbens (NAc) probes. A sustained increase in DA concentration was seen during the 2-hour stimulation period. As expected the increase in the metabolites DOPAC and HVA lagged behind the increase in the concentration of DA. The nominal time represented on the upper abscissa was computed by multiplying the timepoint number by 10 min, the intended sampling interval. The actual sampling intervals were roughly 5% longer.

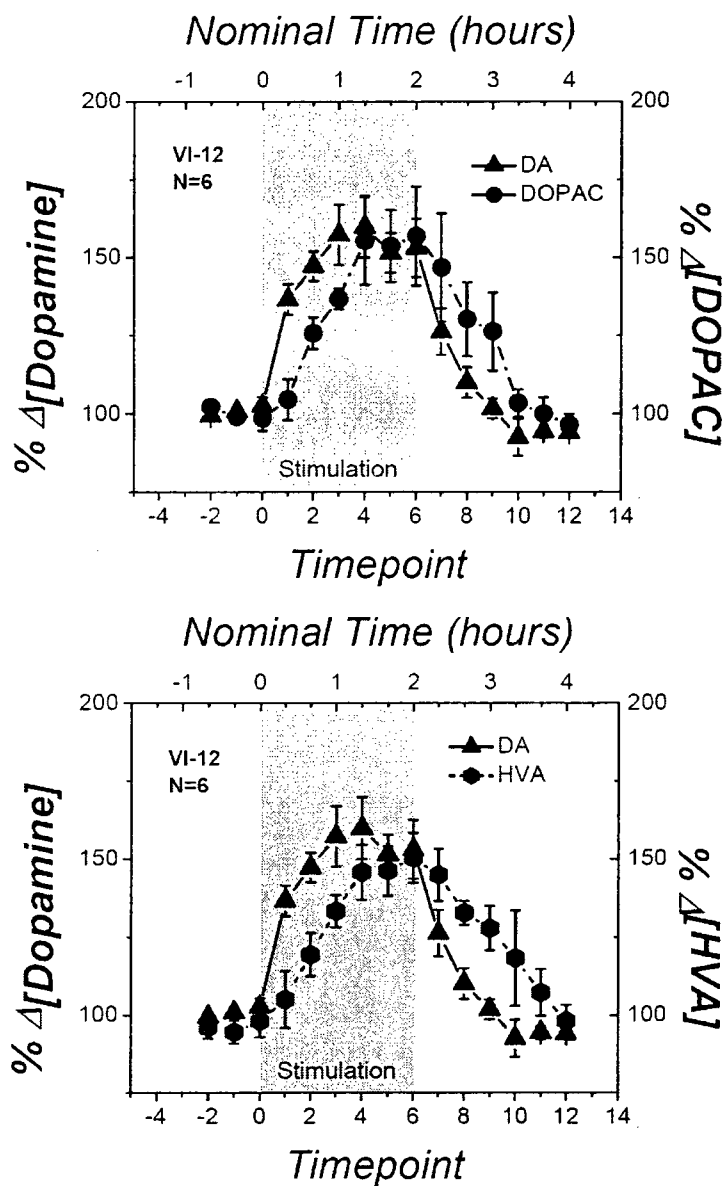


Figure 12. Effect of electrical stimulation of the medial forebrain bundle (MFB) under a variable-interval 12-s (VI-12) schedule on the concentrations of dopamine (DA) and its metabolites, dihydroxyphenylacetic acid (DOPAC) (upper panel) and homovanillic acid (HVA) (lower panel), in dialysate obtained from NAc probes. A sustained increase in DA concentration was seen during the 2-hour stimulation period. As expected the increase in the metabolites DOPAC and HVA lagged behind the increase in the concentration of DA.

levels in parallel with the decline in DA concentration. The average increase of DOPAC during the rewarding stimulation was 139 % \pm 8.5 of the baseline value.

As in the case of DOPAC, HVA concentration (lower panel of Figure 12) increased at slower pace during the stimulation period than the rise in DA. HVA increased steadily from the beginning of the stimulation, and achieved its maximum level, 150% of the baseline value, at the end of the stimulation period. The average increase in HVA concentration during the stimulation period was 133% \pm 7.3 of baseline. The decline in HVA concentration during the post-stimulation period was delayed with respect to the decline in DA concentration.

Statistical comparison of DA levels across schedules

Stimulation of the LH produced a significant increase in DA under both schedules studies (Figure 13). Analysis of variance showed a significant main effect for the time of the sample, $F_{(14,126)} = 56.71$ $p < 0.0001$, but not for the schedule that determined the reward delivery, $F_{(1,9)} = 0.20$ $p = 0.66$, or the interaction between schedule and time of the sample, $F_{(14,126)} = 0.65$ $p = 0.80$. The significant increase of DA during both schedules was stable during the two hours of the stimulation session, and it was slightly higher, but not significantly so, in the group receiving stimulation under the FI-12 schedule. Indeed, Figure 13 shows that the changes in DA concentration during self-stimulation under the FI and VI schedules are nearly superimposable.

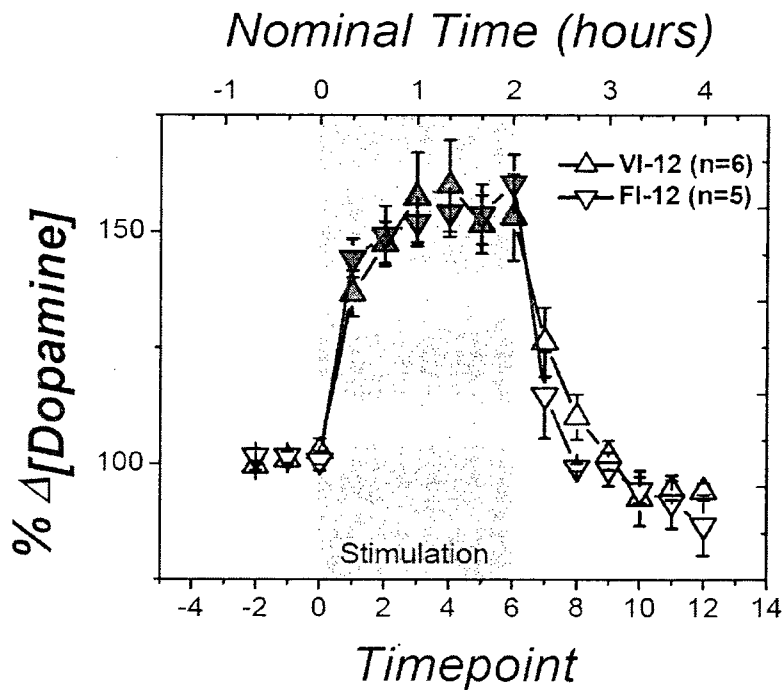


Figure 13. Dopamine concentrations in dialysate obtained from the nucleus accumbens under the two reinforcement schedules (VI-12 = variable-interval 12-s schedule; FI-12 = fixed-interval 12-s schedule). Filled symbols represent significant differences from baseline, as revealed by post hoc tests. The nominal time, represented on the upper abscissa, was computed by multiplying the time point number by 10 min, the intended sampling interval. The actual sampling intervals were roughly 5% longer.

Discussion

The main goal of the present study was to investigate how, in self-stimulating rats, predictability of reward delivery influences DA tone in the NAc. Under the FI-12 schedule, the lever was re-armed 12 s after a train of rewarding stimulation had been earned. Thus, the moment when reward would again become available was predictable. In contrast, the programmed inter-reward intervals under the VI-12 schedule were sampled from a lagged exponential distribution; consequently, the time when reward would next be available was unpredictable. As expected, the difference between the two schedules of reinforcement was manifested in the behaviour of the subjects of each group. Each group of animals showed a pattern of behaviour typical of performance under their respective reinforcement schedule (Figure 10). The subjects working under the FI-12 schedule (squares) showed the expected scalloped pattern, implying that they had learned to predict when the reward would next become available. In contrast, following a short post-reinforcement pause, the subjects in the VI-12 group, maintained a near-constant response rate (circles). The fixed, one second lag, which imposed a minimum inter-reinforcement interval, may have contributed to the post-reinforcement pause. After this lag elapsed, the time of reward availability was unpredictable. Thus, it is not surprising that once responding resumed, the subjects working under the VI-12 schedule performed at a steady rate. Despite the difference in reward predictability and the consequent contrast in the behavior of the two groups of subjects, the DA levels during self-stimulation followed strikingly similar time courses (Figure 13) in the FI-12 and VI-12 groups. Thus, reward predictability had no discernable influence over the aspect of DA signaling registered by microdialysis.

The present results extend the findings of a previous microdialysis study in which Hernandez et al. (2006) showed very similar changes in NAc DA levels in rats passively receiving rewarding MFB stimulation under FT-12 and VT-12 schedules. Given that the subjects in that experiment did not have to work in order to obtain the rewarding stimulation and thus no time-courses of operant responding could be obtained, one cannot be sure that they had indeed learned the predictability of reward delivery under the FT schedule. The results of the present study resolve this ambiguity by providing appropriate behavioral evidence that the rats had learned to predict the availability of reward under the FI-12 schedule.

Hernandez et al. (2006) proposed a modulatory role for DA tone in their feed-forward model of the circuitry responsible for BSR. In this schema, both the directly activated neurons that carry the reward signal and the neurons responsible for the spatio-temporal integration of the reward signal are non dopaminergic. However, transynaptically activated dopaminergic neurons modulate transmission within the circuitry underlying the rewarding effect. Suppression, blockade, or removal of the modulatory DA input attenuates or shuts down transmission between the directly activated neurons and efferent stages of the circuitry whereas boosting DA tone enhances transmission. Thus, the maintenance of self-stimulation performance depends on DA tone and is modulated by manipulations that produce sustained alterations in DA neurotransmission. The results of the present study are consistent with this schema. The rate and intensity of the excitatory drive on the DA neurons, rather than the predictability of this activation, appears to determine the modulatory influence of the dopaminergic neurons on transmission in the circuitry underlying BSR.

In vivo microdialysis preferentially measures DA tone (Wightman & Robinson, 2002). Thus, the present results provide support for the hypothesis (Hernandez et al., 2006; Stefani & Moghaddam, 2006) that reward predictability exerts a differential influence on phasic DA firing and DA tone. These two aspects of DA signaling may well have different functions. Phasic firing may be crucial to learning the operant task (Garris et al., 1999; Kilpatrick et al., 2000; Montague et al., 1996; Reynolds, Hyland, & Wickens, 2001; Schultz et al., 1997; Wightman & Robinson, 2002), initiating responding (Phillips, Stuber, Heien, Wightman, & Carelli, 2003), and in reward expectation (Roitman, Stuber, Phillips, Wightman, & Carelli, 2004; Stuber, Roitman, Phillips, Carelli, & Wightman, 2005) whereas longer-lasting changes in DA tone may play an enabling role (Schultz, 1998, 2002) in processes such as the allocation of effort to task performance (Niv et al., 2006; Salamone, 2002; Salamone et al., 2003; Salamone et al., 1997) and modulation of the circuitry that computes the intensity of incentive stimuli (Blackburn et al., 1992) and rewards (Conover & Shizgal, 2005). A post-synaptic mechanism that can demultiplex the phasic and tonic DA inputs has yet to be established, but a promising proposal has been advanced by West and colleagues (West, Floresco, Charara, Rosenkranz, & Grace, 2003).

Recently, the differential roles of phasic and tonic DA have been investigated in an inducible dopamine transporter (DAT) knockdown mouse line (Cagniard et al., 2006); DA tone can be manipulated in these animals without significantly affecting phasic activity. Increasing DA tone in these animals boosted the rate of responding for food pellets as well as the break point on a progressive ratio schedule but did not change the rate of learning of an appetitive Pavlovian task. These results are consistent with the

notions that 1) DA tone and phasic DA activity play different roles in the modulation and acquisition of goal-directed behaviors and 2) DA tone modulates reward strength (Conover & Shizgal, 2005) and allocation of effort to procurement of rewards (Niv et al., 2006; Salamone, 2002; Salamone et al., 2003; Salamone et al., 1997).

Evidence that DA tone and phasic DA firing are differentially controlled by ventral tegmental area (VTA) afferents is consistent with the hypothesis that DA signaling over different timescales has different functions (Schultz, 1998, 2002). Floresco and co-workers (Floresco, West, Ash, Moore, & Grace, 2003) activated excitatory pedunculopontine inputs to DA neurons and observed a consequent increase in burst firing in the VTA DA neurons. Burst firing is known to enhance phasic release (Garris, Collins, Jones, & Wightman, 1993). Nonetheless, no change in DA tone was registered by a microdialysis probe in the NAc unless reuptake was blocked pharmacologically (Floresco et al., 2003). In contrast, disinhibiting VTA DA cells by suppressing activity of inhibitory ventral pallidal afferents increased the proportion of the VTA DA neurons in the active state without increasing their average firing rate; disinhibiting the VTA DA cells in this way increased tonic DA levels sensed by a microdialysis probe in the NAc. These results suggest that the signal registered by a microdialysis probe is not simply an average of phasic signals impinging on the surrounding region during the sampling interval and that phasic DA signaling and DA tone are differentially influenced by separate afferents to the DA cell bodies.

Future experiments can test alternative interpretations of the differential effect of reward predictability on burst firing in DA neurons and on DA levels observed during experimenter-delivered or self-administered (Figure 13) trains of rewarding MFB

stimulation. In the studies carried out by Schultz and co-workers, the CS-US interval was typically 2 s whereas the intervals tested in the present study were, on average, six times longer. Thus, it is important to assess the impact of reward predictability using intervals within the range of those employed in experiments of Schultz et al. In this way, one could determine whether what appears as differential sensitivity of DA tone and phasic DA release to reward predictability might actually reflect differential sensitivity to events on shorter and longer timescales.

It is also possible that the sustained increase in DA tone observed here could be due to the type of reinforcer employed. There is evidence that unlike the case of phasic DA responses to natural rewards, the phasic response of DA cell bodies to rewarding electrical brain stimulation cannot be “predicted away” as the animal learns to anticipate reward delivery (Fiorillo & Newsome, 2006). In contrast to the findings obtained in rats self-stimulating under a continuous reinforcement schedule (Garris et al., 1999; Kilpatrick et al., 2000) phasic release of DA in the NAc was seen in response to every MFB stimulation train in rats self-stimulating under an FR-1 schedule when a 10-s “time-out” was imposed following reward delivery (Cheer, Heien, Garris, Carelli, & Wightman, 2005). In that experiment, reward delivery was perfectly predictable, yet it continued to trigger phasic DA release. To assess the possibility that the impact of reward predictability depends on the type of reward employed, the present experiment could be repeated, substituting a more natural reward, such as a sucrose solution for the electrical stimulation. Moreover, it would be informative to extend the range of CS-US intervals studied in the Pavlovian conditioning experiments. Finally, voltammetry could be used to investigate the possibility that the pattern of DA release in response to predictable and

unpredictable rewards varies on a time scale finer than the resolution offered by microdialysis sampling.

Given the highly divergent projections of DA neurons and the likelihood that they carry multiple signals multiplexed in time, it is not surprising that these neurons have been implicated in such a diverse range of functions. Experiments on the role of DA neurons in BSR provide one avenue to teasing apart some of these putative roles. The results of the present study are consistent with the notion that DA tone is critical to the maintenance of BSR and does not depend on whether the rewards encountered by the animal are predictable. According to the feedforward model of Hernandez et al. (2006), the modulation of DA tone in the NAc plays a permissive role in the evaluation of rewards. Elevation of DA tone caused by a stream of recent rewards would increase the impact of subsequent rewards, thus helping lock in commitment to a particular objective.

CHAPTER 3

Dopamine tone increases similarly during predictable and unpredictable administration of rewarding brain stimulation at short inter-train intervals

Giovanni Hernandez, Heshmat Rajabi, Jane Stewart, Andreas Arvanitogiannis, &
Peter Shizgal

Hernandez, G., Rajabi, H., Stewart, J., Arvanitogiannis, A., & Shizgal, P. (2008). Dopamine tone increases similarly during predictable and unpredictable administration of rewarding brain stimulation at short inter-train intervals. *Behavioural Brain Research*, 188(1), 227-232. Reproduced with permission.

Introduction

Dopamine (DA) signaling has been implicated in multiple psychological processes, but general agreement about the exact nature of the dopaminergic contribution has yet to be achieved. An influential hypothesis about the function of DA signaling treats the phasic firing of DA neurons as a reward-prediction error that drives associative learning by providing a weight-changing “teaching signal” (Daw & Doya, 2006; Montague et al., 1996; Schultz et al., 1997). Data from classical conditioning experiments are consistent with this view: midbrain DA neurons fire upon receipt of an unpredicted reward but not upon receipt of a reward preceded by a reliable reward-predicting cue (Montague et al., 1996; Schultz, 1998; Schultz et al., 1997).

Phasic release of DA has been monitored in rats working for rewarding electrical brain stimulation. Garris et al. (1999) showed that rats would not learn to self-administer electrical stimulation unless the stimulation electrode was able to trigger phasic release of DA in the nucleus accumbens (NAc) terminal field. However, once the task was acquired, phasic release of DA was only seen at the beginning of the session, declining quickly and no longer observable after a few minutes. If the DA neurons were trans-synaptically activated by the stimulation (Bielajew & Shizgal, 1982, 1986; Shizgal, 1997; Shizgal, Bielajew, Corbett, Skelton, & Yeomans, 1980), then these observations are consistent with the prediction-error model. This model predicts that phasic DA release would be necessary to establish the contingency between lever pressing and delivery of the rewarding stimulation; as the rats learned the contingency, both the reward-prediction error and phasic DA release would decline. (This would not be the case if the DA fibers were directly activated (Montague et al., 1996).)

Recent results suggest that reward predictability plays a very different role in the control of DA tone than in the control of phasic bursting (Hernandez et al., 2006; Stefani & Moghaddam, 2006). Hernandez et al. (2006) showed that DA tone in the NAc, estimated by means of in-vivo microdialysis, remained elevated throughout a long period of experimenter-administered, rewarding brain stimulation; similar DA levels were attained regardless of whether the delivery of the stimulation trains was predictable (one stimulation train every 12 s) or unpredictable (trains delivered at randomly varying intervals, with an average duration of 12 s). Congruent results were obtained when the rats had to work for the stimulation (Hernandez et al., 2007) which was delivered either according to a fixed-interval (predictable) or a variable-interval (unpredictable) reinforcement schedule. Although the temporal patterns of lever pressing were very different in rats responding on the two reinforcement schedules, the time-courses of the elevation in DA levels were indistinguishable. These findings suggest that reward predictability on a fine temporal scale is not important for the control of tonic DA levels.

In the microdialysis experiments that compared predictable and unpredictable delivery of rewarding stimulation, receipt of a stimulation train served as the time marker for predicting when the next train would begin or when the lever would next be armed. The duration of these intervals was long (12 sec) in comparison to the CS-US intervals (typically 2 sec) used in the classical-conditions studies that gave rise to the prediction-error hypothesis of phasic DA signaling (Schultz, 1998; Schultz et al., 1997). Thus, it is of interest to determine whether an effect of predictability would be seen in the microdialysis results when the intervals to be timed were within the range of those typically tested in the classical-conditioning experiments. In this way, one could

determine whether what appears as differential sensitivity of DA tone and phasic DA release to reward predictability might actually reflect differential sensitivity to events on shorter and longer timescales. In the present experiment, the predictable rewarding stimulation was delivered according to a fixed-time 1.5 s schedule (FT1.5: one stimulation train every 1.5 s) whereas the unpredictable stimulation was delivered according to a variable-time 1.5 s schedule (VT1.5: randomly varying inter-train intervals with a mean of 1.5 s).

Materials and Methods

Subjects

Six 300-350-g male Long-Evans rats (Charles-River, St. Constant, QC, Canada) served as subjects. The animals were individually housed in hanging cages on a 12-hr light/dark reverse cycle (lights off from 08:00 to 20:00), with ad libitum access to water and food (Purina Rat Chow). The experimental procedures were performed in accordance with the principles outlined by the Canadian Council on Animal Care.

Surgery

Atropine sulfate (0.5 mg/kg, sc) was administered to reduce bronchial secretions prior to induction of anesthesia with Ketamine-Xylazine (100mg/kg ip). Prior to mounting the rat in the stereotaxic apparatus, the topical anesthetic, xylocaine, was applied to the external auditory meatus to reduce discomfort from the ear bars. Once the rat was mounted in the stereotaxic apparatus, anesthesia was maintained with Isoflurane. A stimulating electrode and a 20 gauge guide cannula (Plastics One, Roanoke, VA) for microdialysis were stereotaxically aimed at the left LH (-2.8 AP, 1.7 ML, and -8.8 DV

from skull) and the NAc (1.5 AP, 2.8 ML, and -5.4 DV from skull at a 10 degree angle) respectively. The monopolar stainless steel electrode (0.25 mm diameter) was insulated with Formvar except for the region extending 0.5 mm from the tip. The anode consisted of two stainless steel screws fixed in the skull, around which the return wire was wrapped. The electrode and the cannula were secured with dental acrylic and skull-screw anchors. At the end of the surgery the rats were injected with buprenorphine (0.05mg/kg, sc) to reduce post-operative pain and with sterile saline solution (1 ml/kg, sc) to facilitate reestablishment of hydromineral balance. The rats recuperated for 5 to 7 days post-surgery before the self-stimulation training began.

Self-stimulation training and stimulation protocol

The self stimulation training was carried out as in previous experiments (Hernandez et al., 2007; Hernandez et al., 2006). Once the rat pressed the lever consistently for trains of constant-current pulses, 0.1 msec in duration and 250 – 400 μ A in amplitude, a rate-frequency curve was obtained by varying the stimulation frequency across trials over a range that drove the number of rewards earned from maximal to minimal levels; the stimulation frequency was decreased from trial to trial by 0.08 \log_{10} units. The frequency used during the subsequent microdialysis sampling was one \log_{10} unit greater than the lowest frequency that supported a maximal response rate, as determined from the rate-frequency curve. Stimulation trains were delivered for 120 minutes according to a FT-1.5 or a VT-1.5 schedule on two different days of microdialysis sampling. The schedules were programmed using LabVIEW software (National Instruments, Austin, TX) installed on an IBM laptop computer. The intervals constituting the VT schedule were drawn from lagged exponential distributions with a

mean of 0.750 seconds; a fixed lag 0.750 seconds was added to each interval in order to prevent the stimulation trains from overlapping in time or occurring at very short temporal offsets. The stimulation was delivered by a Master 8 pulse generator (A.M.P.I., Jerusalem, Israel), and a constant-current amplifier (Mundl, 1980). Microdialysis sampling continued for 120 minutes after the end of the stimulation period.

In vivo microdialysis

Testing was conducted in hexagonal testing chambers (42 x 39 x 33.5 cm), with Plexiglas walls, wooden ceilings, and stainless-steel rod floors; infrared photocells and emitters were mounted in the lateral walls of each box. Each testing chamber was housed in a dark wooden enclosure with a small opening at the front. All testing took place during the dark phase of the circadian schedule. A description of the microdialysis probe can be found in Hernandez et al. (2006).

Sixteen hours before the beginning of each microdialysis experiment, the rats were transported to the testing room and anesthetized lightly with isoflurane. The cannula obturators were removed, and then the microdialysis probes were fixed in position and connected to the microdialysis pump. To prevent occlusion and to help stabilize the probe/brain interface, the probes were perfused with artificial cerebrospinal fluid (ACSF; 145 mM Na⁺, 2.7 mM K⁺, 1.22 mM Ca²⁺, 1.0 mM Mg²⁺, 150mM Cl⁻, 0.2 mM ascorbate, 2 mM Na₂HPO₄, pH = 7.4 ± 0.1) at a rate of 0.7 µl /min. The rats remained in the testing chambers overnight and were provided with ad libitum food and water. Before starting the microdialysis experiment, the food pellets were removed from the testing cages, but the water drinking tubes were left in place. The flow rate was increased to 1.4 µl/min, and dialysate samples were collected every 20 minutes while motor activity was

monitored by a computer system (Hernandez et al., 2006). Baseline sampling continued until the DA concentration of three consecutive microdialysis samples fluctuated by $\leq 5\%$, and delivery of the rewarding stimulation commenced as soon as a stable DA baseline had been attained.

Analytic chemistry

DA was separated from other chemical species present in dialysate samples by high performance liquid chromatography (HPLC) and quantified by electrochemical detection (ED). The samples were loaded into a reverse-phase column (15 x .46 cm Spherisorb-ODS2, 5 μm ; Higgins analytical, Mountain View, CA) through manual injection ports (Rheodyn 7125; Rheodyne LLC, Rhonert Park, CA; 20 μl loop). The separated material passed through dual-channel ESA (Chelmsford, MA) coulometric detectors (Coulochem 5100, with a model 5011 analytical cell), which were connected to a computer. The detectors were set to provide the reduction and oxidation currents for DA and its metabolites, 3,4-dihydroxyphenylacetic acid (DOPAC) and homovanillic acid (HVA); one channel reduced DA whereas the other channel oxidized the metabolites. The equipment was calibrated with standard samples of solutions containing known concentrations of DA and metabolites. The mobile phase (17% acetonitrile 40 mg, 0.076 M SDS, 0.1 M EDTA, 0.058 M NaPO_4 , 0.03 M citric acid, pH = 3.35) was circulated at a flow rate of 1.2 ml/min by Waters 515 HPLC pumps (Lachine, Quebec, Canada). An EZChrom Chromatography Data System (Scientific Software, Inc., San Ramon, CA) was used to analyze and integrate the data obtained for DA, DOPAC, and HVA. Two HPLC-ED systems were used in parallel, and the dialysate samples from a given rat were always analyzed using the same system.

Histology

After the completion of the microdialysis experiment, a lethal dose of sodium pentobarbital was administered. A 1 mA anodal current was passed through the stimulating electrode for 15 sec to deposit iron particles at the site of the electrode tip. The animals were then perfused intracardially with 0.9% sodium chloride, followed by a formalin-Prussian Blue solution (10% formalin, 3% potassium ferricyanide, 3% potassium ferrocyanide, and 0.5% trichloroacetic acid) that forms a blue reaction product with iron particles. The animals were then decapitated and the brains fixed with 10 % formalin solution for at least 7 days. Coronal sections of 30 μ m thickness were cut with a cryostat. The probe and electrode locations were determined microscopically at low magnification with reference to the stereotaxic atlas of Paxinos and Watson (Paxinos & Watson, 1998).

Statistics

The levels of the assayed substances were expressed as concentrations. Basal values are the mean of the three samples obtained prior to the start of the stimulation period.

The effects of the electrical stimulation on DA and its metabolites were analyzed using a two-way analysis of variance with repeated measures over time. Comparison between the baseline levels, stimulation levels, and post-stimulation levels were carried out using Tukey's honestly significant difference (HSD) procedure for equal sample sizes. A level of $p < 0.05$ for a two-tailed test was the criterion for statistical significance. The analysis was carried out using Statistica (Statsoft, Inc., Tulsa, OK).

Results

Location of electrode tips and microdialysis probes

The locations of the microdialysis probes and electrode tips are shown in Figs. 14a and 14b, respectively. The tips of all the microdialysis probes penetrated the shell of the nucleus accumbens, at coronal planes corresponding to plates 13 and 14. All stimulation sites lay within the lateral hypothalamus, at coronal planes corresponding to plates 24 and 25 of the Paxinos and Watson atlas (1998).

Basal extracellular levels of dopamine

Basal amounts of DA per 10 μ l of dialysate were 1.1 ± 0.08 pg for the FT-1.5 schedule and 1.1 ± 0.03 pg for the VT1.5 schedule. Basal level did not vary significantly across conditions, $F_{(1,8)} = 0.005$ $p = 0.94$.

Effect of LH stimulation on concentrations of DA

Stimulation of the LH produced an increase in DA concentration under both reinforcement schedules (Fig. 15). After 20 min of stimulation under a FT-1.5 schedule DA concentration in the dialysate increased to 150% of its baseline value, peaking at 217% after 40 minutes of stimulation. Subsequent to this peak, the DA concentration decreased reaching 161% of its baseline value at the offset of the stimulation. The average DA concentration during the rewarding stimulation was 178% of the baseline value. During the post-stimulation period, DA concentration declined toward the baseline

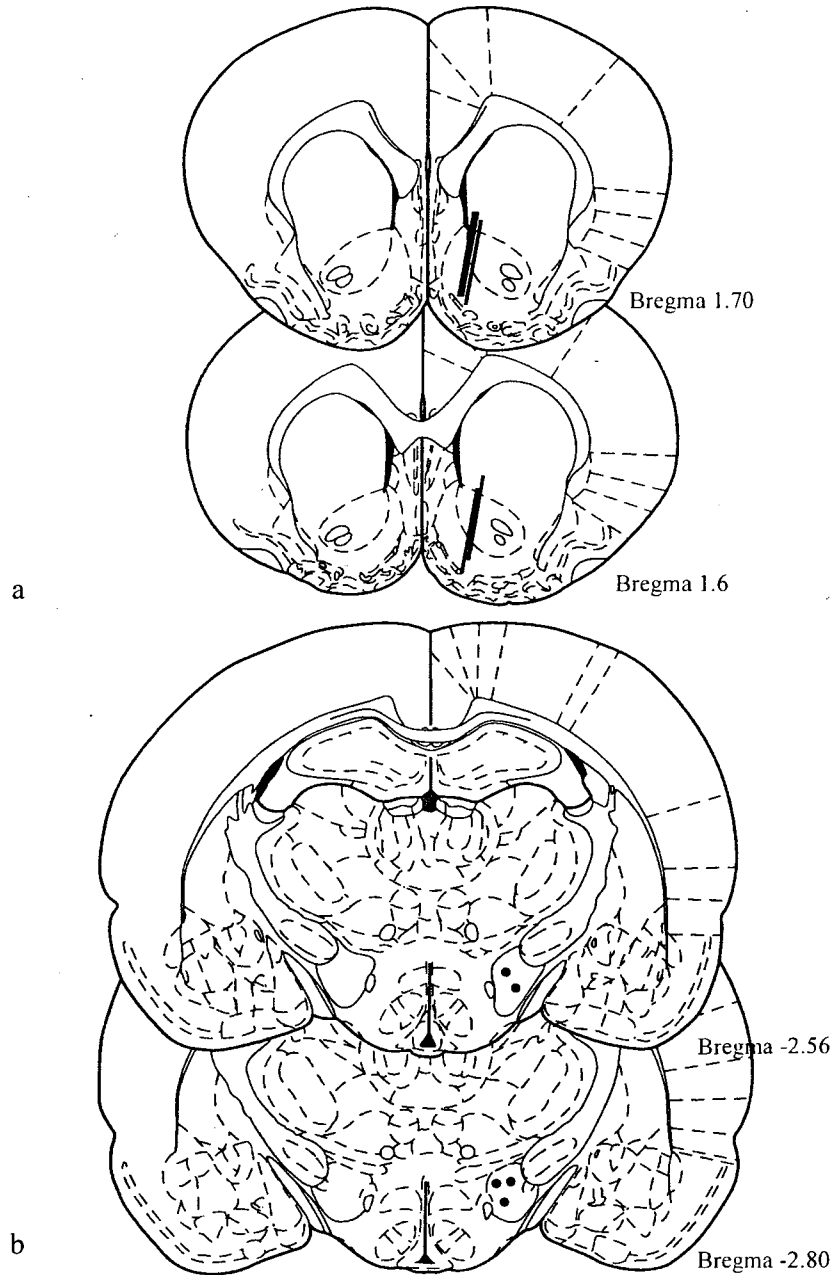


Figure 14. (a) Location of microdialysis probes for the FT and VT groups. The coronal drawings are from the Paxinos and Watson (1998) atlas, plates 13-14.

(b) Location of electrodes tips for the FT and VT groups. The coronal drawings are from the Paxinos and Watson (1998) atlas, plates 24-25.

range. Similarly after 20 minutes of the stimulation onset under a VT-1.5 schedule DA concentration in the dialysate increased to 207% of baseline, peaking at 224% of baseline 40 min after the start of the stimulation. After the peak, DA concentration decreased reaching 171% of baseline at the offset of the stimulation. The average increase of DA during the rewarding stimulation was 196% of baseline. During the post-stimulation period, DA concentration declined toward the baseline range.

The increase in DA concentration observed under both schedules was statistically significant. Analysis of variance showed a significant main effect for time of the sample, $F_{(14,112)} = 29.34, p < 0.05$; but not for the schedule under which the stimulation was delivered, $F_{(1,8)} = 0.20, p = 0.66$; nor for the interaction between schedule and time of the sample, $F_{(14,112)} = 0.98, p = 0.47$.

The stimulation-induced changes in DA concentration followed similar time-courses under the two schedules (Figure 15). The only difference observed between the results obtained under two schedules was the DA concentration 20 minutes after stimulation onset; at this time, the DA concentration in the FT-1.5 sample is significantly lower than in the VT-1.5 sample and not statistically different from the concentrations in the baseline samples, according to a Tukey's HSD post-hoc comparison. The values obtained at the five remaining time points during the stimulation period were indistinguishable. Under both schedules, the DA concentration in the dialysate peaked 40 minutes after the onset of stimulation and then declined progressively throughout the stimulation period.

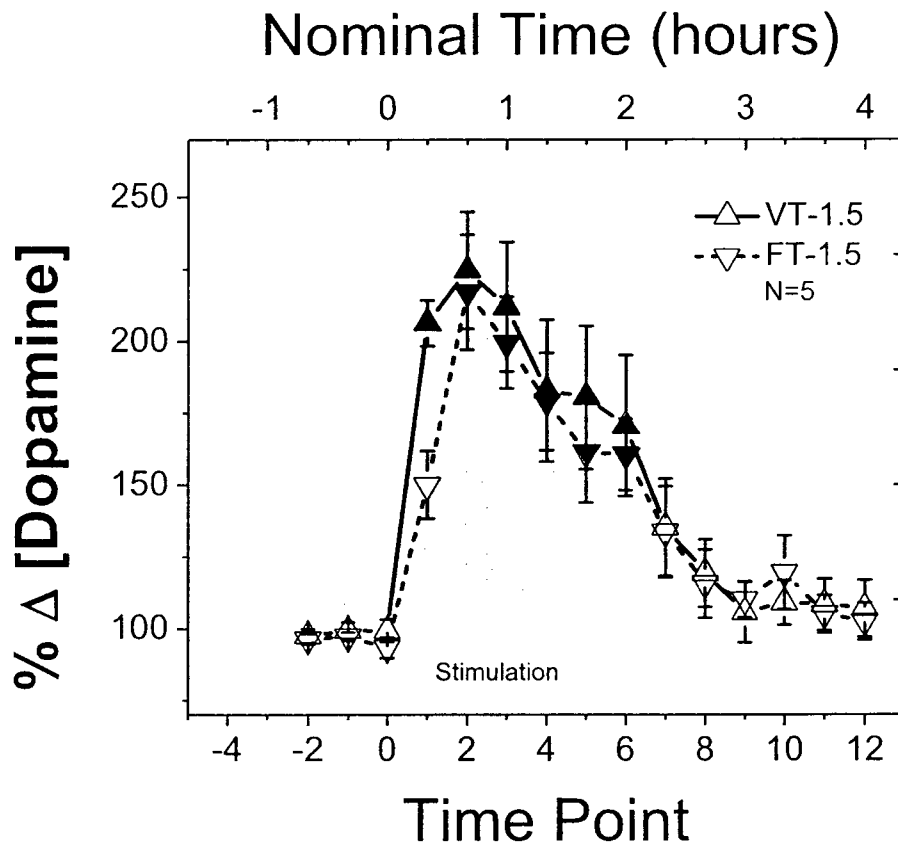


Figure 15. Effect of electrical stimulation of the medial forebrain bundle (MFB) under a fixed-time 1.5-s (FT-1.5) and variable-time(VT-1.5) schedules on the concentrations of dopamine (DA), in dialysate obtained from nucleus accumbens (NAc) probes. A large increase in DA concentration was seen 40 min after the stimulation onset, DA concentration decreased throughout the rest of the stimulation period. The nominal time represented on the upper abscissa was computed by multiplying the time point number by 20 min, the intended sampling interval. The actual sampling intervals were roughly 5% longer. Filled symbols represent statistically significant differences from baseline values.

Discussion

Rewarding electrical brain stimulation has been shown to increase DA tone in the NAc, as measured by means of microdialysis, regardless of whether delivery of the stimulation trains was predictable (Hernandez et al., 2007; Hernandez et al., 2006). These results contrast with the strong dependence of phasic firing in DA neurons (Schultz, 1998; Schultz et al., 1997) and DA release in the NAc (Day, Roitman, Wightman, & Carelli, 2007) on the predictability of natural rewards. However, the time intervals the subjects were asked to predict were much longer in the microdialysis studies of brain stimulation reward (12 s) than in the electrophysiological experiments that gave rise to the prediction-error hypothesis of phasic DA signaling (typically, 2 s) (Ljungberg, Apicella, & Schultz, 1992; Mirenowicz & Schultz, 1994; Romo & Schultz, 1990; Schultz & Romo, 1990). The aim of the present study was to determine whether the predictability of rewarding brain stimulation would influence DA tone in the NAc when the intervals the subjects were asked to predict were similar to those used in the electrophysiological experiments. The results do not support this hypothesis: once again, the magnitude and time course of the stimulation-induced increase in NAc DA levels were strikingly similar in response to rewarding brain stimulation delivered at predictable and unpredictable intervals.

– Under both stimulation schedules, the concentration of DA in the dialysate peaked at the 40-min mark of the stimulation period and then decayed. The decrease during the later part of the stimulation period mirrors what was observed in an earlier study employing high-density electrical stimulation (Hernandez et al., 2006) and is consistent with a computational model of the dynamics of DA release (Montague et al., 2004). The

observed decrease may reflect diminished release capability in the DA neurons due to the persistent, intense afferent drive produced by the LH stimulation. The difference between the DA levels at the first time point could reflect individual variation in microdialysis sampling that was not averaged out due to the relatively small number of subjects (5). Although the direction of this difference is consistent with the prediction of the temporal-difference model (Montague et al., 1996), the remaining data are not: at the remaining five time points, the DA concentration in subjects receiving predictable stimulation is just as high as in subjects receiving unpredictable stimulation.

The rewarding stimulation in the present study was delivered according to a FT-1.5 schedule (one train every 1.5 s) or a VT-1.5 schedule (trains delivered at exponentially distributed intervals averaging 1.5 s). Thus, train onset was predictable under the FT-1.5 schedule and unpredictable under the VT-1.5 schedule. Despite this difference in predictability, the magnitude and time course of DA release were very similar. One way to account for this result and those of prior microdialysis studies (Hernandez et al., 2007; Hernandez et al., 2006) is to take into consideration the multiple modes of DA firing (Schultz, 2002) and attribute dependence on reward predictability to the phasic responses but not to those that evolve over longer time scales. This interpretation is consistent with the proposal of Niv et al. (2006) that DA tone reflects average reward rate as well as with several lines of evidence showing that phasic and tonic release are under differential control and do not necessarily co-vary (Cagniard et al., 2006; Floresco, West, Ash, Moore, & Grace, 2003)

Alternatively, the similarity in the DA release produced by the predictable and unpredictable trains could be due to the type of reinforcer employed. There is evidence

from electrophysiological recordings obtained from DA cell bodies in the monkey that unlike the case of phasic DA responses to natural rewards, the phasic response of DA cell bodies to rewarding electrical brain stimulation cannot be “predicted away” as the animal learns to anticipate reward delivery (Fiorillo & Newsome, 2006). Recent experiments employing fast-scan cyclic voltammetry have been carried out in self-stimulating rats, using a testing paradigm in which a 10 s time-out follows delivery of every stimulation train. Under these conditions, phasic release of DA is observed after every stimulation train, despite the fact that these trains are perfectly predictable (Cheer et al., 2007; Cheer et al., 2005). If so, the nulling of DA release observed earlier by Garris et al. (1999) and Kilpatrick et al. (2000) may be due, not to the predictability of the reward, but rather to the very short intervals that separated the trains self-administered by rats responding at high rates under a continuous reinforcement schedule. Thus, it is not clear whether the results reported here reflect a difference in the role of reward predictability in the control of phasic and tonic DA signaling or a difference in the ability of reward predictions to null the DA-activating effect of natural rewards and rewarding electrical brain stimulation. To choose between the two interpretations, it will be necessary to compare the effects of natural rewards and brain stimulation rewards on phasic and tonic DA release in the same preparation and testing paradigm.

If DA axons were directly activated by the LH stimulation, then it would not be surprising that evoked DA release persists even when reward predictions have become well established. Thus, it is important to emphasize that the stimulation parameters employed in the present experiment weaker than those required in prior studies to directly activate a substantial number of DA fibers (Anderson, Fatigati, & Rompre, 1996;

Yeomans, Maidment, & Bunney, 1988). If so, the evoked DA release was due to trans-synaptic activation of DA neurons. An appropriately timed and anatomically convergent reward-prediction signal should, in principle, be able to counteract such excitatory input. If such cancellation fails to occur in the case of electrically evoked reward signals but does occur in the case of reward signals evoked via normal sensory channels, this could shed light on the structure of the neural networks that underlie the effects of natural and electrically evoked rewards. For example, perhaps the input from the stimulation electrode reaches the DA somata downstream from the synapses where the reward prediction nulls the natural reward signal.

CHAPTER 4

*Dynamic changes in dopamine tone during self-stimulation of the ventral tegmental
area in rats*

Giovanni Hernandez & Peter Shizgal

Hernandez, G., & Shizgal, P. (2009). Dynamic changes in dopamine tone during self-stimulation of the ventral tegmental area in rats. *Behavioural brain research*, 198(1), 91-97. Reproduced with permission.

Introduction

Three principal activity states have been observed in mesencephalic dopamine (DA) neurons (Floresco et al., 2003; Grace, Floresco, Goto, & Lodge, 2007). Under resting conditions, roughly 50% are inactive, due to strong inhibitory drive from GABAergic afferents. Weakening of this inhibitory input reduces the proportion of dopamine neurons in the inactive state, allowing an intrinsic pacemaker mechanism to produce slow, sustained (“tonic”) firing. Excitatory glutamatergic input, coupled with a permissive gating signal from the laterodorsal tegmental nucleus, can induce the dopamine neurons to fire in a “phasic” bursting pattern, provided that the inhibitory GABAergic drive is not too strong.

The different activity states of the mesencephalic cells bodies are reflected in the release of DA in forebrain terminal fields. Experiments carried out by Grace and co-workers suggest that the transition from the inactive to the tonic-firing state increases the background concentration of DA (“dopamine tone”) in the terminal fields, as measured by means of in-vivo microdialysis (Floresco et al., 2003). In contrast, phasic burst-firing is believed to be the origin of the transient, local release measured by means of fast-scan cyclic voltammetry (Wightman & Robinson, 2002).

In several theories of dopaminergic function, different roles are attributed to the tonic and phasic patterns of activity. For example, it has been argued that phasic bursts act as reward-prediction errors that shape synaptic weights so as to maximize reward procurement and optimize predictions of the magnitude and timing of future rewards (Montague, Dayan, & Sejnowski, 1996; Schultz, Dayan, & Montague, 1997). In contrast, Niv and Dayan (2006) have proposed that DA tone encodes the average reward rate and

controls the vigor of reward-procuring behaviors, a view consistent with the proposal of Salamone and co-workers (Salamone, 2002; Salamone, Correa, Mingote, & Weber, 2003; Salamone, Cousins, & Snyder, 1997) that alterations in dopaminergic transmission change the allocation of effort to the pursuit of rewards. In Grace's models of the neural basis of schizophrenia (Grace, 1991; Lodge & Grace, 2007), DA tone regulates the responsiveness of the DA system to phasic activation. It follows from these proposals and the findings on which they are based that the changes in both the phasic and tonic components of DA signaling must be described in order to understand the mechanisms underlying the behavioral consequences of dopaminergic manipulations.

Reward is one of the many functions that have been linked to dopaminergic neurotransmission. The first study on the role of DA in reward was carried out by assessing the effect of alterations in dopaminergic signaling on performance for rewarding electrical brain stimulation (Crow, 1970). The nature of the dopaminergic contribution remains controversial, and the intracranial self-stimulation paradigm continues to see active service in the attempt to determine the role of dopaminergic neurons.

Considerable work has already been done to describe the changes produced by the rewarding stimulation in the activity states of DA neurons and in their patterns of neurotransmitter release. Measurements obtained by means of in-vivo microdialysis show that rewarding stimulation of the medial forebrain bundle (MFB) increases DA tone in the ventral striatal (Fiorino, Coury, Fibiger, & Phillips, 1993; Hernandez et al., 2007; Hernandez et al., 2006; Hernandez, Rajabi, Stewart, Arvanitogiannis, & Shizgal, 2008; Hernandez & Hoebel, 1988; Miliareisis, Emond, & Merali, 1991; Nakahara, Ozaki,

Miura, Miura, & Nagatsu, 1989; Rada, Mark, & Hoebel, 1998; You, Chen, & Wise, 2001) and prefrontal cortical (Nakahara, Fuchikami, Ozaki, Iwasaki, & Nagatsu, 1992) terminal field(s). When repeated pulse trains separated by relatively long intervals (12 s) are delivered, stimulation-induced elevation of DA tone remains stable, or nearly so, during prolonged (2 h) periods of stimulation (Hernandez et al., 2006). Shortening the inter-train interval to 1.5 s increases the peak elevation, but the concentration of DA in the dialysate falls as the stimulation is prolonged; despite the decline from the peak values, the concentration of DA in the dialysate remains elevated above baseline levels at the end of the 2-h stimulation sessions (Hernandez et al., 2006; Hernandez et al., 2008).

Measurements of phasic DA release in response to electrical stimulation of the MFB have been obtained by means of amperometry (Yavich & Tanila, 2007; Yavich & Tiihonen, 2000) and fast-scan cyclic voltammetry (Cheer et al., 2007; Cheer, Heien, Garris, Carelli, & Wightman, 2005; Garris et al., 1999; Kilpatrick, Rooney, Michael, & Wightman, 2000). When the stimulation trains are separated by a 10-s time-out (Cheer et al., 2005), or by imposition of a fixed-ratio 8 reinforcement contingency (Yavich & Tiihonen, 2000), a phasic increase in DA concentration in the nucleus accumbens (NAc) is noted after every stimulation train, and these responses are sustained for at least 3-11 min (Cheer et al., 2005; Yavich & Tiihonen, 2000). However, when a continuous reinforcement schedule was employed, and thus, the inter-train intervals were much shorter, stimulation-induced increases in DA concentration were not always observed and, when detected, the DA transients decreased rapidly in amplitude, often falling below the detection threshold within a minute or so of the onset of the self-stimulation session (Garris et al., 1999; Kilpatrick et al., 2000). In contrast, even when inter-train intervals

are relatively short, elevated DA tone can be seen in microdialysis records over durations more than 100 times longer than those over which electrochemically detected transients have been reported to disappear (Hernandez et al., 2006; Hernandez et al., 2008).

The contrast between the results obtained by means of microdialysis and direct electrochemical sampling (amperometry or voltammetry) may reflect the differential sensitivity of these two measurement methods to the tonic and phasic components of DA release. Alternatively, the reported differences may reflect discrepancies between the conditions under which the measurements have been obtained, such as the stimulation site, the stimulation parameters employed, the amount of stimulation received during training, and whether the stimulation was triggered by the subject or the experimenter. Thus, we used in-vivo microdialysis to sample DA concentrations in the nucleus accumbens under conditions that were otherwise similar to those in the fast-scan cyclic voltammetry study conducted by Garris et al. (1999). In contrast to our previous studies employing short inter-train intervals, and in accord with the study of Garris et al. (1999) stimulation electrodes were aimed at the ventral tegmental area (VTA), longer pulse durations and lower currents were employed, the stimulation was self-administered by the subjects, and the number of stimulation trains received during screening and training was kept to a minimum.

Materials and Methods

Subjects

Eight 300-350-g male Sprague Dawley rats (Charles-River, St. Constant, QC, Canada) served as subjects. The animals were individually housed in hanging cages and maintained on a 12-hr light/dark reverse cycle (lights off from 08:00 to 20:00), with ad

libitum access to water and food (Purina Rat Chow). The experimental procedures were performed in accordance with the principles outlined by the Canadian Council on Animal Care.

Surgery

Atropine sulfate (0.5 mg/kg, s.c.) was administered to reduce bronchial secretions prior to induction of anesthesia with ketamine (10mg/kg), xylazine (100 mg/kg) ip. Before mounting the rat in the stereotaxic apparatus, the topical anesthetic xylocaine was applied to the external auditory meatus to reduce discomfort from the ear bars. An intramuscular injection of Penicillin G (300,000 IU /kg) was given to reduce the chances of sepsis. Once the rat was mounted in the stereotaxic apparatus, anesthesia was maintained with Isoflurane. A 20 gauge cannula (Plastics One, Roanoke, VA), which was to serve as a guide for the microdialysis probe, was stereotaxically aimed at the left NAc shell (1.7 AP, 0.7 ML, and -5.4 DV from skull). Simulation electrodes (0.25 mm diameter) were insulated with Formvar except for a region extending 0.5 mm from the tip and were aimed bilaterally at the VTA (-5.6 AP, 1.0 ML and -8.8 DV). These depth electrodes served as cathodes whereas the anode consisted of two stainless steel screws fixed in the skull. The cannula and the electrode were secured with dental acrylic and skull-screw anchors. At the end of the surgery, the rats were injected with buprenorphine (0.05mg/kg, sc) to reduce post-operative pain and with sterile saline solution (1 ml/kg, sc) to facilitate reestablishment of hydromineral balance. The rats recuperated for 5 to 7 days post-surgery before training.

Self-Stimulation Training

Each rat was shaped to lever press for a 0.4-s train of cathodal, rectangular, constant-current pulses, 1.0 ms in duration. Shaping took place in a Plexiglas operant chamber (30 cm long X 21 cm wide X 51 cm high) equipped with one retractable lever located on the right wall of the box and a cue light positioned 1.5 cm above the lever. A continuous reinforcement schedule was in force. The temporal characteristics of the stimulation were set by digital pulse generators (Master 8 pulse generator A.M.P.I., Jerusalem, Israel), and a constant-current amplifier (Mundl, 1980). The stimulation was controlled using LabVIEW software (National Instruments, Austin, TX).

The stimulation currents were monitored with an oscilloscope, which read the voltage drop across a 1-k Ω resistor (1% precision) in series with the electrode. Initially, low currents (50 μ A) at 60 Hz were used. If sniffing and approach were observed, the rat was trained to press the lever. Otherwise, the stimulation current was increased gradually until either signs of interest or aversion were seen. If the rat displayed signs of aversion, training was discontinued. Once the rat pressed the lever consistently for currents between 125 and 200 μ A. The rats were removed from the boxes until the next day when the microdialysis sessions started.

In vivo microdialysis

Testing was conducted in the same operant boxes in which the animals were shaped, using the stimulation currents determined during the training session. Each test chamber was shielded from light and visual distractions by an opaque Styrofoam panel. All testing took place during the dark phase of the circadian schedule. A description of

the microdialysis probe, electrical slip-ring swivel, and fluid swivel can be found in Hernandez et al.(2006).

Sixteen hours before the beginning of each microdialysis experiment, the rats were transported to the testing room and anesthetized lightly with isoflurane. The obturators were removed from the cannulas, and the microdialysis probes were then fixed in position and connected to the microdialysis pump (Harvard Syringe Pumps model 11; Harvard Apparatus Saint Laurent, QC). To prevent occlusion and to help stabilize the probe/brain interface, the probes were perfused with artificial cerebrospinal fluid (ACSF; 145 mM Na⁺, 2.7 mM, K⁺, 1.22 mM Ca²⁺, 1.0 mM Mg²⁺, 150mM Cl⁻, 0.2 mM ascorbate, 2 mM Na₂HPO₄, pH = 7.4 ± .1) at a rate of 0.3 µl /min. The rats remained in the test chambers overnight and were provided with ad libitum food and water. Before the start of the microdialysis experiment, the food pellets were removed from the test cages, but the water drinking tubes were left in place. The flow rate was increased to 1.0 µl/min, and a 2-hour stabilization period at the new flow rate intervened before the collection of dialysate samples began. Samples were then collected every 10 min and immediately frozen in dry ice. The first 3 hours of collection constituted the baseline condition, and no stimulation was delivered during this period. Following collection of the baseline samples, one of two types of self-stimulation session began. In the “intermittent-access” condition, 10-minute periods of self-stimulation were alternated with 30-minute rest periods whereas in the “continuous-access” condition, stimulation was available continuously for 120 minutes. In both cases, a continuous reinforcement schedule was in effect when the stimulation was available. The rats were assigned at random to either of the two conditions.

After completion of the initial stimulation session, the flow rate was reduced to 0.3 $\mu\text{l}/\text{min}$, a ratio rat chow was placed in the test cage, and the rats were left undisturbed overnight. The next morning, the flow rate was returned to 1.0 $\mu\text{l}/\text{min}$, and collection of a new set of baseline samples began 2 hours later. Then, the rats that had been tested in the continuous-access condition on Day 1 were run in the intermittent-access condition, and the rats that had been tested in the intermittent-access condition on Day 1 were run in the continuous-access condition.

Analytical chemistry

A description of the procedures for analytic chemistry can be found in Hernandez et al.(2006).

Histology

After the completion of the experiment, a lethal dose of sodium pentobarbital was administered. The animals were then perfused intracardially with 0.9% sodium chloride, and decapitated. The brains were removed from the skulls and fixed with 10 % formalin solution for at least 7 days. Coronal sections of 40 μm thickness were cut with a cryostat (Thermo Scientific). The probe location were determined microscopically at low magnification with reference to the stereotaxic atlas of Paxinos and Watson (2007) .

Statistics

The levels of the assayed substances were expressed as concentrations. Basal values are the mean of the three samples obtained prior to the start of the stimulation period. The effects of the electrical stimulation on DA and its metabolites were analyzed using a repeated measures analysis of variance. Comparison between the baseline levels,

stimulation levels, and post-stimulation levels were carried out using Tukey's HSD for equal sample sizes. A level of $p < 0.05$ for a two-tailed test was the criterion for statistical significance. The analysis was carried out using Statistica (Statsoft, Inc., Tulsa, OK)

Results

Location of electrode tips and microdialysis probes

The location of the electrodes tips and microdialysis probes are shown in Figures 16 and 17. All stimulation sites lay within the ventral tegmental area, at coronal planes corresponding to plates 80 to 83 of the Paxinos and Watson atlas (2007). The tips of all the microdialysis probes penetrated the shell of the nucleus accumbens, at coronal planes corresponding to plates 18 to 20.

Behaviour

All rats responded vigorously and reliably for the stimulation throughout both the 10-minute (intermittent-access) and 2-hour (continuous-access) stimulation periods. The rats self-administered trains of rewarding VTA stimulation at an average rate of 0.92 ± 0.03 per second in the intermittent-access condition and 1.08 ± 0.03 per second in the continuous-access condition.

Basal levels

Basal amounts of DA, DOPAC, and HVA per 10 μ l of dialysate were 1.37 ± 0.08 , 944.63 ± 54 pg, and 376 ± 23 pg, respectively, in the intermittent-access condition and 1.4 ± 0.08 pg, 944.6 ± 40 pg, and 336.8 ± 18 pg, respectively, in the continuous-access

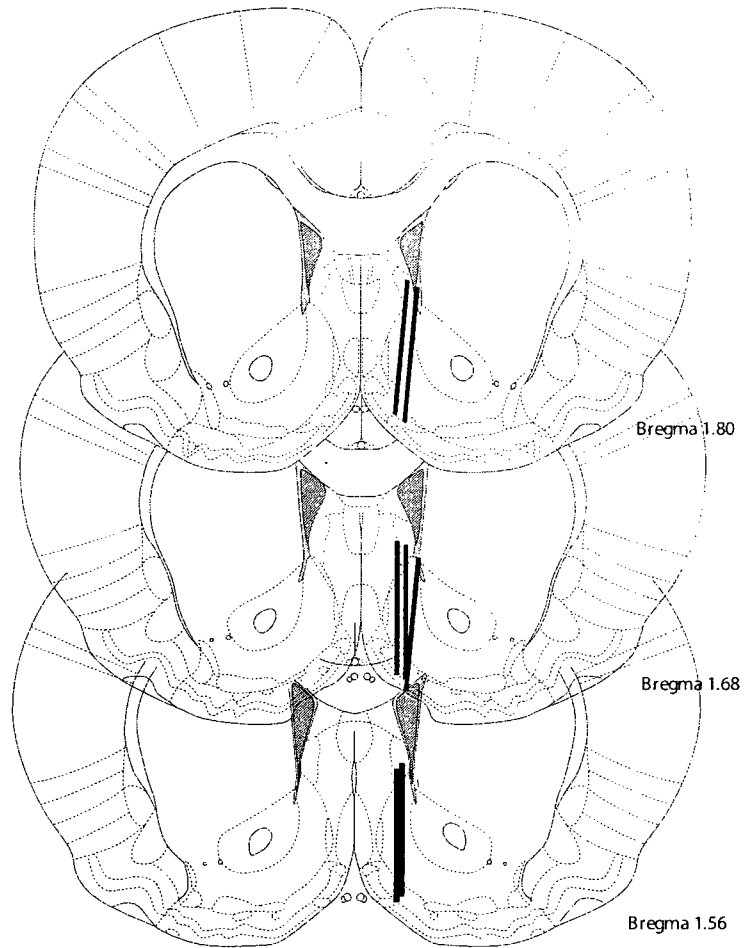


Figure 16. Location of microdialysis probes. All the probes penetrated the shell of the nucleus accumbens. The coronal drawings are from the Paxinos and Watson (2007) atlas, plates 18-20.

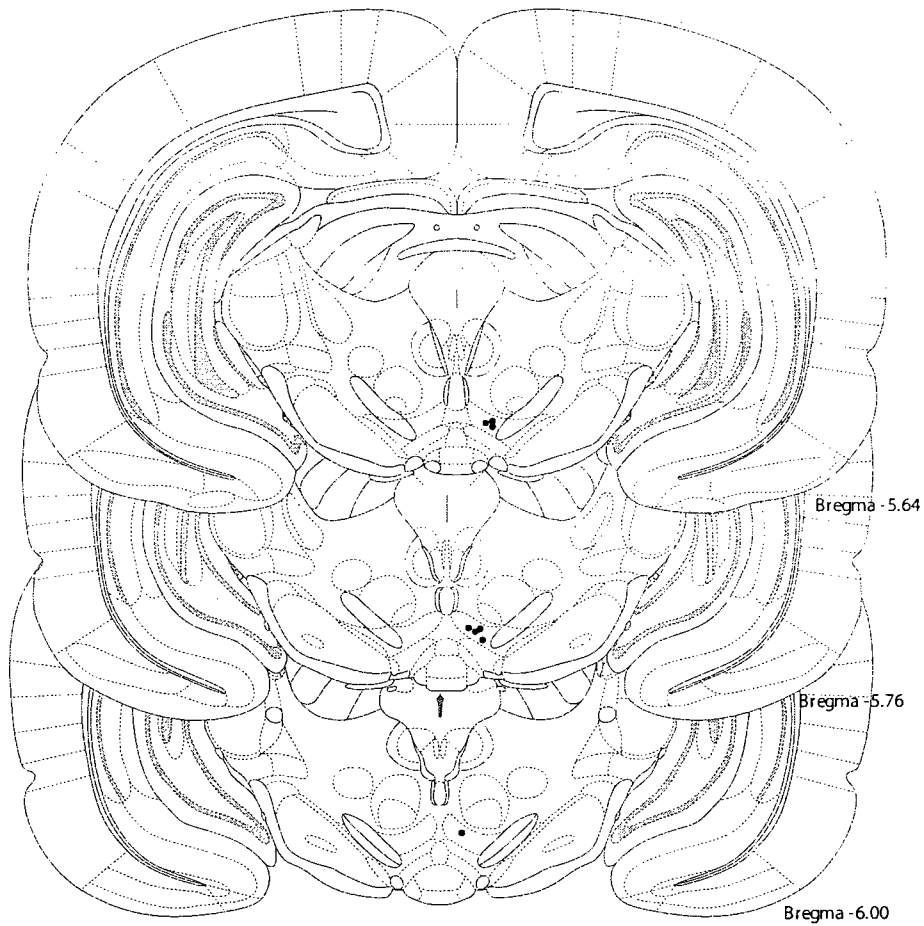


Figure 17. Location of electrodes tips. All stimulation sites lay within the ventral tegmental area. The coronal drawings are from the Paxinos and Watson (2007) atlas, plates 80-83.

condition. Basal levels did not vary significantly across conditions: DA, $F_{(1,7)} = 0.31, p = 0.58$; DOPAC, $F_{(1,7)} = 2.57, p = 0.14$; HVA, $F_{(1,7)} = 1.3, p = 0.28$

Effects of electrical stimulation on the concentration of dopamine in the intermittent-access condition

As shown in Figure 18, the DA concentration in the dialysate sample obtained immediately following each 10-minute bout of self-stimulation was roughly three times higher than the baseline values. In subsequent samples, acquired during the time-out period, the DA concentration declined in an orderly fashion and approached the baseline values by the third post-stimulation sample.

The repeated measures analysis of variance shows a significant main effect for time of the sample, $F_{(19,133)} = 26.81, p < 0.05$. Tukey's HSD post-hoc test indicates that each of the samples taken immediately after the end of the stimulation period is statistically different from baseline values. The only other post-stimulation sample that is significantly different from baseline values is the second post-stimulation sample taken after the first 10-minute stimulation bout.

Effects of electrical stimulation on the concentration of dopamine in the continuous-access condition

Figure 19 shows that after 10 min of stimulation, the DA concentration in the dialysate increased to 258 % of baseline, peaking at 281% of baseline 30 min after stimulation onset. Subsequently, the DA concentration declined smoothly, reaching 146% of the baseline value at the end of the 2-hour period of self-stimulation. A steeper decline

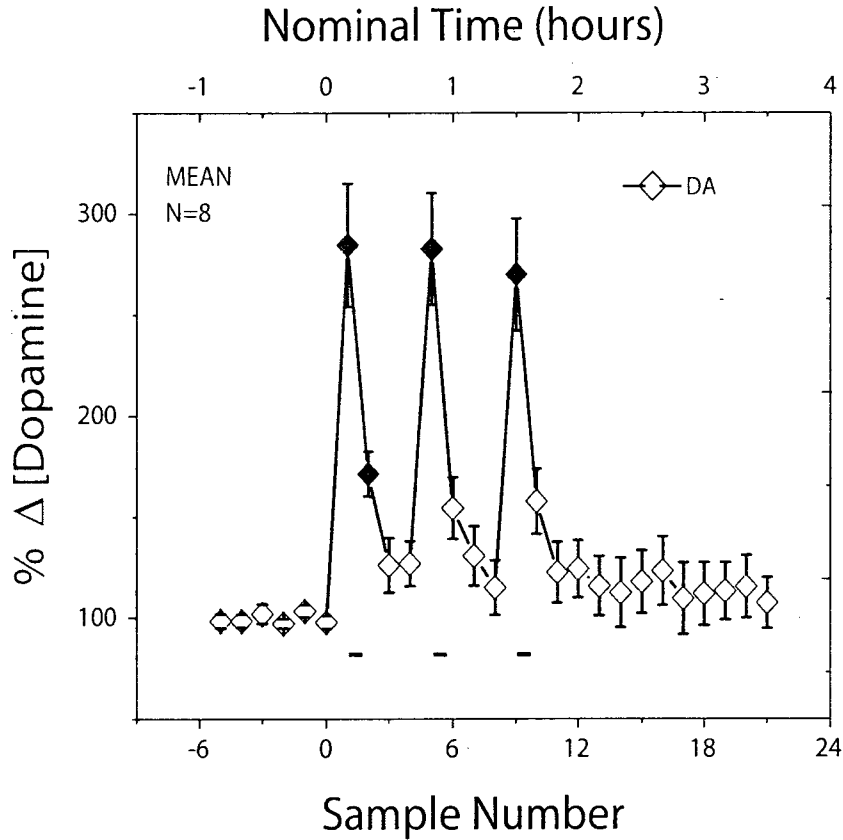


Figure 18. Effect of electrical stimulation of the ventral tegmental area (VTA) throughout 10-minute (intermittent-access) stimulation periods on the concentration of dopamine (DA) in dialysate obtained from nucleus accumbens (NAc) probes. The 10-minute stimulation periods are designated by black lines at the bottom of the graph. A large increase in DA concentration was seen during each self-stimulation period. After access to the stimulation was blocked, the DA concentration declined towards baseline values. The nominal time represented on the upper abscissa was computed by multiplying the sample number by 10 min, the intended sampling interval. Filled symbols represent statistically significant differences from baseline values.

was seen immediately following the post-stimulation period, as the DA concentration returned to the baseline range.

The repeated measures analysis of variance shows a significant main effect for time of the sample, $F_{(27,189)} = 24.68$ $p < 0.05$. Tukey's HSD post-hoc test indicates that the samples taken during the first 100 minutes of the stimulation period, but not during the final 20 minutes, are significantly different from the baseline.

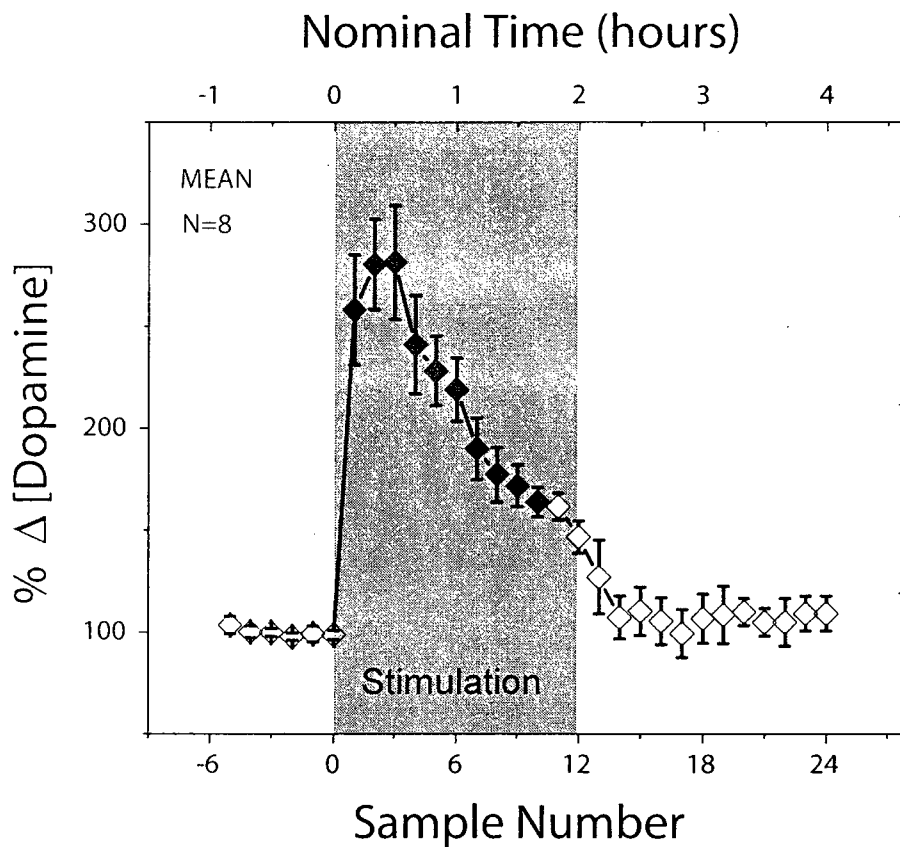


Figure 19. Effect of electrical stimulation of the ventral tegmental area (VTA) under a continuous reinforcement schedule on the concentration of dopamine (DA) in dialysate obtained from nucleus accumbens (NAc) probes. A large increase in DA concentration was seen the first 30 min after the stimulation onset and then DA concentration decreased throughout the rest of the stimulation period. The nominal time represented on the upper abscissa was computed by multiplying the sample number by 10 min, the intended sampling interval. Filled symbols represent statistically significant differences from baseline values.

Discussion

Self-stimulation of the VTA was accompanied by robust increases in the concentration of DA in dialysate samples from the NAc to levels nearly triple the baseline values. In the intermittent condition, the DA concentration declined rapidly during the 30-minute rest periods to approach baseline levels; a second and third 10-minute self-stimulation bout returned the DA concentration to within the range observed during the first bout. In the continuous condition, the DA concentration peaked 30 minutes following the onset of the stimulation session and then declined. Among the possible reasons for this decline are inhibition of release due to the effect of the elevated DA tone on autoreceptors (Grace, 1995) and depletion of the releasable pool of neurotransmitter (Michael, Ikeda, & Justice, 1987a; Michael, Ikeda, & Justice, 1987b).

Notwithstanding the eventual relaxation of DA tone after 30 minutes of self-stimulation, the DA concentration was still more than double the baseline values after 1 hour of self-stimulation and remained significantly elevated during an additional 50 minutes of self-stimulation. The accelerated decline following termination of the self-stimulation session suggests that the persistently elevated DA levels observed while the rats were lever pressing reflects ongoing stimulation-induced release of the neurotransmitter.

These microdialysis findings stand in sharp contrast to the FSCV data reported in the Garris et al. (1999) study. In that experiment, DA release was rarely seen in retrained rats lever pressing for rewarding VTA stimulation; when observed, phasic DA release was seen only at the beginning of the self-stimulation session and fell below the detection limit within 30 seconds or so. Similar results were obtained from FSCV probes in the

caudate/putamen (Kilpatrick et al., 2000). In the contrasting results of the present study, the DA concentration in the dialysate remained significantly elevated until the rats had been self-stimulating for 110 minutes. Garris et al.(1999) reported that a 30-minute rest period failed to restore phasic DA release, as measured by means of FSCV. In the contrasting results of the present study, 30-minute rest periods restored the DA concentration in the dialysate to within the peak range.

Although very different from the results of the Garris et al. (1999) study, the data reported here resemble findings from rats receiving rewarding, experimenter-delivered stimulation at the lateral hypothalamic level of the MFB, at train-repetition rates $\sim 2/3$ those in the present experiment and at much shorter (0.1 msec) pulse durations (Hernandez et al., 2008). In that study, DA levels peaked at the 40-minute mark and then declined, but they were still significantly elevated at the end of the 2-hour stimulation period. Thus, regardless of whether the stimulation is delivered at the lateral hypothalamic or ventral tegmental level of the MFB, whether the stimulation is pre-programmed or self-administered, or whether short or long pulse durations are employed, repeated delivery of rewarding MFB stimulation produces a prolonged elevation in NAc dopamine tone.

One approach towards explaining the discrepancy between the results obtained by means of FSCV and the microdialysis data reported here is to appeal to the differential sensitivity of these two techniques to different transitions between activity states of dopamine neurons. Floresco et al. (2003) showed that activation of excitatory pedunculopontine inputs to the VTA increased burst firing in putative DA neurons but did not increase the concentration of DA obtained from microdialysis probes in the NAc

terminal field unless reuptake was blocked. Conversely, disinhibiting the VTA DA neurons by suppressing input from the ventral pallidum increased the number of DA neurons in the sustained slow-firing (tonic) state and raised the concentration of DA in dialysate obtained from the NAc; no reliable increases in mean firing rate or phasic bursting were noted. FSCV is well-suited to register rapid local changes in DA concentration, but due to the subtraction of the background signal, this method is insensitive to slow, sustained changes in DA tone such as those that accompany an increase in the ratio of DA neurons in the tonic-firing and inactive states. Thus, the discrepancy between the results reported here and those obtained by means of FSCV could have arisen because of the differential sensitivity of the two neurochemical measurement methods to the phasic and tonic activity of DA neurons.

Montague and colleagues (2004) have modeled the dynamics of phasic DA release and have shown that they can account for observations of stimulation-induced release in the caudate-putamen terminal field with three adaptive processes: a short-lasting facilitation, a short-lasting depression, and a longer-lasting depression. If the dynamics of phasic DA release in the NAc are similar to those in the caudate-putamen, the model proposed by Montague et al. may resolve an apparent conundrum: the observations that phasic DA responses disappear rapidly during free-operant self-stimulation but appear reliably following every stimulation train when a 10-second time-out is interposed after the delivery of each reward (Cheer et al., 2005). However, the model does not appear to account for the failure of a 30-minute rest period to restore phasic DA release in the Garris et al. study. The estimated time constant of the longer-lasting depression in the study of Montague et al. was 12-15 minutes, and thus substantial

recovery would be predicted after a 30-minute rest period. Indeed, reliable phasic DA responses to repeated stimulation of the MFB at 20-minute intervals have been observed in numerous studies (Ewing, Bigelow, & Wightman, 1983; Kuhr, Ewing, Near, & Wightman, 1985; Michael, Ikeda, & Justice, 1987a; Michael, Ikeda, & Justice, 1987b). Thus, the failure of the 30-minute rest period to restore phasic DA release in the Garris et al. study remains puzzling.

It would be interesting to repeat the measurements obtained by Montague and colleagues with voltammetry probes located in the NAc. On the basis of the observed DA dynamics and a model linking voltammetric and microdialysis measurements, one could determine whether the observations of DA tone reported here could be predicted from the dynamics of phasic release. Such correspondence would lend force to the view that the microdialysis signal represents nothing more than a lagged spatiotemporal integral of the local transients recorded by means of FSCV. On that view, the discrepancies between the results reported by Garris et al.(1999) and those described here are difficult to reconcile. In contrast, failure to predict the microdialysis signal from the observed dynamics of phasic DA release alone would lend force to the argument that there are processes, such as the transition from the inactive to the tonic activity state of DA neurons, that contribute to DA tone in a manner independent of phasic bursting. That view can readily account for the discrepancies between the results reported by Garris et al.(1999) and those described here.

Schultz (1998; 2002) has argued that DA neurons carry multiplexed signals that vary over different time scales and play different functional roles. This view is consistent with proposals that attribute to DA tone a role in determining response vigor (Niv et al.,

2006; Salamone, 2002; Salamone et al., 2003; Salamone et al., 1997), in regulating responsiveness to phasic DA signaling (Blackburn, Pfau, & Phillips, 1992), or in modulating circuitry that computes reward value (Conover & Shizgal, 2005; Hernandez et al., 2006). Testing these hypotheses requires measurement of the tonic as well as the phasic component of DA signaling. The results reported here complement those obtained by means of FSCV and broaden the description of the DA dynamics that accompany intracranial self-stimulation.

CHAPTER 5

*Potentiation of intracranial self-stimulation during prolonged subcutaneous infusion
of cocaine*

Giovanni Hernandez, Eric Haines, & Peter Shizgal

Hernandez, G., Haines, E., & Shizgal, P. (2008). Potentiation of intracranial self-stimulation during prolonged subcutaneous infusion of cocaine. *Journal of neuroscience methods*, 175(1), 79-87. Reproduced with permission.

Introduction

The neurochemical basis of reward has long been studied by assessing drug-induced changes in operant performance for rewarding electrical brain stimulation (Poschel and Ninteman, 1963; Stein, 1964; Crow, 1970). For several decades, the “curve-shift” method has served as the principal means of measuring such effects. The curve-shift method entails measuring the vigor of performance (e.g., response rate) over a range of stimulation strengths (e.g., pulse frequencies or currents). Variation in the strength of the stimulation required to produce a criterion level of performance is interpreted to reflect drug-induced changes in the strength of the rewarding effect whereas variation in the asymptotic vigor of responding is interpreted to reflect changes in performance capacity (Edmonds and Gallistel, 1974; Gallistel et al., 1982; Gallistel and Freyd, 1987; Rompre and Wise, 1988). The results of such experiments (Franklin, 1978; Gallistel et al., 1982; Gallistel and Freyd, 1987; Rompre and Wise, 1988), serve as a cornerstone for the dopaminergic theory of reward (Wise and Rompre, 1989).

Recently, Arvanitogiannis and Shizgal (2008) have shown that results obtained by means of curve-shift scaling are fundamentally ambiguous. Indistinguishable shifts can be produced by actions of drugs at different stages of the circuitry that translates the stimulation-evoked neural firings into behavior. For example, the same curve shifts can be produced by changes in sensitivity to work requirements and by changes in the reward threshold. Such ambiguity can be removed by measuring operant performance as a function of both the strength and the cost of reward.

Psychomotor stimulants, such as cocaine, produce particularly robust changes in performance for rewarding brain stimulation, as measured by means of curve shifts

(Bauco et al., 1993; Bauco & Wise, 1997b; Carlezon & Wise, 1993; Wise & Munn, 1993). Application of the new testing paradigm proposed by Arvanitogiannis and Shizgal (2008) would help pinpoint both the stage of processing at which drugs produce their performance-modulating effects and the psychological processes (reward, sensitivity to work requirements, etc.) responsible for the observed changes in behavior. However, the new paradigm requires collection of substantially more data than the curve-shift method. In order to obtain a complete dataset in an efficient manner, long test sessions (~4 hours in duration) must be run repeatedly. The validity of the results depends on the stability of the neurochemical effects of the drug treatments and the state of the reward circuitry, both within and across the repeated, long test sessions.

Intraperitoneal (ip) injection has been the most common route of cocaine administration in prior intracranial self-stimulation (ICSS). The relatively short half-life of cocaine, between 24 and 28 min (Carmona et al., 2005), does not pose a serious problem for curve-shift measurements, which can be obtained quickly, but renders intraperitoneal injection an inappropriate method for use with measurement methods, such as the one developed by Arvanitogiannis and Shizgal, that require behavioral and neurochemical stability over several hours. The requisite stability could, in principle, be achieved with an appropriate regimen of intravenous (iv) infusion, but this method is not ideal in the case of studies that extend over several months. The intravenous catheters are prone to infection and loss of patency, which limits their effective lifespan (between 17 and 30 days, according to Foley et al.,(2002).

When injected via the subcutaneous (sc) route, cocaine has a longer half-life, 1.8 to 2 h, than when administered via the ip or iv routes (Nayak, Misra, & Mule, 1976); the

drug does not build up in adipose tissue (Pan, Menacherry, & Justice, 1991). However, cocaine is a potent vasoconstrictive agent, and thus, sc administration at a single locus may lead to necrosis of the skin. To overcome this problem, two methods of infusion had been developed to reduce the local concentration of the drug and hence, the degree of vasoconstriction. Durazzo et al. (1994) reduced the local concentration by greatly increasing the volume of the solution injected at a single point. Joyner et al. (1993) achieved this end by increasing the area of skin under which the drug was infused. They used osmotic minipumps to drive a cocaine solution through a length of tubing fashioned from semipermeable microdialysis membrane.

These infusion methods have been used successfully (Collins, Pahl, & Meyer, 1999; Grigson, Wheeler, Wheeler, & Ballard, 2001; G. King, Kuhn, & Ellinwood, 1993; King, Joyner, Lee, Kuhn, & Ellinwood, 1992), but they are not viable alternatives for studies that require repeated long testing sessions and high rates of drug administration. The first method does not allow a precise infusion rate whereas the second is difficult to adapt to the alternating schedules of cocaine and vehicle administration that are commonly used in studies of the effects of drugs on ICSS.

This paper introduces a new method for subcutaneous administration of cocaine that is appropriate for studies requiring repeated long test sessions, high rates of drug delivery, and alternation between administration of the drug and the vehicle. The drug is dispersed under a large area of skin to avoid necrosis. Perforated Tygon® tubing was substituted for the microdialysis tubing used by Joyner et al. (1993) and a high-capacity external syringe pump for the osmotic minipump (Figure 20). This new method yields long-lasting plateaus in the level of dopamine in the nucleus accumbens, as monitored by

means of in-vivo microdialysis. In addition, stable changes in ICSS were produced by cocaine, both within and across multiple test sessions. Thus, this work sets the stage for application of the new three-dimensional scaling paradigm of Arvanitogiannis and Shizgal (2008) to understand how cocaine acts to alter performance for rewarding brain stimulation.

Materials and Methods

Subjects

Nine (9) 300-350-g male Sprague Dawley rats (Charles-River, St. Constant, QC, Canada) served as subjects. The animals were individually housed in hanging cages and maintained on a 12-h light/dark reverse cycle (lights off from 08:00 to 20:00), with ad libitum access to water and food (Purina Rat Chow). The experimental procedures were performed in accordance with the principles outlined by the Canadian Council on Animal Care.

Surgery

Atropine sulfate (0.5 mg/kg, sc) was administered to reduce bronchial secretions prior to induction of anesthesia with Ketamine (10 mg/kg) - Xylazine (100 mg/kg) ip. Before the rat was mounted in the stereotaxic apparatus, the topical anesthetic, Xylocaine, was applied to the external auditory meatus to reduce discomfort from the ear bars. An intramuscular injection of Penicillin G (300,000 IU/kg) was given to reduce the chances of sepsis. After the rat was mounted in the stereotaxic apparatus, anesthesia was maintained with Isoflurane. A 20 gauge guide cannula (Plastics One, Roanoke, VA) for microdialysis was stereotaxically aimed at the left NAc (1.5 AP, 2.8 ML, and -5.4 DV

from skull at a 10 degree angle). The cannula was secured to the skull with dental acrylic and stainless-steel screw anchors.

As illustrated in Figure 20, a row of perforations, spaced roughly 0.5 cm apart, was made in the central 18-cm segment of a 24 cm length of Tygon® S-54-HL tubing (i.d.: 0.508 mm; o.d.: 1.52 mm; Saint-Gobain Performance Plastics, Akron, OH). The perforations were made with a 25 gauge needle, which produced a puncture with an approximate diameter of 0.23 mm. One end of the Tygon® tubing was thermally sealed and attached with heat-shrinkable tubing to the other end, thus forming a loop. The holes were oriented outwards so as to prevent the drug from pooling within the area enclosed by the loop. The tubing was cold sterilized using CIDEX®-OPA (Johnson & Johnson Gateway, Toronto, ON) for 24 hour prior to implantation and then flushed with sterile saline.

A 2 cm incision was made in the caudal region of the dorsal skin, and a large subcutaneous pocket was opened between this incision and the one that had been made in the scalp for implantation of the cannula. The loop of tubing was then introduced into the pocket with its open end protruding from the incision in the scalp. A length of 22 gauge stainless-steel tubing bent at 90° angle, was attached to the open end. The stainless-steel tubing was secured with dental acrylic and two additional screw anchors.

At the end of the surgery, the rats were injected with buprenorphine (0.05 mg/kg, sc) to reduce post-operative pain and with sterile saline solution (1 ml/kg, sc) to facilitate reestablishment of hydromineral balance. The rats recuperated for 5 to 7 days post-surgery before the microdialysis sessions.

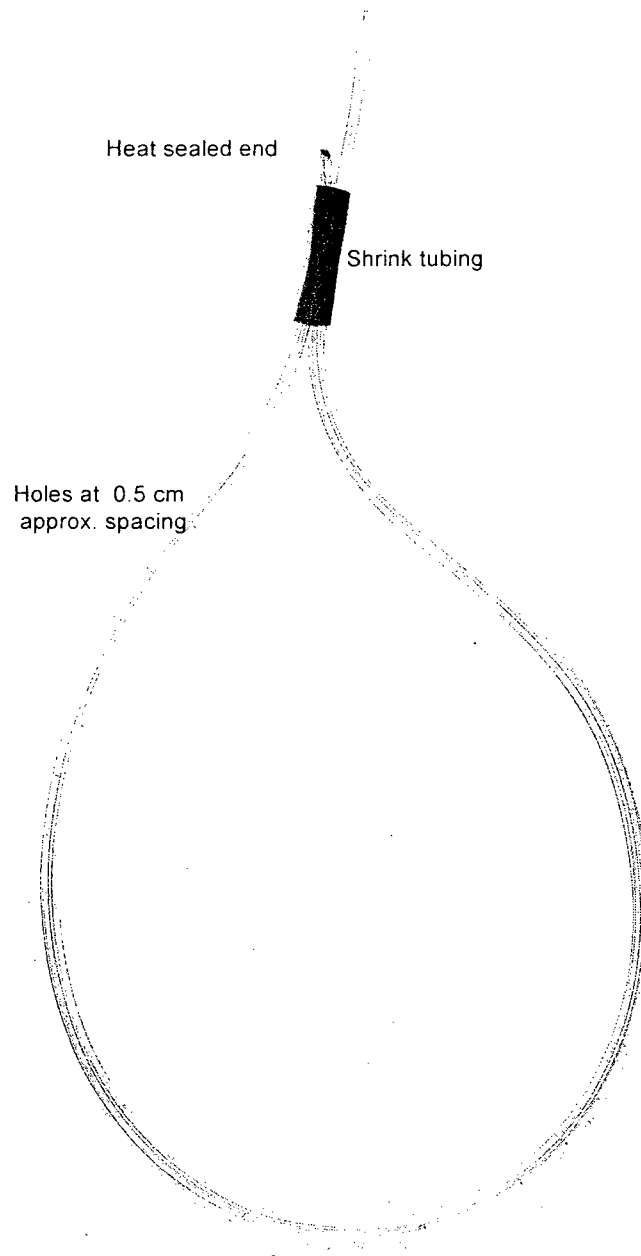


Figure 20. Perforated tubing for prolonged subcutaneous infusion of cocaine.

In-vivo microdialysis

Testing was conducted in operant chambers (from which the levers had been removed) with Plexiglas walls and stainless-steel mesh floors, (30 cm long X 21 cm wide X 51 cm high). Each testing chamber was housed in a dark Styrofoam enclosure with a small opening at the top. All testing took place during the dark phase of the circadian schedule. A description of the microdialysis probe can be found in Hernandez et al. (2006).

Sixteen hours before the beginning of each microdialysis experiment, the rats were transported to the testing room and anesthetized lightly with isoflurane. The cannula obturators were removed, and then the microdialysis probes were fixed in position and connected to the microdialysis pump (Harvard Syringe Pumps model 11; Harvard Apparatus Saint Laurent, QC). To prevent occlusion and to help stabilize the probe/brain interface, the probes were perfused with artificial cerebrospinal fluid (ACSF; 145 mM Na⁺, 2.7 mM K⁺, 1.22 mM Ca²⁺, 1.0 mM Mg²⁺, 150 mM Cl⁻, 0.2 mM ascorbate, 2 mM Na₂HPO₄, pH = 7.4 ± 0.1) at a rate of 0.3 µl/min. The rats remained in the testing chambers overnight and were provided with ad libitum food and water. Before the start of the microdialysis experiment, the food pellets were removed from the testing cages, but the water drinking tubes were left in place. The flow rate was increased to 1.0 µl/min, and dialysate samples were collected every 20 minutes. Baseline sampling continued until the dopamine (DA) concentration in three consecutive microdialysis samples fluctuated by ≤5%.

Subcutaneous infusions

After the DA baseline stabilized, either sterile saline or a solution of cocaine hydrochloride in sterile saline, pH normalized with .1NaOH to 7 ± 0.1 was pumped through the loop of tubing at a rate of 0.375 ml/h by means of an external pump (Harvard Syringe Pumps model 22, Harvard Apparatus Saint Laurent, QC). The drug was delivered at a rate of 10 mg/kg/h. After a six-h period of drug administration and microdialysis sampling, saline-filled syringes were substituted for those containing the drug solution, and the microdialysis probes were removed. The saline infusions then continued overnight. The regimen of cocaine and saline infusions was repeated three times over consecutive days to determine whether skin lesions developed.

Analytical chemistry

High performance liquid chromatography (HPLC) was used to isolate DA from other chemical species present in the dialysate; quantification was carried out using electrochemical detection (ED). Manual injection ports (Rheodyne 7125; Rheodyne LLC, Rohnert Park, CA; 20 μ l loop) were used to load the samples into a reverse-phase column (15 x .46 cm Spherisorb-ODS2, 5 μ m; Higgins analytical, Mountain View, CA) which separated the dialysate contents; then the separated material passed through dual-channel ESA (Chelmsford, MA) coulometric detectors (Coulochem 5100, with a model 5011 analytical cell), which reduced and oxidized DA and its metabolites, 3,4-dihydroxyphenylacetic acid (DOPAC) and homovanillic acid (HVA); one channel reduced DA whereas the other channel oxidized the metabolites. Calibration was carried out with standard samples of known concentrations of DA and metabolites. The mobile phase (17% acetonitrile 40 mg, 0.076 M SDS, 0.1 M EDTA, 0.058 M NaPO₄, 0.03 M

citric acid, pH = 3.35) was circulated at a flow rate of 1.2 ml/min by Waters 515 HPLC pumps (Lachine, QC). The data were analyzed and integrated using an EZChrom Chromatography Data System (Scientific Software, Inc., San Ramon, CA) installed in a PC computer. The samples were analyzed using two HPLC-ED systems running in parallel.

Histology

After the completion of the experiment, a lethal dose of sodium pentobarbital was administered. The animals were then perfused intracardially with 0.9% sodium chloride, and decapitated. Their brains were collected and fixed with 10% formalin solution for at least 7 days. Coronal sections of 30 μ m thickness were cut with a cryostat. Probe locations were determined microscopically at low magnification with reference to the stereotaxic atlas of Paxinos and Watson (1998).

Statistics

The levels of the assayed substances were expressed as concentrations. Basal values are the mean of the three samples obtained prior to the start of the drug infusion.

Due to the presence of outliers, the mean DA concentration at each time point was calculated using Tukey's robust bisquare estimator. A bootstrapping procedure (Efron, 1979), implemented in S-plus software (Insightful Corporation) was used to compute the robust 95% confidence intervals around the robust means.

Results

The location of the microdialysis probes are shown in figure 21. 7 of the 9 probes penetrated the shell of the NAc at coronal planes corresponding to Plates 11 and 12 of Paxinos and Watson's (1998) atlas. The data from the two probes that missed the NAc target were excluded from the analysis.

Time course of DA concentration across conditions

The time course of the changes in DA concentration is shown in figure 22. During the first 2 h 40 min of cocaine infusion, the average concentration of DA in the dialysate increased steadily to 521% of the baseline value. There was little systematic change during the remaining 3 h 20 min. Thus, a relatively stable and long-lasting plateau in the DA concentration was achieved. During the saline infusion, DA levels remained very close to the values observed for the baseline period; the average values remained within 101% to 121% of the baseline value.

From the second sample collected after the beginning of the cocaine infusion, each of the increases in DA concentration is statistically different from the baseline values, as inferred from lack of overlap of the 95% confidence regions. By the same criterion, none of the average values for samples collected more than 2 h 40 min after the start of the cocaine infusions differ from each other. The DA concentration of only two of the samples collected during saline infusion differs from the baseline value; these changes are small (121% of baseline at 220 min and 118% at 340 min). There averages of the DA concentrations in the three sets of baseline samples obtained prior to cocaine or saline infusions were statistically indistinguishable. In contrast, the average values

obtained during the cocaine and saline infusions did differ from the second sample onwards.

Absence of necrosis

Figure 23 presents a photograph of the dorsal surface of seven of the rats in which necrosis of the skin was not evident after cocaine infusions. The tissue immediately surrounding the Tygon tubing appeared normal, on post-mortem inspection. However, an area of necrosis, roughly 1-2 cm in diameter, was seen in two other rats. Post-mortem examination revealed that the Tygon tubing had broken at the junction with the stainless-steel tubing and therefore cocaine was delivered at a single subcutaneous point in these subjects.

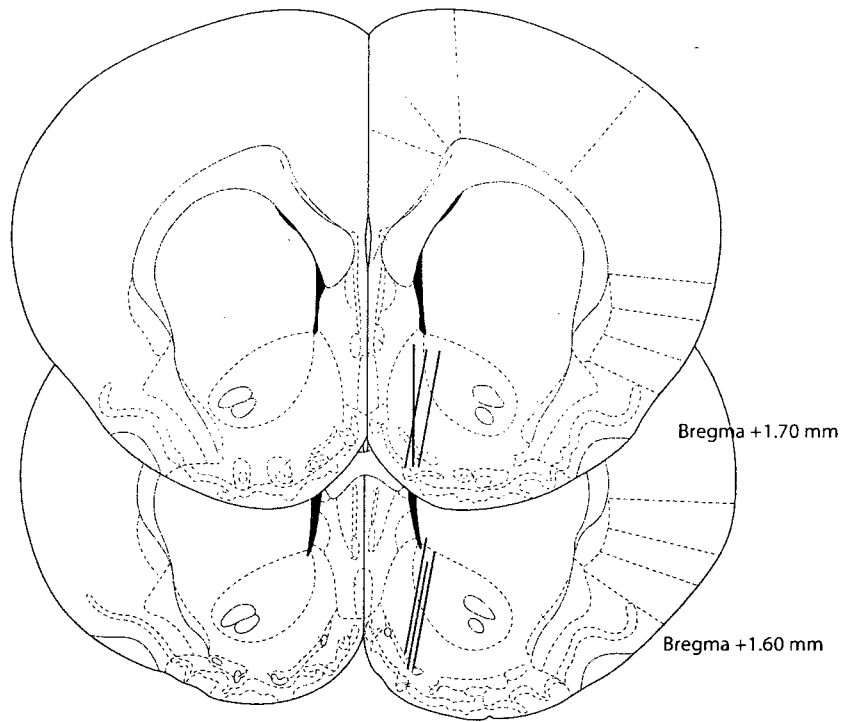


Figure 21. Location of the microdialysis probes. The tip of the probes penetrated the shell of the NAC at coronal planes corresponding to Plates 11 and 12 of Paxinos and Watson's (1998) atlas.

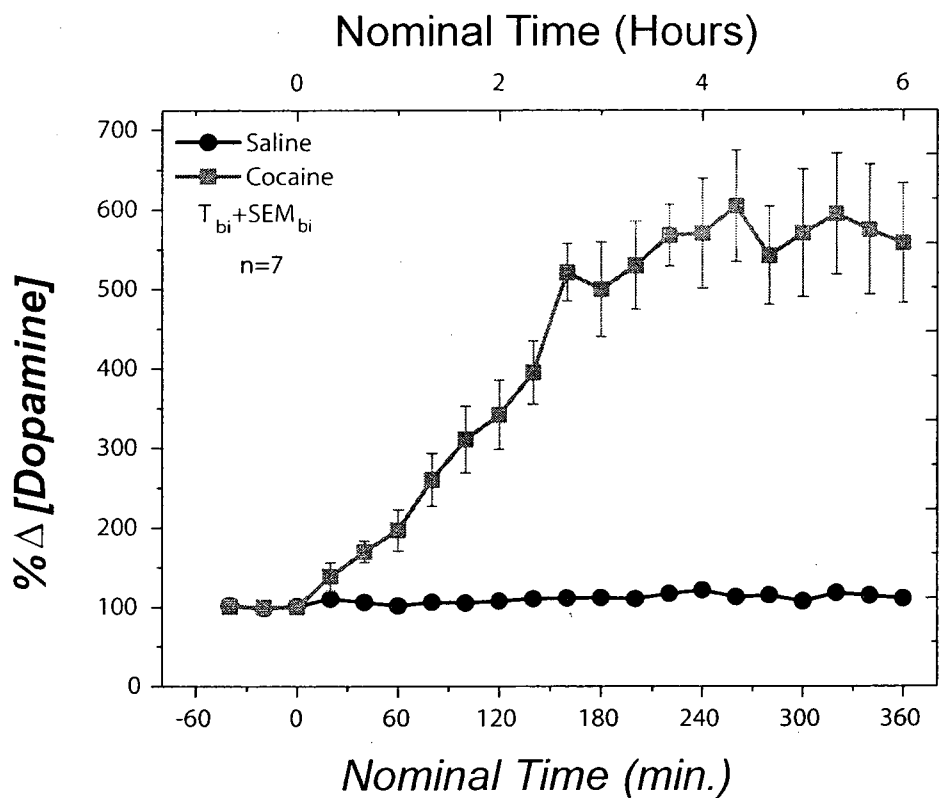


Figure 22. The time course of the changes in DA concentration during subcutaneous infusion of saline or cocaine. The concentration of DA in the dialysate remains nearly constant throughout the 6 h infusion of saline. In contrast, during the cocaine infusion, the DA concentration increased steadily during the first 2 h 40 min and then levelled off, showing little systematic change during the remaining 3 h 20 min.



Figure 23. Photograph of the dorsal surface of the seven rats in which the subcutaneous tubing remained patent. No necrosis of the skin was evident after the cocaine infusions.

Discussion Experiment 1

The results of this experiment demonstrate that the method introduced here for continuous subcutaneous administration of cocaine can produce stable plateaus of elevated DA tone without compromising the integrity of the skin. The neurochemical data suggest that, as intended, a steady state was achieved between absorption and distribution of cocaine on the one hand, and elimination of the drug on the other.

In another experiment, we have used this method successfully with different cocaine dosages over periods as long as 6 months, without evidence of skin lesions. Thus, this method allows stable plateaus in DA concentration in the brain to be achieved repeatedly and safely.

Experiment 2 complements Experiment 1 by asking whether stable behavioral data can be obtained during the continuous-infusion regimen. Changes in the effectiveness of rewarding brain stimulation were measured by means of the curve-shift method during cocaine or saline infusions in multiple sessions spread over many weeks. Thus, Experiment 2 also tests the view that cocaine-induced changes in performance for rewarding brain stimulation undergo neither sensitization nor tolerance during a distributed regimen of sc drug administration (Bauco and Wise, 1997).

Experiment 2

Material and methods

Subjects

Four (4) 300-350-g male Long-Evans rats (Charles-River, St. Constant, QC) served as subjects. The rats were housed as in Experiment 1.

Surgery

The surgery procedures were the same as those in Experiment 1 except that stimulation electrodes were implanted instead of cannulas. The electrodes were aimed bilaterally at the lateral hypothalamic level of the medial forebrain bundle (-2.8 AP, 1.7 ML, and -8.8 DV from skull). The monopole stainless-steel electrode (0.25 mm diameter) was insulated with Formvar except for a 0.5- mm region at the electrode tip. Two stainless steel screws fixed in the skull, around which the return wire was wrapped, served as anode. The ensemble was secured to the skull with dental acrylic.

Self-Stimulation Training

A 0.5-s train of cathodal, rectangular, constant-current pulses, 0.1 ms in duration, was used to shape the experimental subjects to lever press. Shaping took place in similar boxes as the ones used during the microdialysis experiment, but equipped with one retractable lever located on the right wall and a cue light positioned 1.5 cm above the lever. During screening and initial training a continuous reinforcement schedule was in force. The temporal characteristics of the stimulation were set by digital pulse generators, and the amplitude was regulated by constant-current amplifiers. An oscilloscope (Tektronix Model TDS1002, Beaverton, OR), which read the voltage drop across a 1-k Ω

resistor (1% precision) in series with the electrode was used to monitor the stimulation currents. Low currents (200 μ A) and frequencies (25 Hz) were used at the start of shaping and then increased gradually until the rats pressed the lever reliably. Subjects that showed behavioral signs of aversion in response to the stimulation were eliminated from the study.

The experimental subjects used in the present study worked for currents between 250 and 400 μ A. After the rats were trained to press the lever, they were introduced to the procedure for obtaining curves that relate the proportion of time the lever was depressed ("time allocation") to the pulse frequency. The pulse frequency was decreased from trial to trial by 17% over a range that drove time allocation from maximal to minimal levels. During collection of the time-allocation-versus-frequency curves, the rewarding stimulation was delivered according to a 1 s, free-running (zero-hold), variable-interval schedule (FV11). To earn a reward under this schedule, the rat had to be holding down the lever at the time when the programmed inter-reward interval timed out (Conover and Shizgal, 2005).

Procedure

Cocaine hydrochloride dissolved in saline (0.9% sodium chloride) was administered subcutaneously at a constant infusion rate (0.375 ml/h) via an external infusion pump connected to the porous subcutaneous tubing described above. Each animal received six infusions of 3 and 10 mg/kg/h of cocaine in a counterbalanced order. A wash-out and recovery period of 48 or 72 hours was provided following each cocaine infusion. Cocaine was administered on Tuesdays and Fridays. A saline session preceded each cocaine session by 24 h on Mondays and Thursdays.

The self-stimulation tests began two hours after the start of the cocaine or saline infusion. The first determination of the time-allocation-versus-frequency curve was considered a warm-up and not considered in the analysis. Thus, the collection of the behavioral data was almost entirely restricted to the period when the cocaine-induced elevation in DA concentration was shown to be stable in Experiment 1.

Statistical Analysis

A repeated-measures analysis of variance (ANOVA) was used to compare the common logarithms (\log_{10}) of the pulse frequencies that yielded half-maximal time allocation ($\log F_{TA50}$) during infusion of saline and cocaine. The $\log F_{TA50}$ values were derived by fitting a sigmoid curve to the time-allocation values for each determination, as described in an earlier paper (Hernandez et al., 2006), and normalized to the average value for the saline condition. Thus, the average baseline values were set to zero, and the cocaine-induced shifts are represented as deviations, in the logarithmic domain, from this baseline. We refer to the normalized shifts in the $\log F_{TA50}$ values as “curve shifts.” Tukey’s honestly significant difference (HSD) post-hoc test was used for testing the significance pair-wise comparisons. A level of $p < .05$ for a two-tailed test was the criterion for statistical significance.

Results

The histological reconstruction of electrode-tip locations is shown in Figure 24. All of the electrode tips were located within the lateral hypothalamus, in the coronal planes corresponding to Plates 24 and 25 of Paxinos and Watson’s (1998) atlas.

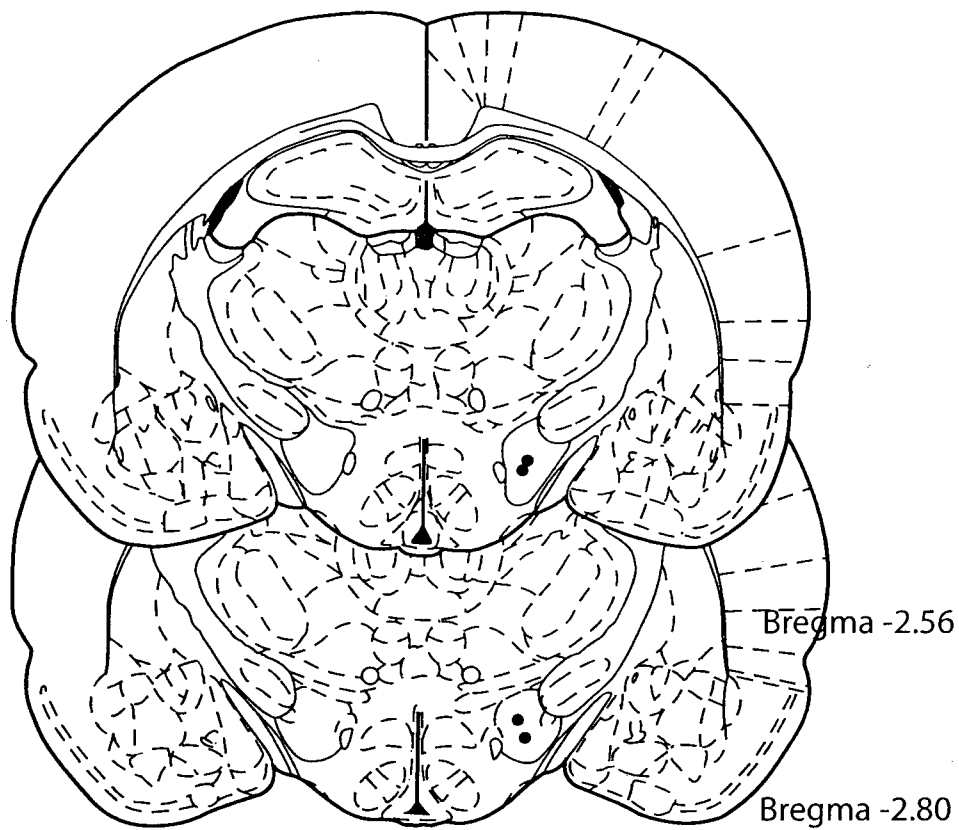


Figure 24. Location of electrode tips. All of the electrode tips were located within the lateral hypothalamus, in the coronal planes corresponding to Plates 24 and 25 of Paxinos and Watson's (Paxinos & Watson, 1998) atlas.

Cocaine-induced curve shifts

In Figure 25, time allocation is plotted as function of pulse frequency for each of the subjects. The mean time allocation for each frequency under each condition is shown along with the corresponding standard error of the mean. All the subjects showed an orderly leftward displacement of the time-allocation-versus-frequency curve, which was scaled by the drug dosage; the 3 mg/kg/h dose produced a smaller leftward displacement, than the 10 mg/kg/h dose. At the 3 mg/kg/h dose, the leftward displacement of the curve ranged from 0.05 log units (subject E6) to 0.16 log units (subject E1) whereas for the 10 mg/kg/h dose, the leftward displacement of the curve ranged from 0.25 log units (subject E5-E6) to 0.31 log units (subject E7).

Figure 26 shows the across-subject and across-session average of the curve shifts observed in each determination. The downward displacement of the cocaine data (gray) in Figure 26 reflects the leftward displacement of the time-allocation-versus-frequency curves in Figure 25. During the saline infusions, the normalized $\log F_{TA50}$ values (black) remained stable across determinations. During the cocaine infusions, there was minor variation in the magnitude of the curve shifts across determinations, but overall, the shifts are quite stable. The average curve shift observed at the 3 mg/kg/h dosage of cocaine was $0.116 \pm 0.0051 \log_{10}$ units whereas at the 10 mg/kg/h the average shift was $0.272 \pm 0.0048 \log_{10}$ units. Mauchly's test shows that the assumption of sphericity has been violated for the main effect of determination, $\chi^2_{(35)} = 55.63, p < 0.05$ and of the interaction between determination and drug dosage $\chi^2_{(135)} = 199.45, p < 0.05$. Therefore, the degrees of freedom were corrected using Greenhouse-Geisser estimates of sphericity ($\epsilon = .548$ for the main effect of determination, and $\epsilon = .366$ for the interaction). The ANOVA shows a

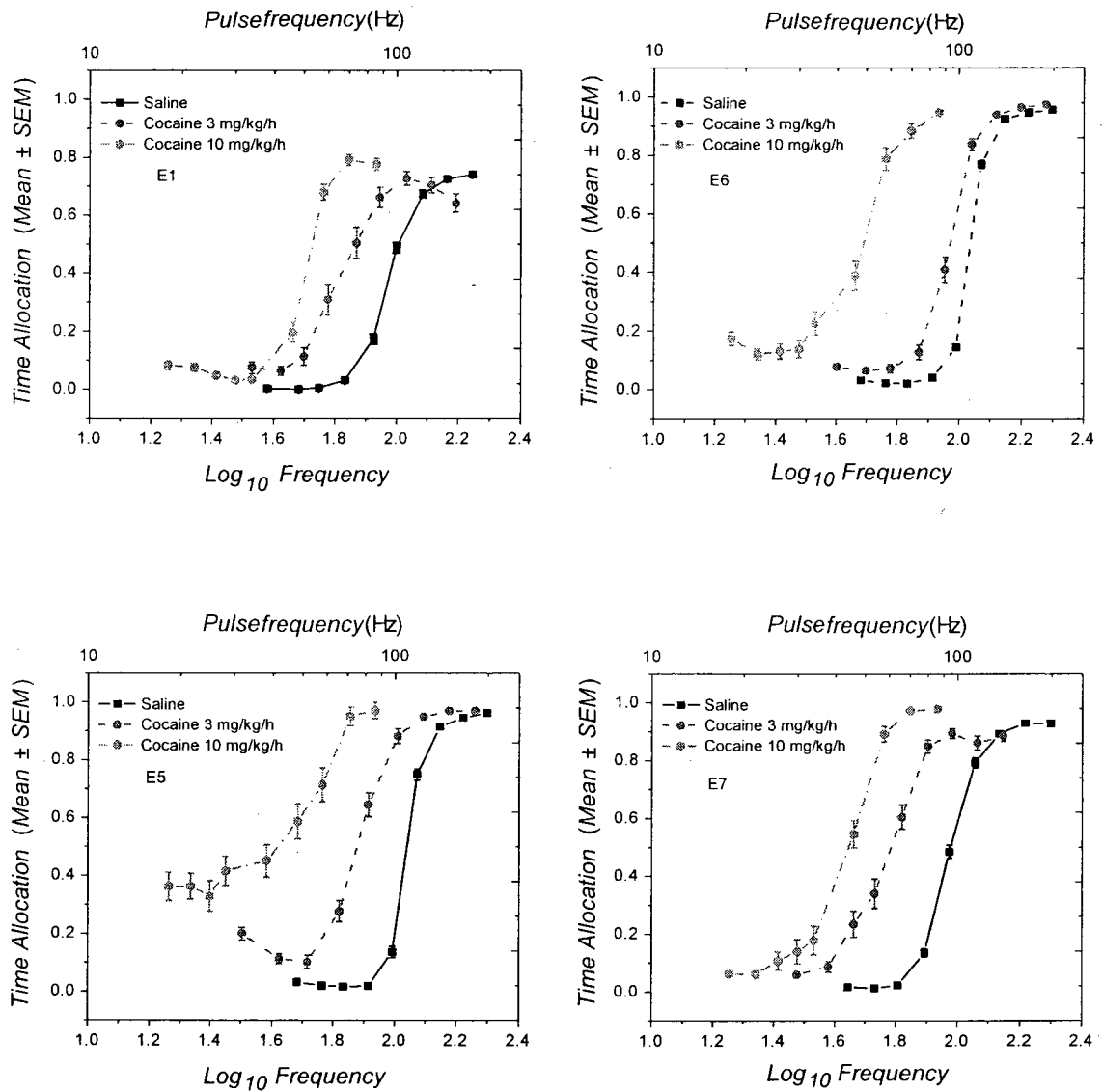


Figure 25. Time allocation is plotted as function of pulse frequency for each of the subjects. All the time-allocation-versus-frequency curves were displaced leftward during cocaine infusions, to a degree scaled by the drug dosage; the 3 mg/kg/h dose produced a smaller leftward displacement than the 10 mg/kg/h dose.

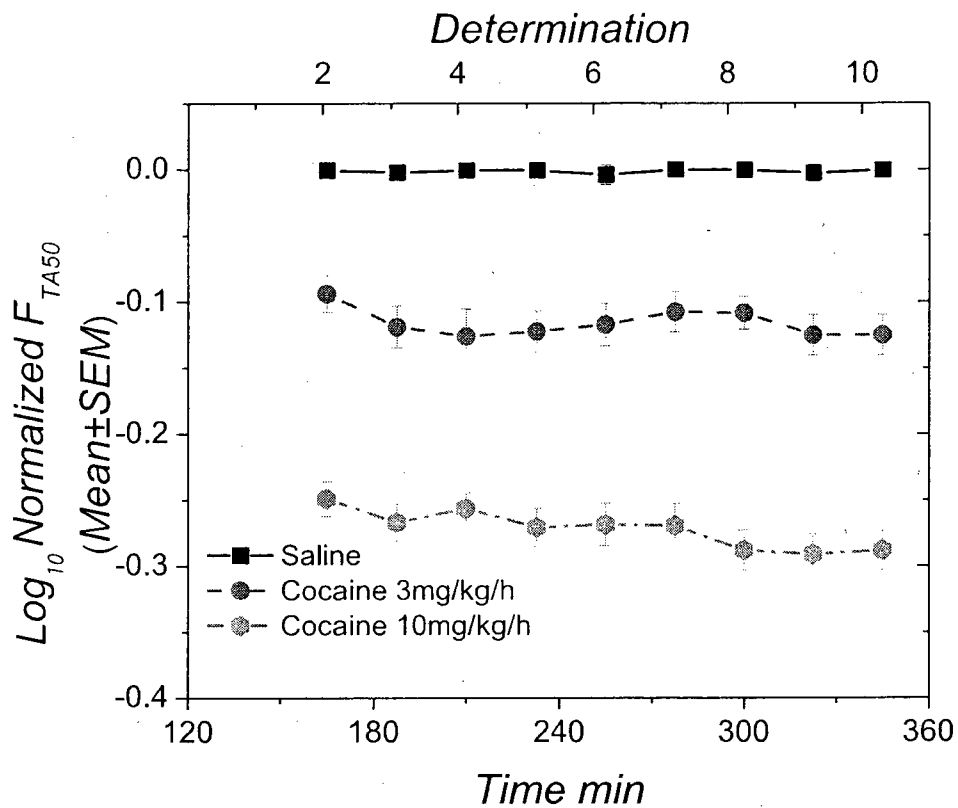


Figure 26. Across-subject and across-session average of the curve shifts observed in each determination. During the saline infusions, the normalized logFTA50 values (black) remained stable across determinations. During the cocaine infusions, there was minor variation in the magnitude of the curve shifts across determinations, but overall, the shifts were quite stable. The average curve shift observed at the 3 mg/kg/h dosage of cocaine was 0.116 ± 0.0051 log10 units whereas at the 10 mg/kg/h dose, the average shift was 0.272 ± 0.0048 log10 units.

main effect for the drug dosage $F_{(2, 38)} = 192.417, p < 0.05$; but not for the determination $F_{(4.387, 83.34)} = 1.645, p > 0.05$ nor for the interaction between the drug dosage and determination $F_{(5.85, 111.3)} = 1.096, p > 0.05$. The data from both drug conditions and the saline condition differed statistically from each other, as revealed by Tukey's HSD post-hoc test, indicating that the magnitude of the curve shift was a function of the drug dosage.

Figure 27 shows the across-subject and across-determination average of the curve shifts observed in each test session. Whereas Figure 26 illustrates the stability of the effect of cocaine within sessions, Figure 27 illustrates the stability of these effects across sessions.

The variability in the data from the saline condition (black) is particularly low. Although there is some drift in the effects of cocaine over multiple test sessions, the changes are minor. Mauchly's test shows that the assumption of sphericity has been met for the main effect of session, $\chi^2_{(14)} = -1.97, p > 0.05$; drug $\chi^2_{(2)} = 1.21, p > 0.05$ and for the interaction between session and drug dosage $\chi^2_{(54)} = 65.36, p > 0.05$. The ANOVA shows a main effect for the drug dosage $F_{(2, 4)} = 88.35, p < 0.05$; but not for the session $F_{(5, 10)} = 1.73, p > 0.05$ nor for the interaction between the drug dosage and session $F_{(10, 20)} = 0.68, p > 0.05$. The data from both drug conditions and the saline condition differed statistically from each other.

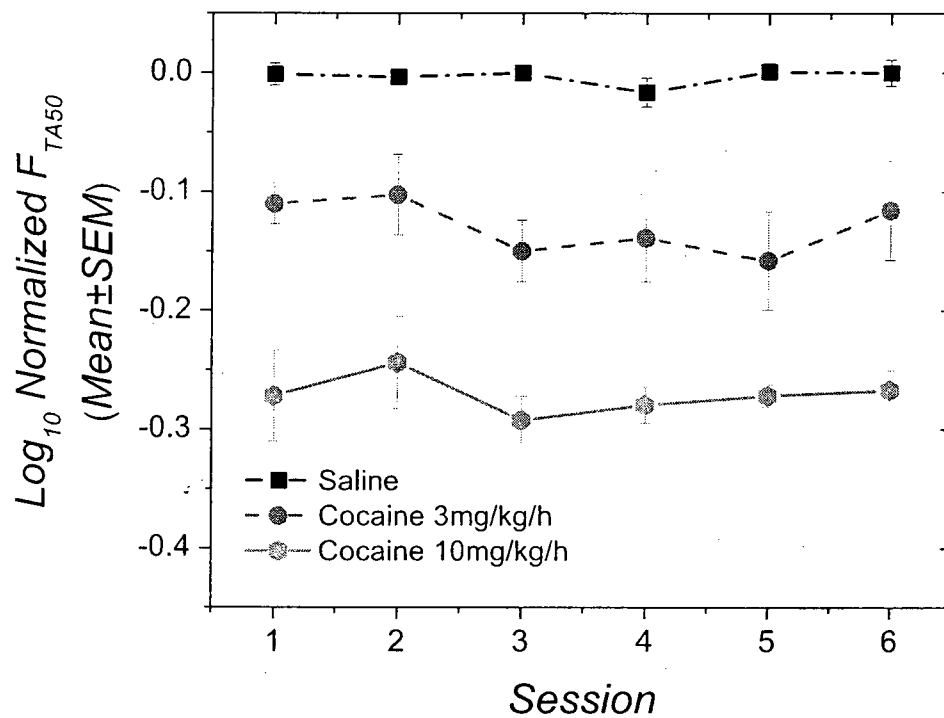


Figure 27. Across-subject and across-determination average of the curve shifts observed in each test session. During the saline infusions, the normalized $\log F_{TA50}$ values (black) remained stable across sessions. During the cocaine infusions, there was minor variation in the magnitude of the curve shifts across sessions, but overall, the shifts were quite stable

Discussion Experiment 2

Continuous subcutaneous infusion of cocaine produced substantial, systematic leftward curve shifts that approached an average of 0.3 \log_{10} units at the 10 mg/kg/h infusion rate (almost halving F_{TA50}) and exceeded an average of 0.1 \log_{10} units at the 3 mg/kg/h infusion rate. These curve shifts were stable over the four-hour test sessions, mirroring the plateau in elevated dopamine levels observed in Experiment 1. The curve shifts were also stable over repeated test sessions, a result consistent with those obtained by Bauco and Wise (1997) and by Frank et al. (1988) with ip injections of cocaine. Similar stability of ICSS data across multiple sessions of drug treatment has also been noted in the case of other drugs of abuse (Baucu et al., 1993; Baucu & Wise, 1994; Carlezon & Wise, 1993; Esposito & Kornetsky, 1977).

In the present study, cocaine was administered twice per week, whereas in the 1992 study of Frank et al. (Experiment 1), cocaine was administered daily, and in Groups 1-4 in the Baucu and Wise study (1997), the drug was administered every 48 h. The maximum dose in the Baucu and Wise study was 32 mg/kg whereas Frank et al. injected 30 mg/kg, and a total dose of 18 - 60 mg/kg was administered in the present study. Measurements of cocaine concentrations in brain and plasma (Carmona et al., 2005) imply that the drug was still present at the time of ICSS testing in all three of these studies. Thus, over a range of doses, injection frequencies and routes of administration, neither tolerance nor sensitization is seen in the cocaine-induced potentiation of intracranial self-stimulation when the behavioral testing period coincides with the direct pharmacological actions of the drug. These results contrast with some of those observed when the effect of cocaine on ICSS was measured following the cessation of an acute

(Frank et al., 1992) or chronic (Kokkinidis & McCarter, 1990) high-dose regimen of administration. Under those conditions, tolerance to the potentiating effect of cocaine on ICSS has been noted.

Dopamine depletion (Dackis & Gold, 1985) and changes in the expression of pre- and post-synaptic receptors (Hammer, Egilmez, & Emmett-Oglesby, 1997) are among the potential mechanisms proposed to explain cocaine tolerance. The twice-weekly regimen of drug administration employed in the present study appears to allow recovery of the dopaminergic system from each cocaine challenge prior to the next ICSS test session. Conceivably, the extensive electrical stimulation of the medial forebrain bundle delivered during the training phase of the study decreases the vulnerability of dopaminergic neurotransmission to repeated cocaine challenges.

In one study, some sensitization of the effect of cocaine was observed when ICSS was assessed 24 h after the cessation of five-day periods of daily cocaine administration (Kokkinidis and McCarter, 1990). The absence of sensitization effects in the current study and several previous ones (Frank et al., 1988; Frank et al., 1992; Bauco and Wise, 1997) may reflect differences in the schedules of drug administration and/or compensatory neuroadaptations to periodic administration of cocaine. Rewarding electrical stimulation of the medial forebrain bundle has been shown to down-regulate the expression of the glutamate receptor type 1 sub-unit (GluR1) in the VTA (Carlezon et al., 2001). In contrast, systemic administration of cocaine up-regulates GluR1 in the VTA (Churchill, Swanson, Urbina, & Kalivas, 1999; Fitzgerald, Ortiz, Hamedani, & Nestler, 1996). These two opposing influences may have cancelled under the conditions of the present study.

General Discussion

The curve-shift method has long served as the principal means of quantifying the influence of drugs on ICSS. Among the advantages of this method is its economy: typically, a curve relating the vigor of behavior to stimulation strength can be obtained in roughly 15 minutes. This feature was particularly useful in the present study, making it possible to repeat the determinations of the time-allocation-versus-frequency function often enough to assess whether a stable potentiation of ICSS had been produced by the continuous subcutaneous infusion of cocaine. The results show that this was indeed the case. The within-session stability of the behavioral data is mirrored by the neurochemical results: by two h 40 min following the onset of the continuous subcutaneous infusion of cocaine, DA levels in the nucleus accumbens attained a plateau, remaining fairly constant for another 3 h 20 min.

The cocaine-induced curve shifts were stable across multiple test sessions as well as within them. Distribution of the drug under a large area of skin circumvented the damage that can ensue from repeated infusions of a vasoconstrictive agent at a single locus. This approach had been used successfully in previous work by Joyner et al. (1993), who used osmotic minipumps to distribute cocaine via microdialysis tubing implanted under the skin. In order to accommodate an intermittent schedule of drug administration, we substituted syringe pumps for the osmotic minipumps, and in order to accommodate the much higher flow rate required in the present study (2.25 ml over 6 h), we substituted perforated silicone tubing for the microdialysis filaments.

The principal objective of this study was to produce stable elevations in DA tone and potentiation of ICSS both within and across repeated, long-duration test sessions, in a

safe sustainable manner. This objective was achieved. As a result, the infusion procedure described here can be used in future work in a conjunction with a more powerful method for measuring changes in ICSS (Arvanitogiannis and Shizgal, 2008). Unlike the curve-shift method used here, this three-dimensional scaling method can distinguish changes in the reward threshold from changes in sensitivity to work requirements. The requirement of this method for repeated, long test sessions necessitated the development of the infusion procedure described here. This procedure should prove useful as well in other behavioral paradigms, such as studies of the modulation of learning by fast-acting drugs, in which repeated long test sessions must be conducted under stable behavioral and neurochemical conditions.

CHAPTER 6

At what stage of processing does cocaine influence performance for brain stimulation reward?

Giovanni Hernandez, Yannick-André Bretron, Kent Conover, & Peter Shizgal

Introduction

The intracranial self stimulation paradigm has been used as a research tool for understanding the neural underpinning of natural rewards ever since the discovery by Olds and Milner (1954) that electrical currents, injected into different brain structures by means of metal electrodes, can serve as a positive reinforcer. During this time, there have been significant advances in methods for measuring brain stimulation reward (BSR). This chapter describes the application of the most recent and powerful of these methods to assess the role of DA in BSR.

Response-rate methods, although popular at the beginning of brain stimulation reward research, proved incapable of distinguishing between variables that affect reinforcement strength and those that affect performance capacity (Valenstein, 1964). Response rate measurements became popular because they offered an immediate gateway for quantitatively studying the properties of rewarding brain stimulation. Their appeal was based in part on the intuitive argument that the average tempo of the instrumental behaviour should be correlated with the strength of the reinforcing effect (Olds, 1966; Valenstein, 1964). Nevertheless, empirical evidence challenged this assumption. It was shown that rats preferred higher-current to lower-current stimulation despite the fact that lower response rates were supported by the higher currents (Hodos & Valenstein, 1962).

The response-rate method is particularly problematic when used to infer the effects of pharmacological agents on BSR. Response rates grow non-linearly as a function of stimulation strength, increasing in an s-shaped manner (Miliaressis, Rompre et al., 1986) and often decreasing at very high stimulation strengths, as various side-

effects of the stimulation interfere with instrumental performance, and response rate declines even as reward strength continues to grow. As a consequence of this non-linear relationship, inferences drawn from drug-induced changes in response-rate will depend on the arbitrary choice of stimulation parameters. For example, if stimulation parameters that sustain a high baseline response rate are used, a reward-potentiating drug will have little or no ability to boost responding. In contrast, if parameters that sustain a low level of baseline responding are used, the same reward-potentiating effect of the drug will produce a large increase in response rate.

The shortcomings of the response-rate method propelled the development of alternatives. The most commonly used of these second-generation paradigms is the curve-shift method (Edmonds & Gallistel, 1974; Miliaressis, Rompre et al., 1986), which adds a second dimension to response-rate measurement. Instead of measuring the vigour of behaviour directed at fixed stimulation trains, a behavioural-output measure, such as response rate, reward rate, or time allocation, is recorded as stimulation strength is varied over a range of values that drives behaviour from minimal to maximal levels. Lateral displacement of the “psychometric” curve relating stimulation strength to behavioural output is commonly interpreted to reflect a change in the strength of the reward whereas a change in asymptotic responding is commonly interpreted to reflect a change in performance capacity (Edmonds & Gallistel, 1974; Miliaressis, Rompre et al., 1986).

The common interpretation of results obtained in the curve-shift paradigm promises unambiguous discrimination of variables that affect performance from those that affect reward strength. Thus, it is not surprising that this paradigm has seen very wide use in studies on the neurochemical basis of BSR. Nevertheless, there is firm

empirical evidence that that not all lateral displacement of the psychometric curve are the product of changes in reward strength; such displacements can be produced by manipulating variables affecting performance capacity, such as changes in the physical effort required to procure the reward (Fouriez et al., 1990; Frank & Williams, 1985); in the case of the Frank & Williams study, the lateral displacement was not accompanied by a change in the asymptotic response rate. Thus, the curve-shift paradigm does not live up to the strong claims made on its behalf.

The case for the curve-shift paradigm was built on the demonstration that the response-rate measure lacked sufficient dimensionality to distinguish between changes in reward strength and changes in performance capacity. An analogous argument can be directed at the curve-shift paradigm. On this view, the curve-shift paradigm is insufficient because its underlying assumptions do not recognize that the behavioural influence of the strength and cost of reward are intertwined. In order to tease apart these two influences, a third dimension must be added to the measurement scheme: Performance must be measured and represented as a function of both the strength and cost of reward. This is the approach that was introduced by Arvanitogianis and Shizgal (2008), in their paper on the “reinforcement mountain.”

At the core of the reinforcement-mountain model is the idea that the neural activity induced by the rewarding stimulation is translated into behaviour by a multistage circuit (Gallistel et al., 1981) (See fig 28). The stimulation pulses trigger a volley of action potentials in reward-related axons coursing near the tip of the electrode; this is referred to in the literature as the “directly stimulated” stage of the circuit (or the “cable”). The output of the directly stimulated stage is integrated, over time and space, by

a later stage that functions as if to count spikes within a time window defined by the train duration. Thus, with train duration held constant, the counter is posited to produce the same output in response to a train of high-frequency, pulses that stimulate relatively few neurons (i.e., at a low current) and a train of low-frequency pulses that stimulates many neurons (i.e. at a high current) and thus elicits the same number of action potentials in the directly stimulated stage (Gallistel, 1978; Gallistel et al., 1981). The output of the integrator is shaped by a logistic *reward-growth* function (Conover & Shizgal, 2005; Leon & Gallistel, 1992; Simmons & Gallistel, 1994; Sonnenschein et al., 2003) into a signal that represents reward intensity (I), the subjective strength of the reward. Then, I gets discounted by two costs: “price” (P), which refers to the opportunity cost of the reward (the total time the rat has to hold down the lever in order to earn a reward) and “effort cost,” the perceived rate of exertion ($1+\xi$) required to perform the lever-pressing task. The comparison between the payoff from the stimulation (U_B) and the payoff from competing activities (U_E), such as exploring, grooming and resting, is described by McDowell’s (2005) extension of Herrnstein’s single operant matching law (Herrnstein, 1970, 1974) which converts U_B and U_E into the allocation of time (time allocation: TA) to the pursuit of BSR.

Combining the equations for each stage of the model proposed by Arvanitogiannis and Shizgal and factoring yields the following expression:

$$TA = \frac{\left(\frac{f^g}{f^g + f_{hm}^g}\right)^a}{\left(\frac{f^g}{f^g + f_{hm}^g}\right)^a + \left(\frac{P}{P_E}\right)^a} \quad (8)$$

where f is the frequency of the stimulation, f_{hm} is the frequency that produces half-maximal reward intensity, P is the price of a stimulation train (total time the lever must be depressed to trigger reward delivery), P_E is the price at which the rat will spend half of its time working for a reward of maximal intensity; g determines the rate at which reward intensity grows as the pulse frequency is increased, and a determines “price sensitivity,” the rate at which time allocation falls as the price of the reward is increased. This expression predicts the proportion of the rat’s time that will be devoted to the pursuit of BSR as a function of the strength and cost of the rewarding stimulation. Thus, the predicted time allocation lies on the surface of a three-dimensional structure.

Variables that affect how stimulation strength is translated into the proportion of maximal reward intensity achieved by a stimulation train act at early stages of the circuit, and displace the three-dimensional structure along the axis representing stimulation strength (e.g., pulse frequency). This displacement will be reflected in a change in the value of f_{hm} . In contrast, variables that affect effort cost act at later stages in the neural circuit, after the reward-intensity signal has been computed, displace the three-dimensional structure along the axis representing opportunity cost. This displacement will be reflected in a change in the value of P_E (Arvanitogiannis & Shizgal, 2008). Changes in the value of competing activities or in the maximum reward intensity will also change P_E .

The reinforcement-mountain model and the associated measurement method offer a new avenue for investigating and revisiting the role of different neurotransmitter systems and neural structures in the pursuit of rewarding stimulation. The present experiment employs these new tools to revisit the role of DA neurotransmission in BSR.

The BSR paradigm was used in the very first experiments on the role of DA in reward. Since that time, the involvement of this neurotransmitter in the computation and pursuit of reward has been the subject of intense study and lively controversy. The reinforcement-mountain model and the associated three-dimensional measurement method make it possible to address these issues from a new and potentially revealing perspective.

DA neurotransmission is believed to play a key role in BSR. Numerous experiments carried out using the curve-shift paradigm have shown that blockade of the DA transporter shifts the psychometric function for BSR leftwards (Bauco and Wise, 1997; Maldonado-Izarry, Stellar and Kelly, 1992): less intense stimulation parameters are needed to produce a given level of performance under the influence of DA transporter blockade. Conversely, DA receptor antagonists shift the psychometric function to the right (Franklin, 1978; Gallistel, Boytim, Gomita, & Klebanoff, 1982; Wise & Rompre, 1989).

A substantial number of hypotheses have been proposed concerning the functions that DA tone modulates. DA has been assigned a preponderant role in determining either the intensity of rewarding effect (Wise & Rompre, 1989), anticipation of reward (Blackburn et al., 1992), incentive salience (Berridge, 2007), attention and motor switching (Redgrave et al., 1999a, 1999b), the proclivity of the subject to invest effort in operant performance (Salamone et al., 2005) or the modulation of response vigour (Niv et al., 2006). Of particular interest for the present experiment are the hypotheses that assign the role of DA tone either to the translation of stimulation strength into a given portion of the maximal reward intensity, or the modulation of subjective effort costs. These two

hypotheses predict orthogonal shifts of the three dimensional structure; the former predicts that changes in DA tone should shift the structure along the frequency axis whereas the later predicts a shift along the opportunity cost axis.

In order to test the role of DA tone in brain stimulation reward, DA tone was upregulated by cocaine-induced blockade of the DA transporter. Cocaine was selected, in part, because of the large existing literature describing the effects of this drug on the pursuit of BSR. The effects of cocaine on BSR undergo neither sensitization nor tolerance over the course of long-term, repeated administration (Bauco et al., 1993; Hernandez, Haines, & Shizgal, 2008), rendering this drug particularly suitable for use with the three-dimensional measurement method.

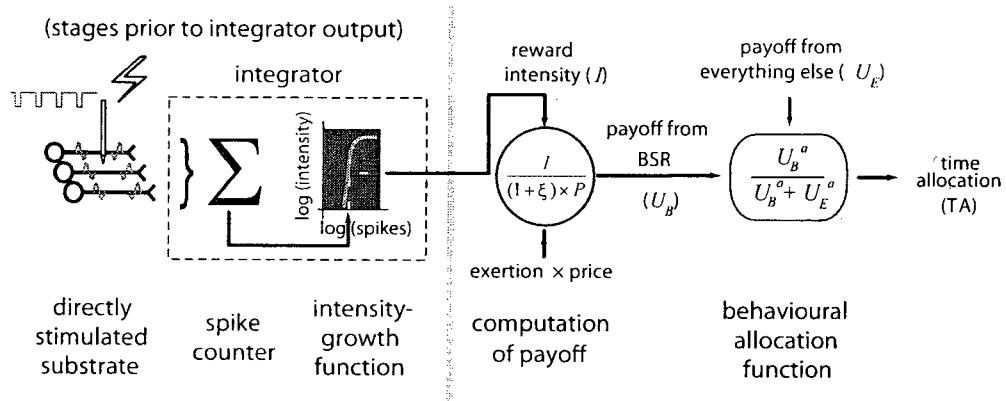


Figure 28. Translation of the stimulation-induced impulse flow into behavior (Adapted from Arvatinogiannis and Shizgal, 2008.)

Method

Subjects

Seven male Long-Evans rats, (Charles-River, St. Constant, QC, Canada) weighing 300-350g at the time of arrival, served as subjects. The animals were individually housed in hanging cages on a 12 hour light/dark reverse cycle (lights off from 08.00 to 20.00 h). with ad libitum access to water and food (Purina Rat Chow). The experimental procedures were performed in accordance with the principles outlined by the Canadian Council on Animal Care.

Surgery

Atropine sulfate (0.5 mg/kg) was administered subcutaneously to reduce bronchial secretions prior to induction of anesthesia with Ketamine (10 mg/kg) - Xylazine (100 mg/kg) ip The topical anesthetic, Xylocaine, was applied to the external auditory meatus to reduce discomfort from the ear bars, prior to mounting the rat in the stereotaxic apparatus. Penicillin G (300,000 IU/kg) was given intramuscularly to minimize the probability of sepsis. After the rat was mounted in the stereotaxic apparatus, anesthesia was maintained with Isoflurane.

Stimulating electrodes were stereotaxically aimed at the lateral hypothalamus bilaterally (-2.8 AP, 1.7 ML, and -8.8 DV from skull). The monopolar stainless steel electrodes (0.25 mm diameter) were insulated with Formvar except for the region extending 0.5 mm from the tip. The anode consisted of two stainless steel screws fixed in the skull, around which the return wire was wrapped. The electrodes were secured with

dental acrylic and skull-screw anchors. A 5- to 7-day period was provided for post-surgical recuperation before the self-stimulation training began.

Self-stimulation training

Self-stimulation of both LH sites was assessed, and the electrode that supported the most vigorous lever-pressing in the absence of motoric side effects was chosen for further testing. Shaping took place in a Plexiglas Skinner Box (30 cm length X 21cm width X 51cm height) equipped with one retractable lever located on the right wall and a cue light positioned 1.5 cm above the lever. A continuous reinforcement schedule was in force. Stimulation consisted of 0.5 s trains of cathodal, constant-current pulses, 0.1 ms in duration. The temporal characteristics of the stimulation were set by digital pulse generators, and the amplitude was regulated by constant-current amplifiers. The stimulation currents were monitored with an oscilloscope, which read the voltage drop across a 1-k Ω resistor (1% precision) in series with the electrode.

Once the rat pressed the lever consistently for currents between 250 – 400 μ A, a curve relating time allocation to pulse frequency was obtained by varying the stimulation frequency across trials over a range that drove the number of rewards earned from maximal to minimal levels; at the beginning of this sequence of trials, the pulse frequency was set to the maximal value to be used and was then decreased successively from trial to trial. The series of trials conducted to obtain a time allocation versus pulse frequency curve is called a “frequency sweep.”

A fixed-cumulative handling time schedule of reinforcement (Y. A. Breton, Marcus, & Shizgal, 2009) controlled the delivery of rewarding stimulation. Under this

schedule, a reward is delivered when the cumulative time that the lever has been depressed reaches a value set by the experimenter (the “price” of the reward). Depression of the lever was accompanied by illumination of the neighbouring cue light. As soon as the response criterion satisfied, the lever was retracted, and a stimulation train was delivered. After a 2-second delay, the lever was re-introduced into the cage, the cumulative timer was reset to zero, and the rat could resume working to obtain another reward.

Each trial consisted of a fixed time during which the price and pulse frequency parameters were held constant. The duration of each trial was sufficient to allow a rat that allocated all of its time to lever pressing to harvest 20 rewards. At the end of each trial and prior to the start of the next one, the lever retracted for 10 seconds, and the house light flashed. Two priming trains were delivered during the final 2-second of the inter-trial interval. The priming stimulation was held constant across trials and was delivered at a pulse frequency that had been shown previously to support vigorous responding; the remaining parameters were the same as those used during the test trials.

During the initial training, the price of the reward was increased from one second to four seconds, the value that would be used during the frequency sweeps throughout the saline condition of the experiment. This price was selected because at this and greater values, objective and subjective prices have been shown to correspond closely (Solomon et al., 2007). Once performance stabilized across successive frequency sweeps, price-sweep testing commenced. During price sweeps, the pulse frequency was set to the maximum value used during the frequency sweeps, and the price of the reward was increased successively from trial to trial. Once performance stabilized across successive

price sweeps, radial-sweep testing commenced. Along a radial sweep, the pulse frequency is decreased and the price is increased successively from trial to trial.

After stable performance was achieved in sessions that included all three sweep types, a second surgery was performed. The rats were anesthetized as described above, and a 24-cm loop of perforated Tygon[®] S-54-HL tubing (i.d.: 0.508 mm; o.d.: 1.52 mm; Saint-Gobain Performance Plastics, Akron, OH) was implanted subcutaneously. The Tygon[®] tubing was attached to a short length of stainless-steel tubing, which was secured to the skull as described in Hernandez, Haines and Shizgal (2008). Following the surgical procedure, a subcutaneous injection of buprenorphine (0.05 mg/kg) was administered and a sterile saline solution (1 ml/kg, sc) was injected to provide fluid therapy. After a recovery period of 1 day, data collection commenced.

Procedure

A sterile saline solution (0.9%) or a solution of cocaine hydrochloride, dissolved in sterile saline, adjusted to a pH of 7 ± 0.1 by means of the addition of .1M NaOH, was administered subcutaneously through the loop of porous subcutaneous tubing. The solutions were delivered at a constant rate (0.375 ml/h) by means of an external infusion pump (Harvard Syringe Pumps model 22, Harvard Apparatus Saint Laurent, QC). The cocaine dose was either 1.75 mg/kg/h (rats MCOC1, MCOC2, MCOC3, MCOC4, MCOC7) or 3.5 mg/kg/h (rats MCOC5, MCOC8). Two different doses were used because differential responding for stimulation trains delivered at different pulse frequencies or prices declined in the case of some subjects when the higher dose was administered during pilot testing.

During vehicle sessions, saline was infused subcutaneously. These sessions were run on Mondays and Thursdays and were composed of pairs of frequency, price, and radial sweeps. The position of each sweep during the session was randomized. During drug sessions, cocaine was infused subcutaneously. These sessions were run on Tuesdays and Fridays. In order to adequately sample the 3D structure acquired under the influence of the drug and to compare its position to the structure acquired during vehicle sessions, a second frequency sweep was added. One of the frequency sweeps acquired during the drug sessions (the “low-price” frequency sweep) was carried out at the same price as the frequency sweep in the vehicle sessions. The second frequency sweep acquired during the drug sessions (the “high-price” frequency sweep) was carried out at a higher price chosen to offset the influence of the drug (see below). The addition of a second frequency sweep, and the need to test higher prices in the drug sessions (see below) made it unfeasible to include all four sweep types in a single drug session. Thus, each drug session consisted of a subset of the four sweep types, and multiple drug sessions were required to obtain enough data to fit the 3D structure.

The self-stimulation tests began 2 hours after the start of the cocaine or saline infusion. The first determination of the time-allocation-versus-frequency curve was considered a warm-up and not considered in the analysis. The collection of the behavioral data was restricted to the period when the cocaine-induced elevation in DA concentration had been shown to be stable for a dose of 10 mg/kg/h (Hernandez et al., 2008) or for a dose of 1.75 mg/kg/hr (see supplementary figure 6). After the first week of experimentation, a preliminary fit of the mountain model to the data was performed, and the results were used to adjust the tested values of pulse frequency and price so as to

optimize sampling. The new values were selected so as to accommodate the drug-induced displacement of the 3D structure and to select the price for the high-price frequency sweep that was included in the drug condition. The price in question was chosen to offset the effect of drug so that the time-allocation versus pulse frequency plot for the high-price frequency sweep carried out in the cocaine condition would overlap the plot obtained at the lower price employed in the saline condition. Thus, the price employed for the high-price frequency sweep exceeded the price employed for the frequency sweep in the vehicle condition by an amount equal to the estimated drug-induced shift of the 3D structure along the price axis (i.e., the drug-induced increase in P_e).

Data analysis

The 3D model was fit separately to the data from the vehicle and drug sessions using the non-linear least-squares routine in the MATLAB Optimization Toolbox (The Mathworks, Natick, MA). One objective of the fitting approach was to obtain an unbiased measure of the dispersion of the parameter estimates. We adopted a resampling strategy (Efron & Tibshirani, 1991) to achieve this. By sampling randomly with replacement from the data, multiple samples were obtained. The 3D model was fit to each of these samples, thus allowing us to compute empirically derived 95% confidence intervals around each of the model parameters as well as around the differences between the estimates of each parameter for the vehicle and drug conditions: The 95% confidence interval around each estimate was defined as the region excluding the lowest 2.5% and highest 2.5% of the estimates. The resampling strategy and the empirically derived confidence intervals it generates avoid making unrealistic assumptions about a lack of correlation between the

estimates of the different parameters and about the normality of the parameter-estimate distributions.

Another objective of the fitting approach was to avoid the bias in slope estimates that is introduced by conventional across-session averaging. This problem can be seen readily in a simplified 2D example (see figure 29). Imagine that time-allocation versus pulse frequency curves are obtained repeatedly across multiple testing sessions. Noise in the determinants of the position parameter will displace these curves leftwards and rightwards. If a curve is constructed from the mean of the time-allocation estimates, its slope will be more gradual than those of any of the individual curves it is supposed to represent. This problem can be circumvented by separately fitting an appropriate model to each of the curves and then averaging the parameter estimates instead of the data points. Generalized to 3D, this is what was done to avoid bias in the estimates of the two parameters (a , g) that determine the slopes of the 3D structure along the pulse-frequency and price axes.

The resampling strategy was adapted to conform to the different structures of the vehicle and drug sessions. Each vehicle session consisted of a two complete sets of sweeps (frequency, price, and radial). Thus, these data were resampled by session. Consider the case of rat MCOC8. Each of the 1000 sets of resampled data consisted of data from nine sessions chosen at random and with replacement from the nine vehicle sessions that were run. Thus, the list of sessions included in a typical resampled data set might consist of the session numbers (1, 2, 2, 4, 6, 7, 7, 8, 9); the list of session included in another resampled data set might be (2, 3, 4, 5, 5, 6, 8, 9, 9). The 3D model was fit separately to the data from each session in the list, with the two location parameters (F_{hm} ,

P_e) free to vary across sessions and common values of the remaining parameters (a , g , TA_{max} , TA_{min}). This approach captures across-session drift in the location parameters while avoiding the explosion in the number of free parameters and the consequent increased uncertainty in their estimates that would obtain had all six parameters been free to vary across sessions. For example, in the case of the 9-session dataset obtained from MCOC8, a 22-parameter model was fit (one estimate per session for each of the two location parameters plus single estimates of the remaining four parameters). Had all six parameters been free to vary across sessions, a 54-parameter model would have been fit. In contrast, had none of the parameters been free to vary across sessions, a model comprising only six parameters would have been fit, but the slope estimates would have been biased downwards due to the averaging artifact illustrated in Figure 29.

On each iteration, the parameter estimates for the resampled data sets (n = number of vehicle sessions) were averaged within sweep type. Thus, in the case of MCOC8, there were nine estimates of each of the location parameters (F_{hm} , P_e), and these were averaged on each iteration to yield a single estimate for each parameter per iteration. One thousand iterations were performed, and the means of the 1000 resulting parameter estimates and the associated 95% confidence intervals were then computed.

Due to the increased time required to test higher prices in the drug condition and due to the addition of a second frequency sweep in that condition, all sweep types were not run in a single session. Therefore, it was not feasible to resample the data by session. Instead, the data were resampled by sweep. One sweep of each type was sampled at random, with replacement, from the pool of consisting of all sweeps of that type so as to create a dataset to which the 3D model could be fit; the number of datasets so constructed

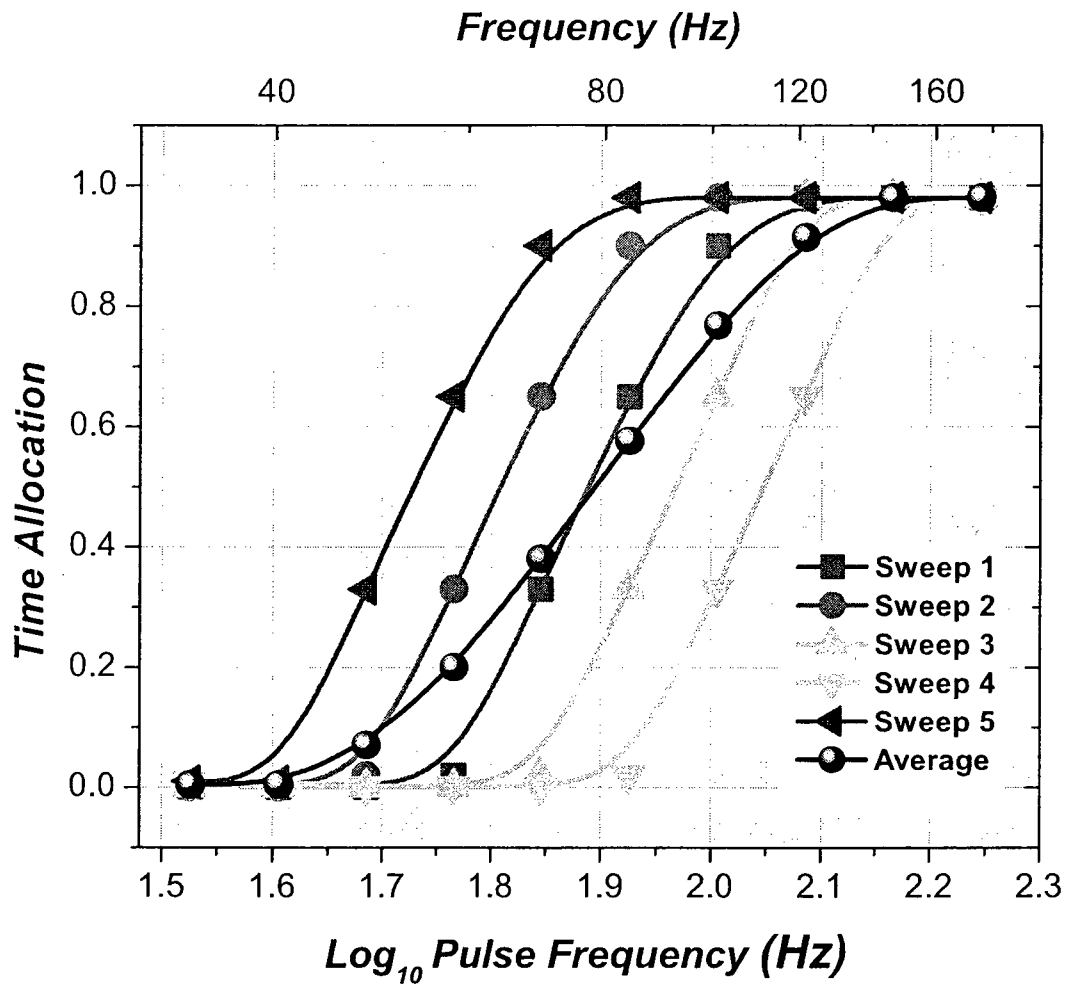


Figure 29. Simulated time allocation-frequency curves and their average. This figure shows that the slope of the average curve is more gradual than any of the slopes of the individual time-allocation versus pulse frequency curves.

equalled the number of sessions run in the drug condition. In some cases, the different pools (low-price frequency sweeps, high-price frequency sweeps, price sweeps, and radial sweeps) contained different numbers of sweeps. This resulted in differential sampling of the pools, with those containing fewer sweeps sampled more heavily than those containing more sweeps. To compensate, the contribution of each sweep type to the fit was weighted by the number of sweeps of that type. The remainder of the fitting procedure was the same as for the vehicle data.

Graphs of the fitted surface defined by the means of the resampled parameter estimates were plotted using Origin (OriginLab Corporation, Northhampton, MA), as were the contour graphs of the 3D structure. Also plotted, for each sweep type, were the time-allocation means, their associated 95% confidence intervals and the 2D projections of the fitted surface.

Histology

After the completion of the experiment, a lethal dose of sodium pentobarbital was administered. A 1 mA anodal current was passed through the stimulating electrode for 15 sec to deposit iron ions at the site of the electrode tip. The animals were then perfused intracardially with 0.9% sodium chloride, followed by a formalin-Prussian Blue solution (10% formalin, 3% potassium ferricyanide, 3% potassium ferrocyanide, and 0.5% trichloroacetic acid) that forms a blue reaction with the iron deposited at the tip of the electrode. Then, the rats were decapitated and their brains were removed and fixed with 10% formalin solution for at least 7 days. Coronal sections of 30 μm thickness were cut with a cryostat (Thermo Scientific) and subsequent stained using the formol-thionin

technique. Tips locations were determined microscopically at low magnification with reference to the stereotaxic atlas of Paxinos and Watson (2007).

Results

Electrode tip location

The histological reconstruction of electrode-tip locations is shown in Figure 30. All of the electrode tips were located within the lateral hypothalamus, in the coronal planes corresponding to Plates 55 and 56 of Paxinos and Watson's (2007) atlas.

Fit of the model to the data and cocaine- induced shifts

The reinforcement mountain model expressed in equation 8 offered an adequate fit, with no visually obvious signs of systematic bias, to the vehicle data from all subjects. The model also offered an adequate fit for the data collected in the cocaine condition for three of the subjects, MCOC4, MCOC7, and MCOC8, as illustrated by Figure 31, which shows the graphical analysis of data from subject MCOC8. Panels *a* and *b* present the behavioural data and the fitted surface obtained for the vehicle and cocaine conditions, respectively. Panels *c* through *g* show the two dimensional projections of the fitted surfaces and the behavioural data. Panel *c* shows the frequency-sweep curves obtained at a price of 4-second obtained in the vehicle (dark red) and cocaine (light red) along with the corresponding 2D projections of the fitted surfaces. The light red curve is displaced leftward from the curve obtained in the vehicle condition. When the price of the frequency curve was adjusted to offset the displacement of the 3D structure along the price axis, both curves overlapped as shown in panel *d*. Panel *e* shows the price data obtained in the vehicle (light blue) and cocaine (dark blue) conditions with the

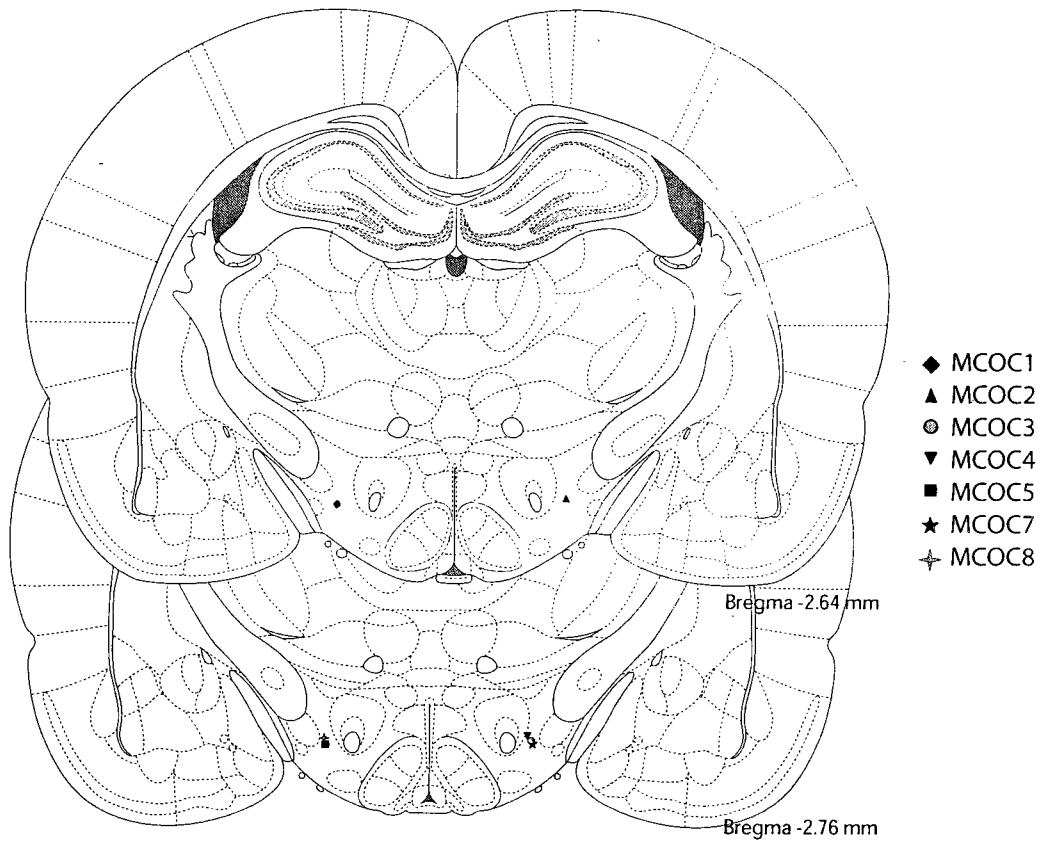


Figure 30. Location of electrode tips. All of the electrode tips were located within the lateral hypothalamus, in the coronal planes corresponding to Plates 55 and 56 of Paxinos and Watson's (2007) atlas.

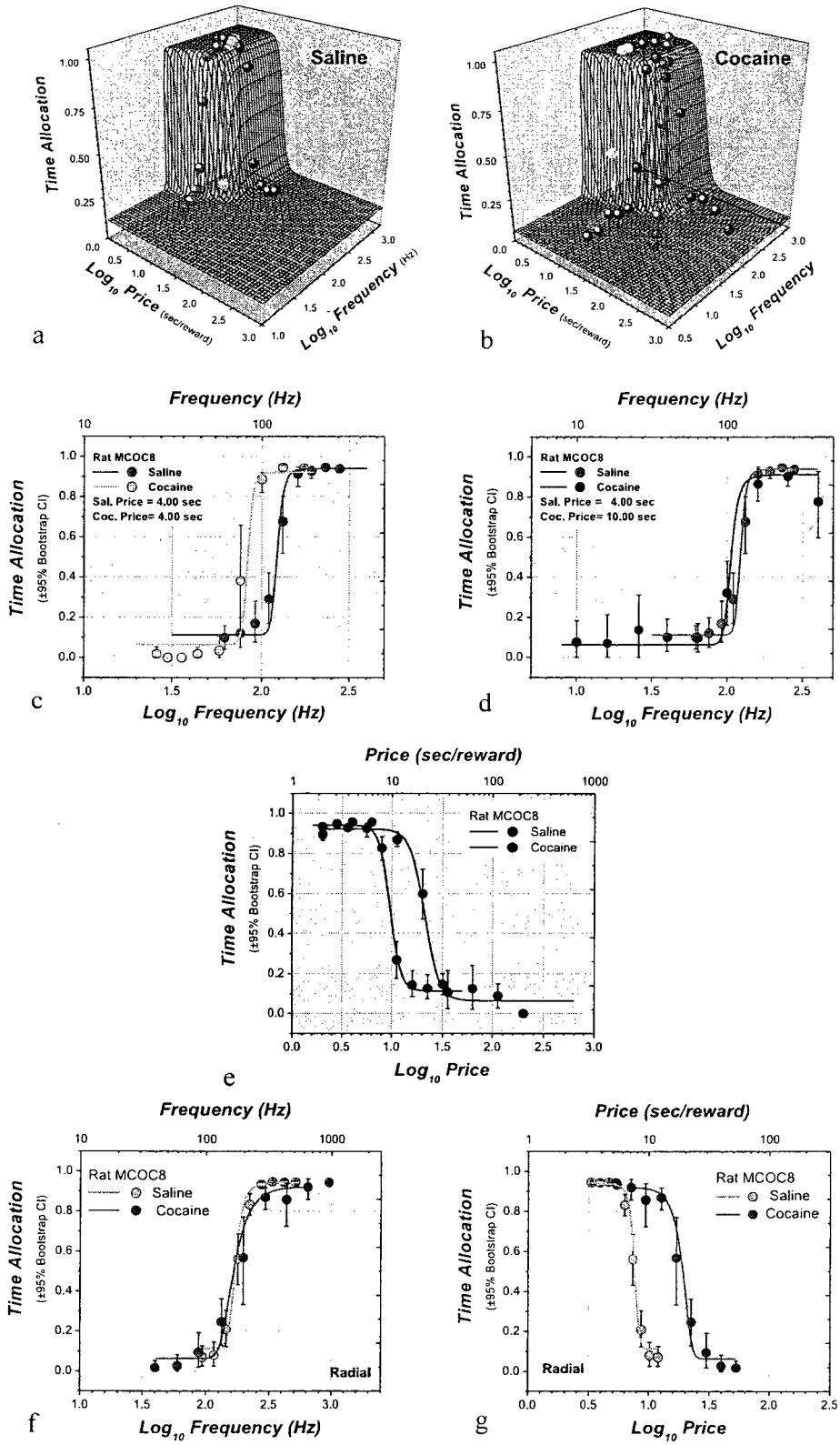


Figure 31.

Figure 31. Time allocation data from rat MCOC8, fitted surfaces and their two dimensional projections. Panels a and b show the behavioural data and the fitted surface obtained for the vehicle condition and cocaine condition respectively. Panels c through g show the two dimensional projections obtained from the fitted surfaces and the behavioural data. Panel c shows the two time allocation-frequency curves at a 4-second price obtained for vehicle (dark red) and cocaine (light red). The light red curve is displaced leftward. When the price is adjusted to offset the displacement of the 3D structure along the price axis, both curves overlap as shown in panel d. Panel e shows the price sweep data from the vehicle (light blue) and cocaine (dark blue) conditions, along with the corresponding projections of the fitted surfaces. Cocaine produced a substantial rightward displacement along the price axis. That the mountain was displaced along the price axis and not along the frequency axis is readily apparent in the plots of the radial-sweep data, which are plotted against the frequency axis in panel f and along the price axis in panel g. The data obtained in the cocaine condition (dark green) overlaps those obtained in the vehicle condition (light green) when projected along the frequency axis (panel f). In contrast, the cocaine data are shifted rightwards when projected along the price axis (panel g).

corresponding 2D projections of the fitted surfaces. Cocaine induced a substantial rightward displacement of the price-sweep data. That the mountain was displaced along the price axis and not along the frequency axis is readily apparent in the plots of the radial-sweep data. When plotted against the frequency axis (panel *f*), the data obtained during the vehicle infusion (light green) and during the cocaine infusion (dark green) overlap. In contrast, when plotted against the price axis (panel *g*), the data obtained during the cocaine infusion are displaced rightward with respect to the data obtained during the vehicle condition.

Figure 32 shows the contour graphs of the surfaces fitted to the data from the saline and cocaine conditions. The contour graphs were obtained by projecting onto a plane the cross-sections obtained after horizontally slicing the fitted surface at fixed intervals representing 10% changes in time allocation. In order to facilitate visualization of shifts along the two axes, the contour graph for the vehicle condition is plotted twice, once in the upper left quadrant and once in the lower right. The parameter values tested are colour-coded by sweep type. The superimposed solid yellow lines represent the location parameters, f_{hm} and P_e , which determine the position of the mountain along the frequency and price axes, respectively. The dotted yellow lines demarcate the 95% confidence interval around each of the location-parameter estimates. As represented by the dark red arrow, the structure moved significantly rightward along the price axis ($0.32 \log_{10}$ units), but only marginally along the frequency axis ($-0.08 \log_{10}$ units). The frequency axis displacement falls within the confidence interval and therefore is not considered reliable. The displacements of the mountain along the frequency and price axes are summarized in the bar graph shown in the upper right quadrant of Figure 32.

In the cases of three subjects, MCOC1, MCOC3 and MCOC5, the prediction of the model in its standard form deviated systematically from some of the data collected in the cocaine condition. In the cocaine data from these subjects, relatively high proportions of trial time were devoted to the pursuit of BSR, even when the pulse frequency was low. Moreover, time allocation on these low-payoff trials in the cocaine condition varied substantially from session to session.

In order to accommodate these patterns, a revised version of the model was developed by adding a constant term to the output of the integrator, as follows:

$$TA = \frac{\left[\left(\frac{f^g}{f^g + f_{hm}^g} \right) + \frac{CR}{I_{max}} \right]^a}{\left[\left(\frac{f^g}{f^g + f_{hm}^g} \right) + \frac{CR}{I_{max}} \right]^a + \left(\frac{P}{P_E} \right)^a} \quad (9)$$

The new term, CR/I_{max} , could be interpreted to represent a fixed conditioned reward or a fixed reward associated with motor performance. The revised 7-parameter model fits the data well and fares better than the 6-parameter model. The addition of the parameter increased the non-linear R^2 values for the fits to the cocaine data from each of the three subjects. For MCOC1 the adjusted R^2 went from 0.949 to 0.953; for MCOC3 the adjusted R^2 went from 0.934 to 0.963; and for MCOC5 the adjusted R^2 went from 0.963 to 0.972.

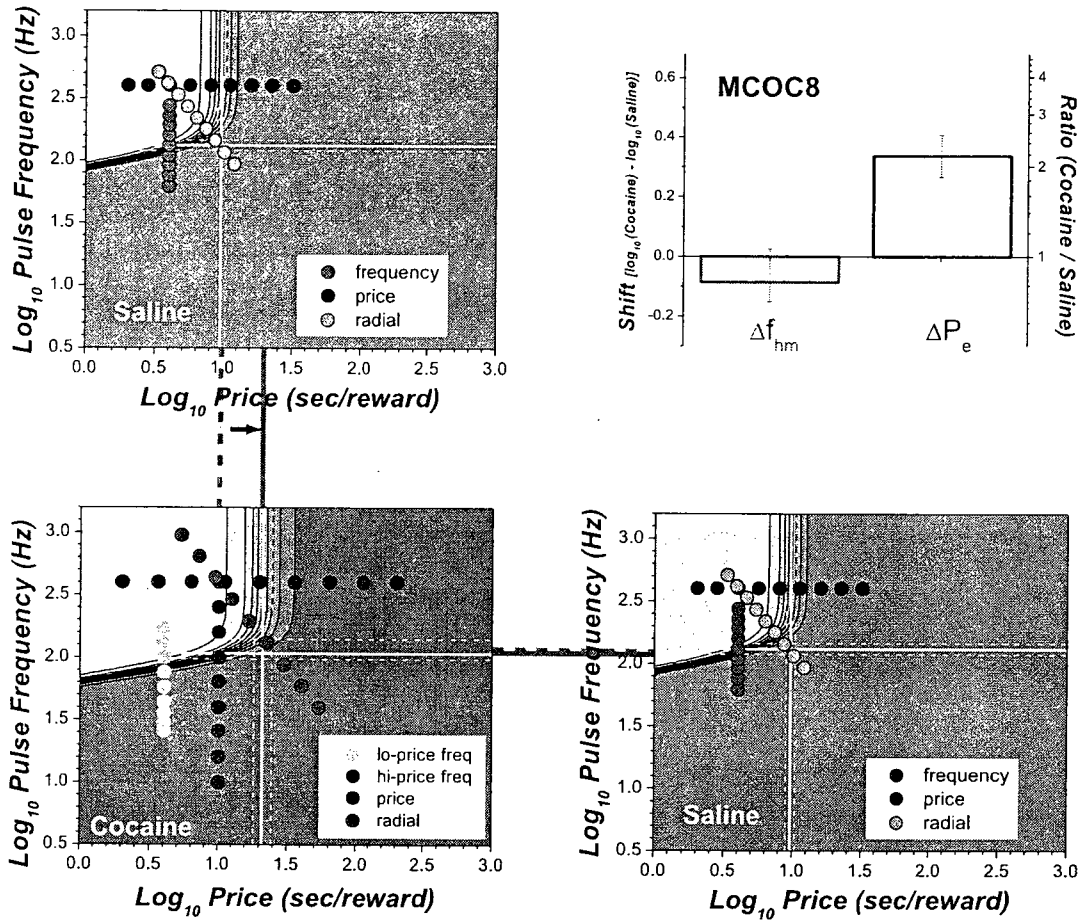


Figure 32. Contour graphs and bar graph showing the displacement of the mountain along the price axis in the case of rat MCOc8. Note that the contour graph for the vehicle condition is plotted twice, so that the shifts along the two axes are readily visualized. The superimposed solid yellow lines represent the position parameters, f_{hm} and P_e , which determine the position of the mountain along the frequency and price axes, respectively. The dotted yellow lines demarcate the 95% confidence interval around each of the parameter estimates. As represented by the dark red arrow, the structure moved significantly rightward along the price axis by $0.32 \log_{10}$ units; but only marginally along the frequency axis by $-0.08 \log_{10}$ units. The bar graph summarizes the two displacements.

Figure 33 shows data from rat MCOC3 that illustrate the improved fit provided by the 7-parameter model. Panel *a* shows the mean TA values obtained during the low-price frequency sweep carried out under the influence of cocaine as well as the data from the frequency sweep carried out in the saline condition. The 6-parameter model was fit to the data in both cases, and the 2D projections of the fitted surfaces are shown as solid lines. Note that the cocaine data deviate systematically from the 2D projection. Panel *c* shows that this systematic deviation is reduced by fitting the 7-parameter model to the data from the cocaine condition. (The 6-parameter model was always fit to the data from the vehicle condition.) In Panels *b* and *d*, the data from the high-price frequency sweep carried out under the influence of cocaine are compared to the same data from the vehicle condition as are shown in Panels *a* and *c*. Note that the increase in price has brought down the TA values obtained at the lower pulse frequencies (and has offset the displacement of the 2D projection along the frequency axis), but that the 7-parameter model still provides a closer fit than the 6-parameter model.

Figure 34 illustrates another advantage of the 7-parameter fit. The TA values from each cocaine session are shown for the low-price frequency sweep along with the 2D projection of the corresponding fitted surface. It is evident that the degree to which TA values are boosted at the low frequencies varies from session to session. As the lower panel shows, allowing the added parameter (CR / I_{max}) to vary across sessions (along with the location parameters, F_{hm} and P_e) captures much of this variance. In contrast, the 6-parameter fit (upper panel), which was carried out with only F_{hm} and P_e free to vary across sessions, fails to describe the across-session variation in TA at low pulse frequencies. The improvement in the fits to the data from the cocaine condition were less

dramatic in the cases of rats MCOC1 and MCOC5, but are nonetheless discernable, particularly in the graphs showing the across-sessions variation in TA (supplementary figure 7).

Figure 35 presents the data and 2D projections of the fitted surface for rat MCOC3, the case in which the benefits of fitting the 7-parameter model were highest. The corresponding contour and bar graphs are shown in Figure 36.

The remaining rat, MCOC2, showed an idiosyncratic pattern of responding along the frequency sweeps performed under the influence of cocaine. Time allocation fell initially as the pulse frequency was decreased but then increased as the pulse frequency was further lowered (figure 37). In order for the surface fit to converge, the uncharacteristic "tails" of the psychometric functions (the portion over the low-frequency range) had to be excluded from the analysis (shaded region of fig 37). Once this was done, the standard 6-parameter model was used to fit the data. (see supplementary figures 8 and 9).

The goodness- of- fit of the model in all subjects, as estimated by the non-linear adjusted R^2 value, ranged from 0.97 to 0.98 for the vehicle condition whereas the goodness- of- fit of 6-parameter or 7-parameter model for the cocaine condition ranged from 0.94 to 0.97. Supplementary figures 10,11,12,13,14,15,16,17 show the 2D and 3D graphical analysis of the data from subjects MCOC1, MCOC2, MCOC4, MCOC7, and MCOC5.

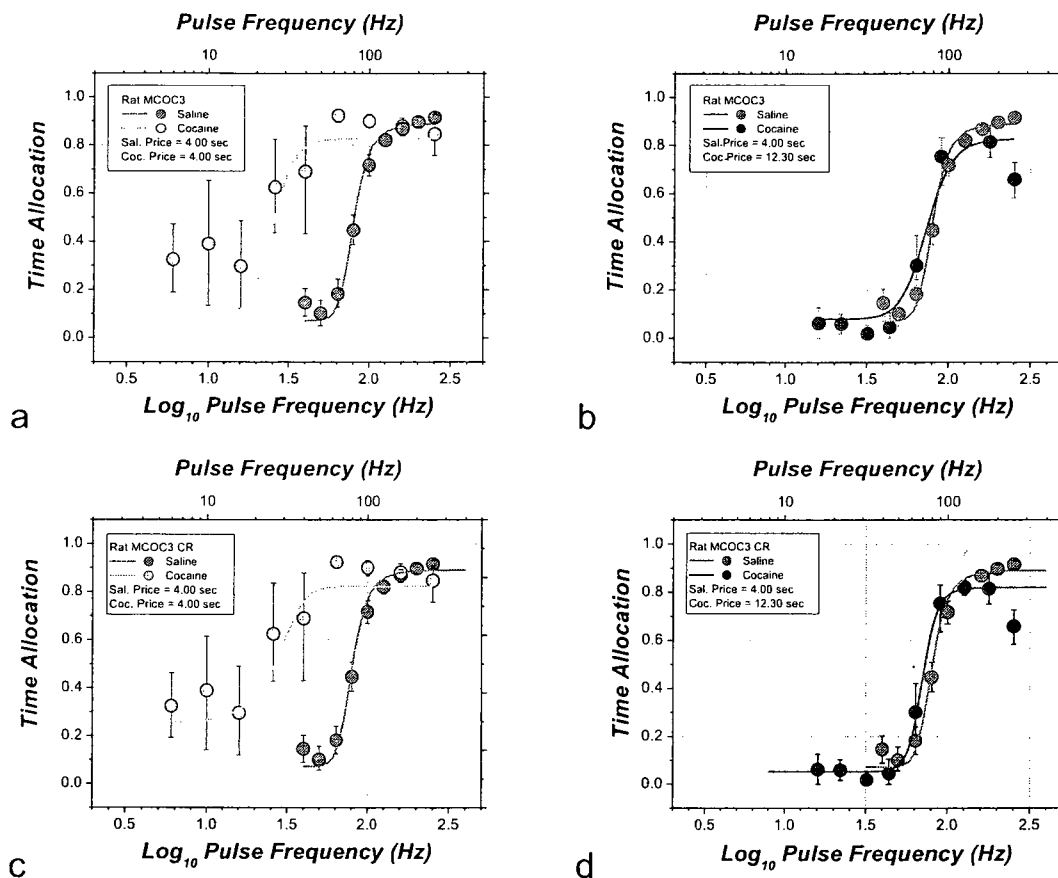


Figure 33 .Fit of the time allocation-frequency curves for rat MCOC3 using the 6-parameter model (panels a and b) and using the 7-parameter model (panels c and d). Panels a and c show the mean TA values obtained during the low-price frequency sweep carried out under the cocaine and the saline condition. The 6-parameter model was fit to the data in both cases, and the 2D projections of the fitted surfaces are shown as solid lines. Note how the solid line deviates from the cocaine data. Panel c shows how the 7-parameter model improves the fit of the model to the data by reducing the gap between the obtained function and the data points. In Panels b and d, the cocaine data from the high-price frequency sweep are compared to the data from the vehicle condition. The increase in price has brought down the TA values obtained at the lower pulse frequencies and compensated for the rightward displacement of the montain.

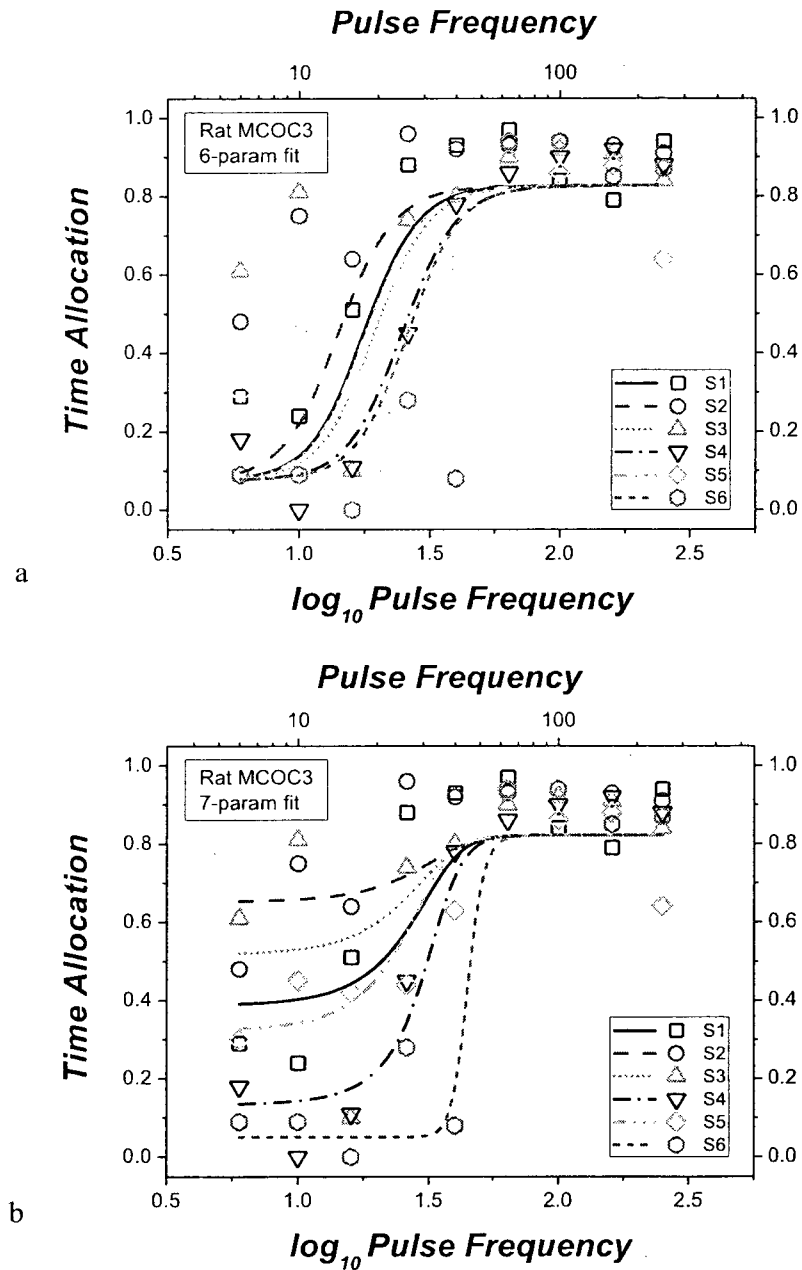


Figure 34. Time allocation data and projections of the fitted surfaces obtained by allowing the location parameters to vary across sessions. Panel a shows projections of the 6-parameter fits whereas panel b shows the projections of the 7-parameter fits. Unlike the 7-parameter model, the 6-parameter model is unable to capture the variance observed across sessions.

Figure 38 shows the bar graphs summarizing the cocaine-induced changes in the values of the location parameters for all rats. As can be seen readily, cocaine produced a significant rightward shift along the price axis in all subjects. These displacements vary between 0.27 and 0.55 \log_{10} units and average 0.388 \log_{10} units (SEM= 0.04). This means that on average, the price at which a TA value halfway between T_{Amin} and T_{Amax} was obtained for a reward of maximum strength was 2.45 times higher under the influence of cocaine than in the saline condition (See table 1).

Table 1. Summary of the location parameter difference P_e for all subjects

Subject	Parameter difference (cocaine -saline)	Confidence interval lower limit	Confidence interval upper limit	Significant displacement
MCOC1	0.3075	0.08788	0.1078	*
MCOC2	0.54727	0.20126	0.27981	*
MCOC3	0.51665	0.11435	0.13464	*
MCOC4	0.32233	0.07121	0.0685	*
MCOC5	0.26983	0.12902	0.14365	*
MCOC7	0.41738	0.06767	0.06918	*
MCOC8	0.33724	0.07132	0.06943	*

The displacement of the mountain along the frequency axis varied across subjects between -0.147 and 0.04 \log_{10} units and averaged -0.061 \log_{10} units (SEM=0.03). This means that on average, the frequency that produced half-maximal reward intensity was 0.87 times as high under the influence of cocaine than in the saline condition. In only two cases (MCOC2 and MCOC5), did the displacement of the mountain along the frequency

axis met the criterion for statistical reliability, and in the case of MCOC2, the shift barely meets this criterion (see table 2).

Table 2. Summary of the location parameter difference Fhm for all subjects

Subject	Parameter difference (cocaine -saline)	Confidence interval lower limit	Confidence interval upper limit	Significant displacement
MCOC1	0.02514	0.09622	0.13585	
MCOC2	-0.14678	0.10283	0.13628	*
MCOC3	0.04485	0.10331	0.14729	
MCOC4	-0.06765	0.0679	0.08041	
MCOC5	-0.14678	0.06469	0.04792	*
MCOC7	-0.0498	0.0451	0.0497	
MCOC8	-0.08586	0.06472	0.11172	

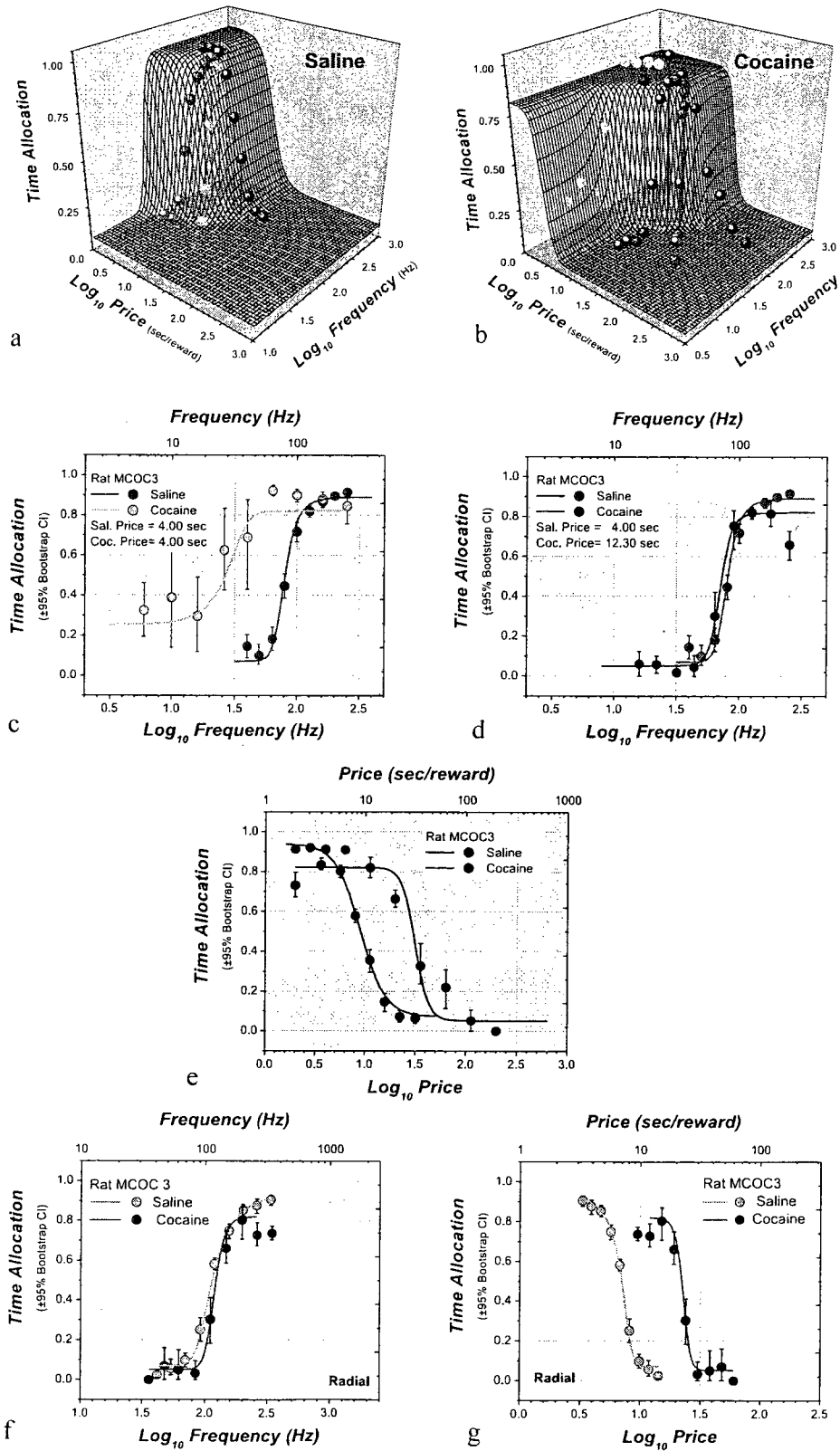


Figure 35

Figure 35. Time allocation data from rat MCOC3, fitted surfaces and their two dimensional projections. Panels a and b show the behavioural data and the fitted surface obtained for the vehicle condition and cocaine condition respectively. Panels c through g show the two dimensional projections obtained from the fitted surfaces and the behavioural data. Panel c shows the two time allocation-frequency curves at a 4-second price obtained for vehicle (dark red) and cocaine (light red). The light red curve is displaced leftward. When the price is adjusted to offset the displacement of the 3D structure along the price axis, both curves overlap as shown in panel d. Panel e shows the price sweep data from the vehicle (light blue) and cocaine (dark blue) conditions, along with the corresponding projections of the fitted surfaces. Cocaine produced a substantial rightward displacement along the price axis. That the mountain was displaced along the price axis and not along the frequency axis is readily apparent in the plots of the radial-sweep data, which are plotted against the frequency axis in panel f and along the price axis in panel g. The data obtained in the cocaine condition (dark green) overlaps those obtained in the vehicle condition (light green) when projected along the frequency axis (panel f). In contrast, the cocaine data are shifted rightwards when projected along the price axis (panel g).

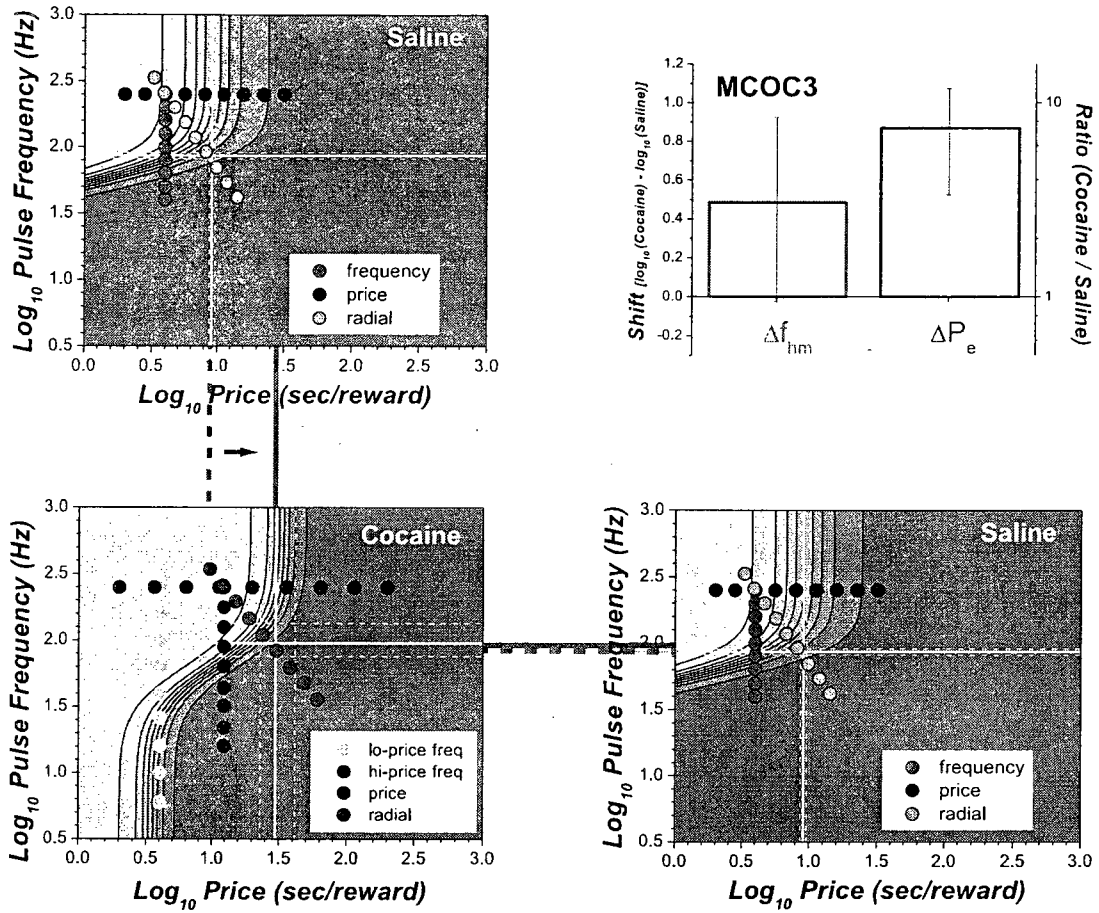


Figure 36. Contour graphs and bar graph showing the displacement of the mountain along the price axis in the case of rat MCOC3. Note that the contour graph for the vehicle condition is plotted twice, so that the shifts along the two axes are readily visualized. The superimposed solid yellow lines represent the position parameters, f_{hm} and P_E , which determine the position of the mountain along the frequency and price axes, respectively. The dotted yellow lines demarcate the 95% confidence interval around each of the parameter estimates. As represented by the dark red arrow, the structure moved significantly rightward along the price axis by $0.51 \log_{10}$ units; but only marginally along the frequency axis by $0.04 \log_{10}$ units. The bar graph summarizes the two displacements.

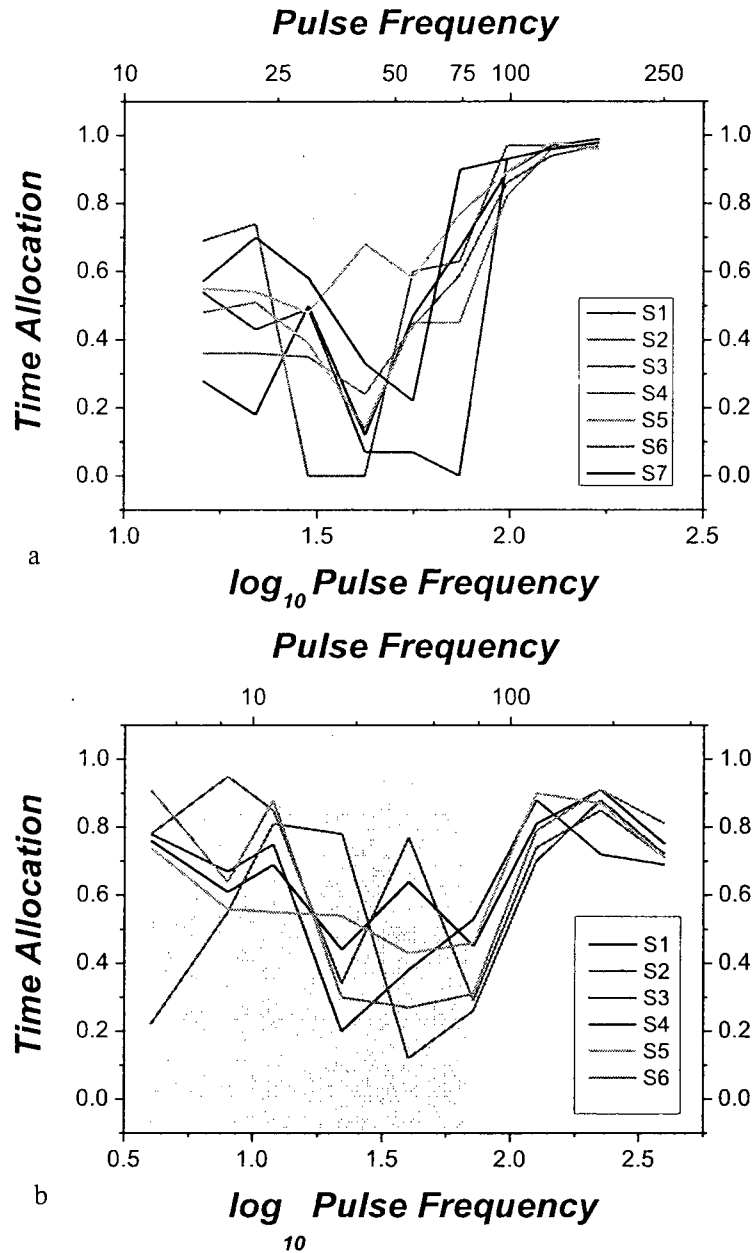


Figure 37. Time allocation vs. frequency curves obtained at a low-price (a) and at a high-price (b) under the influence of cocaine from rat MCOC2. Note the idiosyncratic pattern of responding; time allocation fell initially as the pulse frequency was decreased but then increased as the pulse frequency was further lowered. To fit the model to this subject the portions over the low frequency range were excluded from the analysis (shaded regions).

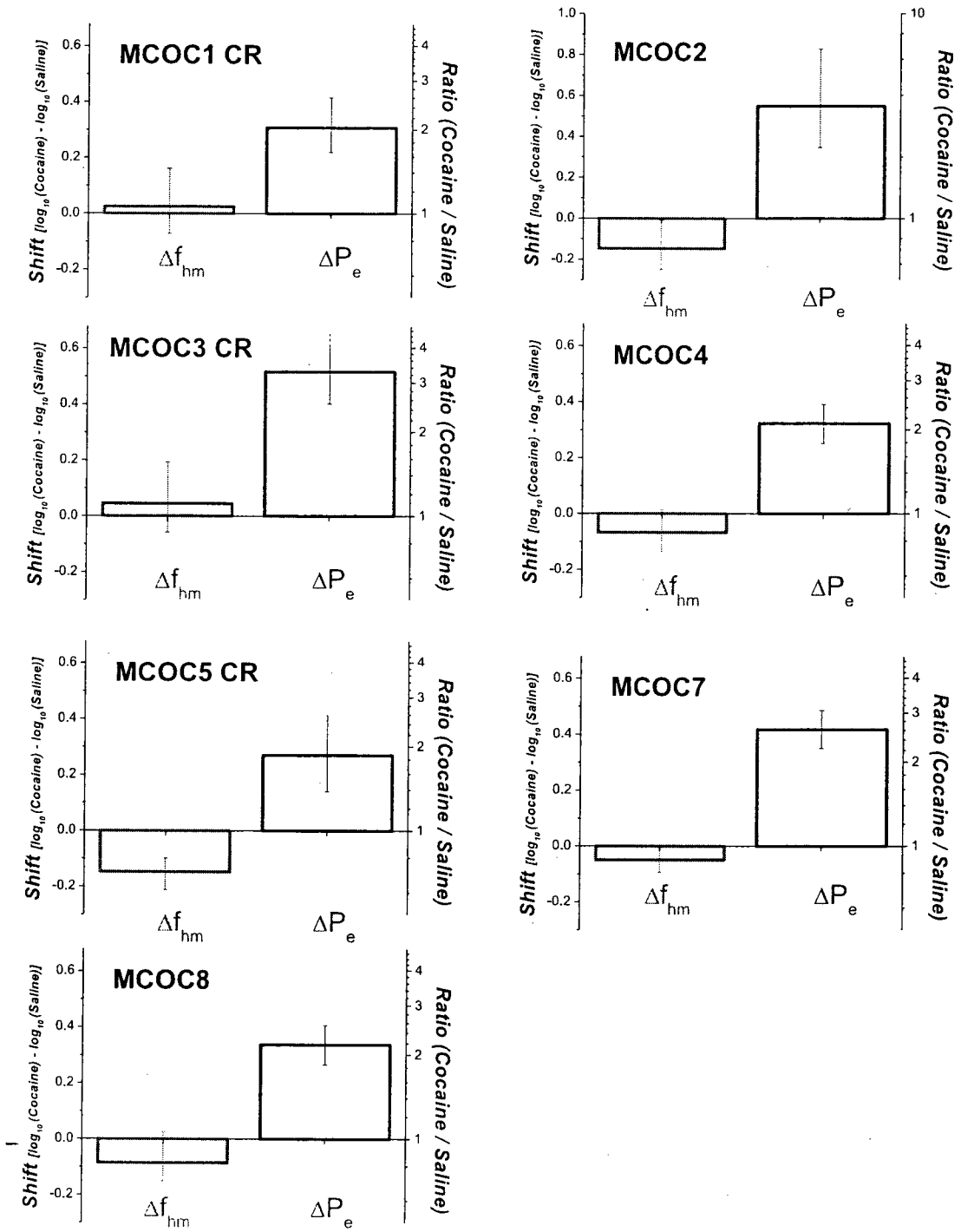


Figure 38. Bar graphs showing the displacement of the mountain for all subjects tested.

The mountain was reliably displaced along the price axis. Of all the subjects only two (MCOC2 and MCOC5) showed a displacement of the mountain along the frequency axis.

Discussion

The goal of the present research was to identify, by means of the reinforcement mountain testing paradigm and model, where the influence of DA tone is brought to bear in the neural circuitry underlying intracranial self-stimulation.

The increase in DA tone brought about by the continuous subcutaneous infusions of cocaine affected the willingness of the experimental subjects to invest time in the pursuit of reward. The three-dimensional structure formed by the time allocation, stimulation frequency and price, reliably shifted rightward along the price axis in all subjects tested, an effect that is orthogonal to those produced by varying the current (Arvanitogiannis & Shizgal, 2008) or train duration (Arvanitogiannis & Shizgal, 2008; Breton, 2006; Breton, Conover, & Shizgal, 2006; Mullet, 2005).

These results imply that DA tone influences the reward circuit at or beyond the integrator output, at a later stage of processing that was initially proposed (Wise, 1980) and has been long believed. The results obtained suggest that the leftward shifts seen when the curve-shift method is used to assess the effect of increased DA tone on intracranial self-stimulation could reflect the movement of the 3D structure along the price axis. This displacement along the price axis cannot be discerned by means of traditional curve-shift measurements. However, due to the diagonal orientation of the mountain surface over the range of frequencies over which time allocation rises steeply, rightward displacement along the price axis produces a leftward displacement of the 2D silhouette of the mountain in the performance-frequency plane, creating the illusion of a leftward shift in the underlying reward-growth function.

According to the model, the observed displacement along the price axis could be product of several factors. DA tone could alter the absolute reward intensity achievable (I_{max}), a change that rescales the reward-growth function. Alternatively, DA tone could alter the subjective effort cost, the perceived exertion required to hold down the lever. This proposition is compatible with Salamone's hypothesis of DA involvement in behaviour (Salamone, 2002; Salamone et al., 2005; Salamone et al., 2001). Alternatively, or in addition, a displacement along the price axis could reflect a devaluation of competing activities, such as grooming, resting or exploring. Future experimentation will be required to delineate the relative contribution of these factors.

In the data from the two of the seven subjects, the 3D structure shifted reliably along the frequency axis under the influence of cocaine, in addition to shifting along the price axis. This shift could be the product of various factors that need to be taken into consideration in planning future experimentation. Heterogeneity of the neural circuitry at the level of the LH could be one of the possible explanations for the disparity in the results. Different electrode location might have activated functionally different circuits and their corresponding integrated outputs (Arvanitogiannis, Waraczynski, & Shizgal, 1996; Fulton, Woodside, & Shizgal, 2006; Shizgal, Fulton, & Woodside, 2001). Thus, some of the activated neurons may have influenced the neural circuitry prior to the integration of the reward signal. However, the histological reconstruction of the electrode tips location does not show a systematic difference between the location of the electrode tips in rats MCOC2 and MCOC5 on the one hand and the remaining rats on the other.

The data were fitted using the 6-parameter model for the saline condition and either the 6-parameter or the 7-parameter model for the cocaine condition. The addition

of an extra parameter to the model was required because under the influence of cocaine, some subjects allocated a relatively high portion of the trial time to the pursuit of BSR even when reward intensity was low. The increased allocation of time to the pursuit of stimulation trains delivered at low pulse frequencies could reflect represent a fixed conditioned reward (Hill, 1970), or a decrease in discrimination between different reward intensities (Evenden, 1988). However, at least in the case of MCOC3, increasing the price reduced or eliminated the increased time allocation seen when both the price and pulse frequency were low, suggesting that discrimination had not been unduly compromised by the drug.

The interaction of the phasic and tonic components of dopamine signalling could be germane to the interpretation of the results. Cocaine increases DA tone by acting as an inhibitor of DA reuptake, by blocking dopamine transporters (Giros, Jaber, Jones, Wightman, & Caron, 1996) and by increasing the amount of dopamine exocytosed through mobilization of vesicles normally unavailable for release (Venton et al., 2006). Also it has been shown that cocaine can act pre-synaptically on DA neurons by blocking the voltage-sensitive sodium channel (VSSC) in VTA GABA neurons, thus inactivating the tonic inhibition of DA neurons and increasing DA phasic firing (Scott et al., 2008). At the terminal level the increase in phasic release after cocaine administration had been captured using FSCV (Aragona et al., 2008).

Phasic and tonic DA release may well play different roles in the reward substrate with phasic DA release acting prior the integration of the reward signal and DA tone influencing variables that act at the level of the integrator or after the integration of the

reward signal has taken place. Why such a division of function would influence the results from only two of seven rats is not clear.

Several means exist for evaluating the role of phasic DA signalling in BSR. For example, it should be possible to reduce or eliminate the influence of DA phasic transients by inactivating VTA GABA neurons with a locally injected mixture of the GABA_A and GABA_B receptor agonists, baclofen and muscimol, as has been done by Aragona et al. (2008). Another promising means of suppressing phasic, but not tonic, DA signalling is inactivation of NMDA-type, ionotropic glutamate receptors in DA neurons, as suggested by Zweifel et al. (2009).

Another fact that should be considered is that cocaine is not a specific DA transport blocker; it affects reuptake of other neurotransmitters, in particular, serotonin, and norepinephrine (Roberts, 1991). Cocaine-induced increases in norepinephrine tone would be of particular interest, since it has been shown that electrical stimulation of the medial forebrain bundle activates norepinephrine releasing neurons located in the locus coeruleus and lateral tegmental A7 cluster (Yasushi et al., 2001). Moreover, intra locus coeruleus injections of the α_1 receptor antagonist, terazosin, produce a rightward, dose-dependent displacement of rate-frequency curves obtained with MFB stimulation (Lin, de Vaca, Carr, & Stone, 2006). These findings suggest that norepinephrine release contributes in some way to the pursuit of rewarding electrical stimulation. In order to reduce the influence of other neurotransmitters in the interpretation of the present results, a specific DA transport blocker, like GBR 12909, should be used instead of cocaine. The result of such experiments should shed light on the specific contribution of DA tone.

The results obtained by applying the reinforcement-mountain model and testing paradigm illustrate how quantitative modeling can be a powerful tool for isolating, manipulating and describing the psychological processes underlying the evaluation and pursuit of rewards and for mapping these processes onto neural circuitry. Moreover, the results showcase the reinforcement mountain model as a powerful analytical tool that opens new avenues for generating, analyzing and interpreting the influence of pharmacological and psychophysical variables on the reward circuit and onto behaviour.

GENERAL DISCUSSION

The goal of the present thesis was to determine the role of tonic dopamine release in brain stimulation reward. In order to fulfill this goal, a series of experiments were carried out. The first five experiments entailed measurement of DA tone in rats receiving or self-administering rewarding electrical stimulation of the MFB. The last experiment addresses directly where in the reward circuit DA contributes to ICSS, an issue germane to the debate over whether changes in DA tone alter subjective reward intensity or subjective effort costs.

Several different reinforcement schedules were used to evaluate the role of predictability in DA tone. Both the predictability (fixed versus variable) and duration (12 sec vs 1.5 sec) of the inter-train interval were varied, as were the response requirements (time versus interval schedules). DA tone was increased consistently by the stimulation, and this increase was not affected by the predictability of train onset. The pattern of changes in DA tone observed when the rats worked for the stimulation resembled those observed when they received the stimulation passively. The time course of operant performance shows clearly that the subjects in the FI12 group learned to predict the availability of the reward whereas the subjects in the VI12 failed to do so, as expected.

What seems to affect the stability of the DA increase is the stimulation duty cycle. When the trains of rewarding stimulation were relatively far apart (12 seconds), DA tone was stable for up to two hours, but when the stimulation trains are spaced closer in time (inter-train interval = 1.5 seconds) DA tone declined sharply and progressively from its peak value. However, trains separated by the short, 1.5 second inter-train interval drove

DA levels to a higher peak than was observed in any of the experiments in which the constant or average inter-train interval was 12 sec.

The predictability of gustatory rewards has a profound influence on whether or not their delivery triggers phasic firing of DA neurons (Ljungberg et al., 1992; Mirenowicz & Schultz, 1994). In contrast, experiments 1-5 show that varying the predictability of train onset had no discernable effect on the time course or amplitude of change in DA tone during delivery of rewarding brain stimulation. Compatible results had been obtained when rats worked for food pellets; DA release in the Nac was similarly elevated regardless of how predictable the task for obtaining a food pellet was (Stefani & Moghaddam, 2006) Thus, predictability has not influenced DA tone measurements obtained via in-vivo microdialysis in studies carried out to date.

It could be argued that the similar pattern of DA release observed during predictable and unpredictable tasks is an artefact of the microdialysis technique. The poor temporal resolution of the technique and the relative large size of the probe would mask the effects of predictability because the measurement obtained by means of microdialysis reflects an average of phasic and tonic release (Donita et al., 2009).

If this argument were correct then different patterns of DA overflow should be observed in response to predictable and unpredictable rewards, even at the low temporal sampling resolution that the microdialysis method offers. Specifically, according to the temporal difference model (Montague et al., 1996), under predictable conditions DA overflow measured by means of microdialysis should be consistently lower than under unpredictable conditions. This pattern was never seen.

The similarity in the profile of tonic DA release is congruent with Niv et al's (2006) proposal that DA tone tracks the average reward rate. On this view, phasic and tonic DA release are differentiable on the basis of their function as well as their dynamics: phasic release signals prediction errors and thus drives learning whereas the slowly evolving DA tone plays an enabling role in several behavioural domains, including initiation and control of movement, cognition, motivation, and mood (W Schultz, 2002). These two release patterns are controlled by distinct neural mechanisms and do not necessarily co-vary. Floresco et al (2003) showed that activation of excitatory pedunculopontine inputs to midbrain DA neurons increases burst firing without increasing DA levels in the nucleus accumbens terminal field, as measured by a microdialysis probe. In contrast, disinhibiting VTA DA neurons by suppressing the activity of inhibitory ventral pallidal afferents increased the proportion of VTA neurons in the active state and, in turn, increased DA tone in the nucleus accumbens without altering burst firing in the VTA DA neurons.

Phasic and tonic release were further differentiated in the experiment described in Chapter 4, which replicates Garris et al's (1999) study, substituting in-vivo microdialysis for FSCV. In the Garris et al (1999) experiment as well as in Kilpatrick et al (2000) study, DA phasic release, as measured by means of FSCV, was transient in response to rewarding stimulation. DA release was observed at the beginning of the self-stimulation behaviour but the signal declined rapidly into the noise band even though the rats continued to self-stimulate.

The results obtained by means of in-vivo microdialysis and reported here contrast sharply with those reported by Garris et al and Kilpatrick et al. A robust increase in DA

tone was observed during each stimulation bout, and DA levels declined rapidly during the resting periods. When the experimental subjects had access to a continuous reinforcement schedule, the DA concentration in the dialysate peaked 30 minutes following the onset of the stimulation and then steadily declined. Nevertheless, the DA concentration remained significantly elevated for 110 minutes. This pattern in tonic DA release, in which DA tone peaks and then steadily declines had been observed in the previous experiments when the experimental subjects were exposed to either the VT or FT 1.5 schedules and when lateral hypothalamic stimulation was delivered using a shorter pulse duration (0.1 msec) than the one used in this experiment (1 msec). In comparison to what was observed in those experiments, DA tone peaked earlier and declined at a slightly faster rate. This could be explained by the fact that inter-train intervals were shorter during the experiment described in Chapter 4 than in the other microdialysis experiments due to the continuous reinforcement schedule employed.

At first glance, the FSCV results reported by Garris et al. (1999) and Kilpatrick et al. (2000) seem to provide evidence that bridge the gap between DA phasic release at the terminal fields, with the electrophysiological data obtained from single-unit midbrain DA neurons spikes at the level of the cell bodies and believed to encode reward-prediction errors (Hollerman & Schultz, 1998; Montague et al., 1996; Montague et al., 2004; Schultz & Dickinson, 2000). If it is assumed that the electrode activates DA neurons trans-synaptically, and since the behaviour of pressing the lever will predict the delivery of rewarding stimulation, then it is not surprising that phasic release is no longer detectable when the contingency has been learned. However, one problem with this interpretation is that when a ten-second time-out was introduced between stimulations,

phasic release was observed after each train (Cheer et al., 2005). In this case, the delivery of the electrical stimulation was as predictable as in previous experiments; yet phasic release was measurable every single time. Thus, the nulling of DA release observed by Garris et al. (1999) and Kilpatrick et al. (2000) may be due not to the predictability of the reward but to the high density of rewarding stimulation that the experimental subjects received.

A formal model of DA phasic release proposed by Montague et al. (2004) may accommodate these data. According to this model, stimulation induced phasic release can be accounted for by three adaptive processes: short lasting facilitation, short lasting depression and long lasting depression. By virtue of the short lasting depression, this model predicts the absence of phasic release when the stimulation is given according to a continuous reinforcement schedule and the emergence of phasic release when a time-out is introduced between stimulations. What this model fails to predict is the absence of phasic release after a 30 min rest period. The time constant for the long lasting depression in the Montague et al. (2004) model was between 12-15 minutes. Thus a considerable recovery of releasable DA is predicted after a 30 min rest period. Indeed, there is empirical evidence that shows DA phasic release recuperates after repeated stimulation of the medial forebrain bundle (MFB) when measured at 20 min intervals (Ewing et al., 1983; Kuhr et al., 1985; Michael et al., 1987a; Michael et al., 1987b). Thus, the absence of phasic DA release detection after a 30 min rest period in the Garris et al. (1999) study is perplexing. A meaningful explanation is required of why this signal falls below the detection threshold after being initially recorded at the start of the stimulation session, and after plenty of time for the releasable DA at the terminals to be replenished; such an

interpretation should address possible limitations of the detection method (Yavich & Tiihonen, 2000).

The discrepancy observed between the Garris et al. (1999) and Kilpatrick et al. (2000) results on the one hand and the microdialysis results here reported on the other, can be seen as further evidence for the dissociation between phasic and tonic release. In our experiment, we observed prolonged increases in DA levels that go well beyond the time limits of the DA overflow reported in the FSCV studies. These results may suggest that the signal measured by means of microdialysis reflects the number of DA neurons in the active state and is not driven solely by the integration DA transients.

The empirical evidence gathered by the multiple experiments carried out shows that tonic DA release is present under circumstances in which phasic DA release is no longer detectable, and unlike phasic firing, it does not seem to be influenced by reward predictability. The presence of tonic DA release when phasic release has been reported to have faded away might suggest that DA tone is the signal that is important to the maintenance of self-stimulation. Convergent evidence seems to support this conclusion. Long standing results obtained using pharmacological manipulations, such as blockade of the DA transporter or DA receptor, show how sensitive the behaviour sustained by BSR is to alterations in tonic DA signalling. Evidence of this sensitivity is also provided by the after-effects of prolonged rewarding stimulation. DA tone is affected by the stimulation density. When the rewarding stimulations are separated by an average interval of 12 sec. DA tone is stable; but when the rewarding stimulations are separated by an average interval of 1.5 sec or less, DA tone shows a dynamic pattern characterized by a peak followed by a steady decline. As expected, these different patterns have implications for

the behaviour sustained by BSR. When the richer stimulation pattern was in effect for 150 minutes and was delivered between the collections of two time allocation-frequency curves, the second time allocation-frequency curve was rightward displaced. However, when the leaner stimulation pattern or no stimulation was interpolated between the two time allocation-frequency curves, no significant displacement of the second curve was observed.

How DA neurons are integrated into the circuit that computes and integrates the reward signal and what role dopamine tone plays circuit function was further investigated. Based on empirical evidence and formal reasoning, a feedforward model of the role of DA neurons in ICSS was postulated. As multiple electrophysiological data have shown, it is very unlikely that DA neurons are the ones directly stimulated by the electrode, and if the data from Garris et al. (1999) experiment are taken at face value DA neurons are unlikely candidates to carry the reward signal. In the feedforward schema, the directly activated neurons project to one or more additional non-dopaminergic populations that process the reward signal and relay it to subsequent stages. DA neurons activated trans-synaptically, in parallel with the non-dopaminergic efferents of the directly-stimulated neurons; their output converges with the main signal-carrying pathway and modulates transmission along it. Manipulations that reduce or eliminate the influence of DA attenuates or shuts down transmission between the directly activated neurons and efferent stages of the circuitry. Manipulations that enhance DA tone boost neurotransmission along the reward circuit.

Where DA tone exerts its influence in the multistage minimal model (Gallistel et al., 1981; Shizgal, 1997) that translates the induced neural firing into behaviour was

investigated using the reinforcement mountain model and testing paradigm. The results obtained show that increases in DA tone, obtained after continuous subcutaneous infusions of cocaine affect the willingness of the experimental subjects to invest time in the pursuit of reward. The 3D structure formed by the time allocation, stimulation frequency and opportunity cost, reliably shifted rightward along the cost axis in all subjects tested; in most subjects this change was not accompanied by a shift along the frequency axis.

The model framework provides some ideas about the parameters influenced by DA tone and the stage of processing at which this influence is brought to bear. Increased DA tone could boost the absolute reward intensity achievable (I_{max}), thus rescaling the reward-growth function. This possibility is compatible with the feedforward model described above and in Chapter 1. Alternatively, upregulation of DA tone could decrease the subjective effort cost, the perceived exertion required to hold down the lever. This last proposition is compatible with Salamone's hypothesis of DA function (Salamone, 2002a; Salamone et al., 2005; Salamone et al., 2001). In addition, it is possible that the displacement along the cost axis is due to a drug-induced decrease in the payoff from alternative activities (U_E). How these factors are influenced by DA tone will be addressed in future research.

The displacement of the mountain along the frequency axis observed in two, of the seven subjects tested, opens the door for inquiry into other factors that could play a role in the pursuit of rewards and thus, has implications for future experiments. One of those factors is the heterogeneity of the reward substrate (Arvanitogiannis et al., 1996; Fulton et al., 2006). Although the stimulation sites in the subjects showing shifts along

both axes do not appear different from the others, the past demonstrations of placement-specific effects have rested on rather subtle spatial differences that required large numbers of placements to discern. Despite the absence of confirming histological evidence, it is possible that the electrodes in this study sampled differentially from functionally distinct sub-populations of reward-related neurons and that dopaminergic neurons occupy different positions within these circuits within which these neurons are embedded.

Cocaine was the drug selected for the mountain experiment, in part because of the abundance of prior research on its effects in the ICSS paradigm. However, cocaine does not have a clean neuropharmacological effect since it acts both at the presynaptic (Aragona et al., 2008; Scott et al., 2008) and at the postsynaptic level (Giros et al., 1996; Venton et al., 2006) of DA releasing neurons. In addition, cocaine affects neurotransmitters other than dopamine, including norepinephrine (Roberts, 1991), a neurotransmitter that is coming back to the spotlight in the study of reward and BSR (Lin et al., 2006; Yasushi et al., 2001). Thus, it will be important to determine how a drug with more specific effects on DA neurotransmission, like the specific DA transport blocker, GBR12909, affects the reinforcement mountain.

The obtained results highlight the promise and power of the reinforcement mountain model and testing paradigm. These findings challenge a long believed effect of DA tone on the reward circuit. It can be inferred from the data that DA tone influences the reward circuit at or beyond the integrator output, at a later stage of processing that was initially proposed (Wise, 1980). Moreover, the data clearly exemplify how by the introduction of a three-dimensional method of testing and analysis can extend and deepen

the interpretation of previous results. The three-dimensional perspective reveals an ambiguity in data obtained by curve-shift scaling that has not been recognized in earlier papers on the role of DA in ICSS. In the light of the current results, it appears that previous investigators have misinterpreted the principal influence of DA tone on ICSS due to movements of the diagonally oriented face of the 3D structure along an axis that has not been considered in conventional curve-shift analysis. The previously documented shifts of psychometric curves along the frequency axis were likely due, in large part, to unmeasured and unappreciated shifts along the price axis.

The reinforcement mountain model offers clear advantages over the traditional curve-shift paradigm. It is based on solid electrophysiological data and extensive, quantitatively rigorous, behavioural measurements. It incorporates multiple factors involved in translating the stream of action potentials elicited by the stimulation into the pursuit of BSR, and it does so in a systematic, step-by-step manner. The formal nature of the mountain model makes it highly amenable to exploration by means of simulation while providing clear avenues for linking key variables to identifiable neural-circuit components and signals. This new analytical tool will increase our understanding of the influence of pharmacological and psychological variables on the reward circuit and on reward-seeking behaviour.

REFERENCES

- Adell, A., & Artigas, F. (2004). The somatodendritic release of dopamine in the ventral tegmental area and its regulation by afferent transmitter systems. *Neuroscience and Biobehavioral Reviews*, 28(4), 415-431.
- Amaral, D. G., & Routtenberg, A. (1975). Locus coeruleus and intracranial self-stimulation: A cautionary note. *Behavioral Biology*, 13(3), 331-338.
- Anderson, R. M., Fatigati, M. D., & Rompre, P. P. (1996). Estimates of the axonal refractory period of midbrain dopamine neurons: their relevance to brain stimulation reward. *Brain Research*, 718(1-2), 83-88.
- Aragona, B. J., Cleaveland, N. A., Stuber, G. D., Day, J. J., Carelli, R. M., & Wightman, R. M. (2008). Preferential Enhancement of Dopamine Transmission within the Nucleus Accumbens Shell by Cocaine Is Attributable to a Direct Increase in Phasic Dopamine Release Events. *Journal of Neuroscience*, 28(35), 8821-8831.
- Arvanitogiannis, A., & Shizgal, P. (2008). The reinforcement mountain: allocation of behavior as a function of the rate and intensity of rewarding brain stimulation. *Behavioral Neuroscience*, 122(5), 1126-1138.
- Arvanitogiannis, A., Waraczynski, M., & Shizgal, P. (1996). Effects of excitotoxic lesions of the basal forebrain on MFB self-stimulation. *Physiology and Behavior*, 59(4-5), 795-806.
- Atalay, J., & Wise, R. A. (1983). Time course of pimozide effects on brain stimulation reward. *Pharmacology Biochemistry & Behavior*, 18, 655-658.

- Bauco, P., Wang, Y., & Wise, R. A. (1993). Lack of sensitization or tolerance to the facilitating effect of ventral tegmental area morphine on lateral hypothalamic brain stimulation reward. *Brain Research*, *617*(2), 303-308.
- Bauco, P., & Wise, R. A. (1994). Potentiation of lateral hypothalamic and midline mesencephalic brain stimulation reinforcement by nicotine: examination of repeated treatment. *The Journal of Pharmacology and Experimental Therapeutics*, *271*(1), 294-301.
- Bauco, P., & Wise, R. A. (1997). Synergistic effects of cocaine with lateral hypothalamic brain stimulation reward: lack of tolerance or sensitization. *Journal of Pharmacology and Experimental Therapeutics*, *283*(3), 1160-1167.
- Bean, A. J., & Roth, R. H. (1991). Extracellular dopamine and neurotensin in rat prefrontal cortex in vivo: effects of median forebrain bundle stimulation frequency, stimulation pattern, and dopamine autoreceptors. *Journal of Neuroscience*, *11*(9), 2694-2702.
- Belluzzi, J. D., Ritter, S., Wise, C. D., & Stein, L. (1975). Substantia nigra self-stimulation: Dependence on noradrenergic reward pathways. *Behavioral Biology*, *13*(1), 103-111.
- Berridge, K. C. (2007). The debate over dopamine's role in reward: the case for incentive salience. *Psychopharmacology (Berl)*, *191*(3), 391-431.
- Bielajew, C., Lapointe, M., Kiss, I., & Shizgal, P. (1982). Absolute and relative refractory periods of the substrates for lateral hypothalamic and ventral midbrain self-stimulation. *Physiology & Behavior*, *28*(1), 125-132.

- Bielajew, C., & Shizgal, P. (1982). Behaviorally derived measures of conduction velocity in the substrate for rewarding medial forebrain bundle stimulation. *Brain Research*, 237(1), 107-119.
- Bielajew, C., & Shizgal, P. (1986). Evidence implicating descending fibers in self-stimulation of the medial forebrain bundle. *Journal of Neuroscience*, 6(4), 919-929.
- Blackburn, J. R., Pfaus, J. G., & Phillips, A. G. (1992). Dopamine functions in appetitive and defensive behaviours. *Progress in Neurobiology*, 39(3), 247-279.
- Blaaha, C. D., & Phillips, A. G. (1990). Application of in vivo electrochemistry to the measurement of changes in dopamine release during intracranial self-stimulation. *Journal of Neuroscience Methods*, 34(1-3), 125-133.
- Blaaha, C. D., & Phillips, A. G. (1996). A critical assessment of electrochemical procedures applied to the measurement of dopamine and its metabolites during drug-induced and species-typical behaviours. *Behavioral Pharmacology*, 7(7), 675-708.
- Breton, Y. (2006). *Further validation of a model for inferring the value of rewarding brain stimulation*. Concordia University, Montreal.
- Breton, Y., Conover, K., & Shizgal, P. (2006). *Further tests of a 3D model of performance for rewarding brain stimulation*. Poster presented at the Society for Neuroscience, 2006.
- Breton, Y. A., Marcus, J. C., & Shizgal, P. (2009). Rattus Psychologicus: construction of preferences by self-stimulating rats. *Behavioral Brain Research*, 202(1), 77-91.

- Brown, J., Bullock, D., & Grossberg, S. (1999). How the basal ganglia use parallel excitatory and inhibitory learning pathways to selectively respond to unexpected rewarding cues. *Journal of Neuroscience*, *19*(23), 10502-10511.
- Bungay, P. M., Newton-Vinson, P., Isele, W., Garris, P. A., & Justice, J. B. (2003). Microdialysis of dopamine interpreted with quantitative model incorporating probe implantation trauma. *Journal of Neurochemistry*, *86*(4), 932-946.
- Cagniard, B., Beeler, J. A., Britt, J. P., McGehee, D. S., Marinelli, M., & Zhuang, X. (2006). Dopamine scales performance in the absence of new learning. *Neuron*, *51*(5), 541-547.
- Carlezon, W. A., Todtenkopf, M. S., McPhie, D. L., Pimentel, P., Pliakas, A. M., Stellar, J. R., et al. (2001). Repeated exposure to rewarding brain stimulation downregulates GluR1 expression in the ventral tegmental area. *Neuropsychopharmacology*, *25*(2), 234-241.
- Carlezon, W. A., & Wise, R. A. (1993). Phencyclidine-induced potentiation of brain stimulation reward: acute effects are not altered by repeated administration. *Psychopharmacology*, *111*(4), 402-408.
- Carlsson, A. (2003). A half-century of neurotransmitter research: impact on neurology and psychiatry. . In H. Jörnvall (Ed.), *Nobel Lectures, Physiology or Medicine 1996-2000* Singapore: World Scientific Publishing Company.
- Carmona, G. N., Schindler, C. W., Greig, N. H., Holloway, H. W., Jufer, R. A., Cone, E. J., et al. (2005). Intravenous butyrylcholinesterase administration and plasma and brain levels of cocaine and metabolites in rats. *European Journal of Pharmacology*, *517*(3), 186-190.

- Cheer, J. F., Aragona, B. J., Heien, M. L., Seipel, A. T., Carelli, R. M., & Wightman, R. M. (2007). Coordinated accumbal dopamine release and neural activity drive goal-directed behavior. *Neuron*, *54*(2), 237-244.
- Cheer, J. F., Heien, M. L. A. V., Garris, P. A., Carelli, R. M., & Wightman, R. M. (2005). Simultaneous dopamine and single-unit recordings reveal accumbens GABAergic responses: Implications for intracranial self-stimulation. *Proceedings of the National Academy of Sciences*, *102*(52), 19150-19155.
- Churchill, L., Swanson, C. J., Urbina, M., & Kalivas, P. W. (1999). Repeated Cocaine Alters Glutamate Receptor Subunit Levels in the Nucleus Accumbens and Ventral Tegmental Area of Rats that Develop Behavioral Sensitization. *Journal of Neurochemistry*, *72*(6), 2397-2403.
- Clavier, R. M., Fibiger, H. C., & Phillips, A. G. (1976). Evidence that self-stimulation of the region of the locus coeruleus in rats does not depend upon noradrenergic projections to telencephalon. *Brain Research*, *113*(1), 71-81.
- Clavier, R. M., & Routtenberg, A. (1976). Brain stem self-stimulation attenuated by lesions of medial forebrain bundle but not by lesions of locus coeruleus or the caudal ventral norepinephrine bundle. *Brain Research*, *101*(2), 251-271.
- Colle, L. M., & Wise, R. A. (1988). Effects of nucleus accumbens amphetamine on lateral hypothalamic brain stimulation reward. *Brain Research*, *459*(2), 361-368.
- Collins, L. M., Pahl, J. A., & Meyer, J. S. (1999). Distribution of cocaine and metabolites in the pregnant rat and fetus in a chronic subcutaneous injection model. *Neurotoxicology and Teratology*, *21*(6), 639-646.

- Conover, K. L., & Shizgal, P. (1994). Competition and Summation Between Rewarding Effects of Sucrose and Lateral Hypothalamic Stimulation in the Rat. *Behavioral Neuroscience*, *108*(3), 537-548.
- Conover, K. L., & Shizgal, P. (2005). Employing labor-supply theory to measure the reward value of electrical brain stimulation. *Games and Economic Behavior*, *52*(2), 283-304.
- Cooper, B. R., Cott, J. M., & Breese, G. R. (1974). Effects of catecholamine-depleting drugs and amphetamine on self-stimulation of brain following various 6-hydroxydopamine treatments. *Psychopharmacology*, *37*(3), 235-248.
- Corbett, D., Fox, E., & Milner, P. M. (1982). Fiber pathways associated with cerebellar self-stimulation in the rat: A retrograde and anterograde tracing study. *Behavioural Brain Research*, *6*(2), 167-184.
- Corbett, D., Skelton, R. W., & Wise, R. A. (1977). Dorsal noradrenergic bundle lesions fail to disrupt self-stimulation from the region of locus coeruleus. *Brain Research*, *133*(1), 37-44.
- Corbett, D., & Wise, R. A. (1980). Intracranial self-stimulation in relation to the ascending dopaminergic systems of the midbrain: A moveable electrode mapping study. *Brain Research*, *185*, 1-15.
- Crow, T. J. (1969). Mode of enhancement of self stimulation in rats by methamphetamine. *Nature*, *224*(5220), 709.
- Crow, T. J. (1970). Enhancement of cocaine of intra-cranial self-stimulation in the rat. *Life Science*, *9*(7), 375-381.

- Crow, T. J. (1972). Catecholamine-containing neurones and electrical self-stimulation. 1. A review of some data. *Psychological Medicine*, 2(4), 414-421.
- Crow, T. J. (1972). A map of the rat mesencephalon for electrical self-stimulation. *Brain Research*, 36(2), 265-273.
- Crow, T. J., Spear, P. J., & Arbuthnott, G. W. (1972). Intracranial self-stimulation with electrodes in the region of the locus coeruleus. *Brain Research*, 36(2), 275-287.
- Dackis, C. A., & Gold, M. S. (1985). New concepts in cocaine addiction: the dopamine depletion hypothesis. *Neuroscience and Biobehavioral Reviews*, 9(3), 469-477.
- Daw, N. D., & Doya, K. (2006). The computational neurobiology of learning and reward. *Current Opinion in Neurobiology*, 16(2), 199-204.
- Daw, N. D., & Touretzky, D. S. (2002). Long-term reward prediction in TD models of the dopamine system. *Neural Computation*, 14(11), 2567-2583.
- Day, J. J., Roitman, M. F., Wightman, R. M., & Carelli, R. M. (2007). Associative learning mediates dynamic shifts in dopamine signaling in the nucleus accumbens. *Nature Neuroscience*, 10(8), 1020-1028.
- Dayan, P., & Balleine, B. W. (2002). Reward, motivation, and reinforcement learning. *Neuron*, 36(2), 285-298.
- Delgado, J. M. R. (1975). New Orientation in self-stimulation in man. In A. Wauquier & E. T. Rolls (Eds.), *Brain-Stimulation Reward*. New York: Elsevier.
- Delgado, J. M. R., Roberts, W. W., & Miller, N. E. (1954). Learning Motivated by Electrical Stimulation of the Brain. *Am J Physiol*, 179(3), 587-593.

- Di Chiara, G., Bassareo, V., Fenu, S., De Luca, M. A., Spina, L., Cadoni, C., et al. (2004). Dopamine and drug addiction: the nucleus accumbens shell connection. *Neuropharmacology*, *47 Suppl 1*, 227-241.
- Donita, L. R., Elaina, C. H., Scott, M., Rueben, A. G., & Wightman, R. M. (2009). Disparity Between Tonic and Phasic Ethanol-Induced Dopamine Increases in the Nucleus Accumbens of Rats. *Alcoholism: Clinical and Experimental Research*, *33*(7), 1187-1196.
- Durazzo, T. C., Gauvin, D. V., Goulden, K. L., Briscoe, R. J., & Holloway, F. A. (1994). Technical report: The subcutaneous administration of cocaine in the rat. *Pharmacology Biochemistry and Behavior*, *49*(4), 1007-1010.
- Edmonds, D. E., & Gallistel, C. R. (1974). Parametric analysis of brain stimulation reward in the rat: III. Effect of performance variables on the reward summation function. *Journal of Comparative and Physiological Psychology*, *87*(5), 876-883.
- Edmonds, D. E., & Gallistel, C. R. (1977). Reward versus performance in self-stimulation: electrode-specific effects of alpha-methyl-p-tyrosine on reward in the rat. *Journal of Comparative and Physiological Psychology*, *91*(5), 962-974.
- Efron, B., & Tibshirani, R. (1991). Statistical Data Analysis in the Computer Age. *Science*, *253*(5018), 390-395.
- Esposito, R., & Kornetsky, C. (1977). Morphine lowering of self-stimulation thresholds: lack of tolerance with long-term administration. *Science*, *195*(4274), 189-191.
- Ettenberg, A., Koob, G. F., & Bloom, F. E. (1981). Response artifact in the measurement of neuroleptic-induced anhedonia. *Science*, *213*(4505), 357-359.

- Evenden, J. I. (1988). Reinforcers and Sequential choice: "Win-Stay" and the role of Dopamine in reinforcement. In Michael L. Commons, Russell M. Church, James R. Stellar & A. R. Wagner (Eds.), *Quantitative analysis of behavior* (Vol. 7, pp. 187-206). Hillsdale: Lawrence Erlbaum
- Ewing, A. G., Bigelow, J. C., & Wightman, R. M. (1983). Direct in vivo monitoring of dopamine released from two striatal compartments in the rat. *Science*, *221*(4606), 169-171.
- Fibiger, H. C. (1978). Drugs and Reinforcement Mechanisms: A Critical Review of the Catecholamine Theory. *Annual Review of Pharmacology and Toxicology*, *18*(1), 37.
- Field, A. (2005). *Discovering statistics with SPSS* (Second ed.). London: Sage.
- Fiorillo, C. D., & Newsome, W. T. (2006, October 18, 2006). *Activation of midbrain dopamine neurons by brain stimulation reward in mediodorsal thalamus*. Poster presented at the 2006 Meeting of the Society for Neuroscience, Atlanta, GA.
- Fiorino, D. F., Cury, A., Fibiger, H. C., & Phillips, A. G. (1993). Electrical stimulation of reward sites in the ventral tegmental area increases dopamine transmission in the nucleus accumbens of the rat. *Behavioural Brain Research*, *55*(2), 131-141.
- Fitzgerald, L. W., Ortiz, J., Hamedani, A. G., & Nestler, E. J. (1996). Drugs of abuse and stress increase the expression of GluR1 and NMDAR1 glutamate receptor subunits in the rat ventral tegmental area: common adaptations among cross-sensitizing agents. *The Journal of Neuroscience*, *16*(1), 274-282.

- Floresco, S. B., West, A. R., Ash, B., Moore, H., & Grace, A. A. (2003). Afferent modulation of dopamine neuron firing differentially regulates tonic and phasic dopamine transmission. *Nature Neuroscience*, 6(9), 968-973.
- Foley, P. L., Barthel, C. H., & Brausa, H. R. (2002). Effect of covalently bound heparin coating on patency and biocompatibility of long-term indwelling catheters in the rat jugular vein. *Comparative medicine*, 52(3), 243-248.
- Forster, G. L., & Blaha, C. D. (2000). Laterodorsal tegmental stimulation elicits dopamine efflux in the rat nucleus accumbens by activation of acetylcholine and glutamate receptors in the ventral tegmental area. *European Journal of Neuroscience*, 12(10), 3596-3604.
- Fouriez, G. (1995). Temporal integration in self-stimulation: A paradox lost? *Behavioral Neuroscience*, 109(5), 965-971.
- Fouriez, G., Bielajew, C., & Pagotto, W. (1990). Task difficulty increases thresholds of rewarding brain stimulation. *Behavioural Brain Research*, 37(1), 1-7.
- Fouriez, G., & Francis, S. (1992). Apomorphine and electrical self-stimulation of rat brain. *Behavioural Brain Research*, 52(1), 73-80.
- Fouriez, G., & Wise, R. A. (1976). Pimozide-induced extinction of intracranial self-stimulation: response patterns rule out motor or performance deficits. *Brain Research*, 103(2), 377-380.
- Frank, R. A., Manderscheid, P. Z., Panicker, S., Williams, H. P., & Kokoris, D. (1992). Cocaine euphoria, dysphoria, and tolerance assessed using drug-induced changes in brain-stimulation reward. *Pharmacology Biochemistry and Behavior*, 42(4), 771-779.

- Frank, R. A., Markou, A., & Wiggins, L. L. (1987). A systematic evaluation of the properties of self-stimulation train-duration response functions. *Behavioral Neuroscience, 101*(4), 546-559.
- Frank, R. A., Martz, S., & Pommering, T. (1988). The effect of chronic cocaine on self-stimulation train-duration thresholds. *Pharmacology Biochemistry and Behavior, 29*(4), 755-758.
- Frank, R. A., & Williams, H. P. (1985). Both response effort and current intensity affect self-stimulation train duration thresholds. *Pharmacology Biochemistry and Behavior, 22*(4), 527-530.
- Franklin, K. B. J. (1978). Catecholamines and self-stimulation: Reward and performance effects dissociated. *Pharmacology Biochemistry and Behavior, 9*(6), 813-820.
- Fulton, S., Woodside, B., & Shizgal, P. (2000). Modulation of brain reward circuitry by leptin. *Science, 287*(5450), 125-128.
- Fulton, S., Woodside, B., & Shizgal, P. (2006). Potentiation of brain stimulation reward by weight loss: evidence for functional heterogeneity in brain reward circuitry. *Behavioural brain research, 174*(1), 56-63.
- Gallistel, C. R. (1978). Self-stimulation in the rat: Quantitative characteristics of the reward pathway. *Journal of Comparative and Physiological Psychology, 92*, 977-998.
- Gallistel, C. R. (1978). Self-stimulation in the rat: quantitative characteristics of the reward pathway. *Journal of Comparative and Physiological Psychology, 92*(6), 977-998.

- Gallistel, C. R., Boytim, M., Gomita, Y., & Klebanoff, L. (1982). Does pimozide block the reinforcing effect of brain stimulation? *Pharmacology Biochemistry and Behavior*, *17*(4), 769-781.
- Gallistel, C. R., Boytim, M., Gomita, Y., & Klebanoff, L. (1982). Does pimozide block the reinforcing effect of brain stimulation? *Pharmacology Biochemistry and Behavior*, *17*, 769-781.
- Gallistel, C. R., & Freyd, G. (1987). Quantitative determination of the effects of catecholaminergic agonists and antagonists on the rewarding efficacy of brain stimulation. *Pharmacology Biochemistry and Behavior*, *26*(4), 731-741.
- Gallistel, C. R., & Karras, D. (1984). Pimozide and amphetamine have opposing effects on the reward summation function. *Pharmacology Biochemistry and Behavior*, *20*(1), 73-77.
- Gallistel, C. R., & Leon, M. (1991). Measuring the subjective magnitude of brain stimulation reward by titration with rate of reward. *Behavioral Neuroscience*, *105*(6), 913-925.
- Gallistel, C. R., Shizgal, P., & Yeomans, J. S. (1981). A portrait of the substrate for self-stimulation. *Psychological Review*, *88*(3), 228-273.
- Garris, P. A., Collins, L. B., Jones, S. R., & Wightman, R. M. (1993). Evoked Extracellular Dopamine In Vivo in the Medial Prefrontal Cortex. *Journal of Neurochemistry*, *61*(2), 637-647.
- Garris, P. A., Kilpatrick, M., Bunin, M. A., Michael, D., Walker, Q. D., & Wightman, R. M. (1999). Dissociation of dopamine release in the nucleus accumbens from intracranial self-stimulation. *Nature*, *398*(6722), 67-69.

- Gerfen, C. R., Herkenham, M., & Thibault, J. (1987). The neostriatal mosaic: II. Patch- and matrix-directed mesostriatal dopaminergic and non-dopaminergic systems. *Journal of Neuroscience*, 7(12), 3915-3934.
- German, D. C., & Bowden, D. M. (1974). Catecholamine systems as the neural substrate for intracranial self-stimulation: a hypothesis. *Brain Research*, 73, 381-419.
- Gibson, W. E. (1965). Intracranial reinforcement compared with sugar-water reinforcement. *Science*, 148, 1357-1359.
- Giros, B., Jaber, M., Jones, S. R., Wightman, R. M., & Caron, M. G. (1996). Hyperlocomotion and indifference to cocaine and amphetamine in mice lacking the dopamine transporter. *Nature*, 379(6566), 606-612.
- Grace, A. A. (1991). Phasic versus tonic dopamine release and the modulation of dopamine system responsivity: a hypothesis for the etiology of schizophrenia. *Neuroscience*, 41(1), 1-24.
- Grace, A. A. (1995). The tonic/phasic model of dopamine system regulation: its relevance for understanding how stimulant abuse can alter basal ganglia function. *Drug and Alcohol Dependence*, 37(2), 111-129.
- Grace, A. A., Floresco, S. B., Goto, Y., & Lodge, D. J. (2007). Regulation of firing of dopaminergic neurons and control of goal-directed behaviors. *Trends in Neuroscience*, 30(5), 220-227.
- Green, L., & Rachlin, H. (1991). Economic substitutability of electrical brain stimulation, food, and water. *Journal of the Experimental Analysis of Behavior*, 55, 133-143.
- Grigson, P. S., Wheeler, R. A., Wheeler, D. S., & Ballard, S. M. (2001). Chronic morphine treatment exaggerates the suppressive effects of sucrose and cocaine,

- but not lithium chloride, on saccharin intake in Sprague-Dawley rats. *Behavioral Neuroscience*, 115(2), 403-416.
- Hamilton, A. L., Stellar, J. R., & Hart, E. B. (1985). Reward, performance, and the response strength method in self-stimulating rats: Validation and neuroleptics. *Physiology & Behavior*, 35(6), 897-904.
- Hammer, R. P., Egilmez, Y., & Emmett-Oglesby, M. W. (1997). Neural mechanisms of tolerance to the effects of cocaine. *Behavioural Brain Research*, 84(1-2), 225-239.
- Heath, R. G. (1964). Pleasure response of human subjects to direct stimulation of the brain: physiologic psychodynamic considerations. In R. G. Heath (Ed.), *The Role of Pleasure in Behavior* (pp. 219-243). New York: Hoeber, Harper and Row.
- Heimer, L., Zahm, D. S., Churchill, L., Kalivas, P. W., & Wohltmann, C. (1991). Specificity in the projection patterns of accumbal core and shell in the rat. *Neuroscience*, 41(1), 89-125.
- Hernandez, G., Haines, E., Rajabi, H., Stewart, J., Arvanitogiannis, A., & Shizgal, P. (2007). Predictable and unpredictable rewards produce similar changes in dopamine tone. *Behavioral Neuroscience*, 121(5), 887-895.
- Hernandez, G., Haines, E., & Shizgal, P. (2008). Potentiation of intracranial self-stimulation during prolonged subcutaneous infusion of cocaine. *Journal of neuroscience methods*, 175(1), 79-87.
- Hernandez, G., Hamdani, S., Rajabi, H., Conover, K., Stewart, J., Arvanitogiannis, A., et al. (2006). Prolonged rewarding stimulation of the rat medial forebrain bundle: neurochemical and behavioral consequences. *Behavioral Neuroscience*, 120(4), 888 - 904.

- Hernandez, L., & Hoebel, B. G. (1988). Feeding and hypothalamic stimulation increase dopamine turnover in the accumbens. *Physiology & Behavior*, *44*(4-5), 599-606.
- Herrnstein, R. J. (1970). On the law of effect. *J Exp Anal Behav*, *13*(2), 243-266.
- Herrnstein, R. J. (1974). Formal properties of the matching law. *J Exp Anal Behav*, *21*(1), 159-164.
- Hill, R. (1970). Facilitation of conditioned reinforcement as a mechanism of psychomotor stimulation. In Costa E. & Garattini S. (Eds.), *Amphetamines and related compounds* (pp. 781-795). New York: Raven Press.
- Hodos, W., & Valenstein, E. S. (1962). An evaluation of response rate as a measure of rewarding intracranial stimulation. *J Comp Physiol Psychol*, *55*, 80-84.
- Hoebel, B. G. (1974). Brain reward and aversion systems in the control of feeding and sexual behavior. In J. K. Cole & T. B. Sonderegger (Eds.), *The Nebraska Symposium on Motivation* (Vol. 22, pp. 49-112): University of Nebraska Press.
- Hollerman, J. R., & Schultz, W. (1998). Dopamine neurons report an error in the temporal prediction of reward during learning. *Nat Neurosci*, *1*(4), 304-309.
- Hooks, M. S., Colvin, A. C., Juncos, J. L., & Justice, J. B., Jr. (1992). Individual differences in basal and cocaine-stimulated extracellular dopamine in the nucleus accumbens using quantitative microdialysis. *Brain Research*, *587*(2), 306-312.
- Hooks, M. S., Jones, G. H., Smith, A. D., Neill, D. B., & Justice, J. B., Jr. (1991). Response to novelty predicts the locomotor and nucleus accumbens dopamine response to cocaine. *Synapse*, *9*(2), 121-128.
- Hornykiewicz, O. (2002). Dopamine miracle: from brain homogenate to dopamine replacement. *Movement Disorders*, *17*(3), 501-508.

- Houck, J. C., Adams, J. L., & Barto, A. G. (1995). A Model of How the Basal Ganglia Generate and Use Neural Signals That predict reinforcement. In J. L. D. James C. Houk , David G. Beiser (Ed.), *Models of Information Processing in the Basal Ganglia* (pp. 249-270). Massachusetts The MIT Press.
- Howarth, C. I., & Deutsch, J. A. (1962). Drive decay: the cause of fast "extinction" of habits learned for brain stimulation. *Science*, *137*, 35-36.
- Joyner, C., King, G., Lee, T. H., & Ellinwood, E. H. (1993). Technique for the continuous infusion of high doses of cocaine by osmotic minipump. *Pharmacology Biochemistry and Behavior*, *44*(4), 971-973.
- Kalivas, P. W., & Stewart, J. (1991). Dopamine transmission in the initiation and expression of drug- and stress-induced sensitization of motor activity. *Brain Research Review*, *16*(3), 223-244.
- Katz, R. J. (1981). The temporal structure of motivation IV: A reexamination of extinction effects in intracranial reward. *Behavioral and Neural Biology*, *32*(2), 191-200.
- Katz, R. J. (1982). Dopamine and the limits of behavioral reduction-or why aren't all schizophrenics fat and happy? *The Behavioral and brain sciences*, *5*, 60-61.
- Kilpatrick, M. R., Rooney, M. B., Michael, D. J., & Wightman, R. M. (2000). Extracellular dopamine dynamics in rat caudate-putamen during experimenter-delivered and intracranial self-stimulation. *Neuroscience*, *96*(4), 697-706.
- King, G., Kuhn, C., & Ellinwood, E. (1993). Dopamine efflux during withdrawal from continuous or intermittent cocaine. *Psychopharmacology*, *111*(2), 179-184.

- King, G. R., Joyner, C., Lee, T., Kuhn, C., & Ellinwood, E. H. (1992). Intermittent and Continuous cocaine Administration: Residual Behavioral states during withdrawal. *Pharmacology Biochemistry and Behavior*, *43*(1), 243-248.
- Kokkinidis, L., & McCarter, B. D. (1990). Postcocaine depression and sensitization of brain-stimulation reward: Analysis of reinforcement and performance effects. *Pharmacology Biochemistry and Behavior*, *36*(3), 463-471.
- Kuczenski, R., & Segal, D. (1989). Concomitant characterization of behavioral and striatal neurotransmitter response to amphetamine using in vivo microdialysis. *Journal of Neuroscience*, *9*(6), 2051-2065.
- Kuhr, W. G., Ewing, A. G., Near, J. A., & Wightman, R. M. (1985). Amphetamine attenuates the stimulated release of dopamine in vivo. *Journal of Pharmacology and Experimental Therapeutics*, *232*(2), 388-394.
- Leon, M., & Gallistel, C. R. (1992). The function relating the subjective magnitude of brain stimulation reward to stimulation strength varies with site of stimulation. *Behavioural Brain Research*, *52*(2), 183-193.
- Liebman, J. M., & Butcher, L. L. (1974). Comparative involvement of dopamine and noradrenaline in rate-free self-stimulation in substantia nigra, lateral hypothalamus, and mesencephalic central gray. *Naunyn Schmiedeberg's Arch Pharmacol*, *284*(2), 167-194.
- Lin, Y., de Vaca, S. C., Carr, K. D., & Stone, E. A. (2006). Role of α 1-Adrenoceptors of the Locus Coeruleus in Self-Stimulation of the Medial Forebrain Bundle. *Neuropsychopharmacology*, *32*(4), 835-841.

- Lippa, A. S., Antelman, S. M., Fisher, A. E., & Canfield, D. R. (1973). Neurochemical mediation of reward: A significant role for dopamine? *Pharmacology Biochemistry and Behavior*, *1*(1), 23-28.
- Ljungberg, T., Apicella, P., & Schultz, W. (1992). Responses of monkey dopamine neurons during learning of behavioral reactions. *Journal of Neurophysiology*, *67*, 145-163.
- Ljungberg, T., Apicella, P., and Schultz, W. . (1992). Responses of monkey dopamine neurons during learning of behavioral reactions. *Journal of Neurophysiology* *67*, 145-163.
- Lodge, D. J., & Grace, A. A. (2007). Aberrant hippocampal activity underlies the dopamine dysregulation in an animal model of schizophrenia. *Journal of Neuroscience*, *27*(42), 11424-11430.
- Maldonado-Irizarry, C. S., Stellar, J. R., & Kelley, A. E. (1994). Effects of cocaine and GBR-12909 on brain stimulation reward. *Pharmacology Biochemistry and Behavior*, *48*(4), 915-920.
- McDowell, J. J. (2005). On the classic and modern theories of matching. *Journal of the Experimental Analysis of Behavior*, *84*(1), 111-127.
- McSweeney, F. K., & Roll, J. M. (1993). Responding changes systematically within sessions during conditioning procedures. *Journal of the Experimental Analysis of Behavior*, *60*(3), 621-640.
- Michael, A. C., Ikeda, M., & Justice, J. B. (1987a). Dynamics of the recovery of releasable dopamine following electrical stimulation of the medial forebrain bundle. *Neuroscience Letters*, *76*(1), 81-86.

- Michael, A. C., Ikeda, M., & Justice, J. J. B. (1987b). Mechanisms contributing to the recovery of striatal releasable dopamine following MFB stimulation. *Brain Research*, 421(1-2), 325-335.
- Miliaressis, E., Emond, C., & Merali, Z. (1991). Re-evaluation of the role of dopamine in intracranial self-stimulat using in vivo microdialysis. *Behavioural Brain Research*, 46, 43-48.
- Miliaressis, E., & Malette, J. (1987). Summation and saturation properties in the rewarding effect of brain stimulation. *Physiology & Behavior*, 41, 595-604.
- Miliaressis, E., Malette, J., & Coulombe, D. (1986). The effects of pimozide on the reinforcing efficacy of central grey stimulation in the rat. *Behavioural Brain Research*, 21(2), 95-100.
- Miliaressis, E., Rompre, P.-P., Laviolette, P., Philippe, L., & Coulombe, D. (1986). The curve-shift paradigm in self-stimulation. *Physiology & Behavior*, 37(1), 85-91.
- Mirenowicz, J., and Schultz, W. . (1994). Importance of unpredictability for reward responses in primate dopamine neurons. . *Journal of Neurophysiology* 72 1024-1027.
- Mirenowicz, J., & Schultz, W. (1994). Importance of unpredictability for reward responses in primate dopamine neurons. *Journal of Neurophysiology*, 72(2), 1024-1027.
- Montague, P. R., Dayan, P., & Sejnowski, T. J. (1996a). A framework for mesencephalic dopamine systems based on predictive Hebbian learning. *Journal of Neuroscience*, 16(5), 1936-1947.

- Montague, P. R., Dayan, P., & Sejnowski, T. J. (1996b). A framework for mesencephalic dopamine systems based on predictive Hebbian learning. *Journal of Neuroscience*, *16*(5), 1936-1947.
- Montague, P. R., McClure, S. M., Baldwin, P. R., Phillips, P. E. M., Budygin, E. A., Stuber, G. D., et al. (2004). Dynamic Gain Control of Dopamine Delivery in Freely Moving Animals. *Journal of Neuroscience*, *24*(7), 1754-1759.
- Mullet, A. (2005). *Linking changes in performance for brain stimulation reward to stages of neural processing*. Concordia University, Montreal.
- Murray, B., & Shizgal, P. (1996). Behavioral measures of conduction velocity and refractory period for reward-relevant axons in the anterior LH and VTA. *Physiology & Behavior*, *59*(4/5), 643-652.
- Nakahara, D., Fuchikami, K., Ozaki, N., Iwasaki, T., & Nagatsu, T. (1992). Differential effect of self-stimulation on dopamine release and metabolism in the rat medial frontal cortex, nucleus accumbens and striatum studied by in vivo microdialysis. *Brain Research*, *574*, 164-170.
- Nakahara, D., Ozaki, N., Miura, Y., Miura, H., & Nagatsu, T. (1989). increased dopamine and serotonin metabolism in rat nucleus accumbens produced by intracranial self-stimulation of medial forebrain bundle as measured by in vivo microdialysis. *Brain Research*, *495*(1), 178-181.
- Nakajima, S., & Patterson, R. L. (1997). The involvement of dopamine D2 receptors, but not D3 or D4 receptors, in the rewarding effect of brain stimulation in the rat. *Brain Research*, *760*(1-2), 74-79.

- Nayak, P. K., Misra, A. L., & Mule, S. J. (1976). Physiological disposition and biotransformation of (3H) cocaine in acutely and chronically treated rats. *Journal of Pharmacology and Experimental Therapeutics*, 196(3), 556-569.
- Niv, Y., Daw, N., & Dayan, P. (2006). How fast to work: response vigor, motivation and tonic dopamine. In Y. Weiss, B. Schölkopf & J. Platt (Eds.), *Advances in Neural Information Processing Systems* (Vol. 18, pp. 1019-1026). Cambridge: MIT Press.
- Olds, J. (1958). Satiation effects in self-stimulation of the brain. *Journal of Comparative and Physiological Psychology*, 51, 675-678.
- Olds, J. (1962). Hypothalamic substrates of reward. *Physiological Review*, 42, 554-604.
- Olds, J. (1966). Brain Centers and Positive Reinforcement. In E. Stellar & J. Sprague (Eds.), *Progress in brain research* (Vol. 2). New York: Academic Press.
- Olds, J., & Milner, P. (1954). Positive reinforcement produced by electrical stimulation of septal area and other regions of rat brain. *Journal of Comparative Physiological Psychology*, 47(6), 419-427.
- Olds, J., & Milner, P. M. (1954). Positive reinforcement produced by electrical stimulation of septal area and other regions of rat brain. *Journal of Comparative and Physiological Psychology*, 47, 419-427.
- Olds, M. E., & Olds, J. (1962). Approach-escape interactions in rat brain. *American Journal of Physiology*, 203(5), 803-810.
- Pan, H.-T., Menacherry, S., & Justice, J. B. (1991). Differences in the Pharmacokinetics of Cocaine in Naive and Cocaine-Experienced Rats. *Journal of Neurochemistry*, 56(4), 1299-1306.

- Paxinos, G., & Watson, C. (1998). *The Rat Brain in Stereotaxic Coordinates* (4th ed.). San Diego: Academic Press.
- Paxinos, G., & Watson, C. (2007). *The rat brain in stereotaxic coordinates* (6th ed.). Amsterdam: Elsevier.
- Phillips, A. G., Coury, A., Fiorino, D., Lepiane, F. G., Brown, E., & Fibiger, H. C. (1992). Self-Stimulation of the Ventral Tegmental Area Enhances Dopamine Release in the Nucleus Accumbens: A Microdialysis Study. *Annals of the New York Academy of Sciences*, 654(1), 199-206.
- Phillips, P. E., Stuber, G. D., Heien, M. L., Wightman, R. M., & Carelli, R. M. (2003). Subsecond dopamine release promotes cocaine seeking. *Nature*, 422(6932), 614-618.
- Poschel, B. P. H., & Ninteman, F. W. (1963). Norepinephrine: A possible excitatory neurohormone of the reward system. *Life Sciences*, 2(10), 782-788.
- Prado-Alcala, R., Streater, A., & Wise, R. (1984). Brain stimulation reward and dopamine terminal fields. II. Septal and cortical projections. *Brain Research*, 301, 209-219.
- Prado-Alcala, R., & Wise, R. A. (1984). Brain stimulation reward and dopamine terminal fields. I. Caudate-putamen, nucleus accumbens and amygdala. *Brain Research*, 297, 265-273.
- Rada, P. V., Mark, G. P., & Hoebel, B. G. (1998). Dopamine release in the nucleus accumbens by hypothalamic stimulation-escape behavior. *Brain Research*, 782(1-2), 228-234.

- Rada, P. V., Mark, G. P., Yeomans, J. J., & Hoebel, B. G. (2000). Acetylcholine release in ventral tegmental area by hypothalamic self-stimulation, eating, and drinking. *Pharmacology Biochemistry & Behavior*, 65(3), 375-379.
- Redgrave, P., Prescott, T. J., & Gurney, K. (1999a). The basal ganglia: a vertebrate solution to the selection problem? *Neuroscience*, 89(4), 1009-1023.
- Redgrave, P., Prescott, T. J., & Gurney, K. (1999b). Is the short-latency dopamine response too short to signal reward error? *Trends Neurosci*, 22(4), 146-151.
- Reynolds, J. N., Hyland, B. I., & Wickens, J. R. (2001). A cellular mechanism of reward-related learning. *Nature*, 413(6851), 67-70.
- Richardson, N. R., & Gratton, A. (1996). Behavior-relevant changes in nucleus accumbens dopamine transmission elicited by food reinforcement: An electrochemical study in rat. *Journal of Neuroscience*, 16(24), 8160-8169.
- Roberts, D. C. S. (1991). *Neural substrates mediating cocaine reinforcement: The role of monoamine system*. Boca Raton: CRC Press.
- Robinson, S., Sandstrom, S. M., Denenberg, V. H., & Palmiter, R. D. (2005). Distinguishing whether dopamine regulates liking, wanting, and/or learning about rewards. *Behavioral Neuroscience*, 119(1), 5-15.
- Roitman, M. F., Stuber, G. D., Phillips, P. E., Wightman, R. M., & Carelli, R. M. (2004). Dopamine operates as a subsecond modulator of food seeking. *Journal of Neuroscience*, 24(6), 1265-1271.
- Roll, S. K. (1970). Intracranial Self-Stimulation and Wakefulness: Effect of Manipulating Ambient Brain Catecholamines. *Science*, 168(3937), 1370-1372.

- Romo, R., & Schultz, W. (1990). Dopamine neurons of the monkey midbrain: contingencies of responses to active touch during self initiated arm movements. *Journal of Neurophysiology*, 63, 592-606.
- Rompré, P.-P., & Baucó, P. (1990). GBR 12909 reverses the SCH 23390 inhibition of rewarding effects of brain stimulation. *European Journal of Pharmacology*, 182(1), 181-184.
- Rompré, P.-P., & Miliaressis, E. (1987). Behavioral determination of refractory periods of the brainstem substrates of self-stimulation. *Behavioural Brain Research*, 23(3), 205-219.
- Rompré, P.-P., & Shizgal, P. (1986). Electrophysiological characteristics of neurons in forebrain regions implicated in self-stimulation of the medial forebrain bundle in the rat. *Brain Research*, 364(2), 338-349.
- Rompré, P. P., & Miliaressis, E. (1985). Pontine and mesencephalic substrates of self-stimulation. *Brain Research*, 359, 246-259.
- Salamone, J. D. (2002). Functional significance of nucleus accumbens dopamine: behavior, pharmacology and neurochemistry. *Behavioural Brain Research*, 137(1-2), 1.
- Salamone, J. D., Correa, M., Mingote, S., & Weber, S. M. (2003a). Nucleus accumbens dopamine and the regulation of effort in food-seeking behavior: implications for studies of natural motivation, psychiatry, and drug abuse. *Journal of Pharmacology and Experimental Therapeutics*, 305(1), 1-8.
- Salamone, J. D., Correa, M., Mingote, S., & Weber, S. M. (2003b). Nucleus Accumbens Dopamine and the Regulation of Effort in Food-Seeking Behavior: Implications

- for Studies of Natural Motivation, Psychiatry, and Drug Abuse. *Journal of Pharmacology and Experimental Therapeutics*, 305(1), 1-8.
- Salamone, J. D., Correa, M., Mingote, S. M., & Weber, S. M. (2005). Beyond the reward hypothesis: alternative functions of nucleus accumbens dopamine. *Current Opinion in Pharmacology*, 5(1), 34-41.
- Salamone, J. D., Cousins, M. S., & Snyder, B. J. (1997). Behavioral functions of nucleus accumbens dopamine: empirical and conceptual problems with the anhedonia hypothesis. *Neuroscience Biobehavioral Review*, 21(3), 341-359.
- Salamone, J. D., Wisniecki, A., Carlson, B. B., & Correa, M. (2001). Nucleus accumbens dopamine depletions make animals highly sensitive to high fixed ratio requirements but do not impair primary food reinforcement. *Neuroscience*, 105(4), 863-870.
- Schaefer, G. J., & Michael, R. P. (1980). Acute effects of neuroleptics on brain self-stimulation thresholds in rats. *Psychopharmacology*, 67(1), 9-15.
- Schultz, W. (1998). Predictive Reward Signal of Dopamine Neurons. *Journal of Neurophysiology*, 80(1), 1-27.
- Schultz, W. (2002). Getting Formal with Dopamine and Reward. *Neuron*, 36(2), 241-263.
- Schultz, W., Dayan, P., & Montague, P. R. (1997). A Neural Substrate of Prediction and Reward. *Science*, 275(5306), 1593-1599.
- Schultz, W., & Dickinson, A. (2000). Neuronal Coding of Prediction Errors. *Annual Review of Neuroscience*, 23(1), 473-500.

- Schultz, W., & Romo, R. (1990). Dopamine neurons of the monkey midbrain: contingencies of responses to stimuli eliciting immediate behavioral reactions. *Journal of Neurophysiology*, 63, 607-624.
- Scott, C. S., Seth, R. T., Malia, L. H., Elise, N. B., Laura, T. L., Sarah, H. S., et al. (2008). Cocaine disinhibits dopamine neurons in the ventral tegmental area via use-dependent blockade of GABA neuron voltage-sensitive sodium channels. *European Journal of Neuroscience*, 28(10), 2028-2040.
- Sharp, T., Zetterstrom, T., Ljungberg, T., & Ungerstedt, U. (1987). A direct comparison of amphetamine-induced behaviours and regional brain dopamine release in the rat using intracerebral dialysis. *Brain Research*, 401(2), 322-330.
- Shizgal, P. (1989). Toward a cellular analysis of intracranial self-stimulation: Contributions of collision studies. *Neuroscience & Biobehavioral Reviews*, 13(2-3), 81-90.
- Shizgal, P. (1997). Neural basis of utility estimation. *Current Opinion in Neurobiology*, 7(2), 198-208.
- Shizgal, P. (2004). Neural mechanisms of reward: Canadian Institutes of Health Research.
- Shizgal, P., Bielajew, C., Corbett, D., Skelton, R., & Yeomans, J. (1980). Behavioral methods for inferring anatomical linkage between rewarding brain stimulation sites. *Journal of Comparative and Physiological Psychology*, 94(2), 227-237.
- Shizgal, P., Bielajew, C., Corbett, D., Skelton, R. W., & Yeomans, J. S. (1980). Behavioral methods for inferring anatomical linkage between rewarding brain

- stimulation sites. *Journal of Comparative and Physiological Psychology*, 94, 227-237.
- Shizgal, P., Bielajew, C., & Rompré, P.-P. (1988). Quantitative characteristics of the directly stimulated neurons subserving self-stimulation of the medial forebrain bundle: Psychophysical inference and electrophysiological measurement. In M. L. Commons, R. M. Church, J. R. Stellar & A. R. Wagner (Eds.), *Quantitative analyses of behavior VII: Biological determinants of reinforcement*. Hillsdale Lawrence Erlbaum Associates.
- Shizgal, P., Fulton, S., & Woodside, B. (2001). Brain reward circuitry and the regulation of energy balance. *International Journal of Obesity and Related Metabolic Disorders*, 25 Suppl 5, S17-21.
- Shizgal, P., & Mathews, G. (1977). Electrical stimulation of the rat diencephalon: differential effects of interrupted stimulation on- and off-responding. *Brain Research*, 129(2), 319-333.
- Shizgal, P., & Murray, B. (1989). Neuronal basis of intracranial self-stimulation. In J. M. Liebman & S. J. Cooper (Eds.), *The Neuropharmacological Basis of Reward*. (pp. 106-163). Oxford: Oxford University Press.
- Simmons, J. M., & Gallistel, C. R. (1994). Saturation of subjective reward magnitude as a function of current and pulse frequency. *Behavioral Neuroscience*, 108, 151-160.
- Simon, H., Le Moal, M., & Cardo, B. (1975). Self-stimulation in the dorsal pontine tegmentum in the rat. *Behavioral Biology*, 13(3), 339-347.
- Skinner, B. F. (1938). *The behavior of organisms*. Cambridge: Copley publishing group.

- Skinner, B. F. (1948). "Superstition" in the pigeon. *Journal of Experimental Psychology*, 38, 168-172.
- Smith, I. D., & Grace, A. A. (1992). Role of the subthalamic nucleus in the regulation of nigral dopamine neuron activity. *Synapse*, 12(4), 287-303.
- Solomon, R. B., Conover, K., & Shizgal, P. (2007). *Estimation of subjective opportunity cost in rats working for rewarding brain stimulation: further progress*. Poster presented at the Society for Neuroscience Annual Meeting.
- Sonnenschein, B., Conover, K., & Shizgal, P. (2003). Growth of brain stimulation reward as a function of duration and stimulation strength. *Behavioral Neuroscience*, 117(5), 978-994.
- Sourkes, T. L. (2000). How dopamine was recognised as a neurotransmitter: a personal view. *Parkinsonism & Related Disorders*, 6(2), 63-67.
- Stefani, M. R., & Moghaddam, B. (2006). Rule learning and reward contingency are associated with dissociable patterns of dopamine activation in the rat prefrontal cortex, nucleus accumbens, and dorsal striatum. *Journal of Neuroscience*, 26(34), 8810-8818.
- Stein, L. (1961). Effects and interactions of imipramine, chlorpromazine, reserpine and amphetamine on self-stimulation: possible neurophysiological basis of depression. *Recent Advances in Biological Psychiatry*, 4, 288-309.
- Stein, L. (1964). Self-Stimulation of Brain and Central Stimulant Action of Amphetamine. *Federation Proceedings*, 23, 836-850.
- Stein, L., & Ray, O. S. (1960). Brain stimulation reward „Thresholds” self-determined in rat. *Psychopharmacology*, 1(3), 251-256.

- Stellar, J. R., Hall, F. S., & Waraczynski, M. (1991). The effects of excitotoxin lesions of the lateral hypothalamus on self-stimulation reward. *Brain Research*, *541*, 29-40.
- Stellar, J. R., Kelley, A. E., & Corbett, D. (1983). Effects of peripheral and central dopamine blockade on lateral hypothalamic self-stimulation: Evidence for both reward and motor deficits. *Pharmacology Biochemistry and Behavior*, *18*(3), 433-442.
- Stellar, J. R., Waraczynski, M., & Wong, K. (1988). The reward summation function in hypothalamic self-stimulation. In A. W. M. Commons, R. Church, & J. R. Stellar (Ed.), *Quantitative analysis of behavior: Biological determinants of behavior* (Vol. 7). Hillsdale, NJ: Erlbaum.
- Stuber, G. D., Roitman, M. F., Phillips, P. E., Carelli, R. M., & Wightman, R. M. (2005). Rapid dopamine signaling in the nucleus accumbens during contingent and noncontingent cocaine administration. *Neuropsychopharmacology*, *30*(5), 853-863.
- Sutton, R. S. (1988). Learning to predict by the methods of temporal differences. *Machine learning*, *3*, 9-44.
- Sutton, R. S., & Barto, A. G. (1998). *Reinforcement learning : an introduction*. Cambridge, Mass: MIT Press.
- Swanson, L. W. (1982). The projections of the ventral tegmental area and adjacent regions: A combined fluorescent retrograde tracer and immunofluorescence study in the rat. *Brain Research Bulletin*, *9*(1-6), 321-353.
- Taber, M. T., & Fibiger, H. C. (1995). Electrical stimulation of the prefrontal cortex increases dopamine release in the nucleus accumbens of the rat: modulation by

- metabotropic glutamate receptors. *The Journal of neuroscience : the official journal of the Society for Neuroscience*, 15(5), 3896-3904.
- Tryon, W. W. (1982). A simplified time-series analysis for evaluating treatment interventions. *Journal of Applied Behavior Analysis*, 15(3), 423-429.
- Valenstein, E. S. (1964). Problems of measurement and interpretation with reinforcing brain stimulation. *Psychological Review*, 71(6), 415-437.
- Venton, B. J., Seipel, A. T., Phillips, P. E., Wetsel, W. C., Gitler, D., Greengard, P., et al. (2006). Cocaine increases dopamine release by mobilization of a synapsin-dependent reserve pool. *Journal of Neuroscience*, 26(12), 3206-3209.
- Vorel, S., Campos, A., & Gardner, E. (2002). Prolonged electrical stimulation of the medial forebrain bundle elicits cocaine-seeking behavior [Electronic Version]. *Society for Neuroscience Abstract Viewer/Itinerary Planner, Program No. 876.8*.
- Wang, R. Y. (1981). Dopaminergic neurons in the rat ventral tegmental area. I. Identification and characterization. *Brain Research Reviews*, 3(2), 123-140.
- Waraczynski, M., & Perkins, M. (1998). Lesions of pontomesencephalic cholinergic nuclei do not substantially disrupt the reward value of medial forebrain bundle stimulation. *Brain Research*, 800(1), 154-169.
- Wauquier, A., & Niemegeers, C. J. (1972). Intracranial self-stimulation in rats as a function of various stimulus parameters. II. Influence of haloperidol, pimozide and pipamperone on medial forebrain bundle stimulation with monopolar electrodes. *Psychopharmacologia*, 27(3), 191-202.

- West, A. R., Floresco, S. B., Charara, A., Rosenkranz, J. A., & Grace, A. A. (2003). Electrophysiological interactions between striatal glutamatergic and dopaminergic systems. *Annals of the New York Academy of Sciences*, 1003, 53-74.
- Wightman, R. M., & Robinson, D. L. (2002). Transient changes in mesolimbic dopamine and their association with 'reward'. *Journal of Neurochemistry*, 82(4), 721-735.
- Wise, C. D., & Stein, L. (1969). Facilitation of Brain Self-Stimulation by Central Administration of Norepinephrine. *Science*, 163(3864), 299-301.
- Wise, R. A. (1978). Catecholamine theories of reward: A critical review. *Brain Research*, 152(2), 215-247.
- Wise, R. A. (1980). Action of drugs of abuse on brain reward systems. *Pharmacology, biochemistry, and behavior*, 13 Suppl 1, 213-223.
- Wise, R. A., & Munn, E. (1993). Effects of repeated amphetamine injections on lateral hypothalamic brain stimulation reward and subsequent locomotion. *Behavioural Brain Research*, 55(2), 195-201.
- Wise, R. A., & Rompre, P. P. (1989). Brain Dopamine and Reward. *Annual Review of Psychology*, 40(1), 191-225.
- Yasushi, I., Masato, N., Kosuke, E., Kaeko, H., Hiroyuki, H., Yoshio, M., et al. (2001). Immunohistochemical characterisation of Fos-positive cells in brainstem monoaminergic nuclei following intracranial self-stimulation of the medial forebrain bundle in the rat. *European Journal of Neuroscience*, 13(8), 1600-1608.
- Yavich, L., & Tanila, H. (2007). Mechanics of self-stimulation and dopamine release in the nucleus accumbens. *Neuroreport*, 18(12), 1271-1274.

- Yavich, L., & Tiihonen, J. (2000). Patterns of dopamine overflow in mouse nucleus accumbens during intracranial self-stimulation. *Neuroscience Letters*, 293(1), 41-44.
- Yeomans, J., & Baptista, M. (1997). Both nicotinic and muscarinic receptors in ventral tegmental area contribute to brain-stimulation reward. *Pharmacology Biochemistry and Behavior*, 57(4), 915-921.
- Yeomans, J. S. (1979). The absolute refractory periods of self-stimulation neurons. *Physiology and Behavior*, 22(5), 911-919.
- Yeomans, J. S. (1988). Mechanisms of brain-stimulation reward. *Progress in Psychobiology and Physiological Psychology*, 13, 227-265.
- Yeomans, J. S., & Davis, J. K. (1975). Behavioral measurement of the post-stimulation excitability of neurons mediating self-stimulation by varying the voltage of paired pulses. *Behavioral Biology*, 15(4), 435-447.
- Yeomans, J. S., Maidment, N. T., & Bunney, B. S. (1986). Excitability properties of medial forebrain bundle axons of putative A10 dopamine cells. *Society for Neuroscience Abstracts*, 12, 1517.
- Yeomans, J. S., Maidment, N. T., & Bunney, B. S. (1988). Excitability properties of medial forebrain bundle axons of A9 and A10 dopamine cells. *Brain Research*, 450(1-2), 86-93.
- Yeomans, J. S., Mathur, A., & Tampakeras, M. (1993). Rewarding brain stimulation: role of tegmental cholinergic neurons that activate dopamine neurons. *Behavioral Neuroscience*, 107, 1077-1087.

- Yeomans, J. S., Matthews, G. G., Hawkins, R. D., Bellman, K., & Doppelt, H. (1979). Characterization of self-stimulation neurons by their local potential summation properties. *Physiological Behavior*, 22(5), 921-929.
- You, Z.-B., Chen, Y.-Q., & Wise, R. A. (2001). Dopamine and glutamate release in the nucleus accumbens and ventral tegmental area of rat following lateral hypothalamic self-stimulation. *Neuroscience*, 107(4), 629-639.
- You, Z.-B., Tzschentke, T. M., Brodin, E., & Wise, R. A. (1998). Electrical Stimulation of the Prefrontal Cortex Increases Cholecystokinin, Glutamate, and Dopamine Release in the Nucleus Accumbens: an In Vivo Microdialysis Study in Freely Moving Rats. *The Journal of neuroscience : the official journal of the Society for Neuroscience*, 18(16), 6492-6500.
- Zald, D. H., Boileau, I., El-Dearedy, W., Gunn, R., McGlone, F., Dichter, G. S., et al. (2004). Dopamine transmission in the human striatum during monetary reward tasks. *Journal of Neuroscience*, 24(17), 4105-4112.
- Zweifel, L. S., Parker, J. G., Lobb, C. J., Rainwater, A., Wall, V. Z., Fadok, J. P., et al. (2009). Disruption of NMDAR-dependent burst firing by dopamine neurons provides selective assessment of phasic dopamine-dependent behavior. *Proceedings of the National Academy of Sciences*, 106(18), 7281-7288.

APPENDICES

Appendix 1: Supplementary material Chapter 1

Basal extracellular levels of DOPAC and HVA.

Basal amounts of DOPAC and HVA per 10 μ l of dialysate were 1404 ± 32 pg and 530 ± 9 pg for the FT12 schedule, 1211 ± 21 pg and 487 ± 9 pg for the VT12 schedule, and 1199 ± 39 pg and 573 ± 17 pg for the VT 1.5 schedule. Basal levels did not vary significantly across conditions (DOPAC $F_{(8,42)} = 0.36$, $p = 0.99$; HVA $F_{(8,42)} = 0.61$, $p = 0.75$).

Effect of LH stimulation under an FT12 schedule on concentrations of DOPAC and HVA.

As shown in Figure S1a, the increase in the dialysate concentration of DOPAC during the stimulation period lagged behind the increase in the concentration of DA and rose more gradually, approaching plateau levels 60 min following stimulation onset. The DOPAC concentration achieved its maximum value, 184%, at the end of the stimulation period and then declined toward baseline levels in parallel with the decline in DA concentration. The average concentration of DOPAC during the rewarding stimulation was 159 % of the baseline value.

As in the case of DOPAC, the increase in the HVA concentration during the stimulation period was delayed with respect to the rise in DA concentration and was more gradual (Figure S2a). The maximum level achieved was 201 % of the baseline value, at the end of the stimulation period. The average HVA concentration during the stimulation period was 156.83% of the baseline value. The decline in HVA concentration during the

post-stimulation period was delayed with respect to the decline in DA and DOPAC concentrations.

Effect of LH stimulation under a VT12 schedule on concentrations of DOPAC and HVA.

As shown in Figure S1b, the increase in the dialysate concentration of DOPAC during the stimulation period lagged behind the increase in the concentration of DA and rose more gradually, approaching a plateau 60 min after the stimulation onset. The DOPAC concentration achieved its maximum level, 150.86% at the end of the stimulation period and then declined toward baseline levels in parallel with the decline in DA concentration. The average increase of DOPAC during the rewarding stimulation was 140.55 % of baseline.

As in the case of DOPAC, HVA concentration (Figure S2b) increased at slower pace during the stimulation period than the rise in DA. HVA increased steadily from the beginning of the stimulation, and achieved its maximum level, 160.78 %, at the end of the stimulation period. The average increase in HVA concentration during the stimulation period was 139.56% of baseline. The decline in HVA concentration during the poststimulation period was delayed with respect to the decline in DA and DOPAC concentrations.

Effect of LH stimulation under a VT1.5 schedule on concentrations of DOPAC and HVA.

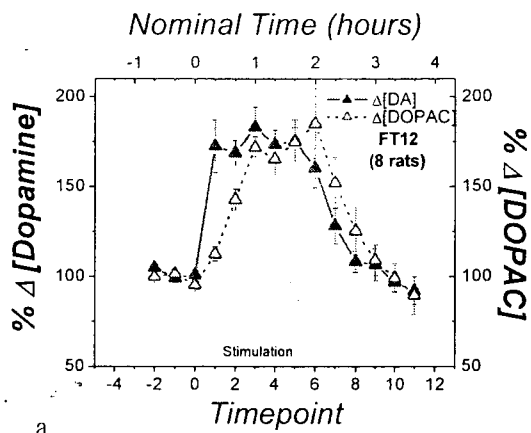
As shown in Figure S1c, the increase in the dialysate concentration of DOPAC during the stimulation lagged behind the increase in the concentration of DA. DOPAC reached its peak, 193.44%, 80 min after the onset of the stimulation and then declined to

150.22 % at the offset of the stimulation period. During the post-stimulation period, DOPAC concentration declined in parallel with the decline in DA, and dropped to values below the baseline, leveling off around 80%. The average increase of DOPAC during the rewarding stimulation was 168.95 % of baseline.

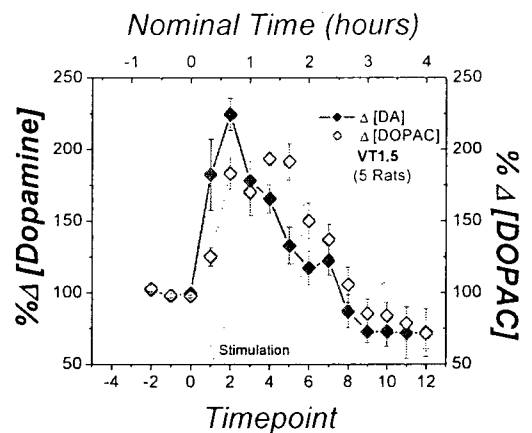
As in the case DOPAC, the increase in the HVA concentration (Figure S2c) lagged behind the rise in DA, reaching its maximum level, 216.53%, 80 min after onset of the stimulation, and declining prior, to the offset of the stimulation. The average HVA concentration during this period was 171.60% of baseline. The decline in HVA concentration during the post-stimulation period was delayed with respect to the decline in DA and DOPAC concentrations.

Statistical comparison of DOPAC and HVA levels across schedules.

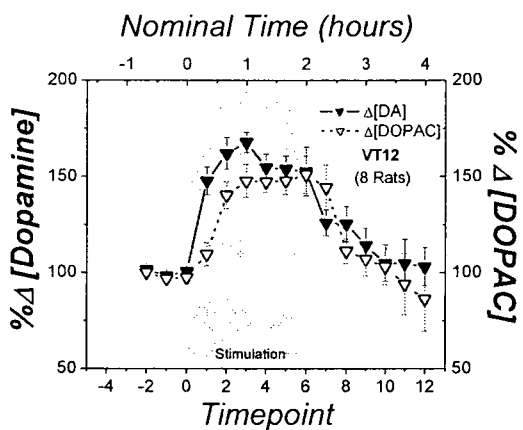
DOPAC increased significantly during the stimulation period in all three schedules studied, but according to different time-courses (Figure S1d). Analysis of variance showed significant effects for time of the sample, $F_{(14,252)} = 65.46, p < 0.01$, and the interaction between schedule and time of the sample, $F_{(28,252)} = 3.45, p < 0.01$; but not for the schedule under which the stimulation was delivered $F_{(2,18)} = 1.03, p = 0.38$. Under all three schedules, significant increases in DOPAC were observed 40 minutes after the stimulation started; the DOPAC concentration remained significantly elevated until 20 minutes after the stimulation was finished under the VT12 and FT12 schedules and until 20 minutes prior to stimulation offset in the VT1.5 condition. HVA also increased significantly during the stimulation period under all three schedules studied, but according to different time-courses (Figure S2d). Analysis of variance showed a significant main effect for time of the sample, $F_{(14,252)} = 53.22, p < 0.01$; but not for the



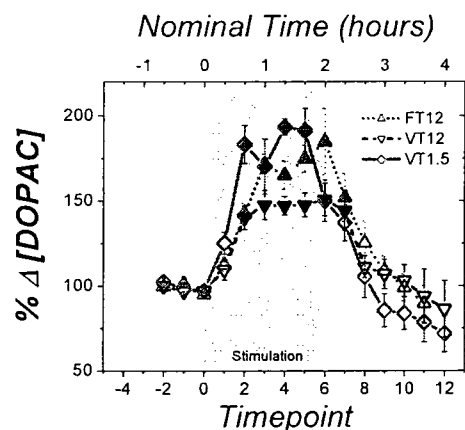
a



c



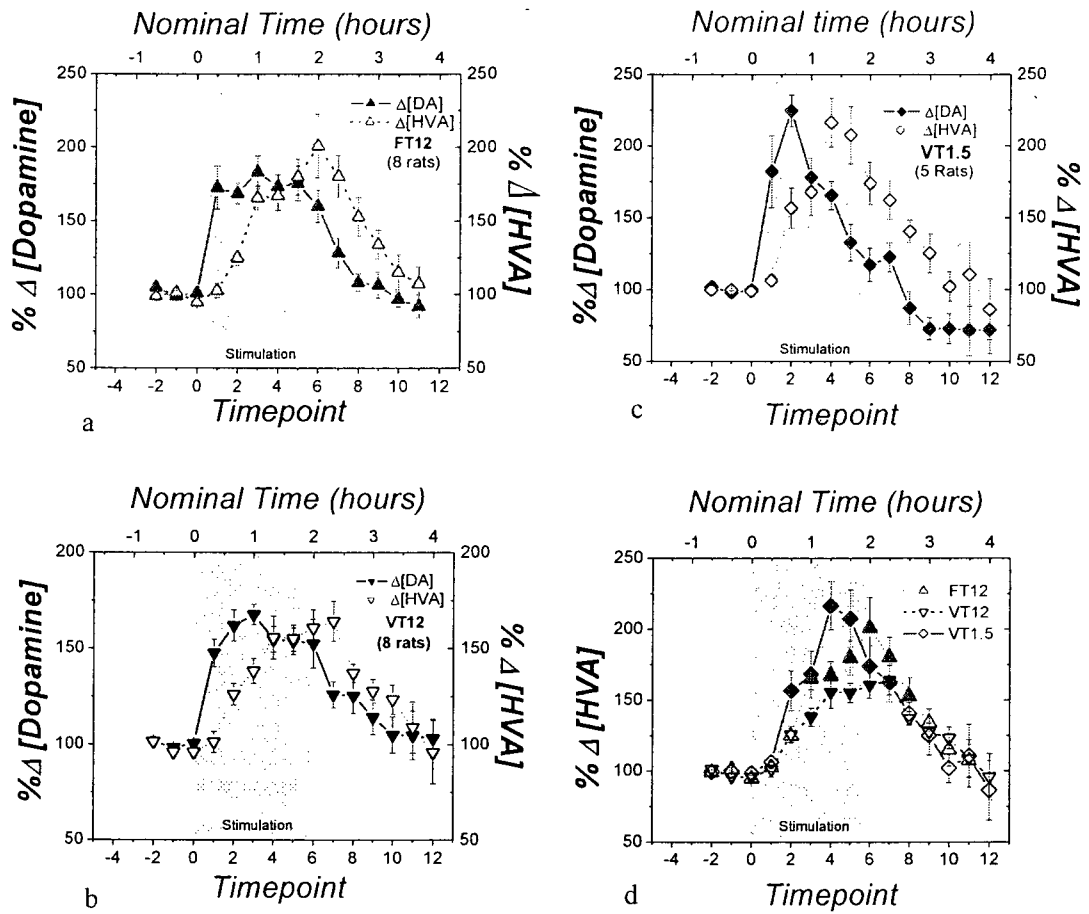
b



d

Supplementary figure 1

Figure Supplementary 1. (a) Effect of electrical stimulation of the MFB under a FT12 schedule on extracellular DA and DOPAC. The onset of stimulation trains is predictable under this schedule. A sustained increase in DA concentration is seen during the 2 hour period of stimulation whereas the changes in DOPAC lag behind the changes in DA concentration, as expected. (b) Effect of electrical stimulation of the MFB under a VT12 schedule on extracellular DA and DOPAC. The onset of stimulation trains is unpredictable under this schedule. A sustained increase in DA concentration is seen during the 2 hour period of stimulation whereas the changes in DOPAC lag behind the changes in DA concentration, as expected. (c) Effect of electrical stimulation of the MFB under a VT1.5 schedule on extracellular DA and DOPAC. A large increase in DA concentration is seen during the first 40 min but is not sustained; the DA measurements return to the baseline range before the end of the 2 hour period of stimulation and trend lower after stimulation offset. The changes in DOPAC lag behind the changes in DA concentration, as expected. (d) DOPAC concentrations in dialysate obtained from the NAc under the three stimulation schedules. Filled symbols represent significant differences from baseline, as revealed by post-hoc tests.



Supplementary figure 2

Figure Supplementary 2. (a) Effect of electrical stimulation of the MFB under a FT12 schedule on extracellular DA and HVA. The onset of stimulation trains is predictable under this schedule. A sustained increase in DA concentration is seen during the 2 hour period of stimulation whereas the changes in HVA lag behind the changes in DA concentration, as expected. (b) Effect of electrical stimulation of the MFB under a VT12 schedule on extracellular DA and HVA. The onset of stimulation trains is unpredictable under this schedule. A sustained increase in DA concentration is seen during the 2 hour period of stimulation whereas the changes in DOPAC lag behind the changes in DA concentration, as expected. (c) Effect of electrical stimulation of the MFB under a VT1.5 schedule on extracellular DA and HVA. (d) HVA concentrations in dialysate obtained from the NAc under the three stimulation schedules. Filled symbols represent significant differences from baseline, as revealed by post-hoc tests.

Appendix 2: Supplementary material Chapter 3
Effect of LH stimulation under a FT-1.5 schedule on concentrations of DA, DOPAC,
and HVA and locomotion.

Delivery of LH stimulation on the FT-1.5 schedule produced an increase in the concentrations of DA, DOPAC and HVA (Supplementary figure 3). After 20 min of stimulation the DA concentration in the dialysate increased to 150% of its baseline value, peaking at 217 % after 40 minutes of stimulation. Subsequent to this peak, the DA concentration decreased reaching 161% of its baseline value at the offset of the stimulation. The average DA concentration during the rewarding stimulation was 178% of the baseline value. During the post-stimulation period, DA concentration declined toward the baseline range. The increase in the dialysate concentration of DOPAC during the stimulation period lagged behind the increase in the concentration of DA (Supplementary figure 3a) and rose more gradually, approaching its maximum value, 182%, 60 min following stimulation onset; after this peak DOPAC stabilized at around 170% of its baseline value. DOPAC started to decline 40 minutes after the stimulation offset, in parallel with the decline in DA concentration, reaching values similar to those observed during the baseline by the end of the sampling period.

As in the case of DOPAC, the increase in the HVA concentration during the stimulation period was delayed with respect to the rise in DA concentration and was more gradual (Supplementary figure 3b). The maximum level achieved was 187 % of the baseline value, at the end of the stimulation period. The average HVA concentration during the stimulation period was 163% of the baseline value. The decline in HVA concentration during the post-stimulation period was delayed with respect to the decline

in DA, reaching values similar to those observed during the baseline by the end of the sampling period.

Delivery of LH stimulation under a FT-1.5 schedule produced an increase in locomotor activity (Supplementary figure 3c), which was defined as consecutive interruption of the two photocell beams. In other words, if a given beam was interrupted two or more times in a row, this was not counted as locomotion, but if interruption of a given beam followed interruption of the second beam, then the locomotor count was incremented. During baseline sampling, locomotor counts ranged from 1 to 32 across subjects (mean = 5). During the first 20 min of stimulation, the average locomotor count increased to 242 counts and remained around this value for the rest of the stimulation period. Twenty minutes after the stimulation offset the mean locomotion score declined and soon returned to the baseline value.

Effect of LH stimulation under a VT-1.5 on concentrations of DA, DOPAC, HVA and locomotion.

Similar effects to those observed under the FT-1.5 schedule were found during the LH stimulation under a VT-1.5 schedule. The rewarding stimulation delivered during this schedule produced an increase in DA, DOPAC, and HVA levels (Supplementary figure 4).

After 20 min of stimulation, the DA concentration in the dialysate increased to 207 % of baseline, peaking at 224% of baseline 40 min after the start of the stimulation. After the peak, DA concentration decreased reaching 171% of baseline at the offset of the stimulation. The average increase of DA during the rewarding stimulation was 196 % of

baseline. During the post-stimulation period, DA concentration declined toward the baseline range. The increase in the dialysate concentration of DOPAC during the stimulation period lagged behind the increase in the concentration of DA (Supplementary figure 4a) and rose more gradually, approaching a plateau 60 min after the stimulation onset. The DOPAC concentration achieved its maximum level, 189%, 100 minutes after the stimulation onset. The average increase in DOPAC concentration during the rewarding stimulation was 170 % of the baseline value. After the stimulation period, DOPAC declined in parallel with the decline in DA concentration, reaching values similar to those observed during baseline 60 minutes after stimulation offset.

As in the case of DOPAC, HVA concentration increased at slower pace than DA concentration (Supplementary figure 4b), achieving its maximum level, 195 %, at the end of the stimulation period. The average increase in HVA concentration during the stimulation period was 162 % of the baseline value. The decline in HVA concentration during the post-stimulation period was delayed with respect to the decline in DA and DOPAC concentrations, reaching values similar to those observed during baseline 100 minutes after stimulation offset.

Following stimulation onset, locomotor activity increased rapidly (Supplementary figure 4c), from a baseline value of 7 reaching a peak of 264 counts, 80 min after stimulation onset. The average locomotor activity during the stimulation period was 246. During the post stimulation period, the locomotor activity returned rapidly to the baseline range.

Comparison of locomotor activity across schedules

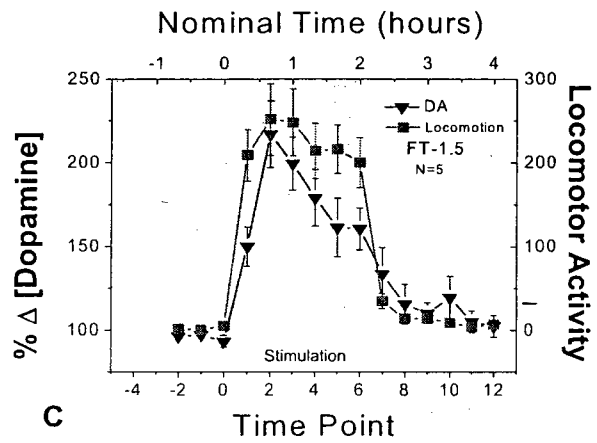
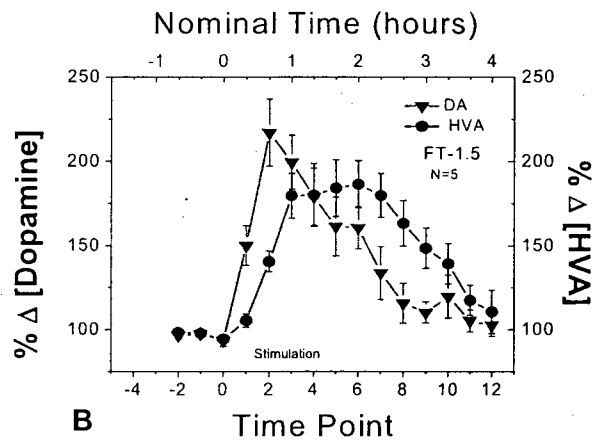
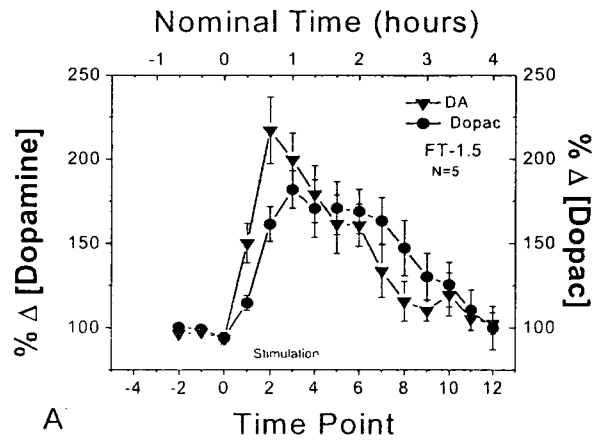
Stimulation of the LH produced a significant increase in locomotor activity under both schedules studied (Supplementary Figure 5; filled symbols represent statistically significant differences from baseline values). Analysis of variance showed a significant main effect for time of the sample, $F_{(14,112)} = 54.67$, $p < 0.05$; but not for the schedule under which the stimulation was delivered, $F_{(1,8)} = 0.15$, $p = 0.70$ nor for the interaction between schedule and time of the sample, $F_{(14,112)} = 0.44$, $p = 0.95$. The increase under the VT-1.5 schedule was slightly greater and more stable than the one observed under the FT1.5 schedule, but this difference did not meet the criterion for statistical reliability in a Tukey's HSD post-hoc comparison.

The initial increase in DA concentration and locomotion occurred at the same time point, suggesting that any delay between behaviourally meaningful changes in DA tone in the NAc terminal field and the concentration of DA in the dialysate due to the sheath of damaged tissue around the microdialysis probe (Bungay et al., 2003) was insignificant at the available temporal resolution. Locomotor activity persisted after the concentration of DA in the dialysate began to fall. This may reflect “superstitious” behavior (Skinner, 1948) arising from the frequent coincidence of locomotion and delivery of rewarding stimulation trains.

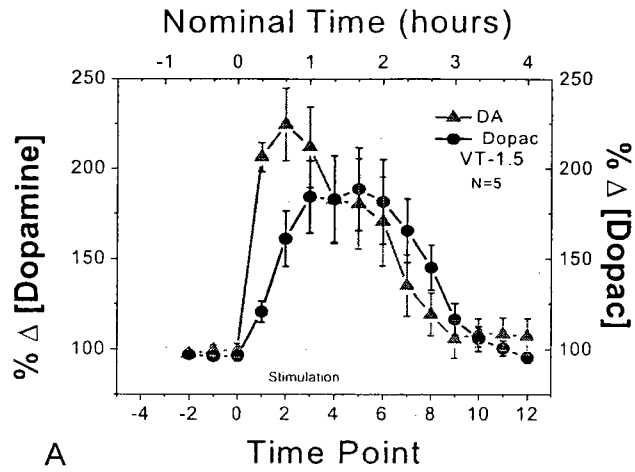
References:

Bungay, P. M., Newton-Vinson, P., Isele, W., Garris, P. A., & Justice, J. B. (2003). Microdialysis of dopamine interpreted with quantitative model incorporating probe implantation trauma. *Journal of Neurochemistry*, *86*, 932–946.

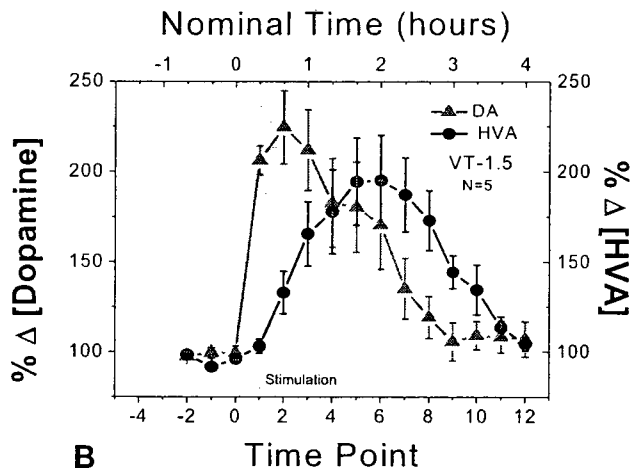
Skinner, B. F. (1948) "Superstition" in the pigeon. *Journal of Experimental Psychology*, 38, 168-172.



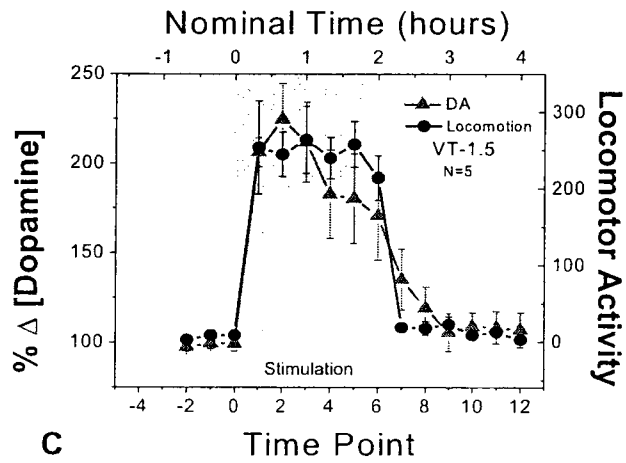
Supplementary figure 3. Comparison of Dopamine efflux under a FT1.5 reinforcement schedule against its metabolites (a) Dopac, (b) HVA, and (c) locomotor activity



A

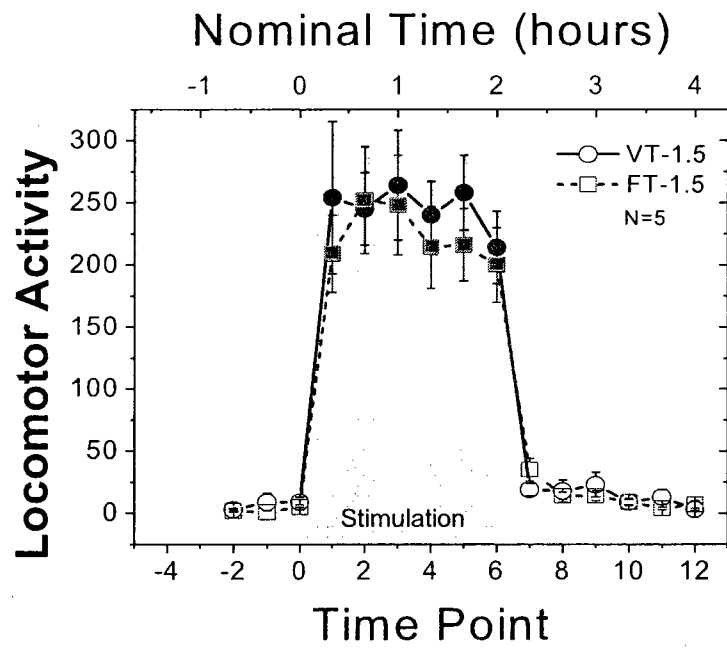


B

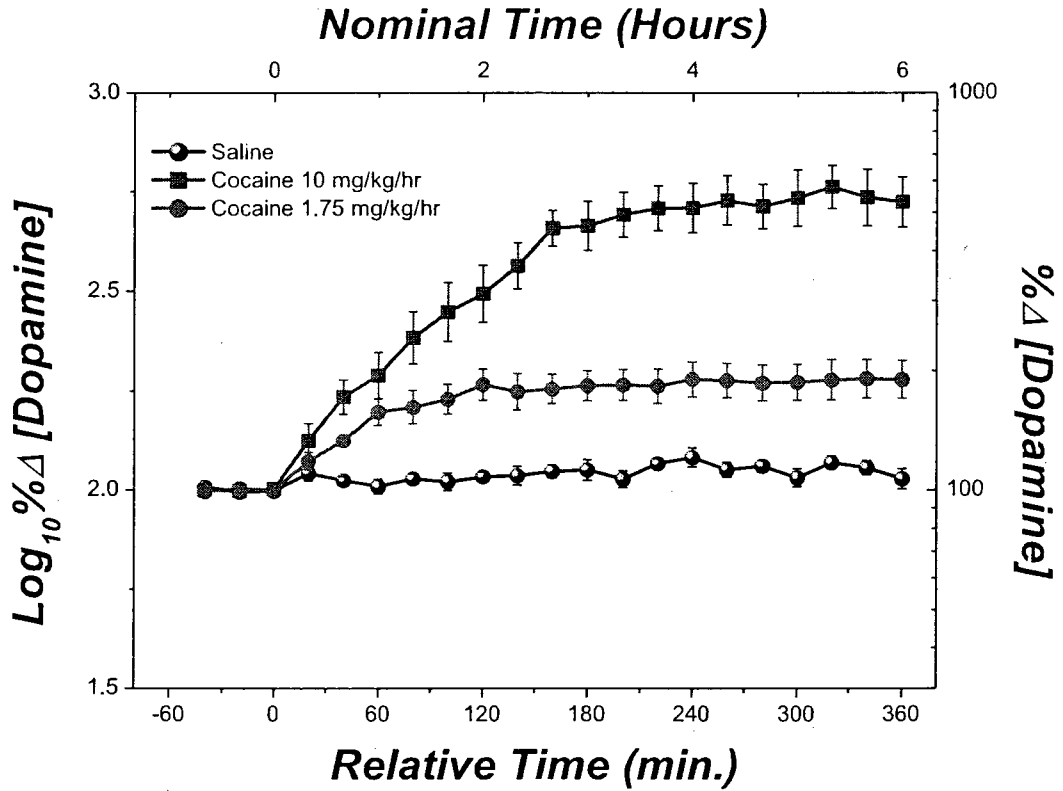


C

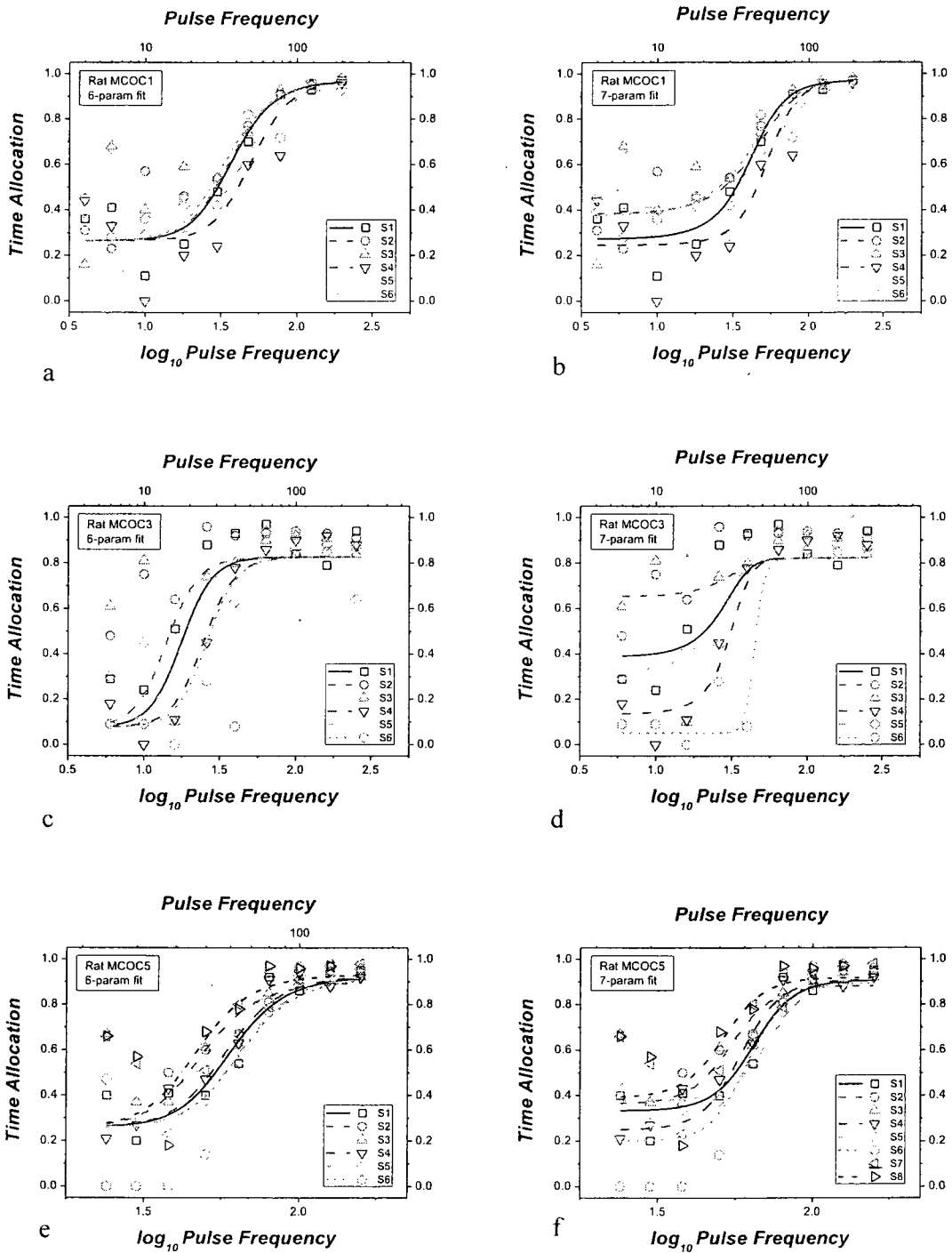
Supplementary figure 4. Comparison of Dopamine efflux under a FT1.5 reinforcement schedule against its metabolites (a) Dopac, (b) HVA, and (c) locomotor activity.



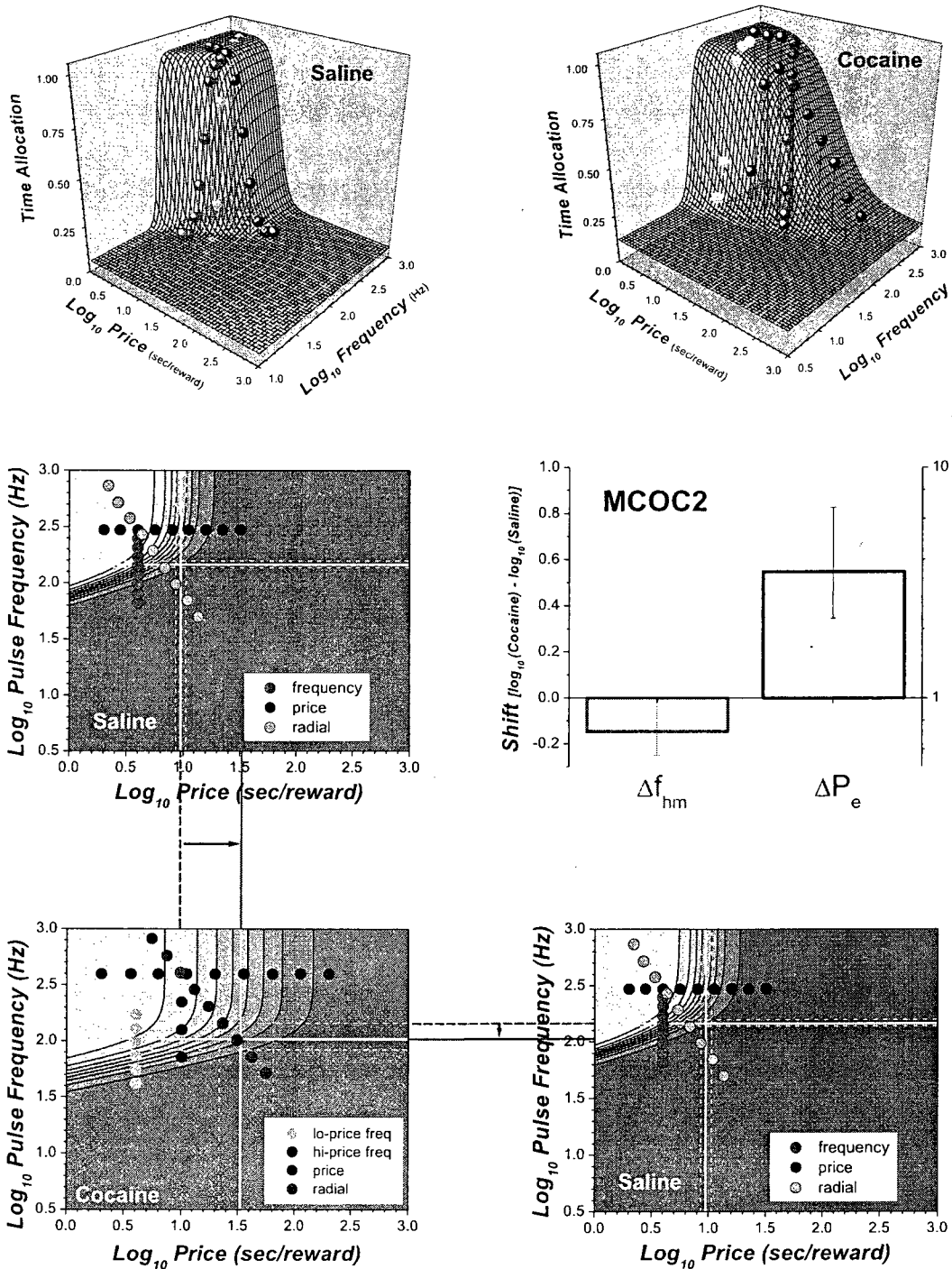
Supplementary figure 5. Comparison of locomotor activity induced by the LH stimulation under a FT 1.5 and VT 1.5 schedule of reinforcement.



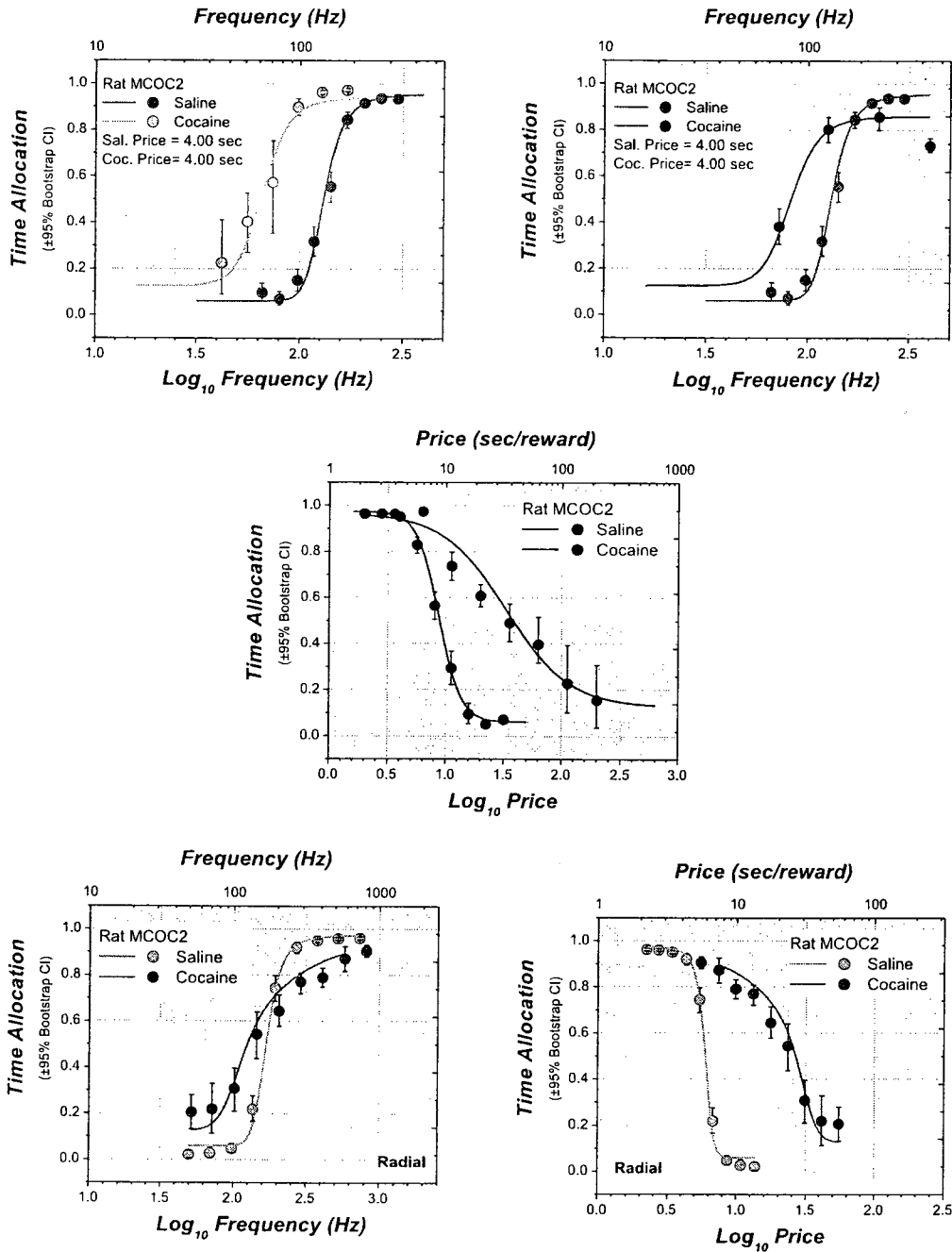
Supplementary Figure 6. DA efflux observed after continuous infusion of cocaine (10mg/kg/hr or 1.75 mg/kg/hr) and saline.



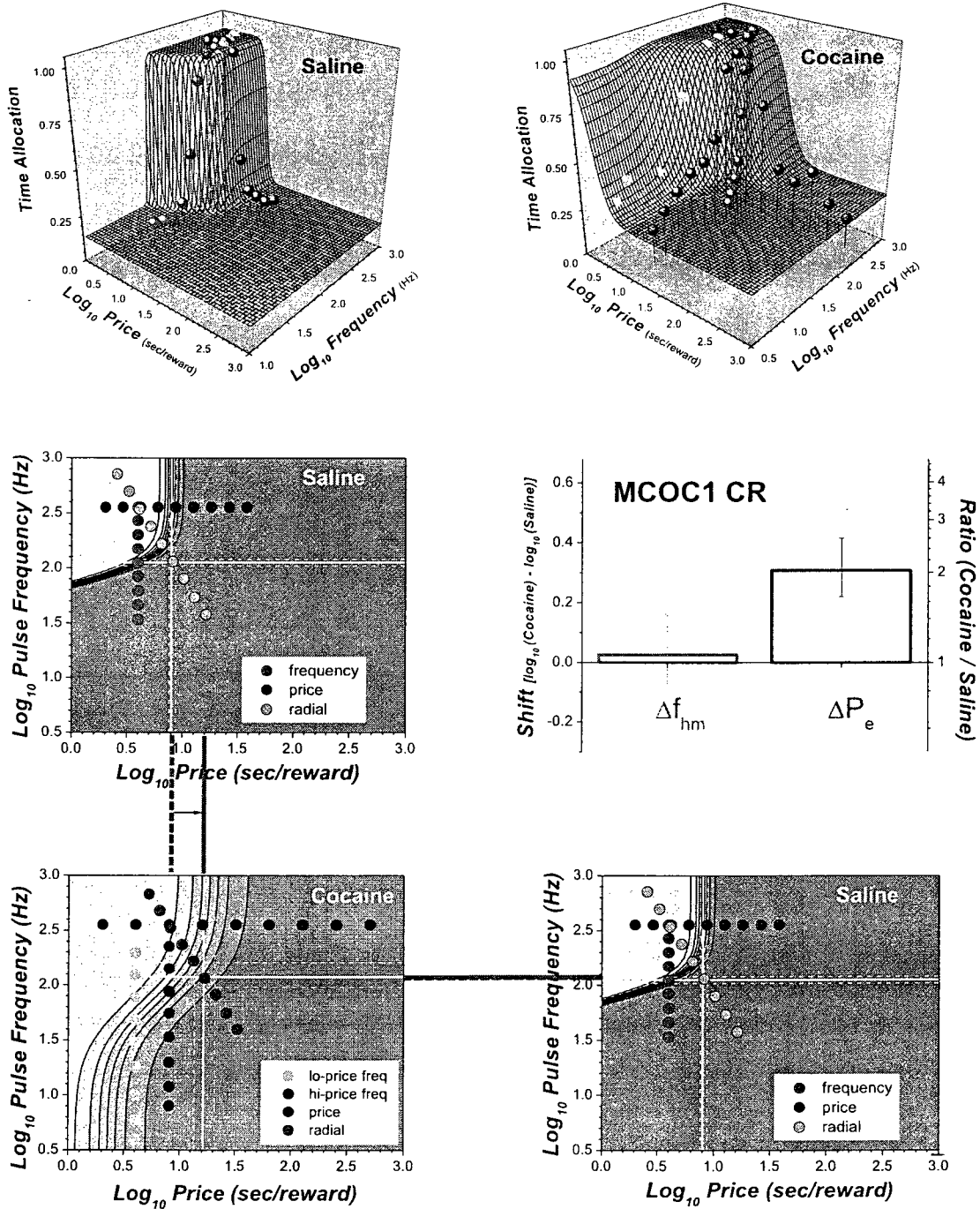
Supplementary figure 7. The 7-parameter model (right column) provides a better fit to the data from MCO1, MCO3 and MCO5 than the 6-parameter model (left column).



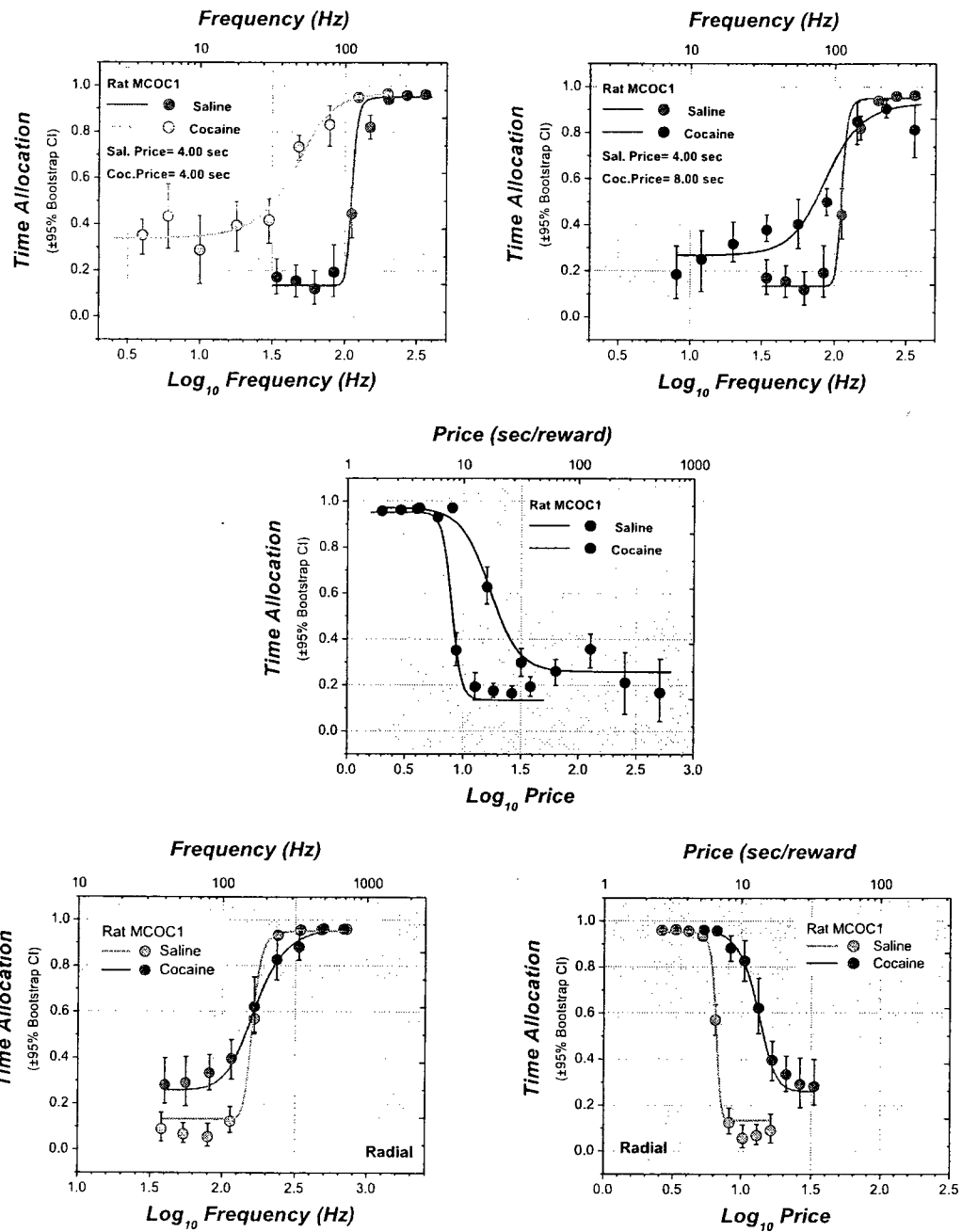
Supplementary figure 8. MCO2. Time allocation data, fitted surfaces, contours graphs and bar graph summarizing the shifts of the position parameters.



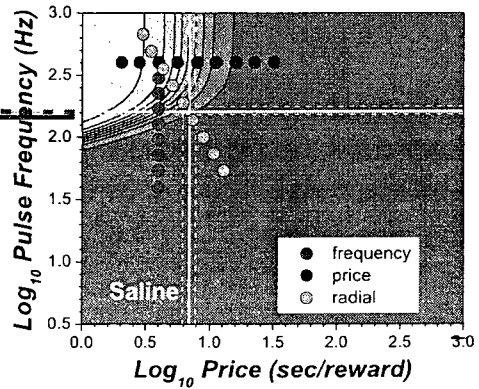
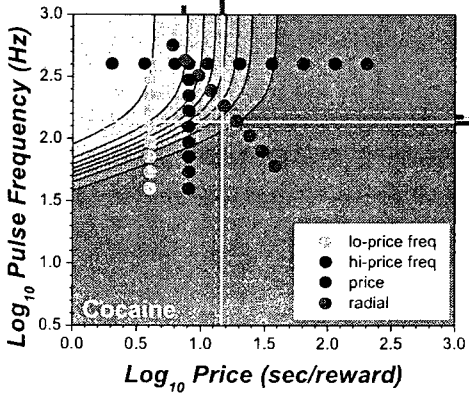
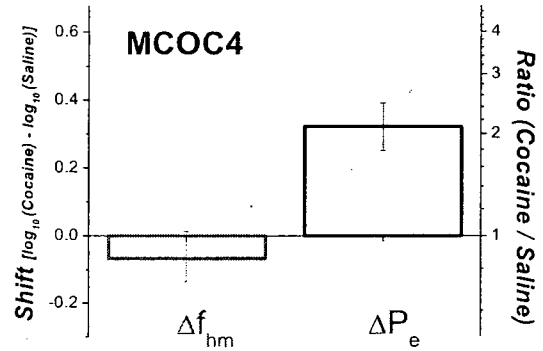
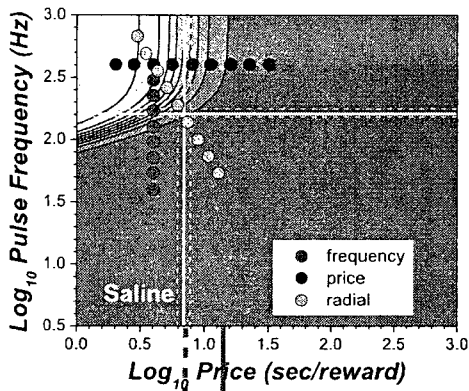
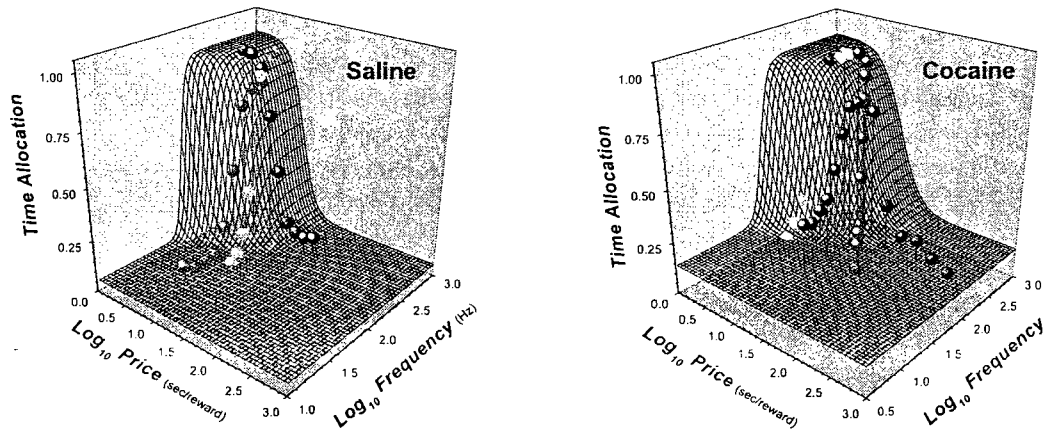
Supplementary figure 9. 2D projections of the surfaces fitted to the data from rat MCOC2.



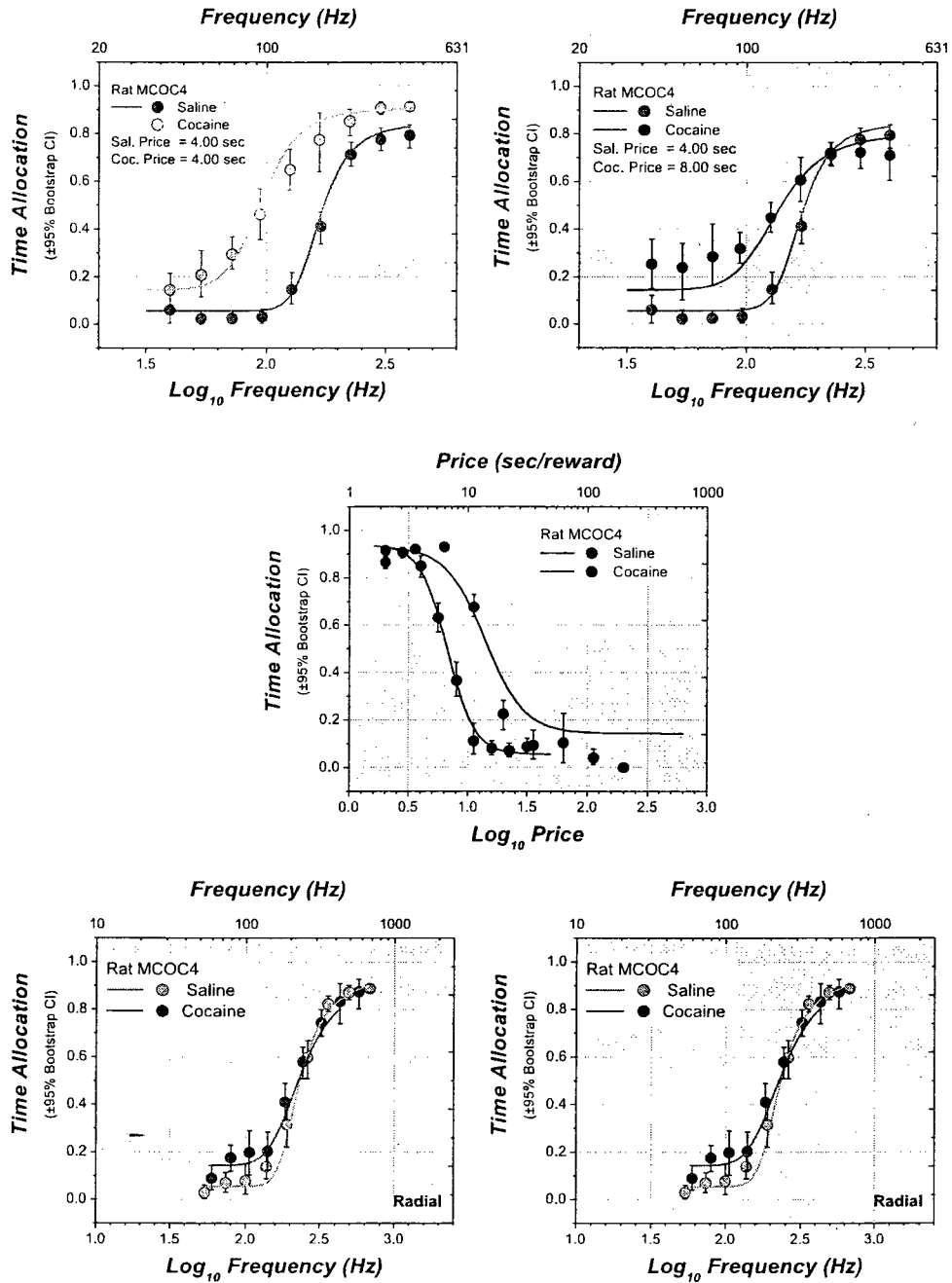
Supplementary figure 10. MCOCl Time allocation data, fitted surfaces, contours graphs and bar graph summarizing the shifts of the position parameters.



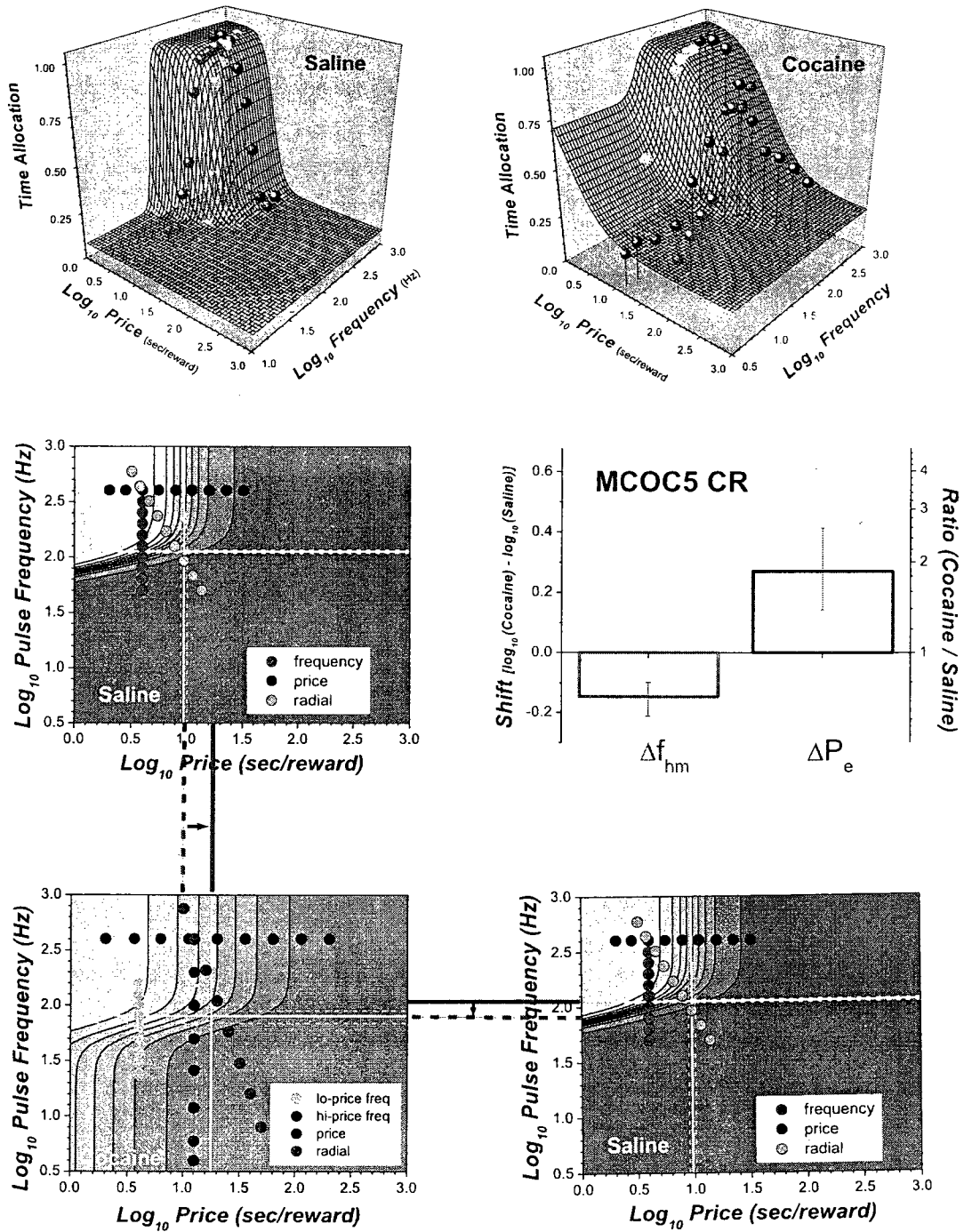
Supplementary figure 11. 2D projections of the surfaces fitted to the data from rat MCOC1.



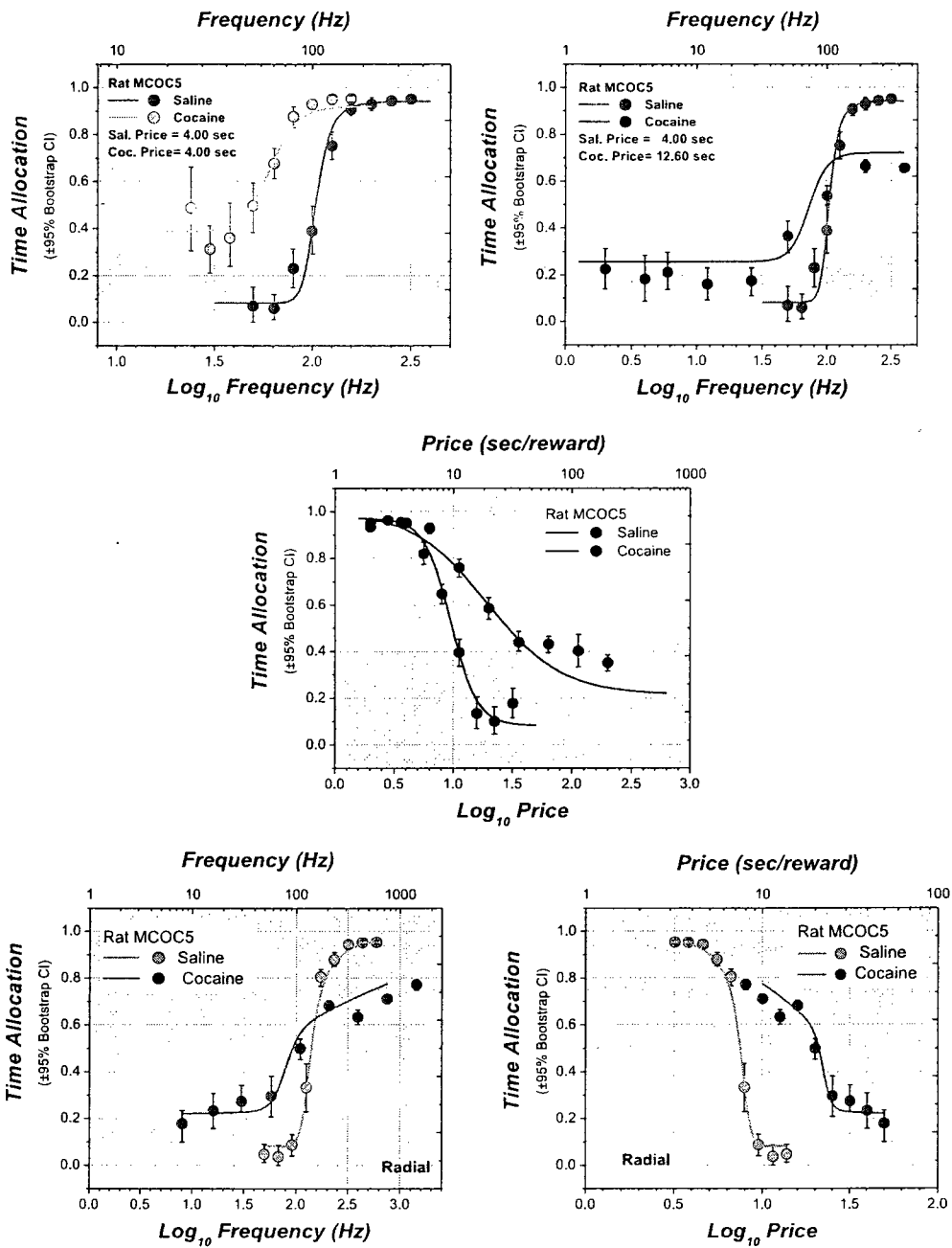
Supplementary figure 12. MCO4 . Time allocation data, fitted surfaces, contours graphs and bar graph summarizing the shifts of the position parameters.



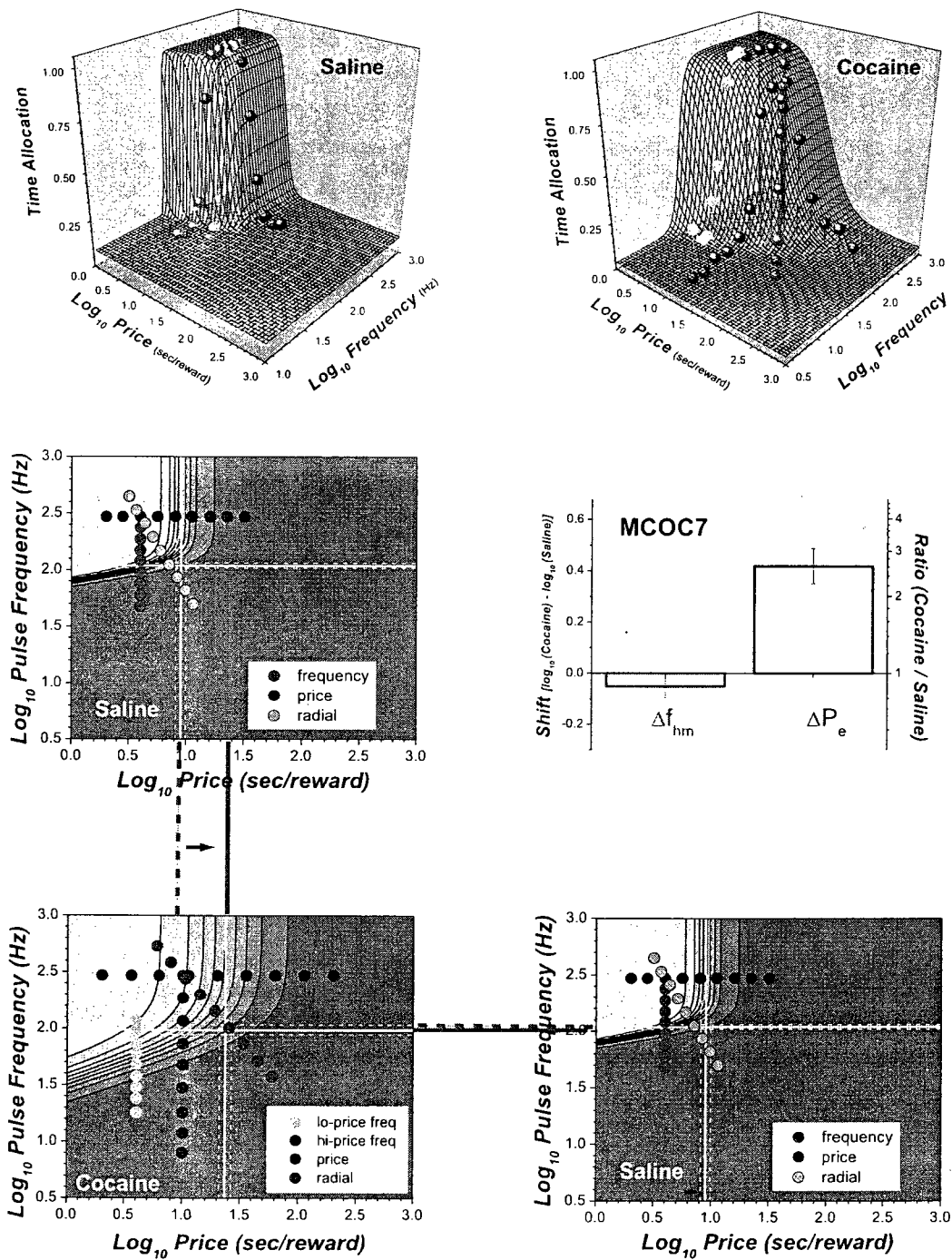
Supplementary figure 13. 2D projections of the surfaces fitted to the data from rat MCOC4.



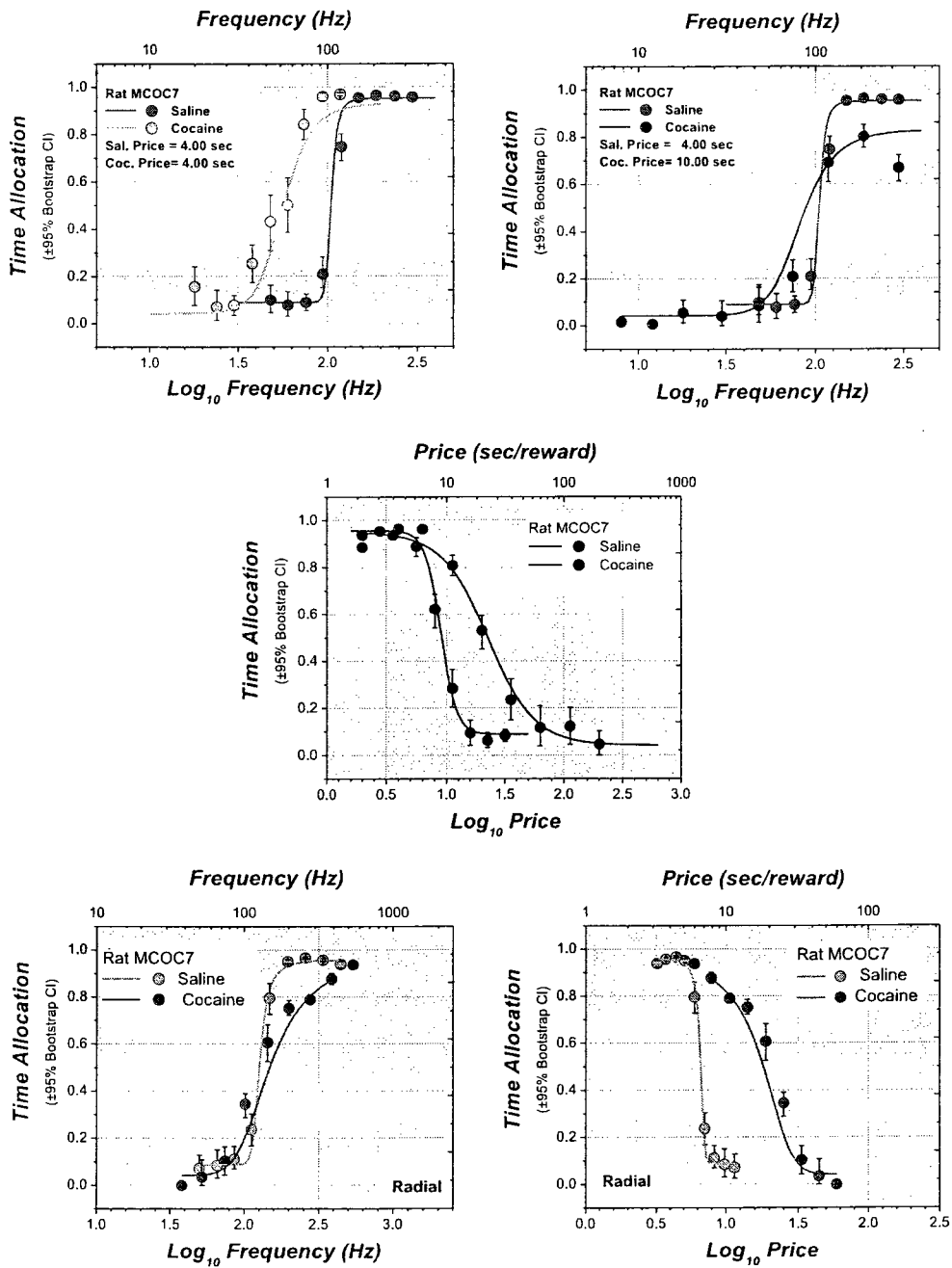
Supplementary figure 14. MCO5. Time allocation data, fitted surfaces, contours graphs and bar graph summarizing the shifts of the position parameters.



Supplementary figure 15. 2D projections of the surfaces fitted to the data from rat MCOCS.



Supplementary figure 16. MCO7. Time allocation data, fitted surfaces, contours graphs and bar graph summarizing the shifts of the position parameters.



Supplementary figure 17. 2D projections of the surfaces fitted to the data from rat MCOC7.